# **APPENDIX J**

Babich, P., Wang, P-Y., Allen, G., Sioutas, C. and P. Koutrakis, 1999: Development and Evaluation of a Continuous PM <sub>2.5</sub> Mass Monitor, submitted *to Aerosol Science and Technology*, July

VAN LOY, M., SAXENA, P., AND ALLAN, M. A., 1999: CHARACTERISTICS OF PM 2.5, SAMPLING METHOD INTERCOMPARISON AND FINE PARTICULATE COMPOSITION AT SIX URBAN SITES, DRAFT FINAL REPORT PREPARED FOR EPRI, SCE, AND CALIFORNIA ENERGY COMMISSION, SEPTEMBER

# DEVELOPMENT AND EVALUATION OF A CONTINUOUS AMBIENT $PM_{2.5}$ MASS MONITOR

Peter Babich<sup>a,\*</sup>, Peng-Yau Wang<sup>b</sup>, George Allen<sup>a</sup>, Constantinos Sioutas<sup>c</sup> and Petros Koutrakis<sup>a</sup>

<sup>a</sup> Harvard School of Public Health, Department of Environmental Health, 665 Huntington Ave. Bldg 1, Rm G2, Boston, MA 02115

<sup>b</sup> National Central University, Graduate Institute of Environmental Engineering, Chungli, Taiwan

<sup>c</sup> University of Southern California, Department of Civil and Environmental

Engineering, Los Angeles, CA 90089

Manuscript submitted for publication to *Aerosol Science and Technology*July, 1999

\* Author to whom correspondence should be addressed

# **ABSTRACT**

A Continuous Ambient Mass Monitor (CAMM) for fine particle mass (PM<sub>2.5</sub>) has recently been developed at the Harvard School of Public Health. The principle of this method is based on the measurement of the increase in pressure drop across a membrane filter (Fluoropore<sup>TM</sup>) during particle sampling. The monitor consists of a conventional impactor/inlet to remove particles larger than 2.5 μm, a diffusion dryer to remove particle-bound water, a filter tape to collect particles, a filter tape transportation system to allow unassisted sampling, and a data acquisition and control unit. For each sampling period (typically 30 to 60 minutes), a new segment of the filter tape is exposed so that particles remain close to equilibrium with the sample air during their collection. This results in minimization of volatilization and adsorption artifacts during sampling. Furthermore, since the required flow rate for the fine particle mass monitoring channel is only 0.3 L/min, the relative humidity of the air sample can be easily reduced to 40% or less using a Nafion<sup>TM</sup> diffusion dryer to remove particle-bound water. The CAMM has a detection limit of less than 5μg/m<sup>3</sup> for PM<sub>2.5</sub> concentrations averaged over one hour.

The performance of the newly developed monitor was investigated through laboratory and field studies. Laboratory tests included a calibration of the CAMM using polystyrene latex (PSL) and silica particles. A series of field studies were conducted in seven cities with presumably different PM<sub>2.5</sub> chemical composition. The 24 one-hour CAMM measurements were averaged and compared to Harvard Impactor (HI) 24-hour PM<sub>2.5</sub> integrated measurements. Based on 211 valid sampling days, the measurements obtained from the Harvard Impactor and the CAMM were highly correlated ( $r^2 = 0.90$ ). The average CAMM-to-HI concentration ratio was  $1.07 (\pm 0.18)$ .

#### INTRODUCTION

The U.S. Environmental Protection Agency (U.S. EPA) has recently promulgated a new National Ambient Air Quality Standard (NAAQS) for fine particulate matter (PM<sub>2.5</sub>; particulate matter  $\leq 2.5\mu m$  aerodynamic diameter). This new standard is in addition to the existing one for PM<sub>10</sub> which includes particles with aerodynamic diameter  $\leq 10\mu m$ . For both the PM<sub>10</sub> and PM<sub>2.5</sub> standards, the Federal Reference Method (FRM) is based on the gravimetric analysis of particles collected on filters over a period of twenty-four hours. The gravimetric analysis was selected because most of the particle data used for the epidemiological studies investigating associations between mortality and morbidity outcomes and ambient particle exposures are based on filter measurements (Dockery et al., 1993 and Ito and Thurston, 1996).

The technology that the U.S. EPA has implemented as the reference method for PM<sub>2.5</sub> is a Teflon membrane filter preceded by an inertial impactor that has a 50% collection efficiency at 2.5µm and manufactured according to design specifications of the EPA. In operation, a 24-hour integrated sample is collected on a filter, which is later equilibrated at controlled temperature and relative humidity (RH) conditions in a laboratory, and then weighed to determine the mass of the deposited particulate matter (PM). According to the Federal Register, sampling must be conducted at ambient temperature conditions (within 5°C), and the collected samples must be equilibrated at 30-40% RH and 20-23°C for 24 hours prior to their gravimetric analysis (Federal Register, 1997). This specified method will then be used to evaluate potential equivalent methods. This approach is necessary in order to minimize discrepancies among different equivalent samplers. It must be pointed out, however, that the accuracy of the FRM itself is questionable due to the volatilization of the semi-volatile inorganic and organic compounds which are continually interchanging between the particle and gas phases.

The PM<sub>2.5</sub> FRM presents the following drawbacks: a) it requires a sequential sampling unit to collect two to seven daily samples per week; b) it requires both an environmentally controlled balance room and extensive labor to weigh the filters and; c) it does not provide short term measurements. Capital investment and labor costs can be significant for the implementation of the fine particle mass standard, while very little will be learned about the diurnal variability of fine particle concentrations. A 24-hour average measurement may not adequately represent actual human exposure. Therefore, a semi-continuous monitor that can provide accurate hourly measurements is essential for exposure assessment. Detailed temporal information is needed for both understanding particle health effects and developing sound mitigation strategies. Because of its sensitivity, the gravimetric method may not be adequate to obtain short term measurements (less than 12-24 hours). In addition, attempts to obtain a finer resolution on ambient particle concentrations on a regular basis using filter based methods for large monitoring networks are cost-prohibitive and impractical. Finally, the proposed FRM can not provide immediate data that are necessary to calculate Air Pollution Indices (APIs). Therefore, development of equivalent continuous fine particle methods will make it possible to obtain richer data sets and to establish comprehensive monitoring networks that provide information on temporal and spatial variability of particle mass concentration in a cost-effective way.

In this paper we describe the development as well as the laboratory and field evaluation of a semi-continuous fine particle mass sampler that can provide one-hour measurements or less. Our method is based on the continuous measurement of the increase in pressure drop across a Fluoropore<sup>TM</sup> membrane filter during particle sampling. We have designed and constructed a filter tape transportation system that allows for unassisted particle sampling. For each sampling period (varying from 30 to 60 minutes) a new segment of the filter tape is exposed. Considering

that the time scale for variation in ambient air composition is usually much longer than one hour, it is expected that particles remain in or close to equilibrium with the sample air during their collection. This method combines measurement at ambient temperature, short sampling durations, and low face velocity, all of which result in reducing sampling artifacts. These sampling artifacts are related to losses of volatile PM constituents and/or adsorption of gases by already collected particles, and are more likely to occur over longer sampling periods (Appel et al., 1984). In addition, because this technique requires a low flow rate (0.3 L/min) the relative humidity of the air sample can be controlled to 40% or less by passing the air sample through a Nafion<sup>TM</sup> diffusion dryer prior to its collection. This is in accordance with the PM<sub>2.5</sub> FRM, which requires that particle filter samples should be conditioned prior to gravimetric measurement at a relative humidity of 30-40% to remove particle-bound water.

#### **METHODS**

# **CAMM description**

A schematic of the CAMM is shown in Figure 1 and it consists of the following components: 1) a Well Impactor Ninety Six (WINS; Federal Register, 1997)  $PM_{2.5}$  size selective inertial impactor; 2) two round-nozzle virtual impactors, having 50% cutpoints of 1.0 and 0.40  $\mu$ m in aerodynamic diameter, respectively; 3) the  $PM_{2.5}$  monitoring channel, and; 4) a data acquisition and control system.

The key feature of the CAMM is the PM<sub>2.5</sub> particle-monitoring channel, which consists of a filter tape transportation system and the pressure transducers. The principal components of this system include a microprocessor-controlled drive to advance the tape and a mechanism to allow

release and resealing of the filter tape each time the filter tape is advanced. The use of a filter tape transportation system makes it possible to expose a new segment of the filter membrane for each of the different sampling periods to minimize adsorption/desorption phenomena. The fine particle sample is divided into two channels of equal flows (0.3 L/min each). A high efficiency particle air (HEPA) filter is used to remove particles from one of the two channels (the reference channel).

For each sampling period, the filter transportation system exposes two circular filter surface areas (radius of 3.2 mm) of the Fluoropore<sup>TM</sup> filter tape (PTFE Teflon membrane, laminated to a layer of porous polyethylene, pore size: 3 µm, Millipore Corporation, Medford, MA), to the fine particle and the reference channels, respectively. During sampling, the pressure drop across the collection medium for the sample and reference areas is measured continuously using pressure transducers (full range 0-25" H<sub>2</sub>O, Model PX653-25D5V, Omega Engineering Inc., Stamford, CT). The pressure drop across the Fluoropore<sup>TM</sup> filter is approximately 7.5x10<sup>3</sup> dyn/cm<sup>2</sup>. The pressure drop across the reference channel depends on the filter characteristics, flow rate, relative humidity and temperature. Similarly, the pressure drop across the fine particle sample channel depends on the same parameters plus the particles that deposit onto the filter. Therefore, the difference in pressure drop between the particle sample channel and the reference channel can be attributed to the particles collected on the filter medium. A filter was also placed downstream of both the sample and reference channels. Another set of pressure transducers (full range 0-2" H<sub>2</sub>O, Model PX653-02D5V) are used to monitor the pressure drop difference between the sample and reference channel for both the upstream and downstream filters. This second set of pressure transducers are used to measure the increase in pressure drop associated with the particle loading in order to determine the particle mass concentration. This dual channel with

downstream filter design is not affected by small flow fluctuations or changes in relative humidity and temperature. Therefore, this monitoring technique does not require costly flow or temperature controls. The latter is one of the main features of our method because it makes it possible to conduct measurements at ambient temperatures.

The original design of this instrument included the use of a porous membrane Nuclepore™ filter (Wang, 1997). Nuclepore™ filters have uniform circular pores that are normal to the surface. By properly choosing filter face velocity and pore size, the increase in pressure drop per unit time in these filters can become independent of particle size for particles in the range of 0.1-2 µm. Despite this significant advantage of Nuclepore filters, we have recently found that the particle collection efficiency was not constant and varied with both filter porosity and pore diameter which varied not only between batches, but also within the same batch (Sioutas et al. 1998). This led us to investigate the possibilities of using a different filter material in the system. We have chosen a filter, such as Fluoropore™, because of the structural consistency as well as the abundant literature on pressure drop with loading for various fibrous filters (Novick et al., 1992; Gupta et al., 1993; Japuntich et al., 1994). These studies have shown that the change in the pressure across the filter per concentration and time to be inversely proportional to the particle diameter (d<sub>p</sub>). As part of our laboratory experiments (described below), we have also investigated the relationship between the increase in pressure drop per unit time and particle mass concentrations in Fluoropore<sup>TM</sup> filters, confirming this inverse relationship.

In order to make the increase in pressure drop per unit time and concentration independent of particle size, a series of two virtual impactors were employed to enrich the concentration of the larger particles. The impactor size cutpoints were selected in such a way so

that the enrichment factor of different particles in the size range 0.1 to  $1.0~\mu m$  is proportional to their size and it varies between 1 and 10 times. This renders the response of the method independent of particle diameter. The virtual impactors were placed as shown in Figure 1 after the WINS PM<sub>2.5</sub> size selective inlet and before the sampling channel. The first impactor has a 50% cutpoint at  $1.0~\mu m$  and operates with a minor-to-total flow ratio of 0.2. The second impactor has a 50% cutpoint at  $0.40~\mu m$  and operates at the same minor-to-total flow ratio. The minor flow of the second virtual impactor contains the air sample in which larger particles are enriched with respect to smaller particles.

# **Experimental**

The relationship between the increase in pressure drop with particle loading across the Fluoropore ™ membrane filter was investigated as a function of particle concentration and size. First, tests were conducted without the virtual impactors, and then with the two virtual impactors. The experimental setup is shown in Figure 2. Suspensions of monodisperse fluorescent yellow-green latex microspheres (Fluoresbrite, Polysciences, Warrington, PA) were atomized with a pocket nebulizer (Retec X-70/N) using filtered room air at 20 psi. Particle size ranged from 0.05 to 2.3 µm. The volumetric flow rate of the nebulizer was estimated to be approximately 5.5 LPM and the output was approximately 0.25 cm³/min of fluorescent suspension. The nebulizer was connected to a syringe pump in order to atomize large amounts (120 mL) of the fluorescent suspension. In addition, the output of the nebulizer was maintained constant to ensure a stable atomization process. The generated aerosol was mixed with clean (particle-free) air with controlled relative humidity (RH). RH was controlled by adjusting the flow rates of a dry and a

moist airstream, as shown in Figure 2. The aerosol was then drawn through a 1-L cylindrical chamber where ten  $^{210}$ Po ionizing units were placed (Staticmaster, NRD Inc.) to reduce electrostatic charges carried by the generated particles to the Boltzmann equilibrium distribution. The aerosol was then drawn through a manifold with a RH/Temperature probe connected to it; part of the aerosol was drawn through a Teflon filter used as a reference to determine the mass concentration of the input aerosol. The test sample was drawn through the CAMM at 0.3 L/min. In order to investigate the effect of particle density (or equivalently, specific gravity), suspensions of monodisperse silica beads ( $\rho_p$ =2.2 g/cm<sup>3</sup>, Bangs Laboratories, Inc., Carmel, IN) were also atomized.

At the end of each experiment, the reference Teflon filter was weighed in a controlled RH and temperature room to determine the mass concentration of the generated aerosols. Filters were weighed after 24-hours of equilibration ( $40 \pm 5\%$  RH,  $70 \pm 5$  °F). The measured increase in pressure drop per unit time was then divided by the mass concentration of the aerosol to obtain its normalized value ( $3.23 \pm 0.1 \times 10^{-6}$  dyn/cm<sup>2</sup>/s per  $\mu$ g/m<sup>3</sup>).

# **Field Study**

A series of field studies, sponsored by EPRI (Palo Alto, CA), were conducted to test the CAMM in different U.S. urban environments and compare it with the gravimetric PM method. Because the composition of ambient particles varies with geographic location and season, studies were conducted in different areas of the United States which have distinctly different ambient air particulate compositions and densities. These sites include: Riverside, CA, Boston, MA, Chicago, IL, Dallas, TX, Phoenix, AZ, Bakersfield, CA, and Philadelphia, PA. At each site we

set out to collect 30 days of valid data. Table 1 shows a schedule of the field tests and their location.

The PM<sub>2.5</sub> FRM and Harvard Impactor (HI; Marple et al., 1987) were used for the integrated fine particle mass measurements. Similar to the FRM, the Harvard Impactor utilizes a measurement principle based on gravimetric analysis. The FRM was used only at Riverside and Bakersfield while the HI was used at every site. The comparison of the FRM and HI showed excellent agreement in both Riverside ( $r^2 = 0.99$ , slope = 0.92, the FRM measured less mass) and Bakersfield ( $r^2 = 0.99$ , slope = 1.00), thereby substantiating the decision to use only the HI as a surrogate FRM at all the other sites. The FRM uses a 47mm Teflon membrane filter (Teflo<sup>TM</sup>, Gelman Sciences) at a flow rate of 16.7 L/min. The PM<sub>2.5</sub> HI collects particles on 37 mm Teflon filters (Teflo<sup>TM</sup>, Gelman Sciences) at a flow rate of 10 L/min. The filters for both the FRM and HI were equilibrated in a temperature and relative humidity controlled weighing room at least 48 hours prior to being weighed, both before and after sampling. All final weighings were done within 10 days after sampling following EPA guidelines as described in the Federal Register.

Since the Harvard Impactor sampler was used as the reference to which the CAMM would be compared, several quality assurance steps were taken. At each site, field blanks (10% of total sample size), replicate samples (20% for PM<sub>10</sub> HIs and 100% for PM<sub>2.5</sub> HIs), and laboratory blanks (5% of total sample size), were collected in order to assess the precision and limit of detection of HI samples. Duplicate PM<sub>2.5</sub> HIs were used for each sampling day to ensure maximum data capture for the 24-hour integrated fine particle mass measurements. Field blanks were treated identically to the samples. The field blanks were intended to account for collection of particles on the filter that occurs during handling. Replicate samples, which refer to two identical, collocated samples, were used to assess the precision of the method. Laboratory blanks

were designed to assess the consistency of the weighing procedure. Filters were weighed twice before and after sampling to improve precision; if the difference between two weighings exceeded 10µg, the filter was weighed a third time. Flow rates were kept within  $\pm$  5% of the target flow, 10 L/min. Relative precision of a single HI PM sample was calculated as the standard deviation of the difference between collocated samples divided by the mean of the collocated samples, divided by  $\sqrt{2}$ . The limit of detection was computed as three times the standard deviation of the mass increase of the field blanks (Keith, et al., 1983; Thomas, et al., 1993). Precision of the CAMM method was also determined in Philadelphia where two CAMM systems were utilized.

Sampling time for the HI was 24 hours while the CAMM was set to advance the filter tape every hour. The 24 one-hour CAMM measurements were then averaged and compared to the corresponding Harvard Impactor 24-hour integrated measurement.

The Harvard-EPA Annular Denuder System (HEADS; Koutrakis et. al., 1988) was used during the field studies to measure particulate ion concentrations (NH<sub>4</sub><sup>+</sup>, SO<sub>4</sub><sup>-2</sup>, NO<sub>3</sub><sup>-</sup>) and inorganic gases (SO<sub>2</sub>, HNO<sub>3</sub>, NH<sub>3</sub>). Organic and elemental carbon was measured using a 47mm pre-fired quartz fiber filter and analyzed by the thermal optical reflectance (TOR) method (Chow et. al., 1993). Both the HEADS and the carbon samplers were operated at 10 L/min for 24 hours. Total particulate nitrate was measured to determine whether any of the differences between the mass measurements obtained from the CAMM and the Harvard Impactor could be explained by the losses of nitrate from the Teflon filter of the HI. The loss of particulate organic carbon (OC) from the Teflon filter could not be quantified so the particulate OC was measured to determine if there was any relationship between the differences between the mass measurements obtained from the CAMM and the HI and the total particulate OC measured. The HEADS and carbon

samplers were run concurrent with the HI and CAMM.

#### **RESULTS AND DISCUSSION**

# CAMM Configuration without the virtual impactors

Results from the characterization of the CAMM configuration without the virtual impactors are shown in Figure 3. The experiments show that the increase in the pressure drop, per unit time and particle mass concentration ( $\Delta P/(c_m \cdot t)$ ) can be expressed by the following equation:

$$\frac{\Delta P}{c_m t} \propto \frac{1}{\rho_p d_p \sqrt{C_c}} \quad (1)$$

where  $\rho_p$  is the particle density,  $d_p$  is the physical particle diameter and  $C_c$  is the particle slip correction factor. Similar relationships have also been derived in studies conducted in fibrous filters by Novick et al. (1992), Gupta et al. (1993) and Hinds and Kadrichu (1997). The dependence of the instrument response on particle diameter makes it difficult to use this method without any modifications that would negate this effect. Hence, we used the two virtual impactors to enrich the concentration of larger particles with respect to smaller particles of  $PM_{2.5}$  as an inverse function of size.

# CAMM Configuration with the Two Virtual Impactors

Results from the first series of tests are summarized in Figure 4. This figure shows

separately the concentration enrichment achieved by the 1.0 µm and the 0.40 µm virtual impactors, respectively, as well as the overall concentration enrichment when both impactors are used in series. The enrichment of the both virtual impactors were determined by generating monodisperse fluorescent aerosols and by connecting a Scanning Mobility Particle Sizer (SMPS, TSI Model 3934) and an Aerodynamic Particle Sizer (APS, TSI Model 3310A) upstream and downstream of the virtual impactor. For each particle size, the SMPS (for PSL particles less than 0.5µm in diameter) and the APS (for PSL particles greater than 0.5µm in diameter) sampled for approximately 10 minutes upstream of the impactor, then downstream of the impactor for additional 10 minutes. The upstream and downstream measurements were repeated at least one more time for each particle size to ensure stable readings as well as to incorporate the effects of possible fluctuations in the concentrations of the generated aerosols.

The combined enrichment of the two virtual impactors, also shown in Figure 4, shows that for particles in the aerodynamic size range of 0.1 to 1.1  $\mu$ m, the enrichment depends linearly on the product of aerodynamic diameter and the square root of the Cunningham slip correction. The regression line for particles in the range of 0.1 to 1.1  $\mu$ m is also shown. The enrichment in concentration achieved by the series of the two virtual impactors can be expressed as follows:

Concentration Enrichment = 
$$-0.20 + 9.74 d_a C_c^{1/2} = -0.20 + 9.74 d_p (\rho_p C_c)^{1/2}$$
 (2)

where  $d_a$  is the particle aerodynamic diameter. A high correlation for equation (2) was obtained ( $r^2$ =0.97). The intercept of the regression line is not significantly different from zero (p value=0.36), and thus can be neglected.

By combining equations (1) and (2), the increase in pressure drop per unit time for

particles in the range of 0.1-1.1 µm can be expressed as follows:

$$\frac{\Delta P}{t} \propto \frac{c_m}{\sqrt{\rho_{pc}}} \quad (3)$$

This relationship was experimentally confirmed and the results are shown in Figure 5. The values of the pressure drop, per unit time and particle concentration ( $\Delta P/(c_m \cdot t)$ ) are plotted as a function of aerodynamic particle diameter, for both polystyrene latex and silica particles. The average increase in pressure drop per unit time and mass concentration for the system with the two round nozzle virtual impactors is equal to 3.23 ( $\pm$  0.1) x 10<sup>-6</sup> dyn/cm<sup>2</sup>/s per  $\mu g/m^3$ . This value is independent of particle aerodynamic diameter for particles in the range of 0.05 to 1.1  $\mu$ m. Figure 6 shows the results of laboratory calibrations of the CAMM using PSL particles ( $\rho_p$  = 1.05 g/cm<sup>3</sup>), silica particles ( $\rho_p$  = 2.2 g/cm<sup>3</sup>), ammonium sulfate ((NH<sub>4</sub>)<sub>2</sub>SO<sub>4</sub>;  $\rho_p$  = 1.8 g/cm<sup>3</sup>), and ammonium bisulfate (NH<sub>4</sub>HSO<sub>4</sub>;  $\rho_p$  = 1.8 g/cm<sup>3</sup>). All CAMM measurements were corrected by the square root of density as described below.

It is important to point out that there is a reduced response for particles greater than 1.1  $\mu$ m as demonstrated by the results shown in Figure 4. The concentration enrichment achieved by the combination of two virtual impactors does not increase linearly with the parameter ( $d_a \cdot C_c^{0.5}$ ) for particles larger than about 1.1  $\mu$ m. Therefore, the dependence of ( $\Delta P/(c_m \cdot t)$ ) on the inverse of particle aerodynamic diameter is not negated by the concentration enrichment of particles in that size range. From a practical standpoint, this will have a negligible effect since the majority of  $PM_{2.5}$  mass is associated with particles in the range 0.1 to 1.1  $\mu$ m, with typically less than 5% of

the mass contribution from particles in the range 1.0 to 2.5  $\mu$ m (Whitby and Svendrup, 1980). In areas where the coarse to fine mass ratio is high, the CAMM may underestimate the PM<sub>2.5</sub> mass due to the contribution of particles in the range from 1.0 to 2.5  $\mu$ m from the coarse fraction. In these areas the CAMM may not be the most suitable method to measure PM<sub>2.5</sub>.

The results shown in Figure 5 and 6 also suggest that the increase in pressure drop per unit time and concentration ( $\Delta P/(c_m \cdot t)$ ) is inversely proportional to the square root of density (equation 3). Therefore, it is necessary to estimate the average particle density in order to determine particle concentration for the field studies. The non-aqueous components of ambient fine particles consist primarily of ammonium sulfate ( $\rho_p=1.8~g/cm^3$ ), ammonium nitrate ( $\rho_p=1.7~g/cm^3$ ), elemental carbon ( $\rho_p=2~g/cm^3$ ) and organic compounds ( $\rho_p=0.9-1.5~g/cm^3$ ). The ratio of organic to elemental carbon typically ranges from 1.8-2.5 (Allen et al., 1998) thus the density of the composite carbon mixture will be in the range 1.3-1.9  $g/cm^3$ . Hence the density of a dry PM<sub>2.5</sub> aerosol should be in the range 1.4-2.0  $g/cm^3$ . A density of 1.7  $g/cm^3$  was used as the estimated average density to correct the CAMM data in this study. Stein et. al. (1994) found a similar average density that varied between 1.60 and 1.79  $g/cm^3$ . Given the expected density range (1.4-2.0  $g/cm^3$ ) and the square root of density dependency, assuming an average particle density of 1.7  $g/cm^3$  introduces a mass concentration uncertainty of less than  $\pm$  10%.

# Field Study Results

Based on 211 valid daily samples collected in seven U.S. cities, the correlation between the gravimetric method and the CAMM method was high ( $r^2 = 0.90$ ). The average CAMM concentration was 18.9  $\mu$ g/m<sup>3</sup> and the average HI concentration was 17.7  $\mu$ g/m<sup>3</sup> with a CAMM to HI mean ratio of 1.07 ( $\pm$  0.18). Table 2 provides a summary of the data for the seven cities

where sampling was conducted. Figure 7 is a plot of the combined data set for the seven cities of the particle mass concentration determined by the gravimetric analysis (Harvard Impactor) and the CAMM method. These values are density-corrected, assuming a particle density of 1.7 g/cm<sup>3</sup> for all sites.

The data shown in Table 2 do not indicate any significant dependence of the CAMM-to-HI concentration ratio on the sampling location. Furthermore, not knowing the true particle density in each location makes it difficult to conclude whether the somewhat higher CAMM readings (by 2-11%) are due to loss of volatile compounds from the HI particle filter or to uncertainties related to the assumed density value of 1.7 g/cm<sup>3</sup>. Finally, high correlations were obtained for all sampling sites individually, with r<sup>2</sup> values ranging from 0.84 to 0.97.

CAMM precision tests conducted in Philadelphia resulted in 14 valid sample days and 296 valid sample hours. The coefficient of variation (CV) for the 24-hour CAMM measurements was 15.9% for a mean concentration of 22.3  $\mu$ g/m³. The two instruments showed good agreement (slope = 0.95) and were highly correlated ( $r^2 = 0.89$ ) for 24-hour measurements. Comparison of one-hour CAMM data resulted in an  $r^2$  of 0.75, a slope of 0.97, and a CV of 28.1%. Harvard Impactor precision tests across all cities showed good precision with a CV of 4.6% (222 sample days,  $r^2 = 0.99$ , slope = 1.006). The high CV observed for the CAMM precision can partly be explained by the sealing mechanism of the Fluoropore filter. The inconsistent sealing resulted in leaks of the system which led to a variable baseline. Much work is currently being done on the design of the CAMM in order to better seal the filter material and thereby reduce some of the instability of the hourly CAMM measurements.

In an effort to examine whether the differences of the mass measurements between the HI and CAMM are due to losses of the semivolatiles, we investigated the relationship between the

observed differences and the total nitrate, nitrate lost and total organic carbon. No relationships were found for the individual sites or for all sites combined. A possible explanation is that the precision of the CAMM hourly measurements was not sufficient enough to investigate whether a relationship existed between the differences in the mass concentrations and the semivolatile components. By improving the sealing mechanism we hope to address this issue in the future.

A comparison of one-hour averages for the CAMM and the Tapered Element Oscillating MicroBalance (TEOM®; Rupprecht and Patashnick) was done during an indoor study in Swampscott, MA in November of 1998. The two methods were highly correlated ( $r^2 = 0.90$ ) for 124 valid sample hours. The regression equation for the two methods is: TEOM ( $\mu g/m^3$ ) = CAMM\*0.90 - 1.83. The CAMM concentrations were corrected using an estimated average density of 1.7 g/cm³. Figure 8 shows the relationship between the one-hour PM<sub>2.5</sub> concentrations for the CAMM and TEOM.

# **CONCLUSIONS**

A novel monitoring technique has been developed that makes it possible to continuously measure fine particle mass. Features of this continuous monitor include: a) measurement of particle mass at ambient temperature; b) use of a filter tape transport system that makes it possible to expose a new segment of the filter membrane for sampling periods of 60 minutes or less to minimize adsorption/desorption phenomena; c) use of a Nafion<sup>TM</sup> diffusion dryer system that reduces relative humidity to 40% or below to remove particle-bound water; e) use of a single pumping unit for all sampling channels and; g) unattended operation because of its filter transport system. The response is independent of particle size, however, it does depend on the square root of the particle density and this can introduce uncertainties on the order of 10% for

typical atmospheric measurements. Reducing the relative humidity to below 40% with the Nafion<sup>TM</sup> diffusion dryer may cause an increase of the nitrate lost through volatilization of ammonium nitrate. However, the 1-hour sampling duration, sampling at ambient temperatures and the small pressure drop across the filter are all characteristics to overall minimize losses of semi-volatile species.

A series of field studies, conducted in seven U.S. cities with different PM<sub>2.5</sub> chemical compositions indicated excellent overall agreement between the CAMM and the Harvard Impactor. Based on 211 valid daily samples, the correlation between the 24-hour average Harvard Impactor and the CAMM concentrations was high ( $r^2 = 0.90$ ). The average CAMM-to-HI concentration ratio was 1.07 (± 0.18). Both Boston and Philadelphia showed high correlations (r<sup>2</sup> of 0.97 and 0.94 respectively; Table 2). This is expected given the stable nature of the Northeast aerosol which, particularly in the summertime, is dominated by sulfates. Conversely, Riverside, the only site in which a significant fraction of nitrate loss was observed, showed the lowest correlation (0.84), which may be a result of a less stable aerosol with high concentrations of ammonium nitrate. In Riverside, approximately 40% of the nitrate (10% of total mass) was lost off the Harvard Impactor (or the FRM) sample as compared with the total particulate nitrate as measured by the HEADS. However, as discussed earlier, the lack of an observable relationship between the differences of the mass measured by the CAMM and HI for each sample day and the measured nitrate and organic carbon, may again, be attributed to the insufficient seal of the Fluoropore filter. Future laboratory and field studies, using a reengineered instrument that sufficiently seals the filter material, will focus on assessing and quantifying the ability of the CAMM to measure semi-volatile compounds with minimal losses.

In conclusion, the laboratory and field studies have demonstrated that the CAMM is a

suitable and cost-effective method for semi-continuous particulate mass measurements. Currently, our research efforts related to this technology include the development of other monitors that can be used to measure particle size, particle density, and microenvironmental and personal PM exposures.

# Acknowledgments

The field testing of the Continuous Ambient Mass Monitor was supported by EPRI under contract #96-0000-1326. A special thanks to the project manager, Dr. Pradeep Saxena, for his contributions to the project. The authors would like to thank Mark Davey of Thermo Environmental Instruments, Inc. for his participation in the field study. Also, we would like to thank Chris Long for the indoor PM<sub>2.5</sub> data for the CAMM and TEOM. The laboratory testing of the CAMM was supported by the Center of Indoor Air Research (CIAR) under contract #96-08A and the U.S. Environmental Protection Agency research grant #822816-01.

#### REFERENCES

Allen, G., Lawrence J., and Koutrakis, P., (1998). Field validation of a semi-continuous method for aerosol black carbon (Aethalometer) and temporal patterns of summertime hourly black carbon measurements in southwestern PA. *Atmos. Environ.* (In Press).

Appel B.R., Tokiwa Y., Haik M. and Kothny E.L., (1984). Artifact particulate sulfate, and nitrate formation on filter media. *Atmos. Environ.* 18: 409.

Bergman, W., Taylor, R.D., Miller, H.H., Biermann, A.H., Hebard, H.D., daRoza, R.A. and Lum, B.Y. (1979). Enhanced filtration program at LLL-A progress report, 15<sup>th</sup> *DOE Nuclear Air Cleaning Conference*, 1058-1081.

Chow, J.C., Watson, J.G., Pritchett, L.C., Pierson, W.R., Frazier, C.A. and Purcell, R.G. (1993). The DRI thermal/optical reflectance carbon analysis system: description, evaluation and applications in U.S. air quality studies, *Atmos. Environ.*, 27A:1185-1201.

Dockery D. W., Pope C. A. III, Xu X., Spengler J. D., Ware J. H., Fay M. E., Ferris B. G., and Speizer F. E. (1993). An association between air pollution and mortality in six U. S. Cities, *New Engl. J Med.* 329:1753-1759.

Federal Register, National Ambient Air Quality Standards for Particulate Matter. 40 CFR Part 50.7 Section 8.2, Vol. 62, No.138, July 18, 1997.

Gupta, A., Novick, V.J., Biswas, P. and Monson, P.R. (1993). Effect of humidity and particle hygroscopicity on the mass loading capacity of high efficiency particulate air (HEPA) filters, *Aerosol Sci. and Technol.* 19:94-107

Ito K. and Thurston G. D. (1996). Daily PM<sub>10</sub>/mortality associations: an investigation of at-risk sub-populations, *J. Expos. Anal. and Environ. Epidemiol.* 6:79-95.

Hinds W.C. and Kadrichu, N.P. (1997). The effect of dust loading on penetration and resistance of glass fiber filters. *Aerosol Sci. and Technol.*, 27:162-173

Japuntich, D.A., Stenhouse, J.I.T., and Liu, B.Y.H. (1994). Experimental results of solid monodisperse particle clogging of fibrous filters, *J. Aerosol Sci.* 25:385-393.

Keith, L.H., Crummett, W., Deegan, J., Libby, R.A., Taylor, J.K., and Wentler G. (1983). Principles of environmental analysis, *Anal. Chem.*, 55:2210-2218.

Koutrakis, P., Wang, P.Y., Sioutas, C., and Wolfson, J.M. (1996). Methods and apparatus to measure particulate mass in gas, U.S. Patent 5,571,945.

Koutrakis, P., Wolfson, J.M., Slater, J.L., Brauer, M., and Spengler, J.D., and Stevens, R.K. (1988). Evaluation of an annular denuder/filter pack system to collect acidic aerosols and gases. *Environ. Sci. and Technol.*, 22:1463-1468.

Marple, V., Rubow, K.L., Turner, W. and Spengler, J. (1987). Low flow rate sharp cut impactors for indoor air sampling: design and calibration, *J. Air Pollut. Control Assoc.* 37:1303-1307.

Novick, V.J., Monson, P.R., and Ellison, P.E. (1992). The effect of solid particle mass loading on the pressure drop of HEPA filters, *J. Aerosol Sci.*, 23:657-665.

Pataschnick, H. and Rupprecht, E.G. (1991). Continuous PM-10 measurements using the tapered element microbalance, *J. Air Waste Manage*. *Assoc*. 41:1079-1083.

Smith, T.N. and Phillips, C.R. (1975). Environ. Sci. Technol. 9:564-568.

Sioutas, C., Koutrakis, P., Wang, P.Y, Babich, P.C., and Wolfson, J.M. (1998). Experimental investigation of pressure drop with particle loading in Nuclepore filters. *Aerosol Sci. Technol.*, in press.

Stein, S.W., Turpin, B.J., Cai, X.P., Huang, C.P.F., and McMurry, P.H. (1994). Measurements of relative humidity-dependent bounce and density for atmospheric particles using the DMA-impactor technique, *Atmos. Environ.*, 28:1739-1746.

Thomas, K.W., Pellizzari, E.D., Clayton, C.A., Whitaker, D.A., Shores, R.C., Spengler, J.D., Ozkaynak, H., Froelich, S.E., and Wallace, L.A. (1993). Particle Total Exposure Assessment Methodology (PTEAM) 1990 Study: Method Performance and Data Quality for Personal, Indoor,

and Outdoor Monitoring, J. Expos. Anal. and Environ. Epidemiol., 3:203-226.

U. S. Environmental Protection Agency (1996). Review of the national ambient air quality standards for particulate matter: policy assessment of scientific and technical information. OAQPS Staff Paper.

Wang, P.Y. (1997). Continuous Aerosol Mass Measurement by Flow Obstruction. S.D. Thesis, Harvard University, School of Public Health, Boston, MA.

Whitby, K.T., and Svendrup, G.M. (1980). California aerosols: their physical and chemical characteristics, *Environ. Sci. Technol.* 10:477.

TABLE 1. Sampling locations and schedule.

Sampling Location	Sampling schedule
Riverside, CA	15 August 1997 - 20 September 1997
Boston, MA	10 September 1997 - 30 September 1997
Chicago, IL	10 October 1997 – 15 November 1997
Dallas, TX	5 December 1997 - 20 January 1998
Phoenix, AZ	10 December 1997 – 25 January 1998
Bakersfield ,CA	10 February 1998 – 25 March 1998
Philadelphia, PA	1 August 1998 – 1 September 1998

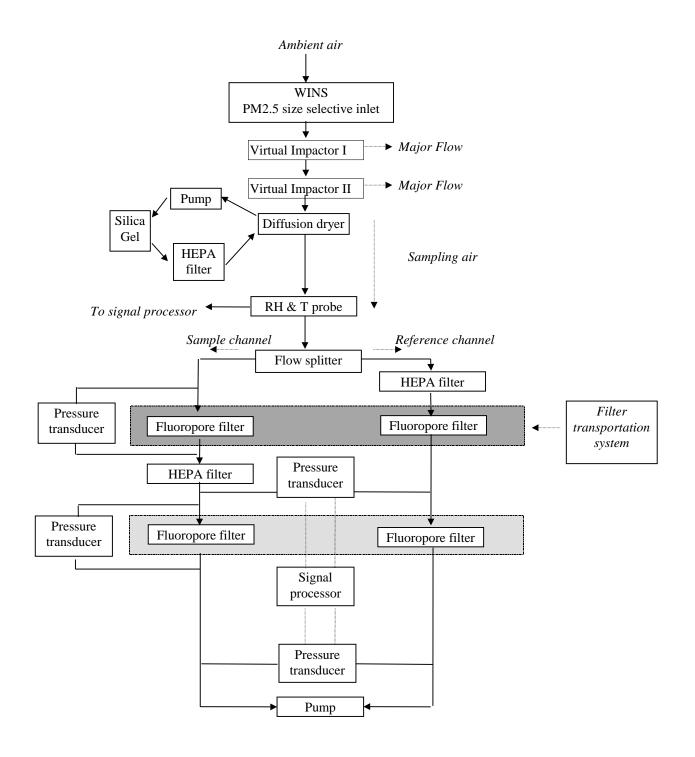
TABLE 2: Results of CAMM and Harvard Impactor measurements from seven cities

		Average					
		Harvard	Average				
		Impactor	CAMM	CAMM	Valid		
Site	Season	Concentration	Concentration	/HI	Sampling	Correlation	Slope
		$(\mu g/m^3)$	$(\mu g/m^3)$	Ratio	Days	$(\mathbf{r}^2)$	
Bakersfield	Spring	18.4	20.6	1.12	46	0.95	1.09
Boston	Summer	15.2	17.1	1.12	18	0.97	1.16
Chicago	Fall	16.8	17.8	1.06	31	0.90	1.06
Dallas	Winter	11.7	12.1	1.04	34	0.90	1.03
Philadelphia	Summer	21.1	21.8	1.04	18	0.94	0.95
Phoenix	Winter	22.5	23.1	1.02	32	0.86	0.98
Riverside	Summer	18.4	20.3	1.11	32	0.84	1.08
Combined		17.7	18.9	1.07	211	0.90	1.05

TABLE 3: Average concentrations of chemical components in seven cities. Sulfate and nitrate concentrations are determined from the HEADS. Organic carbon (OC) and elemental carbon (EC) concentrations are determined using the thermal/optical reflectance (TOR) method from particles collected on a quartz filter. The OC measurements were multiplied by the hydrocarbon conversion factor (1.4).

	Valid Sampling	Sulfate (SO <sub>4</sub> <sup>+2</sup> )	Nitrate (NO <sub>3</sub> <sup>-</sup> )	Organic carbon (OCx1.4)	Elemental carbon (EC)
Site	Days	$(\mu g/m^3)$	$(\mu g/m^3)$	$(\mu g/m^3)$	$(\mu g/m^3)$
Bakersfield	46	1.0	5.6	6.8	1.5
Boston	18	4.6	0.4	6.4	1.2
Chicago	31	3.0	3.2	5.2	1.4
Dallas	34	1.8	2.1	5.4	1.3
Philadelphia	18	7.7	0.6	6.0	1.5
Phoenix	32	0.7	3.9	10.6	3.7
Riverside	32	2.8	4.4	9.1	1.9

FIGURE 1: Schematic of the Continuous Ambient Mass Monitor (CAMM)



 $\label{thm:continuous} \textbf{FIGURE 2: Schematic of the experimental set-up for the laboratory characterization of the CAMM }$ 

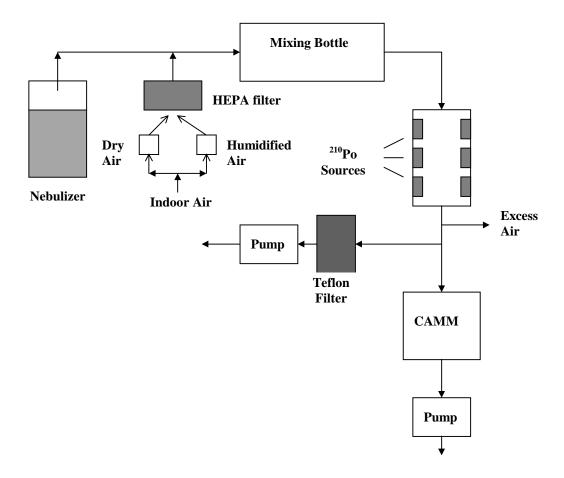
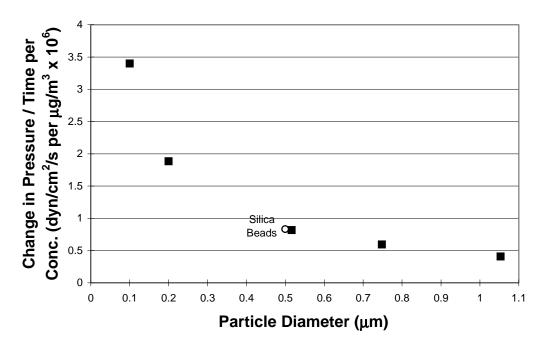


FIGURE 3: Increase in pressure drop per unit time and mass concentration vs. aerodynamic particle diameter for CAMM without virtual impactors. The silica beads have been corrected for density.



<sup>\*</sup>All points represent PSL particles except the one labeled Silica Beads

FIGURE 4: Concentration enrichment as a function of particle aerodynamic diameter for the 1.0 $\mu$ m 50% cutpoint virtual impactor (1st virtual impactor), the 0.40 $\mu$ m 50% cutpoint virtual impactor (2nd virtual impactor) and the two virtual impactors in series

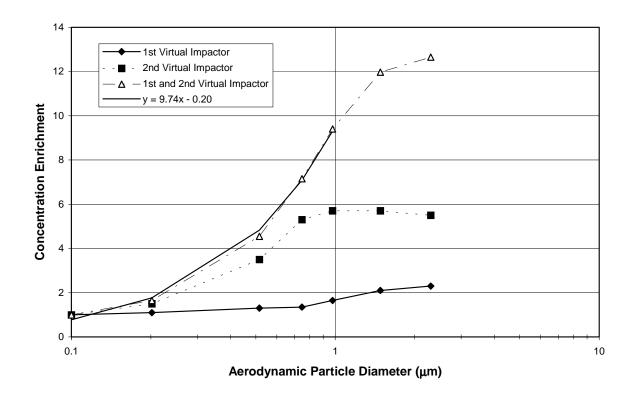


FIGURE 5: Increase in pressure drop per unit time and mass concentration vs. particle aerodynamic diameter for CAMM with two round nozzle virtual impactors. The silica beads have been corrected for density.

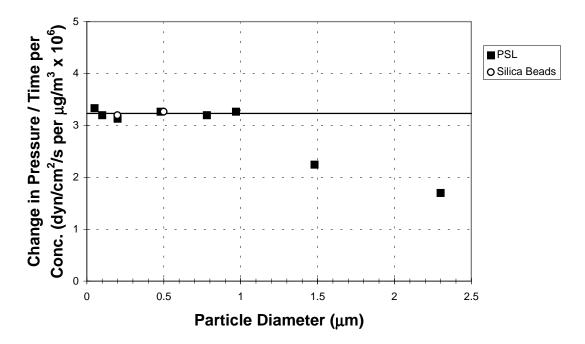


FIGURE 6: CAMM laboratory calibrations using Teflon filter as mass reference. All CAMM concentrations have been corrected for density.

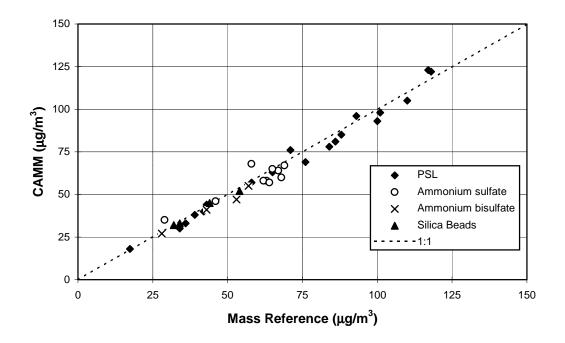


FIGURE 7: CAMM vs Harvard Impactor 24-hour average PM<sub>2.5</sub> concentrations for seven cities (Riverside, Chicago, Boston, Phoenix, Dallas, Bakersfield and Philadelphia)

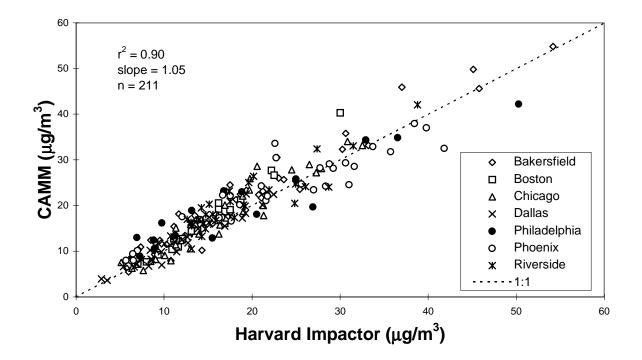
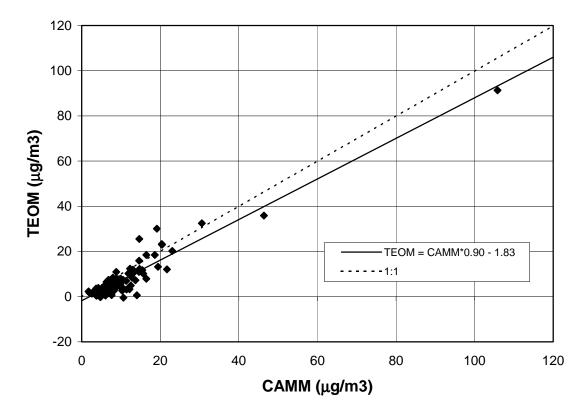


FIGURE 8: The relationship between 124 one-hour indoor  $PM_{2.5}$  concentrations for the CAMM and TEOM in Swampscott, MA ( $r^2 = 0.90$ ). The CAMM concentrations have been corrected for density using the estimated average density of 1.7 g/cm<sup>3</sup>.





# Draft Report - Characteristics of PM<sub>2.5</sub>

Sampling Method Intercomparison and Fine Particle Composition at Six Urban Sites

### Characteristics of PM<sub>2.5</sub>

Sampling Method Intercomparison and Fine Particle Composition at Six Urban Sites

Final Report, Draft: September 9, 1999

Prepared by Michael Van Loy, Pradeep Saxena<sup>1</sup>, Mary Ann Allan EPRI 3412 Hillview Avenue Palo Alto, California 94304-1395

With Assistance from Peter Babich, Petros Koutrakis, George Allen, Harvard School of Public Health Yanbo Pang and Delbert Eatough, Brigham Young University Susanne Hering, Aerosol Dynamics Inc. John Molenar, Air Resource Specialists, Inc.

Prepared for EPRI Southern California Edison California Energy Commission

EPRI Project Managers Mary Ann Allan Pradeep Saxena<sup>1</sup>

<sup>&</sup>lt;sup>1</sup> Current address: Sun Microsystems, 901 San Antonio Road, MIL 03-06 Palo Alto, CA 94303

### **ACKNOWLEDGEMENTS**

This research study has been sponsored by several organizations, all under the technical management of EPRI. The field measurements, sample analyses and quality assurance audits were supported under EPRI agreement WO9152. The majority of the data analyses and comparative interpretation, including this report, were supported under EPRI agreement WO9185, sponsored by Southern California Edison Company, California Energy Commission, and EPRI.

We would like to thank the many people who attended to the measurement details in the laboratories and field sites, including: Mark Davey of Thermo Environmental Instruments, Norman Eatough of California State Polytechnic University, Fida Obeidi and Yiming Ding of Brigham Young University, Mark Stolzenburg and Nathan Kreisberg of Aerosol Dynamics, Inc., Joe Adlhoch of Air Resource Specialists. Special thanks to Fred Rogers and Jim Bowen of Desert Research Institute for conducting external field and laboratory audits. And to the many organizations and individuals across the country who cut through red tape and made room for us to operate our samplers at their facilities, we could not have done it without you:

California Air Resources Board, Bakersfield Illinois Institute of Technology, Chicago Fire Station #25, Dallas Air Monitoring Services Laboratory, Philadelphia Baxter Water Treatment Plant, Philadelphia Arizona Department of Environmental Protection, Phoenix University of California, Riverside

### **EXECUTIVE SUMMARY**

We describe the results of a six-city (Riverside, Chicago, Dallas, Phoenix, Bakersfield, and Philadelphia) study of inorganic and organic constituents of PM<sub>2.5</sub> (particles with aerodynamic diameters smaller than 2.5 µm). Data from a variety of samplers operated by the Harvard School of Public Health (HSPH), Brigham Young University (BYU), Aerosol Dynamics Inc. (ADI), and Air Resource Specialists Inc. (ARS) are analyzed to characterize the effectiveness of a variety of established and novel sampling techniques for PM<sub>2.5</sub> mass and chemical speciation based on quartz, Teflon, nylon, and/or carbon-impregnated filter collection of discrete aerosol samples. Some samplers employed denuders to remove gas-phase compounds such as nitric acid, sulfur dioxide, and volatile organic compounds which might be expected to confound accurate quantification of particle phase chemical speciation. In addition, several in situ samplers including the ADI nitrate analyzer, the HSPH Continuous Aerosol Mass Monitor (CAMM), a black carbon aethalometer, and a nephelometer were used and their results compared with those from the discrete samplers. Data from the samplers provide snapshot, approximately 1-month characterizations of 24-h and study average PM<sub>2.5</sub> composition at the six urban locations. Additionally, we used the results of field tests of carbon denuder efficiency at Bakersfield and comparisons of different carbon sampler configurations at Riverside, Chicago, Dallas, Phoenix, and Bakersfield to characterize the impacts of sampling assumptions typically made by different investigators to estimate PM<sub>2.5</sub> carbon concentrations.

PM<sub>2.5</sub> mass measurements on the Federal Reference Method (FRM)-equivalent Harvard Impactor (HI) agreed within approximately 15% with PM<sub>2.5</sub> mass estimates based on reconstructions from discrete chemical component samplers on study averages. At Riverside and Dallas, most reconstructed mass estimates exceeded the HI mass measured, but at the other sites, the reconstructed masses were smaller than that measured on HI. We hypothesize that the unidentified mass may be attributable to particle-phase water. Despite the relatively close agreement between the FRM equivalent sampler and the mass reconstructions on a study average basis, larger discrepancies were

apparent on 24-hour averages. Increasing sampling temperature tends to increase losses of volatile components from HI samples while increasing RH increases the fraction of HI-collected mass that is unaccounted for in chemical speciation analyses.

# **TABLE OF CONTENTS**

Acknowledgements	i
Executive Summary	ii
Table of Contents	iv
List of Tables and Figures	vi
Introduction	1
Background	1
PM <sub>2.5</sub> Sampling Issues	1
Study Objectives	4
Experimental	6
Sampling Locations and General Conditions	
Discrete (Filter-Based) PM <sub>2.5</sub> Samplers	
Mass	
Inorganic Ions (Sulfate, Nitrate, Ammonium)	
Carbon	
Continuous (In Situ) PM <sub>2.5</sub> Samplers	
Nitrate	
Black Carbon	
Inorganic Gas Measurements	
Meteorology and Light Scattering	
Data Analysis Methodology	15
Sampler Intercomparison	
Guide to Analyses	
Carbon Field Denuder Tests.	
Carbon Sampling	
Results	22
Sampler Intercomparisons	
Sulfate	
Nitrate	
HEADS Ion Balances	
HSPH Carbon Denuder Field Tests at Bakersfield	
Carbon	
Inorganic Gases	
Continuous Sampler Tests.	
PM2.5 Mass	
Nitrate	
Carbon	
Light Scattering	
Continuous PM <sub>2.5</sub> Sampler Correlations	
PM <sub>2.5</sub> Speciation	
L 171 / 5 A D D A //(III V /II	

Conclusions	35
References	38
Appendix: Deming Regression	42
Tables	44
Figures	61

# LIST OF TABLES AND FIGURES

Table 1	Summary of sampling dates and sampling locations for the 6 study	
	sites.	44
Table 2	Summary of discrete particle-phase sulfate samplers.	45
Table 3	Summary of discrete particle-phase nitrate samplers.	46
Table 4	Summary of discrete particle-phase ammonium samplers	47
Table 5	Summary of particle-phase carbon samplers.	48
Table 6	Summary of temperature data for all study sites except Philadelphia.	49
Table 7	Summary of relative humidity data for all study sites except Philadelphia.	49
Table 8	PM <sub>2.5</sub> sulfate concentration statistics for the six study sites.	50
Table 9	PM <sub>2.5</sub> nitrate concentration statistics for the six study sites	52
Table 10	PM <sub>2.5</sub> ammonium concentration statistics for the six study sites.	53
Table 11	PM <sub>2.5</sub> elemental carbon concentration statistics for the six study sites.	54
Table 12	Organic carbon concentration statistics for the six study sites.	55
Table 13	Gas-phase nitric acid concentration statistics for the six study sites.	56
Table 14	Gas-phase sulfur dioxide concentration statistics for the six study sites.	57
Table 15	Gas-phase ammonia concentration statistics for the six study sites.	58
Table 16	PM <sub>2.5</sub> mass concentration statistics for the six study sites.	59
Figure 1	Harvard – EPA Annular Denuder Sampler (HEADS) schematic.	61
Figure 2	BYU Annular Denuder and ChemSpec Sampler schematics.	62
Figure 3	High Volume BYU Organic Sampler System (BIG BOSS) schematic.	63
Figure 4	Particle Concentrator BYU Organic Sampler System (PC-BOSS) schematic.	64
Figure 5	Schematic of HSPH Carbon Samplers.	65
Figure 6	Schematic of the Continuous Ambient Mass Monitor (CAMM)	66
Figure 7	Schematic of the Aerosol Dynamics Inc. Continuous Nitrate Monitor (ACNM)	67
Figure 8	Schematic diagrams of commonly used PM <sub>2.5</sub> carbon samplers.	68

Figure 9A	Sulfate: Full HEADS F1 vs. Nylon HEADS F1 (Teflon) filter at all sites.	69
Figure 9R	Sulfate: Full HEADS F1 vs. Nylon HEADS F1 (Teflon) filter at Riverside.	70
Figure 9C	Sulfate: Full HEADS F1 vs. Nylon HEADS F1 (Teflon) filter at Chicago.	71
Figure 9D	Sulfate: Full HEADS F1 vs. Nylon HEADS F1 (Teflon) filter at Dallas.	72
Figure 9P	Sulfate: Full HEADS F1 vs. Nylon HEADS F1 (Teflon) filter at Phoenix.	73
Figure 9B	Sulfate: Full HEADS F1 vs. Nylon HEADS F1 (Teflon) filter at Bakersfield.	74
Figure 10A	Sulfate: Harvard Impactor vs. Full HEADS F1 (Teflon) filter at all sites.	75
Figure 10R	Sulfate: Harvard Impactor vs. Full HEADS F1 (Teflon) filter at Riverside.	76
Figure 10C	Sulfate: Harvard Impactor vs. Full HEADS F1 (Teflon) filter at Chicago.	77
Figure 10D	Sulfate: Harvard Impactor vs. Full HEADS F1 (Teflon) filter at Dallas.	78
Figure 10P	Sulfate: Harvard Impactor vs. Full HEADS F1 (Teflon) filter at Phoenix.	79
Figure 10B	Sulfate: Harvard Impactor vs. Full HEADS F1 (Teflon) filter at Bakersfield.	80
Figure 11A	Sulfate: Harvard Impactor vs. Nylon HEADS F1 (Teflon) filter at all sites.	81
Figure 11R	Sulfate: Harvard Impactor vs. Nylon HEADS F1 (Teflon) filter at Riverside.	82
Figure 11C	Sulfate: Harvard Impactor vs. Nylon HEADS F1 (Teflon) filter at Chicago.	83
Figure 11D	Sulfate: Harvard Impactor vs. Nylon HEADS F1 (Teflon) filter at Dallas.	84
Figure 11P	Sulfate: Harvard Impactor vs. Nylon HEADS F1 (Teflon) filter at Phoenix.	85
Figure 11B	Sulfate: Harvard Impactor vs. Nylon HEADS F1 (Teflon) filter at Bakersfield.	86

Figure 11F	Philadelphia.	87
Figure 12A	Sulfate: Collocated Annular Denuder Sampler Teflon filters at all sites.	88
E' 10D		88
Figure 12R	Sulfate: Collocated Annular Denuder Sampler Teflon filters at Riverside.	89
Figure 12B	Sulfate: Collocated Annular Denuder Sampler Teflon filters at Bakersfield.	90
Figure 13A	Sulfate: Collocated ChemSpec Sampler Teflon filters at all sites.	91
Figure 13R	Sulfate: Collocated ChemSpec Sampler Teflon filters at Riverside.	92
Figure 13B	Sulfate: Collocated ChemSpec Sampler Teflon filters at Bakersfield.	93
Figure 14A	Sulfate: Collocated Big BOSS quartz filters at all sites.	94
Figure 14R	Sulfate: Collocated Big BOSS quartz filters at Riverside.	95
Figure 14B	Sulfate: Collocated Big BOSS quartz filters at Bakersfield.	96
Figure 15A	Sulfate: Collocated PC-BOSS minor flow quartz filters at all sites.	97
Figure 15R	Sulfate: Collocated PC-BOSS minor flow quartz filters at Riverside.	98
Figure 15B	Sulfate: Collocated PC-BOSS minor flow quartz filters at	
	Bakersfield.	99
Figure 16A	Sulfate: Collocated PC-BOSS minor flow Teflon filters at all sites.	100
Figure 16R	Sulfate: Collocated PC-BOSS minor flow Teflon filters at Riverside.	101
Figure 16B	Sulfate: Collocated PC-BOSS minor flow Teflon filters at Bakersfield.	102
Figure 17A	Sulfate: Collocated PC-BOSS major flow quartz filters at all sites.	103
Figure 17R	Sulfate: Collocated PC-BOSS major flow quartz filters at Riverside.	104
Figure 17B	Sulfate: Collocated PC-BOSS major flow quartz filters at	
9	Bakersfield.	105
Figure 18A	Sulfate: Annular Denuder Sampler vs. ChemSpec sampler Teflon filters at all sites.	106
Figure 18R	Sulfate: Annular Denuder Sampler vs. ChemSpec sampler Teflon filters at Riverside.	107
Figure 18B	Sulfate: Annular Denuder Sampler vs. ChemSpec sampler Teflon filters at Bakersfield.	108
Figure 19A	Sulfate: Annular Denuder Sampler Teflon filter vs. Big BOSS quartz filter at all sites.	109

Figure 19R	Sulfate: Annular Denuder Sampler Teflon filter vs. Big BOSS quartz filter at Riverside.	110
Figure 19B	Sulfate: Annular Denuder Sampler Teflon filter vs. Big BOSS quartz filter at Bakersfield.	111
Figure 20A	Sulfate: Annular Denuder Sampler Teflon filter vs. PC-BOSS A and B minor + major quartz filters at all sites.	112
Figure 20R	Sulfate: Annular Denuder Sampler Teflon filter vs. PC-BOSS A and B minor + major quartz filters at Riverside.	113
Figure 20B	Sulfate: Annular Denuder Sampler Teflon filter vs. PC-BOSS A and B minor + major quartz filters at Bakersfield.	114
Figure 21A	Sulfate: Annular Denuder Sampler Teflon filter vs. PC-BOSS A and B minor Teflon + major quartz filters at all sites.	115
Figure 21R	Sulfate: Annular Denuder Sampler Teflon filter vs. PC-BOSS A and B minor Teflon + major quartz filters at Riverside.	116
Figure 21B	Sulfate: Annular Denuder Sampler Teflon filter vs. PC-BOSS A and B minor Teflon + major quartz filters at Bakersfield.	117
Figure 22A	Sulfate: ChemSpec Sampler Teflon filter vs. Big BOSS quartz filter at all sites.	118
Figure 22R	Sulfate: ChemSpec Sampler Teflon filter vs. Big BOSS quartz filter at Riverside.	119
Figure 22B	Sulfate: ChemSpec Sampler Teflon filter vs. Big BOSS quartz filter at Bakersfield.	120
Figure 23A	Sulfate: ChemSpec Sampler Teflon filter vs. PC-BOSS A and B minor + major quartz filters at all sites.	121
Figure 23R	Sulfate: ChemSpec Sampler Teflon filter vs. PC-BOSS A and B minor + major quartz filters at Riverside.	122
Figure 23B	Sulfate: ChemSpec Sampler Teflon filter vs. PC-BOSS A and B minor + major quartz filters at Bakersfield.	123
Figure 24A	Sulfate: ChemSpec Sampler Teflon filter vs. PC-BOSS A and B minor Teflon + major quartz filters at all sites.	124
Figure 24R	Sulfate: ChemSpec Sampler Teflon filter vs. PC-BOSS A and B minor Teflon + major quartz filters at Riverside.	125
Figure 24B	Sulfate: ChemSpec Sampler Teflon filter vs. PC-BOSS A and B minor Teflon + major quartz filters at Bakersfield.	126
Figure 25A	Sulfate: Big BOSS quartz filter vs. PC-BOSS A and B minor + major quartz filters at all sites.	127

Figure 25R	Sulfate: Big BOSS quartz filter vs. PC-BOSS A and B minor + major quartz filters at Riverside.	128
Figure 25B	Sulfate: Big BOSS quartz filter vs. PC-BOSS A and B minor + major quartz filters at Bakersfield.	129
Figure 26A	Sulfate: Big BOSS quartz filter vs. PC-BOSS A and B minor Teflon + major quartz filters at all sites.	130
Figure 26R	Sulfate: Big BOSS quartz filter vs. PC-BOSS A and B minor Teflon + major quartz filters at Riverside.	131
Figure 26B	Sulfate: Big BOSS quartz filter vs. PC-BOSS A and B minor Teflon + major quartz filters at Bakersfield.	132
Figure 27A	Sulfate: Full and Nylon HEADS F1 (Teflon) filter vs. Annular Denuder Sampler Teflon filter at all sites.	133
Figure 27R	Sulfate: Full and Nylon HEADS F1 (Teflon) filter vs. Annular Denuder Sampler Teflon filter at Riverside.	134
Figure 27B	Sulfate: Full and Nylon HEADS F1 (Teflon) filter vs. Annular Denuder Sampler Teflon filter at Bakersfield.	135
Figure 28A	Sulfate: Full and Nylon HEADS F1 (Teflon) filter vs. ChemSpec Sampler Teflon filter at all sites.	136
Figure 28R	Sulfate: Full and Nylon HEADS F1 (Teflon) filter vs. ChemSpec Sampler Teflon filter at Riverside.	137
Figure 28B	Sulfate: Full and Nylon HEADS F1 (Teflon) filter vs. ChemSpec Sampler Teflon filter at Bakersfield.	138
Figure 29A	Sulfate: Full and Nylon HEADS F1 (Teflon) filter vs. Big BOSS quartz filter at all sites.	139
Figure 29R	Sulfate: Full and Nylon HEADS F1 (Teflon) filter vs. Big BOSS quartz filter at Riverside.	140
Figure 29B	Sulfate: Full and Nylon HEADS F1 (Teflon) filter vs. Big BOSS quartz filter at Bakersfield.	141
Figure 30A	Sulfate: Full and Nylon HEADS F1 (Teflon) filter vs. PC-BOSS minor + major quartz filters at all sites.	142
Figure 30R	Sulfate: Full and Nylon HEADS F1 (Teflon) filter vs. PC-BOSS minor + major quartz filters at Riverside.	143
Figure 30B	Sulfate: Full and Nylon HEADS F1 (Teflon) filter vs. PC-BOSS minor + major quartz filters at Bakersfield.	144
Figure 31A	Sulfate: Full and Nylon HEADS F1 (Teflon) filter vs. PC-BOSS minor Teflon + major quartz filters at all sites.	145

Figure 31R	Sulfate: Full and Nylon HEADS F1 (Teflon) filter vs. PC-BOSS minor Teflon + major quartz filters at Riverside.	146
Figure 31B	Sulfate: Full and Nylon HEADS F1 (Teflon) filter vs. PC-BOSS minor Teflon + major quartz filters at Bakersfield.	147
Figure 32A	Nitrate: Full HEADS F1 + F2 – F3 filters vs. Nylon HEADS F1 + FN filters at all sites.	148
Figure 32R	Nitrate: Full HEADS F1 + F2 – F3 filters vs. Nylon HEADS F1 + FN filters at Riverside.	149
Figure 32C	Nitrate: Full HEADS F1 + F2 – F3 filters vs. Nylon HEADS F1 + FN filters at Chicago.	150
Figure 32D	Nitrate: Full HEADS F1 + F2 – F3 filters vs. Nylon HEADS F1 + FN filters at Dallas.	151
Figure 32P	Nitrate: Full HEADS F1 + F2 – F3 filters vs. Nylon HEADS F1 + FN filters at Phoenix.	152
Figure 32B	Nitrate: Full HEADS F1 + F2 – F3 filters vs. Nylon HEADS F1 + FN filters at Bakersfield.	153
Figure 33A	Nitrate: Full HEADS F1 (Teflon) filter vs. F1 (Teflon) + F2 – F3 (sodium carbonate) filters at all sites.	154
Figure 34A	Nitrate: Nylon HEADS F1 (Teflon) filter vs. F1 (Teflon) + FN (nylon) filters at all sites.	155
Figure 35A	Nitrate: Harvard Impactor vs. Full HEADS F1 $+$ F2 $-$ F3 filters at all sites.	156
Figure 35R	Nitrate: Harvard Impactor vs. Full HEADS F1 $+$ F2 $-$ F3 filters at Riverside.	157
Figure 35C	Nitrate: Harvard Impactor vs. Full HEADS F1 + F2 – F3 filters at Chicago.	158
Figure 35D	Nitrate: Harvard Impactor vs. Full HEADS F1 + F2 – F3 filters at Dallas.	159
Figure 35P	Nitrate: Harvard Impactor vs. Full HEADS F1 + F2 – F3 filters at Phoenix.	160
Figure 35B	Nitrate: Harvard Impactor vs. Full HEADS F1 + F2 – F3 filters at Bakersfield.	161
Figure 36A	Nitrate: Harvard Impactor vs. Nylon HEADS F1 + FN filters at all sites.	162
Figure 36R	Nitrate: Harvard Impactor vs. Nylon HEADS F1 + FN filters at Riverside.	163

Figure 36C	Nitrate: Harvard Impactor vs. Nylon HEADS F1 + FN filters at Chicago.	164
Figure 36D	Nitrate: Harvard Impactor vs. Nylon HEADS F1 + FN filters at Dallas.	165
Figure 36P	Nitrate: Harvard Impactor vs. Nylon HEADS F1 + FN filters at Phoenix.	166
Figure 36B	Nitrate: Harvard Impactor vs. Nylon HEADS F1 + FN filters at Bakersfield.	167
Figure 36F	Nitrate: Harvard Impactor vs. Nylon HEADS F1 + FN filters at Philadelphia.	168
Figure 37A	Nitrate: Harvard Impactor vs. Full HEADS F1 filter at all sites.	169
Figure 38A	Nitrate: Harvard Impactor vs. Nylon HEADS F1 filter at all sites.	170
Figure 39A	Nitrate: Collocated Annular Denuder Sampler Teflon + nylon filters at all sites.	171
Figure 39R	Nitrate: Collocated Annular Denuder Sampler Teflon + nylon filters at Riverside.	172
Figure 39B	Nitrate: Collocated Annular Denuder Sampler Teflon + nylon filters at Bakersfield.	173
Figure 40A	Nitrate: Annular Denuder Sampler Teflon filter vs. Teflon + nylon filters at all sites.	174
Figure 41A	Nitrate: Collocated ChemSpec Sampler Teflon + nylon filters at all sites.	175
Figure 41R	Nitrate: Collocated ChemSpec Sampler Teflon + nylon filters at Riverside.	176
Figure 41B	Nitrate: Collocated ChemSpec Sampler Teflon + nylon filters at Bakersfield.	177
Figure 42A	Nitrate: ChemSpec Sampler Teflon filter vs. Teflon + nylon filters at all sites.	178
Figure 43A	Nitrate: Collocated PC-BOSS minor flow quartz + Empore + major flow quartz filters at all sites.	179
Figure 43R	Nitrate: Collocated PC-BOSS minor flow quartz + Empore + major flow quartz filters at Riverside.	180
Figure 43B	Nitrate: Collocated PC-BOSS minor flow quartz + Empore + major flow quartz filters at Bakersfield.	181
Figure 44A	Nitrate: Collocated PC-BOSS minor flow Teflon + nylon + major flow quartz filters at all sites.	182

Figure 44K	Nitrate: Collocated PC-BOSS minor flow Teflon + nylon + major flow quartz filters at Riverside.	183
Figure 44B	Nitrate: Collocated PC-BOSS minor flow Teflon + nylon + major flow quartz filters at Bakersfield.	184
Figure 45A	Nitrate: Collocated PC-BOSS major flow quartz filters at all sites.	185
Figure 46A	Nitrate: PC-BOSS minor flow quartz filter vs. minor flow quartz + Empore filters at all sites.	186
Figure 47A	Nitrate: PC-BOSS minor flow Teflon filter vs. minor flow Teflon + nylon filters at all sites.	187
Figure 48A	Nitrate: PC-BOSS minor flow quartz vs. minor flow Teflon filters at all sites.	188
Figure 49A	Nitrate: Annular Denuder Sampler Teflon + nylon filters vs. ChemSpec Sampler Teflon + nylon filters at all sites.	189
Figure 49R	Nitrate: Annular Denuder Sampler Teflon + nylon filters vs. ChemSpec Sampler Teflon + nylon filters at Riverside.	190
Figure 49B	Nitrate: Annular Denuder Sampler Teflon + nylon filters vs. ChemSpec Sampler Teflon + nylon filters at Bakersfield.	191
Figure 50A	Nitrate: Annular Denuder Sampler Teflon + nylon filters vs. PC-BOSS A and B minor flow quartz + Empore + major flow quartz	
	filters at all sites.	192
Figure 50R	Nitrate: Annular Denuder Sampler Teflon + nylon filters vs. PC-BOSS A and B minor flow quartz + Empore + major flow quartz	100
	filters at Riverside.	193
Figure 50B	Nitrate: Annular Denuder Sampler Teflon + nylon filters vs. PC-BOSS A and B minor flow quartz + Empore + major flow quartz filters at Bakersfield.	194
Figure 51A	Nitrate: Annular Denuder Sampler Teflon + nylon filters vs. PC-BOSS A and B minor flow Teflon + nylon + major flow quartz	
E' 51D	filters at all sites.	195
Figure 51R	Nitrate: Annular Denuder Sampler Teflon + nylon filters vs. PC-BOSS A and B minor flow Teflon + nylon + major flow quartz filters at Riverside.	196
Figure 51B	Nitrate: Annular Denuder Sampler Teflon + nylon filters vs. PC-BOSS A and B minor flow Teflon + nylon + major flow quartz	170
	filters at Bakersfield.	197

Figure 52A	Nitrate: ChemSpec Sampler Teflon + nylon filters vs. PC-BOSS A	
	and B minor flow quartz + Empore + major flow quartz filters at all	
	sites.	198
Figure 52R	Nitrate: ChemSpec Sampler Teflon + nylon filters vs. PC-BOSS A	
	and B minor flow quartz + Empore + major flow quartz filters at	
	Riverside.	199
Figure 52B	Nitrate: ChemSpec Sampler Teflon + nylon filters vs. PC-BOSS A	
	and B minor flow quartz + Empore + major flow quartz filters at	
	Bakersfield.	200
Figure 53A	Nitrate: ChemSpec Sampler Teflon + nylon filters vs. PC-BOSS A	
	and B minor flow Teflon + nylon + major flow quartz filters at all	
	sites.	201
Figure 53R	Nitrate: ChemSpec Sampler Teflon + nylon filters vs. PC-BOSS A	
S	and B minor flow Teflon + nylon + major flow quartz filters at	
	Riverside.	202
Figure 53B	Nitrate: ChemSpec Sampler Teflon + nylon filters vs. PC-BOSS A	
O	and B minor flow Teflon + nylon + major flow quartz filters at	
	Bakersfield.	203
Figure 54A	Nitrate: Full HEADS F1 + F2 – F3 and Nylon HEADS F1 + FN	
G	filters vs. Annular Denuder Sampler Teflon + nylon filters at all	
	sites.	204
Figure 54R	Nitrate: Full HEADS F1 + F2 – F3 and Nylon HEADS F1 + FN	
	filters vs. Annular Denuder Sampler Teflon + nylon filters at	
	Riverside.	205
Figure 54B	Nitrate: Full HEADS F1 + F2 – F3 and Nylon HEADS F1 + FN	
	filters vs. Annular Denuder Sampler Teflon + nylon filters at	
	Bakersfield.	206
Figure 55A	Nitrate: Full HEADS F1 + F2 – F3 and Nylon HEADS F1 + FN	
	filters vs. ChemSpec Sampler Teflon + nylon filters at all sites.	207
Figure 55R	Nitrate: Full HEADS F1 + F2 – F3 and Nylon HEADS F1 + FN	
	filters vs. ChemSpec Sampler Teflon + nylon filters at Riverside.	208
Figure 55B	Nitrate: Full HEADS F1 + F2 – F3 and Nylon HEADS F1 + FN	
J	filters vs. ChemSpec Sampler Teflon + nylon filters at Bakersfield.	209
Figure 56A	Nitrate: Full HEADS F1 + F2 – F3 and Nylon HEADS F1 + FN	
J	filters vs. PC-BOSS A minor flow quartz + Empore + major flow	
	quartz filters at all sites.	210

filters vs. PC-BOSS A minor flow quartz + Empore + major frequartz filters at Riverside.  Figure 56B Nitrate: Full HEADS F1 + F2 – F3 and Nylon HEADS F1 + F	low
<b>Figure 56B</b> Nitrate: Full HEADS F1 + F2 – F3 and Nylon HEADS F1 + F	011
•	211
filters vs. PC-BOSS A minor flow quartz + Empore + major f	
quartz filters at Bakersfield.	212
<b>Figure 57A</b> Nitrate: Full HEADS F1 + F2 – F3 and Nylon HEADS F1 + F	
filters vs. PC-BOSS A minor flow Teflon + nylon + major flo	
quartz filters at all sites.	213
<b>Figure 57R</b> Nitrate: Full HEADS F1 + F2 – F3 and Nylon HEADS F1 + F	
filters vs. PC-BOSS A minor flow Teflon + nylon + major flo	
quartz filters at Riverside.	214
<b>Figure 57B</b> Nitrate: Full HEADS F1 + F2 – F3 and Nylon HEADS F1 + F	
filters vs. PC-BOSS A minor flow Teflon + nylon + major flo	
quartz filters at Bakersfield.	215
Figure 58A Ion Balance: Anion vs. cation equivalents for ammonium, acid	
nitrate, and sulfate collected on Full HEADS F1 (Teflon) filte	
sites.	216
Figure 58R Ion Balance: Anion vs. cation equivalents for ammonium, acid	•
nitrate, and sulfate collected on Full HEADS F1 (Teflon) filte Riverside.	
	217
Figure 58C Ion Balance: Anion vs. cation equivalents for ammonium, acid	•
nitrate, and sulfate collected on Full HEADS F1 (Teflon) filte	er at 218
Chicago.	
E' FOD I D-1 A	•
Figure 58D Ion Balance: Anion vs. cation equivalents for ammonium, acid	r ot
nitrate, and sulfate collected on Full HEADS F1 (Teflon) filte	
nitrate, and sulfate collected on Full HEADS F1 (Teflon) filte Dallas.	219
nitrate, and sulfate collected on Full HEADS F1 (Teflon) filte Dallas.  Figure 58P Ion Balance: Anion vs. cation equivalents for ammonium, acid	219 dity,
nitrate, and sulfate collected on Full HEADS F1 (Teflon) filte Dallas.  Figure 58P Ion Balance: Anion vs. cation equivalents for ammonium, acid nitrate, and sulfate collected on Full HEADS F1 (Teflon) filte	219 dity, er at
nitrate, and sulfate collected on Full HEADS F1 (Teflon) filte Dallas.  Figure 58P Ion Balance: Anion vs. cation equivalents for ammonium, acid nitrate, and sulfate collected on Full HEADS F1 (Teflon) filte Phoenix.	219 dity, er at 220
nitrate, and sulfate collected on Full HEADS F1 (Teflon) filte Dallas.  Figure 58P Ion Balance: Anion vs. cation equivalents for ammonium, acid nitrate, and sulfate collected on Full HEADS F1 (Teflon) filte Phoenix.  Figure 58B Ion Balance: Anion vs. cation equivalents for ammonium, acid	219 dity, er at 220 dity,
nitrate, and sulfate collected on Full HEADS F1 (Teflon) filte Dallas.  Figure 58P Ion Balance: Anion vs. cation equivalents for ammonium, acid nitrate, and sulfate collected on Full HEADS F1 (Teflon) filte Phoenix.	219 dity, er at 220 dity,
nitrate, and sulfate collected on Full HEADS F1 (Teflon) filte Dallas.  Figure 58P Ion Balance: Anion vs. cation equivalents for ammonium, acid nitrate, and sulfate collected on Full HEADS F1 (Teflon) filte Phoenix.  Figure 58B Ion Balance: Anion vs. cation equivalents for ammonium, acid nitrate, and sulfate collected on Full HEADS F1 (Teflon) filte Bakersfield.	dity, er at 220 dity, er at 221
nitrate, and sulfate collected on Full HEADS F1 (Teflon) filte Dallas.  Figure 58P Ion Balance: Anion vs. cation equivalents for ammonium, acid nitrate, and sulfate collected on Full HEADS F1 (Teflon) filte Phoenix.  Figure 58B Ion Balance: Anion vs. cation equivalents for ammonium, acid nitrate, and sulfate collected on Full HEADS F1 (Teflon) filte	dity, er at 220 dity, er at 221 dity,

Figure 59R	Ion Balance: Anion vs. cation equivalents for ammonium, acidity, nitrate, and sulfate collected on Nylon HEADS F1 (Teflon) filter at Riverside.	223
Figure 59C	Ion Balance: Anion vs. cation equivalents for ammonium, acidity, nitrate, and sulfate collected on Nylon HEADS F1 (Teflon) filter at Chicago.	224
Figure 59D	Ion Balance: Anion vs. cation equivalents for ammonium, acidity, nitrate, and sulfate collected on Nylon HEADS F1 (Teflon) filter at Dallas.	225
Figure 59P	Ion Balance: Anion vs. cation equivalents for ammonium, acidity, nitrate, and sulfate collected on Nylon HEADS F1 (Teflon) filter at Phoenix.	226
Figure 59B	Ion Balance: Anion vs. cation equivalents for ammonium, acidity, nitrate, and sulfate collected on Nylon HEADS F1 (Teflon) filter at Bakersfield.	227
Figure 60A	Ion Balance: Anion vs. cation equivalents for ammonium, acidity, nitrate, and sulfate collected on Full HEADS F1 (Teflon) + backup filters at all sites.	228
Figure 60R	Ion Balance: Anion vs. cation equivalents for ammonium, acidity, nitrate, and sulfate collected on Full HEADS F1 (Teflon) + backup filters at Riverside.	229
Figure 60C	Ion Balance: Anion vs. cation equivalents for ammonium, acidity, nitrate, and sulfate collected on Full HEADS F1 (Teflon) + backup filters at Chicago.	230
Figure 60D	Ion Balance: Anion vs. cation equivalents for ammonium, acidity, nitrate, and sulfate collected on Full HEADS F1 (Teflon) + backup filters at Dallas.	231
Figure 60P	Ion Balance: Anion vs. cation equivalents for ammonium, acidity, nitrate, and sulfate collected on Full HEADS F1 (Teflon) + backup filters at Phoenix.	232
Figure 60B	Ion Balance: Anion vs. cation equivalents for ammonium, acidity, nitrate, and sulfate collected on Full HEADS F1 (Teflon) + backup filters at Bakersfield.	233
Figure 61A	Ion Balance: Anion vs. cation equivalents for ammonium, acidity, nitrate, and sulfate collected on Full HEADS backup filters (F2 – F3 and F4) at all sites.	234

Figure 61R	Ion Balance: Anion vs. cation equivalents for ammonium, acidity, nitrate, and sulfate collected on Full HEADS backup filters (F2 – F3 and F4) at Riverside.	235
Figure 61C	Ion Balance: Anion vs. cation equivalents for ammonium, acidity, nitrate, and sulfate collected on Full HEADS backup filters (F2 – F3 and F4) at Chicago.	236
Figure 61D	Ion Balance: Anion vs. cation equivalents for ammonium, acidity, nitrate, and sulfate collected on Full HEADS backup filters (F2 – F3 and F4) at Dallas.	237
Figure 61P	Ion Balance: Anion vs. cation equivalents for ammonium, acidity, nitrate, and sulfate collected on Full HEADS backup filters (F2 – F3 and F4) at Phoenix.	238
Figure 61B	Ion Balance: Anion vs. cation equivalents for ammonium, acidity, nitrate, and sulfate collected on Full HEADS backup filters (F2 – F3 and F4) at Bakersfield.	239
Figure 62B	Carbon denuder test: organic carbon on front quartz filter $(Q_a)$ of denuded sampler without prefilter (DEN) vs. denuded sampler with Teflon prefilter (DPF) at Bakersfield.	240
Figure 63B	Carbon denuder test: organic carbon on front quartz filter $(Q_a)$ of undenuded sampler without prefilter (UND) vs. undenuded sampler with Teflon prefilter (UPF) at Bakersfield.	241
Figure 64B	Carbon denuder test: organic carbon on front quartz filter $(Q_a)$ of denuded sampler with Teflon prefilter (DPF) vs. undenuded sampler with Teflon prefilter (UPF) at Bakersfield.	242
Figure 65B	Carbon denuder test: calculated gas-quartz filter adsorption equilibrium constant vs. 23-h average reciprocal Kelvin temperature at Bakersfield.	243
Figure 66B	Carbon denuder test: calculated gas-quartz filter adsorption equilibrium constant vs. 23-h average relative humidity at Bakersfield.	244
Figure 67B	Carbon denuder test: calculated denuder efficiency vs. 23-h average reciprocal Kelvin temperature at Bakersfield.	245
Figure 68B	Carbon denuder test: calculated denuder efficiency vs. 23-h average relative humidity at Bakersfield.	246
Figure 69A	Elemental carbon: denuded (DEN) vs. undenuded (UND) Harvard carbon Sampler front quartz filter $(Q_{\text{a}})$ at all sites.	247
Figure 69R	Elemental carbon: denuded (DEN) vs. undenuded (UND) Harvard carbon Sampler front quartz filter (O <sub>2</sub> ) at Riverside.	248

Figure 69C	Elemental carbon: denuded (DEN) vs. undenuded (UND) Harvard carbon Sampler front quartz filter $(Q_a)$ at Chicago.	249
Figure 69D	Elemental carbon: denuded (DEN) vs. undenuded (UND) Harvard carbon Sampler front quartz filter $(Q_a)$ at Dallas.	250
Figure 69P	Elemental carbon: denuded (DEN) vs. undenuded (UND) Harvard carbon Sampler front quartz filter ( $Q_a$ ) at Phoenix.	251
Figure 69B	Elemental carbon: denuded (DEN) vs. undenuded (UND) Harvard carbon Sampler front quartz filter ( $Q_a$ ) at Bakersfield.	252
Figure 70A	Elemental carbon: collocated Big BOSS quartz filter at all sites.	253
Figure 70R	Elemental carbon: collocated Big BOSS quartz filter at Riverside.	254
Figure 70B	Elemental carbon: collocated Big BOSS quartz filter at Bakersfield.	255
Figure 71A	Elemental carbon: collocated PC-BOSS minor + major flow quartz filters at all sites.	256
Figure 71R	Elemental carbon: collocated PC-BOSS minor + major flow quartz filters at Riverside.	257
Figure 71B	Elemental carbon: collocated PC-BOSS minor + major flow quartz filters at Bakersfield.	258
Figure 72A	Elemental carbon: Big BOSS quartz filter vs. PC-BOSS A minor + major flow quartz filters at all sites.	259
Figure 72R	Elemental carbon: Big BOSS quartz filter vs. PC-BOSS A minor + major flow quartz filters at Riverside.	260
Figure 72B	Elemental carbon: Big BOSS quartz filter vs. PC-BOSS A minor + major flow quartz filters at Bakersfield.	261
Figure 73A	Elemental carbon: denuded (DEN) and undenuded (UND) Harvard Carbon Sampler front filters (Q <sub>a</sub> ) vs. Big BOSS quartz filter at all	
	sites.	262
Figure 73R	Elemental carbon: denuded (DEN) and undenuded (UND) Harvard Carbon Sampler front filters ( $Q_a$ ) vs. Big BOSS quartz filter at	
	Riverside.	263
Figure 73B	Elemental carbon: denuded (DEN) and undenuded (UND) Harvard Carbon Sampler front filters (Q <sub>a</sub> ) vs. Big BOSS quartz filter at	
	Bakersfield.	264
Figure 74A	Elemental carbon: denuded (DEN) and undenuded (UND) Harvard Carbon Sampler front filters (Q <sub>a</sub> ) vs. PC-BOSS minor flow quartz +	
	major flow quartz filters at all sites.	265

Figure 74R	Elemental carbon: denuded (DEN) and undenuded (UND) Harvard Carbon Sampler front filters (Q <sub>a</sub> ) vs. PC-BOSS minor flow quartz +	
	major flow quartz filters at Riverside.	266
Figure 74B	Elemental carbon: denuded (DEN) and undenuded (UND) Harvard Carbon Sampler front filters ( $Q_a$ ) vs. PC-BOSS minor flow quartz + major flow quartz filters at Bakersfield.	267
Figure 75A	Total carbon: denuded (DEN) vs. undenuded (UND) Harvard Carbon Sampler front quartz filter $(Q_a)$ at all sites.	268
Figure 75R	Total carbon: denuded (DEN) vs. undenuded (UND) Harvard Carbon Sampler front quartz filter $(Q_a)$ at Riverside.	269
Figure 75C	Total carbon: denuded (DEN) vs. undenuded (UND) Harvard Carbon Sampler front quartz filter $(Q_a)$ at Chicago.	270
Figure 75D	Total carbon: denuded (DEN) vs. undenuded (UND) Harvard Carbon Sampler front quartz filter $(Q_a)$ at Dallas.	271
Figure 75P	Total carbon: denuded (DEN) vs. undenuded (UND) Harvard Carbon Sampler front quartz filter $(Q_a)$ at Phoenix.	272
Figure 75B	Total carbon: denuded (DEN) vs. undenuded (UND) Harvard Carbon Sampler front quartz filter $(Q_a)$ at Bakersfield.	273
Figure 76A	Total carbon: denuded (DEN) vs. undenuded (UND) Harvard Carbon Sampler back quartz filter $(Q_b)$ at all sites.	274
Figure 76R	Total carbon: denuded (DEN) vs. undenuded (UND) Harvard Carbon Sampler back quartz filter $(Q_b)$ at Riverside.	275
Figure 76C	Total carbon: denuded (DEN) vs. undenuded (UND) Harvard Carbon Sampler back quartz filter $(Q_b)$ at Chicago.	276
Figure 76D	Total carbon: denuded (DEN) vs. undenuded (UND) Harvard Carbon Sampler back quartz filter $(Q_b)$ at Dallas.	277
Figure 76D	Total carbon: denuded (DEN) vs. undenuded (UND) Harvard Carbon Sampler back quartz filter $(Q_b)$ at Phoenix.	278
Figure 76B	Total carbon: denuded (DEN) vs. undenuded (UND) Harvard Carbon Sampler back quartz filter $(Q_b)$ at Bakersfield.	279
Figure 77A	Total carbon: Harvard Carbon Sampler undenuded (UND) front filter $(Q_a)$ and front – back filter $(Q_a - Q_b)$ vs. denuded (DEN) front + back $(Q_a + Q_b)$ at all sites.	280
Figure 77R	Total carbon: Harvard Carbon Sampler undenuded (UND) front filter $(Q_a)$ and front – back filter $(Q_a - Q_b)$ vs. denuded (DEN) front	200
	+ back $(Q_a + Q_b)$ at Riverside.	281

Figure 77C	Total carbon: Harvard Carbon Sampler undenuded (UND) front	
	filter $(Q_a)$ and front – back filter $(Q_a - Q_b)$ vs. denuded (DEN) front	
	$+$ back $(Q_a + Q_b)$ at Chicago.	282
Figure 77D	Total carbon: Harvard Carbon Sampler undenuded (UND) front	
	filter $(Q_a)$ and front – back filter $(Q_a - Q_b)$ vs. denuded (DEN) front	202
	$+$ back $(Q_a + Q_b)$ at Dallas.	283
Figure 77D	Total carbon: Harvard Carbon Sampler undenuded (UND) front	
	filter $(Q_a)$ and front – back filter $(Q_a - Q_b)$ vs. denuded (DEN) front	204
	+ back $(Q_a + Q_b)$ at Phoenix.	284
Figure 77B	Total carbon: Harvard Carbon Sampler undenuded (UND) front	
	filter $(Q_a)$ and front – back filter $(Q_a - Q_b)$ vs. denuded (DEN) front	205
T-' 70 A	+ back $(Q_a + Q_b)$ at Bakersfield.	285
Figure 78A	Total carbon: collocated Big BOSS quartz + Empore filters at all sites.	286
Eigung 70D		200
Figure 78R	Total carbon: collocated Big BOSS quartz + Empore filters at Riverside.	287
Figure 78B		207
rigure /ob	Total carbon: collocated Big BOSS quartz + Empore filters at Bakersfield.	288
Figure 79A	Total carbon: collocated PC-BOSS minor flow quartz + Empore +	200
riguit 17A	major flow quartz filters at all sites.	289
Figure 79R	Total carbon: collocated PC-BOSS minor flow quartz + Empore +	20)
rigure //ik	major flow quartz filters at Riverside.	290
Figure 79B	Total carbon: collocated PC-BOSS minor flow quartz + Empore +	
119010 172	major flow quartz filters at Bakersfield.	291
Figure 80A	Total carbon: collocated PC-BOSS major flow quartz filters at all	
8	sites.	292
Figure 80R	Total carbon: collocated PC-BOSS major flow quartz filters at	
O	Riverside.	293
Figure 80B	Total carbon: collocated PC-BOSS major flow quartz filters at	
G	Bakersfield.	294
Figure 81A	Total carbon: Big BOSS quartz + Empore filters vs. PC-BOSS A	
	minor quartz + Empore + major flow quartz filters at all sites.	295
Figure 81R	Total carbon: Big BOSS quartz + Empore filters vs. PC-BOSS A	
	minor quartz + Empore + major flow quartz filters at Riverside.	296
Figure 81B	Total carbon: Big BOSS quartz + Empore filters vs. PC-BOSS A	
	minor quartz + Empore + major flow quartz filters at Bakersfield.	297

Figure 82A	Total carbon: Harvard Carbon Sampler denuded (DEN) front + back quartz filters $(Q_a + Q_b)$ and undenuded (UND) front filter $(Q_a)$ vs. Big BOSS quartz + Empore filters at all sites.	298
Figure 82R	Total carbon: Harvard Carbon Sampler denuded (DEN) front + back quartz filters $(Q_a + Q_b)$ and undenuded (UND) front filter $(Q_a)$ vs. Big BOSS quartz + Empore filters at Riverside.	299
Figure 82B	Total carbon: Harvard Carbon Sampler denuded (DEN) front + back quartz filters ( $Q_a + Q_b$ ) and undenuded (UND) front filter ( $Q_a$ ) vs. Big BOSS quartz + Empore filters at Bakersfield.	300
Figure 83A	Total carbon: Harvard Carbon Sampler denuded (DEN) front + back quartz filters $(Q_a + Q_b)$ and undenuded (UND) front filter $(Q_a)$ vs. PC-BOSS A minor flow quartz + Empore + major flow quartz filters at all sites.	301
Figure 83R	Total carbon: Harvard Carbon Sampler denuded (DEN) front + back quartz filters ( $Q_a + Q_b$ ) and undenuded (UND) front filter ( $Q_a$ ) vs. PC-BOSS A minor flow quartz + Empore + major flow quartz filters at Riverside.	302
Figure 83B	Total carbon: Harvard Carbon Sampler denuded (DEN) front + back quartz filters ( $Q_a + Q_b$ ) and undenuded (UND) front filter ( $Q_a$ ) vs. PC-BOSS A minor flow quartz + Empore + major flow quartz filters at Bakersfield.	303
Figure 84A	Gas-phase nitric acid: Full HEADS sodium carbonate denuder (D1) vs. Nylon HEADS D1 at all sites. For Bakersfield data (off scale here), see Figure 84B.	304
Figure 84R	Gas-phase nitric acid: Full HEADS sodium carbonate denuder (D1) vs. Nylon HEADS D1 at Riverside.	305
Figure 84C	Gas-phase nitric acid: Full HEADS sodium carbonate denuder (D1) vs. Nylon HEADS D1 at Chicago.	306
Figure 84D	Gas-phase nitric acid: Full HEADS sodium carbonate denuder (D1) vs. Nylon HEADS D1 at Dallas.	307
Figure 84P	Gas-phase nitric acid: Full HEADS sodium carbonate denuder (D1) vs. Nylon HEADS D1 at Phoenix.	308
Figure 84B	Gas-phase nitric acid: Full HEADS sodium carbonate denuder (D1) vs. Nylon HEADS D1 at Bakersfield.	309
Figure 85A	Nitrate gas-particle distribution: Full HEADS gas-phase nitric acid (D1) vs. filter nitrate $(F1 + F2 - F3)$ at all sites.	310
Figure 85R	Nitrate gas-particle distribution: Full HEADS gas-phase nitric acid (D1) vs. filter nitrate (F1 + F2 – F3) at Riverside.	311

Figure 85C	Nitrate gas-particle distribution: Full HEADS gas-phase nitric acid (D1) vs. filter nitrate (F1 + F2 – F3) at Chicago.	312
Figure 85D	Nitrate gas-particle distribution: Full HEADS gas-phase nitric acid (D1) vs. filter nitrate $(F1 + F2 - F3)$ at Dallas.	313
Figure 85P	Nitrate gas-particle distribution: Full HEADS gas-phase nitric acid (D1) vs. filter nitrate $(F1 + F2 - F3)$ at Phoenix.	314
Figure 85B	Nitrate gas-particle distribution: Full HEADS gas-phase nitric acid (D1) vs. filter nitrate $(F1 + F2 - F3)$ at Bakersfield.	315
Figure 86A	Nitrate gas-particle distribution: Nylon HEADS gas-phase nitric acid (D1) vs. filter nitrate (F1 $+$ FN) at all sites.	316
Figure 86R	Nitrate gas-particle distribution: Nylon HEADS gas-phase nitric acid (D1) vs. filter nitrate (F1 + FN) at Riverside.	317
Figure 86C	Nitrate gas-particle distribution: Nylon HEADS gas-phase nitric acid (D1) vs. filter nitrate (F1 + FN) at Chicago.	318
Figure 86D	Nitrate gas-particle distribution: Nylon HEADS gas-phase nitric acid (D1) vs. filter nitrate (F1 + FN) at Dallas.	319
Figure 86P	Nitrate gas-particle distribution: Nylon HEADS gas-phase nitric acid (D1) vs. filter nitrate (F1 + FN) at Phoenix.	320
Figure 86B	Nitrate gas-particle distribution: Nylon HEADS gas-phase nitric acid (D1) vs. filter nitrate (F1 + FN) at Bakersfield.	321
Figure 87A	Gas-phase ammonia: Full HEADS citric acid denuder (D3) vs. Nylon HEADS D3 at all sites.	322
Figure 87R	Gas-phase ammonia: Full HEADS citric acid denuder (D3) vs. Nylon HEADS D3 at Riverside.	323
Figure 87C	Gas-phase ammonia: Full HEADS citric acid denuder (D3) vs. Nylon HEADS D3 at Chicago.	324
Figure 87D	Gas-phase ammonia: Full HEADS citric acid denuder (D3) vs. Nylon HEADS D3 at Dallas.	325
Figure 87P	Gas-phase ammonia: Full HEADS citric acid denuder (D3) vs. Nylon HEADS D3 at Phoenix.	326
Figure 87B	Gas-phase ammonia: Full HEADS citric acid denuder (D3) vs. Nylon HEADS D3 at Bakersfield.	327
Figure 88A	Ammonia gas-particle distribution: Full HEADS gas-phase ammonia (D3) vs. filter ammonium (F1 + F4) at all sites.	328
Figure 88R	Ammonia gas-particle distribution: Full HEADS gas-phase ammonia (D3) vs. filter ammonium (F1 + F4) at Riverside.	329

Figure 88C	Ammonia gas-particle distribution: Full HEADS gas-phase ammonia (D3) vs. filter ammonium (F1 + F4) at Chicago.	330
Figure 88D	Ammonia gas-particle distribution: Full HEADS gas-phase ammonia (D3) vs. filter ammonium (F1 + F4) at Dallas.	331
Figure 88P	Ammonia gas-particle distribution: Full HEADS gas-phase ammonia (D3) vs. filter ammonium (F1 + F4) at Phoenix.	332
Figure 88B	Ammonia gas-particle distribution: Full HEADS gas-phase ammonia (D3) vs. filter ammonium (F1 + F4) at Bakersfield.	333
Figure 89A	Continuous-discrete mass measurement comparison: 23-h averaged CAMM mass vs. Harvard Impactor at all sites.	334
Figure 89R	Continuous-discrete mass measurement comparison: 23-h averaged CAMM mass vs. Harvard Impactor at Riverside.	335
Figure 89C	Continuous-discrete mass measurement comparison: 23-h averaged CAMM mass vs. Harvard Impactor at Chicago.	336
Figure 89D	Continuous-discrete mass measurement comparison: 23-h averaged CAMM mass vs. Harvard Impactor at Dallas.	337
Figure 89P	Continuous-discrete mass measurement comparison: 23-h averaged CAMM mass vs. Harvard Impactor at Phoenix.	338
Figure 89B	Continuous-discrete mass measurement comparison: 23-h averaged CAMM mass vs. Harvard Impactor at Bakersfield.	339
Figure 90R	Continuous-discrete nitrate measurement comparison: 23-h averaged ADI nitrate monitor vs. Nylon HEADS F1 + FN and Full HEADS F1 + F2 – F3 at Riverside.	340
Figure 91R	Continuous-discrete nitrate measurement comparison: 23-h averaged ADI nitrate monitor vs. ADS Teflon + nylon filters and CSS Teflon + nylon filters at Riverside.	341
Figure 92R	Continuous-discrete nitrate measurement comparison: 23-h averaged ADI nitrate monitor vs. PC-BOSS minor flow quartz + Empore + major flow quartz filters and PC-BOSS minor flow	
Figure 93A	Teflon + nylon + major flow quartz filters at Riverside.  Continuous-discrete carbon measurement comparison: 23-h averaged aethalometer black carbon mass vs. undenuded Harvard Carbon Sampler (UND) front filter (Q <sub>a</sub> ) elemental carbon at all sites.	342 343
	01000.	JTJ

Figure 93R	Continuous-discrete carbon measurement comparison: 23-h	
	averaged aethalometer black carbon mass vs. undenuded Harvard	
	Carbon Sampler (UND) front filter $(Q_a)$ elemental carbon at	
	Riverside.	344
Figure 93C	Continuous-discrete carbon measurement comparison: 23-h	
	averaged aethalometer black carbon mass vs. undenuded Harvard	
	Carbon Sampler (UND) front filter (Qa) elemental carbon at	
	Chicago.	345
Figure 93D	Continuous-discrete carbon measurement comparison: 23-h	
	averaged aethalometer black carbon mass vs. undenuded Harvard	
	Carbon Sampler (UND) front filter (Qa) elemental carbon at Dallas.	346
Figure 93P	Continuous-discrete carbon measurement comparison: 23-h	
	averaged aethalometer black carbon mass vs. undenuded Harvard	
	Carbon Sampler (UND) front filter (Qa) elemental carbon at	
	Phoenix.	347
Figure 93B	Continuous-discrete carbon measurement comparison: 23-h	
	averaged aethalometer black carbon mass vs. undenuded Harvard	
	Carbon Sampler (UND) front filter (Qa) elemental carbon at	
	Bakersfield.	348
Figure 94A	Comparison of 23-h averaged continuous-nephelometer scattering	
	coefficient data with Harvard Impactor mass at all sites.	349
Figure 94R	Comparison of 23-h averaged continuous-nephelometer scattering	
	coefficient data with Harvard Impactor mass at Riverside.	350
Figure 94C	Comparison of 23-h averaged continuous-nephelometer scattering	
G	coefficient data with Harvard Impactor mass at Chicago.	351
Figure 94D	Comparison of 23-h averaged continuous-nephelometer scattering	
8	coefficient data with Harvard Impactor mass at Dallas.	352
Figure 94P	Comparison of 23-h averaged continuous-nephelometer scattering	
119410 > 11	coefficient data with Harvard Impactor mass at Phoenix.	353
Figure 94B	Comparison of 23-h averaged continuous-nephelometer scattering	
	coefficient data with Harvard Impactor mass at Bakersfield.	354
Figure 95R	Correlations between 1-h average measurements collected by	
rigure /SK	CAMM (mass), ADI sampler (nitrate), and aethalometer (black	
	carbon) at Riverside.	355
Figure 95C	Correlations between 1-h average measurements collected by	555
riguit 33C	CAMM (mass) and aethalometer (black carbon) at Chicago.	356
Figure 05D		550
Figure 95D	Correlations between 1-h average measurements collected by CAMM (mass) and aethalometer (black carbon) at Dallas	357
	A PARTICIO DE LA PARTICIONA DE LA PARTICIO DELLA PARTICIO DELLA PARTICIO DE LA PARTICIO DE LA PARTICIO DELLA PARTICIONE DELLA PAR	11/

Figure 95P	Correlations between 1-h average measurements collected by	
	CAMM (mass) and aethalometer (black carbon) at Phoenix.	358
Figure 95B	Correlations between 1-h average measurements collected by	
	CAMM (mass) and aethalometer (black carbon) at Bakersfield.	359
Figure 96R	Correlations between 1-h average measurements collected by	
	CAMM (mass), ADI sampler (nitrate), and nephelometer (light	
	scattering)at Riverside.	360
Figure 96C	Correlations between 1-h average measurements collected by	
	CAMM (mass) and nephelometer (light scattering)at Chicago.	361
Figure 96D	Correlations between 1-h average measurements collected by	
	CAMM (mass) and nephelometer (light scattering)at Dallas.	362
Figure 96P	Correlations between 1-h average measurements collected by	2 - 2
	CAMM (mass) and nephelometer (light scattering)at Phoenix.	363
Figure 96B	Correlations between 1-h average measurements collected by	2-1
	CAMM (mass) and nephelometer (light scattering)at Bakersfield.	364
Figure 97R	Daily average chemical composition estimates for PM <sub>2.5</sub> based on	
	Full HEADS and DEN Harvard carbon sampler measurements at	
	Riverside. A negative unidentified fraction indicates that the 24-h	365
E' 050	average reconstructed mass exceeded the HI mass.	303
Figure 97C	Daily average chemical composition estimates for PM <sub>2.5</sub> based on Full HEADS and DEN Harvard carbon sampler measurements at	
	Chicago. A negative unidentified fraction indicates that the 24-h	
	average reconstructed mass exceeded the HI mass.	366
Figure 97D	Daily average chemical composition estimates for PM <sub>2.5</sub> based on	
119010 > 12	Full HEADS and DEN Harvard carbon sampler measurements at	
	Dallas. A negative unidentified fraction indicates that the 24-h	
	average reconstructed mass exceeded the HI mass.	367
Figure 97P	Daily average chemical composition estimates for PM <sub>2.5</sub> based on	
	Full HEADS and DEN Harvard carbon sampler measurements at	
	Phoenix. A negative unidentified fraction indicates that the 24-h	
	average reconstructed mass exceeded the HI mass.	368
Figure 97B	Daily average chemical composition estimates for $PM_{2.5}$ based on	
	Full HEADS and DEN Harvard carbon sampler measurements at	
	Bakersfield. A negative unidentified fraction indicates that the 24-h	0
	average reconstructed mass exceeded the HI mass.	369

Figure 98R	Daily average chemical composition estimates for PM <sub>2.5</sub> based on Full HEADS and UND Harvard carbon sampler measurements at Riverside. A negative unidentified fraction indicates that the 24-h average reconstructed mass exceeded the HI mass.	370
Figure 98C	Daily average chemical composition estimates for PM <sub>2.5</sub> based on Full HEADS and UND Harvard carbon sampler measurements at Chicago. A negative unidentified fraction indicates that the 24-h average reconstructed mass exceeded the HI mass.	371
Figure 98D	Daily average chemical composition estimates for PM <sub>2.5</sub> based on Full HEADS and UND Harvard carbon sampler measurements at Dallas. A negative unidentified fraction indicates that the 24-h average reconstructed mass exceeded the HI mass.	372
Figure 98P	Daily average chemical composition estimates for PM <sub>2.5</sub> based on Full HEADS and UND Harvard carbon sampler measurements at Phoenix. A negative unidentified fraction indicates that the 24-h average reconstructed mass exceeded the HI mass.	373
Figure 98B	Daily average chemical composition estimates for PM <sub>2.5</sub> based on Full HEADS and UND Harvard carbon sampler measurements at Bakersfield. A negative unidentified fraction indicates that the 24-h average reconstructed mass exceeded the HI mass.	373
Figure 99R	Daily average chemical composition estimates for PM <sub>2.5</sub> based on Nylon HEADS and DEN Harvard carbon sampler measurements at Riverside. A negative unidentified fraction indicates that the 24-h average reconstructed mass exceeded the HI mass.	374
Figure 99C	Daily average chemical composition estimates for PM <sub>2.5</sub> based on Nylon HEADS and DEN Harvard carbon sampler measurements at Chicago. A negative unidentified fraction indicates that the 24-h average reconstructed mass exceeded the HI mass.	376
Figure 99D	Daily average chemical composition estimates for PM <sub>2.5</sub> based on Nylon HEADS and DEN Harvard carbon sampler measurements at Dallas. A negative unidentified fraction indicates that the 24-h average reconstructed mass exceeded the HI mass.	377
Figure 99P	Daily average chemical composition estimates for PM <sub>2.5</sub> based on Nylon HEADS and DEN Harvard carbon sampler measurements at Phoenix. A negative unidentified fraction indicates that the 24-h	
	average reconstructed mass exceeded the HI mass.	378

Figure 99B	Daily average chemical composition estimates for PM <sub>2.5</sub> based on Nylon HEADS and DEN Harvard carbon sampler measurements at Bakersfield. A negative unidentified fraction indicates that the 24-h average reconstructed mass exceeded the HI mass.	379
Figure 100R	Daily average chemical composition estimates for PM <sub>2.5</sub> based on Nylon HEADS and UND Harvard carbon sampler measurements at Riverside. A negative unidentified fraction indicates that the 24-h average reconstructed mass exceeded the HI mass.	380
Figure 100C	Daily average chemical composition estimates for PM <sub>2.5</sub> based on Nylon HEADS and UND Harvard carbon sampler measurements at Chicago. A negative unidentified fraction indicates that the 24-h average reconstructed mass exceeded the HI mass.	381
Figure 100D	Daily average chemical composition estimates for PM <sub>2.5</sub> based on Nylon HEADS and UND Harvard carbon sampler measurements at Dallas. A negative unidentified fraction indicates that the 24-h average reconstructed mass exceeded the HI mass.	382
Figure 100P	Daily average chemical composition estimates for PM <sub>2.5</sub> based on Nylon HEADS and UND Harvard carbon sampler measurements at Phoenix. A negative unidentified fraction indicates that the 24-h average reconstructed mass exceeded the HI mass.	383
Figure 100B	Daily average chemical composition estimates for PM <sub>2.5</sub> based on Nylon HEADS and UND Harvard carbon sampler measurements at Bakersfield. A negative unidentified fraction indicates that the 24-h average reconstructed mass exceeded the HI mass.	384
Figure 100F	Daily average chemical composition estimates for PM <sub>2.5</sub> based on Nylon HEADS and UND Harvard carbon sampler measurements at Philadelphia. A negative unidentified fraction indicates that the 24-h average reconstructed mass exceeded the HI mass.	385
Figure 101R	Study average chemical composition estimates for PM <sub>2.5</sub> based on Full HEADS and DEN Harvard carbon sampler measurements at Riverside	386
Figure 101C	Study average chemical composition estimates for PM <sub>2.5</sub> based on Full HEADS and DEN Harvard carbon sampler measurements at Chicago.	387
Figure 101D	Study average chemical composition estimates for PM <sub>2.5</sub> based on Full HEADS and DEN Harvard carbon sampler measurements at Dallas.	388

Figure 101P	Study average chemical composition estimates for PM <sub>2.5</sub> based on	
	Full HEADS and DEN Harvard carbon sampler measurements at	
	Phoenix.	389
Figure 101B	Study average chemical composition estimates for PM <sub>2.5</sub> based on	
	Full HEADS and DEN Harvard carbon sampler measurements at	
	Bakersfield.	390
Figure 102R	Study average chemical composition estimates for PM <sub>2.5</sub> based on	
	Full HEADS and UND Harvard carbon sampler measurements at	
	Riverside	391
Figure 102C	Study average chemical composition estimates for PM <sub>2.5</sub> based on	
	Full HEADS and UND Harvard carbon sampler measurements at	
	Chicago.	392
Figure 102D	Study average chemical composition estimates for PM <sub>2.5</sub> based on	
	Full HEADS and UND Harvard carbon sampler measurements at	
	Dallas.	393
Figure 102P	Study average chemical composition estimates for PM <sub>2.5</sub> based on	
	Full HEADS and UND Harvard carbon sampler measurements at	
	Phoenix.	394
Figure 102B	Study average chemical composition estimates for PM <sub>2.5</sub> based on	
	Full HEADS and UND Harvard carbon sampler measurements at	
	Bakersfield.	395
Figure 103R	Study average chemical composition estimates for PM <sub>2.5</sub> based on	
	Nylon HEADS and DEN Harvard carbon sampler measurements at	
	Riverside	396
Figure 103C	Study average chemical composition estimates for PM <sub>2.5</sub> based on	
	Nylon HEADS and DEN Harvard carbon sampler measurements at	
	Chicago.	397
Figure 103D	Study average chemical composition estimates for PM <sub>2.5</sub> based on	
	Nylon HEADS and DEN Harvard carbon sampler measurements at	
	Dallas.	398
Figure 103P	Study average chemical composition estimates for PM <sub>2.5</sub> based on	
	Nylon HEADS and DEN Harvard carbon sampler measurements at	
	Phoenix.	399
Figure 103B	Study average chemical composition estimates for PM <sub>2.5</sub> based on	
	Nylon HEADS and DEN Harvard carbon sampler measurements at	
	Bakersfield.	400

Figure 102R	Study average chemical composition estimates for PM <sub>2.5</sub> based on Nylon HEADS and UND Harvard carbon sampler measurements at	101
	Riverside	401
Figure 102C	Study average chemical composition estimates for PM <sub>2.5</sub> based on Nylon HEADS and UND Harvard carbon sampler measurements at Chicago.	402
E: 102D		702
Figure 102D	Study average chemical composition estimates for PM <sub>2.5</sub> based on Nylon HEADS and UND Harvard carbon sampler measurements at Dallas.	403
Figure 102P	Study average chemical composition estimates for $PM_{2.5}$ based on Nylon HEADS and UND Harvard carbon sampler measurements at Phoenix.	404
Figure 102B	Study average chemical composition estimates for $PM_{2.5}$ based on Nylon HEADS and UND Harvard carbon sampler measurements at Bakersfield.	405
Figure 102F	Study average chemical composition estimates for $PM_{2.5}$ based on Nylon HEADS and UND Harvard carbon sampler measurements at Philadelphia.	406
Figure 105A	Exploration of observed disagreements between reconstructed and Harvard Impactor mass: HI mass – Reconstructed Mass 4 (see Table 16) vs. average daily temperature at all sites.	407
Figure 105R	Exploration of observed disagreements between reconstructed and Harvard Impactor mass: HI mass – Reconstructed Mass 4 (see Table 16) vs. average daily temperature at Riverside.	408
Figure 105C	Exploration of observed disagreements between reconstructed and Harvard Impactor mass: HI mass – Reconstructed Mass 4 (see Table 16) vs. average daily temperature at Chicago.	409
Figure 105D	Exploration of observed disagreements between reconstructed and Harvard Impactor mass: HI mass – Reconstructed Mass 4 (see	410
E: 105D	Table 16) vs. average daily temperature at Dallas.	410
rigure 105P	Exploration of observed disagreements between reconstructed and Harvard Impactor mass: HI mass – Reconstructed Mass 4 (see Table 16) vs. average daily temperature at Phoenix.	411
Figure 105B	Exploration of observed disagreements between reconstructed and Harvard Impactor mass: HI mass – Reconstructed Mass 4 (see	.11
	Table 16) vs. average daily temperature at Bakersfield.	412

Figure 106A	Exploration of observed disagreements between reconstructed and	
	Harvard Impactor mass: HI mass – Reconstructed Mass 4 (see	440
	Table 16) vs. daily one hour maximum temperature at all sites.	413
Figure 106R	Exploration of observed disagreements between reconstructed and	
	Harvard Impactor mass: HI mass – Reconstructed Mass 4 (see	
	Table 16) vs. daily one hour maximum temperature at Riverside.	414
Figure 106C	Exploration of observed disagreements between reconstructed and	
	Harvard Impactor mass: HI mass – Reconstructed Mass 4 (see	
	Table 16) vs. daily one hour maximum temperature at Chicago.	415
Figure 106D	Exploration of observed disagreements between reconstructed and	
	Harvard Impactor mass: HI mass – Reconstructed Mass 4 (see	
	Table 16) vs. daily one hour maximum temperature at Dallas.	416
Figure 106P	Exploration of observed disagreements between reconstructed and	
	Harvard Impactor mass: HI mass – Reconstructed Mass 4 (see	
	Table 16) vs. daily one hour maximum temperature at Phoenix.	417
Figure 106B	Exploration of observed disagreements between reconstructed and	
	Harvard Impactor mass: HI mass – Reconstructed Mass 4 (see	
	Table 16) vs. daily one hour maximum temperature at Bakersfield.	418
Figure 107A	Exploration of observed disagreements between reconstructed and	
	Harvard Impactor mass: HI mass – Reconstructed Mass 4 (see	
	Table 16) vs. average daily relative humidity at all sites.	419
Figure 107R	Exploration of observed disagreements between reconstructed and	
	Harvard Impactor mass: HI mass – Reconstructed Mass 4 (see	400
	Table 16) vs. average daily relative humidity at Riverside.	420
Figure 107C	Exploration of observed disagreements between reconstructed and	
	Harvard Impactor mass: HI mass – Reconstructed Mass 4 (see	404
	Table 16) vs. average daily relative humidity at Chicago.	421
Figure 107D	Exploration of observed disagreements between reconstructed and	
	Harvard Impactor mass: HI mass – Reconstructed Mass 4 (see	400
	Table 16) vs. average daily relative humidity at Dallas.	422
Figure 107P	Exploration of observed disagreements between reconstructed and	
	Harvard Impactor mass: HI mass – Reconstructed Mass 4 (see	400
	Table 16) vs. average daily relative humidity at Phoenix.	423
Figure 107B	Exploration of observed disagreements between reconstructed and	
	Harvard Impactor mass: HI mass – Reconstructed Mass 4 (see	40.4
	Table 16) vs. average daily relative humidity at Bakersfield.	424

Figure 108A	Exploration of observed disagreements between reconstructed and	
	Harvard Impactor mass: HI mass – Reconstructed Mass 4 (see	
	Table 16) vs. daily one hour maximum relative humidity at all	
	sites.	425
Figure 108R	Exploration of observed disagreements between reconstructed and	
	Harvard Impactor mass: HI mass – Reconstructed Mass 4 (see	
	Table 16) vs. daily one hour maximum relative humidity at	
	Riverside.	426
Figure 108C	Exploration of observed disagreements between reconstructed and	
	Harvard Impactor mass: HI mass – Reconstructed Mass 4 (see	
	Table 16) vs. daily one hour maximum relative humidity at	
	Chicago.	427
Figure 108D	Exploration of observed disagreements between reconstructed and	
G	Harvard Impactor mass: HI mass – Reconstructed Mass 4 (see	
	Table 16) vs. daily one hour maximum relative humidity at Dallas.	428
Figure 106P	Exploration of observed disagreements between reconstructed and	
	Harvard Impactor mass: HI mass – Reconstructed Mass 4 (see	
	Table 16) vs. daily one hour maximum relative humidity at	
	Phoenix.	429
Figure 106B	Exploration of observed disagreements between reconstructed and	
	Harvard Impactor mass: HI mass – Reconstructed Mass 4 (see	
	Table 16) vs. daily one hour maximum relative humidity at	
	Bakersfield.	430

### INTRODUCTION

### Background

In July, 1997, the United States Environmental Protection Agency (EPA) promulgated new standards regulating concentrations of fine particulate matter in the lower atmosphere. These regulations 1) retained the previously established limits for  $PM_{10}$  (particles with aerodynamic diameters smaller than  $10~\mu m$ ), 2) set new limits on the concentration of particles with aerodynamic diameters smaller than  $2.5~\mu m$  ( $PM_{2.5}$ ), and 3) established a Federal Reference Method (FRM) for sampling to determine compliance with the standard. Elevated concentrations of fine particles have been correlated with adverse health outcomes in epidemiological studies. Fine particles are also a major contributor to visibility impairment by regional haze. The proposed standards would regulate PM on both a 24-h and annual basis.

We describe here the results of a study undertaken shortly after promulgation of the new standard and FRM designation. This research was designed to respond to the urgent need for improved data on fine particle concentrations in urban areas of the United States and to test new and existing methods for sampling PM<sub>2.5</sub>. Prior to promulgation of the new standard, PM<sub>2.5</sub> concentrations were not routinely collected in most areas of the United States. As such, implementation of the standards was delayed to allow completion of three years of monitoring (through July, 2000) to determine the NAAQS attainment status of every county in the United States. These determinations as well as the future attainment status of currently out of compliance areas will be based on measurements collected with the newly designated FRM.

### PM<sub>2.5</sub> Sampling Issues

The prescribed Federal Reference Method (FRM) for  $PM_{2.5}$  mandates collection of particulate matter passing through a 2.5  $\mu$ m size-selective inlet on a single Teflon filter. In operation, a 24-hour integrated sample is collected on a filter, which is later equilibrated at controlled temperature and relative humidity (RH) conditions in a laboratory, and then weighed to determine the mass of the deposited particulate matter

(PM). Sampling must be conducted at ambient temperature conditions (within 5°C), and the collected samples must be equilibrated at 30-40% RH and 20-23°C for 24 hours prior to their gravimetric analysis (Federal Register, 1997). This specified method will also be used to evaluate potential equivalent methods to minimize discrepancies among different equivalent samplers. However, the accuracy of the FRM itself for determining aerosol mass at the point of sampling is questionable due to potential errors introduced by volatilization or condensation of inorganic and organic compounds such as ammonium nitrate and some hydrocarbons which readily partition between the gas and particle phases. Furthermore, most existing PM<sub>2.5</sub> data collected with FRM samplers have been gathered in rural settings. The differences in chemistry and PM composition between urban and rural settings raise questions about the adequacy of the FRM for assessing PM<sub>2.5</sub> concentrations in higher population density areas.

The PM<sub>2.5</sub> FRM presents additional limitations: 1) it requires a sequential sampling unit to collect two to seven daily samples per week; 2) it requires both an environmentally controlled balance room and extensive labor to weigh the filters and; 3) it does not provide short term measurements. Capital investment and labor costs for purchase and operation are substantial, but very little will be learned about the diurnal variability of fine particle concentrations. A 24-hour average measurement may not adequately represent actual human exposure. Detailed temporal information is needed for both understanding particle health effects and developing sound mitigation strategies. Because of sensitivity limitations, the FRM gravimetric method may not be adequate to obtain short term measurements (less than 12-24 hours). Finally, the proposed FRM can not provide immediate data that are necessary to calculate Air Pollution Indices (APIs). Development of equivalent continuous fine particle methods will make it possible to obtain richer data sets and to establish comprehensive monitoring networks that provide information on temporal and spatial variability of particle mass concentration in a cost-effective way.

While particle mass is the parameter subject to regulation, data on particle chemical composition and size are needed to understand their origins and sources, and to evaluate the relationships between specific chemical constituents and potential

environmental and health consequences. Automated monitoring methods, such as are now available for specific gaseous pollutants such as ozone and carbon monoxide, have made it possible to obtain high-time resolution, continuous ambient concentration data for these gases at reasonable cost. Equivalent monitoring methods are needed for fine particles. Filter-based particle collection and analysis as is now done is costly, and often results are not known until some months after the sample was collected. As the need for particle data grows with new regulation, advances in particle measurement methods will become essential. However, before automated methods can be used routinely, they must be tested against the more traditional filter-based approaches including the Federal Reference Method for PM<sub>2.5</sub>. While we are beginning to understand the limitations of the filter-based approaches, the reliability and limitations of newer automated methods remain to be explored.

Many PM<sub>2.5</sub> components are either volatile or chemically reactive. The volatile components of greatest concern include ammonium nitrate, whose gas-solid equilibrium constant varies substantially with air temperature, and condensable organic compounds (COCs). Compounds we refer to here as COCs have been widely labeled as semivolatile organic compounds (SVOCs or SOCs). SVOCs are classified using an organic compound's vapor pressure to estimate whether it is likely to exist predominantly in the gas phase, predominantly in the particle phase, or in some dynamic equilibrium between the phases. However, vapor pressure alone may not be sufficient to assess a compound's tendency to fractionate into one phase or the other. Additional factors such as water solubility of the compound and water content or chemical composition of the aerosol particles may also impact gas-particle partitioning in the atmosphere (Saxena and Hildemann, 1996). To differentiate our terminology from that previously used, we define COCs as organic compounds that have at least 1% of their airborne mass in both the particle and gas phases.

Performance of the FRM is expected *a priori* to be a function of the sampling location and time of the year. For instance, in locations such as Southern California and Phoenix where nitrate and organics are known to constitute a substantial portion of the fine particle mass, the FRM-measured PM<sub>2.5</sub> concentration may underestimate PM<sub>2.5</sub>

actually present in the air as it enters the sampler. In eastern U.S. locations, these errors should increase during the winter and decrease during the summer because nitrate contributions to PM<sub>2.5</sub> are generally larger during the winter than the summer. Clean Air Act Title IV mandated sulfur dioxide emission reductions during the years 1995-2000 have already begun to alter the composition of eastern U.S. aerosol. Labile substances may constitute a larger portion of the fine particle mass in the future. Thus, tests being conducted during 1996-97 may overstate the performance for "post-Title IV" aerosol in the eastern U.S. Considering all these factors, a credible evaluation of the FRM ought to demonstrate the relationship between the method performance and the particle composition over a broad range of locations.

#### Study Objectives

This study has two main objectives: 1) investigate the extent to which PM<sub>2.5</sub> measurements made with Teflon filter-based samplers differ in mass and chemical composition from aerosol particles at the point of sampling or inhalation and 2) test and intercompare several continuous and discrete samplers designed to quantify PM<sub>2.5</sub> mass or chemical composition. The first objective requires quantification of the amount and composition of labile fine PM lost from single filter-based sampling methods (e.g., the proposed FRM) as a function of season and location. Because this objective requires accurate chemical characterization of particle mass and chemical component concentrations, we address the second goal of testing new and existing particle sampling methods first in this report. This is accomplished through intercomparisons of data from several collocated samplers including continuous monitors for mass, nitrate, light scattering, and black carbon and discrete monitors for mass, sulfate, nitrate, ammonium, organic and elemental carbon, and other elements. In addition, we also measure inorganic gas-phase compounds (sulfur dioxide, nitric acid, and ammonia) which could potentially act as interferents to particle-phase measurements, as well as temperature and relative humidity. The results reported here will have immediate value in providing more robust fine particle sampling and concentration data to be considered in the debate concerning the promulgation of the fine particle standard and the selection of the FRM. Over the longer term, by quantifying the reliability of the FRM and conventional particle

sampling technology we hope to create an impetus for improving these methods. In the coming decade a proliferation of private and public sector multiyear experiments in urban and nonurban locations is expected. These experiments will create the data needed for designating nonattainment areas and for preparing the state implementation plans (SIPs). Our study can act as a technology assessment forerunner to help design these multiyear, multilocation particle sampling networks.

### **EXPERIMENTAL**

### Sampling Locations and General Conditions

PM<sub>2.5</sub> measurements were conducted at sites in six cities at the places and dates listed in Table 1. The six sites represent a cross section of regional and climatological conditions. Riverside in August, 1997 and Philadelphia in August, 1998 may be representative of western and eastern cities, respectively, in the summer. Chicago provided data from an eastern city in the fall, although the weather was unseasonably cold and perhaps more representative of winter. Phoenix, Bakersfield, and Dallas provide data from two western cities and one southern city the winter. The study period in Dallas was characterized by extremely clean conditions. Precipitation was uncharacteristically frequent and heavy at Bakersfield during the study. Sampling protocols used at the six sites were pilot tested in a brief study conducted in Birmingham, AL in November, 1996 (HSPH report, 1998). While data from the brief sampling periods at each site (between 18 and 56 days) do not allow complete characterization of the seasonal or annual trends in aerosol composition or mass, they give a "snapshot" look at conditions that may occur.

# Discrete (Filter-Based) PM<sub>2.5</sub> Samplers

#### **Mass**

Discrete PM<sub>2.5</sub> mass samples were collected at all six sites with a Harvard Impactor (HI), a low flow particle sampler that uses an oiled impactor plate to minimize particle bounce and provide a sharp cut point. The PM<sub>2.5</sub> HI sampler consists of an inlet, an impaction plate, and filter mounted in a plastic holder. In its standard configuration, the HI sampler flow is 10 L min<sup>-1</sup>. The concentration of particles was determined from the calculated mass change on a 37 mm Teflon filter (Teflo<sup>TM</sup>, Gelman Sciences) by precise weighing under controlled temperature and relative humidity conditions and the total volume of air sampled (at local temperature and pressure). To improve the precision of the HI for method comparison studies, filters were weighed twice before and twice after exposure, and the mean of the two on and two off weights was used to determine the

net mass. If the difference between any pair of filter weights exceeded 10  $\mu$ g, a third weighing was done. Filters were equilibrated in a temperature and relative humidity controlled weighing room at least 48 hours prior to being weighed, both before and after sampling. These techniques reduced the uncertainty of the net exposed filter mass to less than 10  $\mu$ g, or the equivalent of less than 0.8  $\mu$ g/m<sup>3</sup> PM concentration for the 10 L min<sup>-1</sup> HI configuration and a 24 hour sample duration.

### **Inorganic Ions (Sulfate, Nitrate, Ammonium)**

Several methods to quantify concentrations of PM<sub>2.5</sub> inorganic ions were used in this study. The methods for each ion are summarized in Tables 2 – 4. The Harvard-EPA Annular Denuder Sampler (HEADS) method (Figure 1) is described and evaluated in Koutrakis et al. (1988), Ellestad, et al. (1991), and an ORD-USEPA publication (1992). Briefly, each of the two HEADS systems use a Teflon front filter (F1) to collect PM<sub>2.5</sub> particles. Air sampled at 10 L min<sup>-1</sup> first travels through the inlet section where a glass impactor removes particles larger than 2.1 µm and then through two annular denuders coated with sodium carbonate (D1) or citric acid (D3) to remove acidic and alkaline gases, respectively. The HEADS systems differ in the backup filters employed to capture particle phase constituents (nitrate and ammonium in Full HEADS and nitrate in the Nylon configuration) volatilized from the Teflon front filter during sampling. Full HEADS employs a pair of sodium carbonate coated glass fiber filters (F2 and F3) to collect volatilized nitrate and a citric acid coated glass fiber filter to trap ammonium. The F2 filter collects nitric acid from the nitrate volatilized off of the F1 Teflon filter, and the F3 filter is used to correct the nitrate found on the F2 filter for possible interference from ambient NO2 (the nitrate lost from the F1 filter is F2 nitrate minus F3 NO<sub>3</sub>). The total nitrate value for this method is thus the nitrate concentration measured on F1+F2-F3. In Nylon HEADS, the filter pack has only Teflon and Nylon filters – there are no coated glass fiber filters. The Nylon (Gelman Nylasorb) filter (FN) is sandwiched immediately downstream from the Teflon filter to absorb any volatilized HNO<sub>3</sub> from the Teflon filter with minimal losses from other surface reactions in the filter holder. Nitrate in this system is given by nitrate on F1+FN. Only a Nylon HEADS was available at Philadelphia.

The BYU Annular Denuder and ChemSpec Samplers (ADS and CCS, respectively, Figure 2) both incorporate a set of sodium carbonate/glycerine-coated annular denuders to remove sulfur dioxide and nitric acid. The ChemSpec was also sometimes equipped with a sodium chloride denuder designed to enhance removal of ammonia. In both samplers, the denuders were preceded in the sample train by a Teflon-coated impactor inlet with a 50% cutpoint at 2.5 µm and a flow rate of 18 L min<sup>-1</sup>. Teflon and nylon filters analyzed for nitrate and sulfate by IC followed the denuders. Negligible sulfate was detected on the nylon filters in either sampler, so PM<sub>2.5</sub> sulfate is simply that collected on the Teflon filter. Nitrate is the sum of the two filters.

The High Volume BYU Organic Sampler System (Big BOSS, Figure 3) has been described previously by Eatough *et al.* (1993) and Cui *et al.* (1998). Air sampled at 170 to 210 L min<sup>-1</sup> passed first through a multi-channel diffusion denuder whose surfaces were coated with carbon impregnated filter paper sheets and then through a quartz and an Empore carbon-impregnated filter in series. The flow through the Empore filter was controlled by a mass flow controller to less than 25 L min<sup>-1</sup>. Nitrate and sulfate on the two filters were quantified by ion chromatography (IC) in BYU's laboratory. PM<sub>2.5</sub> sulfate is calculated as the mass collected on the quartz filter while nitrate is the sum of the quartz and Empore filter measurements. At the Big BOSS sample flow rates, the denuder's ability to quantitatively remove gas-phase interferents suffers (Cui *et al.*, 1998).

The Particle Concentrator-BYU Organic Sampling System (PC-BOSS, Figure 4), a new sampler recently described by Eatough *et al.* (1999), removes gas-phase carbonaceous compounds, nitric acid and ammonia from the aerosol stream using a particle concentrator designed to separate the incoming air flow into minor and major flow channels. Air entered the particle concentrator after passing through the size selective inlet at approximately 200 L min<sup>-1</sup>. In the concentrator, the air stream was split into two flows: the minor flow contained concentrated particles in the 0.1 to 2.5 μm diameter range, and the major flow contained approximately 75% of the gas volume and the majority of the particles smaller than 0.1 μm in diameter. Small losses (on the order of 5-10%) of particles from the air stream occurred in the particle concentrator. The

minor flow stream then passed through a carbon denuder assumed to remove the remaining gas-phase carbon, nitric acid, and ammonia. Following the denuder, this flow path was split again with half passing through a quartz filter followed by an Empore carbon filter designed to capture particle-phase carbon and nitrate volatilized from the quartz filter during sampling and the remainder passing through a Teflon front filter followed by a nylon back-up filter to catch nitrate volatilized from the Teflon filter. Particles were also collected from the major flow path using a single quartz filter with no back-up filter. All filters were analyzed for nitrate and sulfate by IC. PM<sub>2.5</sub> sulfate is the sum of the minor flow quartz or Teflon filter and the major flow quartz filter measurements. For nitrate, volatilized nitrate collected on the Empore or nylon backup filters is added as well.

#### Carbon

Particle-phase carbon samplers used in this study are summarized in Table 5. Big BOSS and PC-BOSS quartz and Empore filters were analyzed for carbon by temperature programmed volatilization (TPV) (Cui et al., 1998; Eatough et al., 1989; Eatough et al., 1990). Briefly, gases evolved with a linear temperature ramp were converted to carbon dioxide (CO<sub>2</sub>) at 1200 °C over a barium chromate-silver catalyst bed and detected using a non-dispersive infrared detector. The total integrated area from 50 to 750°C gives total carbonaceous material on the filter. Carbon evolved above 500 °C is assumed to be elemental carbon. In the Big BOSS, PM<sub>2.5</sub> elemental carbon is that collected on the quartz filter. Total PM<sub>2.5</sub> carbon is obtained by summing the front filter quartz and the Empore values. Because of slight denuder breakthrough by gas-phase organic carbon, the front quartz filter total carbon measurement was corrected by ignoring carbon evolved in the first thermogram peak (below 170 °C) in the TPV analysis. This adjustment is justified based on comparisons of denuded and undenuded filter analyses (Cui et al., 1998). PC-BOSS total carbon is calculated by summing the minor flow quartz and Empore filters with the major flow quartz filter. Since the major flow is undenuded, the carbon mass collected on this filter was corrected as described for Big BOSS.

The two Harvard Carbon Sampler configurations used at all sites in this study are shown schematically in Figure 5. These samplers are labeled UND and DEN to denote

undenuded and denuded, respectively. Each sampler configuration consisted of two 47-mm diameter quartz fiber filters arranged in series following a virtual impactor with a nominal particle aerodynamic diameter cut point of  $2.5~\mu m$ . Only an undenuded sampler was employed at Philadelphia. Air was sampled at  $10~L~min^{-1}$ . The front quartz filter in all samplers is designated as Quartz Filter A ( $Q_a$ ) and the backup as Quartz Filter B ( $Q_b$ ). In sampler UND, the air stream passed directly from the size selective inlet to  $Q_a$  and then to  $Q_b$ . An aluminum parallel plate denuder with charcoal–impregnated filter surfaces was inserted into the air stream between the inlet and  $Q_a$  in sampler DEN. The denuder was replaced with clean carbon-impregnated filter paper approximately every 2 weeks in an attempt to mitigate errors caused by gas-phase breakthrough of gas phase organic carbon. However, theoretical denuder efficiency calculations depend on several assumptions including complete, irreversible adsorption of gas-phase contaminants on denuder surfaces and laminar flow through the denuder chamber. More accurate estimates of denuder field efficiency could be determined experimentally by quantifying the inlet and outlet concentrations of the gas-phase compound or compounds of interest.

We attempted to quantify field denuder performance using two additional sampler configurations at Bakersfield. These samplers, labeled as UPF (undenuded with prefilter) and DPF (denuded with prefilter) in Figure 5, were analogous to samplers UND and DEN. However, the additional samplers at Bakersfield included Teflon pre–filters (TPF) immediately after the size selective inlet. The TPF in samplers UPF and DPF was intended to selectively remove airborne particles from the sampled air stream without significantly disturbing the gas-phase COC concentration. For sampler UPF, the Teflon pre–filter preceded  $Q_a$  and  $Q_b$ . No denuder was used. For sampler DPF, the TPF was followed by a denuder and then by  $Q_a$  and  $Q_b$ . The Teflon filter in sampler DPF removed particle-phase material prior to the air stream entering the denuder, so carbon detected on  $Q_a$  and  $Q_b$  originated from gas-phase or volatilized particle-phase organics that the denuder failed to collect. We used carbon detected on  $Q_a$  and  $Q_b$  in the UPF sampler to estimate the gas phase concentration entering the DPF denuder as described below.

Prior to sampling, all filters used in this study were pre-fired in an oven at 900 °C for at least four hours to remove any carbon contamination. The filters were tested for

carbon levels before use. Those filters that exceeded 1.5  $\mu$ g cm<sup>-2</sup> organic carbon, 0.5  $\mu$ g cm<sup>-2</sup> elemental carbon, or 2.0  $\mu$ g cm<sup>-2</sup> total carbon were discarded. The average pre-fired blank levels were 0.41  $\pm$  0.2  $\mu$ g organic carbon cm<sup>-2</sup> of filter area, 0.03  $\pm$  0.2  $\mu$ g elemental carbon cm<sup>-2</sup>, and 0.44  $\pm$  0.2  $\mu$ g total carbon cm<sup>-2</sup>. Because pre-fired filters may absorb organic vapors during shipping and storage, the lower quantifiable limit (LQL) for analysis of filters from each city was determined from the variability in the results of analysis of dynamic (field) blanks from each site and in regularly collected collocated samples. The average field blank filter masses for all of the sampling sites were 0.27  $\pm$  0.15  $\mu$ g for organic carbon, 0.01  $\pm$  0.04  $\mu$ g for elemental carbon, and 0.29  $\pm$  0.18  $\mu$ g for total carbon. We defined the LQL as 3 times the larger of the standard deviation in the field blank values and the average root mean squared (RMS) difference in replicate analyses of selected filters. For all five study sites, the average RMS difference in the replicate sample analyses was greater then the standard deviation of the field blank values. The average LQL concentrations for the five sites were 1.22  $\mu$ g m<sup>-3</sup> for organic carbon, 0.55  $\mu$ g m<sup>-3</sup> for elemental carbon, and 1.60  $\mu$ g m<sup>-3</sup> for total carbon.

Harvard Carbon Sampler filters were analyzed for total carbon by Thermal Optical Reflectance (TOR) as described elsewhere (Chow *et al.*, 1993) at the Desert Research Institute in Nevada. For sample deposits containing more than  $10 \,\mu g \, cm^{-2}$  of carbon, precision is better than  $\pm$  3%. Precision (reproducibility in replicate analyses of the same filter) of the split between the organic and elemental carbon fractions is generally better than 5% of the total measured carbon. The accuracy of the TOR method for total carbon determined by analyzing a known amount of carbon is  $\pm$  5% (Chow *et al.*, 1993).

# Continuous (In Situ) PM<sub>2.5</sub> Samplers

#### Mass

A Continuous Ambient Mass Monitor System (CAMM, Figure 6), which measures particle mass concentrations based on the continuous measurement of the pressure drop across a porous membrane filter (Nuclepore  $^{TM}$ ) was used at all sites to determine 5-minute average  $PM_{2.5}$  mass. Pressure drop across the filter is proportional to the particle mass concentration. The filter face velocity is chosen such that pore

obstruction by interception is the dominant cause of particle related pressure drop change over time. The monitor is comprised of a filter tape to collect particles, a filter tape transportation system to allow for several weeks of unassisted particle sampling, a system to measure the pressure drop across the filter, a diffusion dryer to remove particle-bound water, and an air sampling pump. The monitor exposes a new segment of filter tape every 20 to 60 minutes for particle collection. During this period, particles collected on the filter are expected to remain in equilibrium with the sample air since the composition of ambient air is assumed to not vary substantially over this short time period. Volatilization and adsorption errors are expected to be minimized relative to those encountered with discrete samplers, since measurements are made at ambient temperature for short time periods and at low face velocity. This technique maintains a constant gasparticle equilibrium for SVM components of the aerosol after collection on the filter which should theoretically reduce errors due to volatilization of collected particle-phase compounds. Furthermore, since the sample air is passed through a Nafion<sup>TM</sup> diffusion dryer prior to its collection, the method is consistent with the Federal Reference Method (FRM), which requires particle mass to be measured at a relative humidity of 40% to remove particle-bound water. The CAMM method for PM<sub>2.5</sub> has a detection limit of 2 μg m<sup>-3</sup> for a 1-hour mean.

#### **Nitrate**

The Automated Nitrate Monitor developed by Aerosol Dynamics Inc. (Figure 7) was used to measure PM<sub>2.5</sub> nitrate at Riverside. The instrument provides automated measurement of PM<sub>2.5</sub> nitrate concentrations with a time resolution of 10 minutes. Analysis of collected nitrate is accomplished using a similar approach to the manual method that has been used for over twenty years to measure the size distribution of sulfate aerosols (Hering and Friedlander, 1982). However, in the ADI instrument, particle collection and analysis have been combined into a single integrated collection and vaporization cell (ICVC), which facilitates automation. Particles are collected on a metal strip in the ICVC for 8 minutes using a humidified impaction process. Humidification of the sampled air stream eliminates particle rebound from the collection surface without the use of grease (Winkler, 1974 and Stein *et al.*,1994). Interference

from vapors such as nitric acid is minimized by a denuder upstream of the humidifier. At the end of the 8 minute particle collection phase, the cell is purged with clean nitrogen gas and the metal strip is rapidly heated to flash vaporize nitrate from the collected particles into the nitrogen stream. Nitrate is quantified by a chemiluminescent NO<sub>x</sub> analyzer, similar to that described by Yamamota and Kousaka (1994). The integral of the resulting NO<sub>x</sub> peak is proportional to the deposited aerosol nitrate. After a 90 second analysis step, the system returns to sample collection mode, initiating the next 8-min sample at the beginning of the next 10-min period. Additional detail on the development and testing of the ADI nitrate monitor has been reported elsewhere (Hering *et al.*, 1999).

#### **Black Carbon**

An aethalometer was used at all study sites to continuously (5 minute averages) measure black carbon concentrations using light absorption. Black carbon is expected to compare well with EC measured on the quartz filter because elemental carbon is the dominant optically absorbing material in submicron PM (Hansen and Rosen, 1990; Gundel et al., 1984; Hansen et al., 1984; Wolff, 1981, Allen et al., 1999). The aethalometer operates at a flow of 4 L min<sup>-1</sup> and passes ambient air through a quartz-fiber filter tape which is compared optically to a reference portion of the tape to determine the increment of light absorbing material per unit volume of sampled air. At a constant airflow, the deposition rate of BC on the filter is proportional to its mass concentration and gives a corresponding rate of increase of the optical attenuation. This rate of increase is converted to a black carbon concentration by dividing by a conversion factor of 19 m<sup>2</sup> g<sup>-1</sup>. The method is described in further detail elsewhere (Hansen, et al., 1984, Allen et al., 1999). The model AE-16U Aethalometer which measures optical absorption at 880 nm was used in Bakersfield, Chicago, Dallas, Phoenix and Riverside, and the model AE-20UV Aethalometer with a dual channel design that measures BC at 880 nm absorption and also optical absorption at 325 nm in the near ultraviolet was used in Philadelphia. The UV channel responds strongly to species present in fresh diesel exhaust and tobacco smoke, but was not analyzed for this paper.

### Inorganic Gas Measurements

Three inorganic gases (sulfur dioxide, nitric acid, and ammonia) were quantified at the six measurement sites by extracting the HEADS denuders and analyzing by IC. The sodium carbonate denuders captured sulfur dioxide and nitric acid while the citric acid denuder collected ammonia.

# Meteorology and Light Scattering

Continuous temperature, relative humidity, and nephelometry data were collected at all sites except Philadelphia by Air Resource Specialists. These data were averaged over 5-minute periods throughout each study period. Light scattering data were collected with an Optec NGN-2 Ambient Nephelometer equipped with a solar radiation shield and temperature and relative humidity were measured with a Rotronic MP-100F Air Temperature/Relative Humidity Sensor equipped with and aspirated shield. Both instruments were mounted on towers at a height of approximately 4 m above the ground surface. Temperature data from the Rotronic sensor and pressure data from state monitoring sites near the study sites were converted to 24-hour averages to correspond with discrete sampler collection periods. These averages facilitated calculation of pollutant concentrations at ambient temperature and pressure. Overall study site statistics for 24-h temperature and relative humidity averages are summarized in Tables 6 and 7.

# **DATA ANALYSIS METHODOLOGY**

### Sampler Intercomparison

We approached the problem of comparing data from different samplers with two goals: 1) assuring that the samplers were expected to measure the same quantity and 2) investigating whether any observed differences are due to sampler performance and data quality issues, to natural variability in the atmospheric components, or to fundamental differences in the aerosol components actually being measured. In the following section, data from samplers measuring the same observable are intercompared wherever the measurements are expected to be similar. For instance, sulfate in PM is nonvolatile, so sulfate collected on discrete sampler front filter surfaces in different samplers are expected to agree closely. In contrast, nitrate tends to volatilize from Teflon filters under sampling conditions. Sampler air flow rates may impact front filter collection of nitrate. However, backup filters such as nylon or sodium bicarbonate-impregnated glass fibers which chemically bind nitrate and "continuous" monitors which analyze nitrate in situ are expected to quantitatively capture nitrate. Thus, we compare sampler nitrate measurements between samplers only for the sum of front and backup filters in discrete samplers. In the case of nitrate, we also investigate the effectiveness of the Harvard impactor for collecting nitrate and sulfate by comparing HI and HEADS measurements.

# Guide to Analyses

As stated above, the second goal of this report (PM<sub>2.5</sub> sampling methodology testing) is addressed first. Toward this end, we first present discrete sampler intercomparison data including PM<sub>2.5</sub> inorganic ions and carbon and inorganic gases. Collocated samples collected with the same sampler are presented first followed by intercomparisons with other samplers measuring the same observable. Next, we present the results of our analysis of the Harvard Carbon Sampler denuder efficiency whose approach is described below. Then, discrete sampler data are compared to corresponding averages from the continuous samplers to test the performance of these newer sampler systems. Finally, we present calculations of PM<sub>2.5</sub> mass reconstructed from the sum of

individual component concentrations on both daily and study averages as part of the first study objective: characterization of seasonal and geographical variations in PM<sub>2.5</sub> composition and potential implications for use of the FRM mass sampler. Composition analyses from the different study sites are compared and differences in the "snapshot" results are discussed. Each sampler correlation figure includes a statistical summary listing means, medians, and variances for data on days when both samplers produced valid measurements; the Deming regression slope (See Appendix) and intercept and associated standard errors and 95% confidence intervals; and the Spearman and Pearson correlation coefficients. In most cases, each sampler number includes more than one figure if a given sampler intercomparison or other analysis was conducted at more than one site. Figures are labeled with the figure number and a letter denoting the site to which it refers: R = Riverside, C = Chicago, D = Dallas, P = Phoenix, B = Bakersfield, F = Philadelphia. For each correlation analysis performed at two or more sites, there is an additional figure: A = all sites.

### Carbon Field Denuder Tests

Sampling methods for carbon in PM currently suffer from a decided lack of consensus in the scientific and air pollution monitoring communities regarding how best to accurately determine airborne concentrations at the point of sampling. The samplers we employed were intended either to duplicate and intercompare commonly employed sampling techniques or to attempt to improve on the current state of the art.

Denuder systems are sometimes used in carbon samplers to mitigate adsorption of gas-phase organic compounds on quartz filters by reducing the gas-phase organic carbon concentration to which a quartz filter is exposed. A denuder exploits the several orders of magnitude slower diffusion rates of particles compared to gas molecules in air to selectively remove gas-phase compounds from an air stream. To achieve a near 100% removal of gas-phase organic carbon, the time scale for air flow from the denuder inlet to its outlet must be greater than the time scale for diffusion of organic molecules from the air stream to the adsorbent surfaces inside the denuder. In addition, the adsorption process at the air-sorbent interface must be rapid relative to the rate at which diffusive

transport delivers molecules to the interface, and the sorbent must have a very large sorption capacity for the compounds it is designed to remove.

Laboratory measurements of the gas phase organic carbon (OC) removal efficiency of denuders are commonly reported as greater than 99%. However, field sampling conditions tend to degrade denuder efficiency. Like all physical adsorption processes, sorption on activated carbon is governed by a reversible equilibrium – net adsorption occurs during periods of elevated gas-phase concentration, but net desorption begins if the gas-phase concentration drops below the value in equilibrium with OC sorbed on the denuder. This dynamic equilibrium leads to slow transport of organic compounds along the length of the denuder similar to the process used to separate compounds through gas or liquid chromatography. In addition, other atmospheric gases, such as water vapor, may adsorb on the denuder adsorbent surfaces and interfere with OC sorption on the denuder surfaces and decrease its OC removal efficiency.

In our study at Bakersfield, we employed two modified Harvard carbon samplers in addition to the two configurations operated at the other sampling sites. These additional samplers, illustrated in Figure 5, added a Teflon filter to the sampling train immediately after the PM<sub>2.5</sub> cutpoint impactor. The Teflon filters remove particles from the sampled air prior to contact with the denuder or filters. We use the results of these two samplers, one with a denuder and one without, to estimate denuder efficiency as described below.

Denuder efficiency is related to the penetration ratio of organic gases through the denuder,  $\eta$ , which is the ratio of the outlet to the inlet concentration. Efficiency,  $\epsilon$ , is simply  $1-\eta$  or

$$\varepsilon = 1 - \eta = 1 - \frac{C_{g,out}}{C_{g,in}}$$
 (1)

where  $C_{g,out}$  and  $C_{g,in}$  are the gas phase organic compound concentrations at the denuder outlet and inlet, respectively. For laboratory tests with single or multiple known compounds,  $C_{g,out}$  and  $C_{g,in}$  are readily obtained by sampling a portion of the inlet gas and outlet gas with a gas chromatograph or similar instrument. For analytical convenience,  $C_{g,in}$  is normally held constant. Field efficiency tests are complicated by variable inlet

concentrations and organic compound composition and by more difficult quantification of the denuder inlet and outlet concentrations.

The Teflon pre-filter is assumed to remove particles from the air stream before they encounter the front quartz filter, so carbon detected on the quartz filters should only be due to gas-phase OC or volatilized particle-phase OC which pass through the Teflon pre-filter (and denuder in DPF). This assumption is confirmed by elemental carbon analysis of the front quartz filter in the two modified samplers which detected negligible EC on either front quartz filter. At low (significantly smaller than individual organics' saturation vapor pressures) gas-phase OC concentrations, sorption of organics on quartz is generally assumed to be governed by a linear isotherm (Goss, 1993; Storey *et al.*, 1995):

$$m_s = K_q C_g \tag{2}$$

where  $m_s$  is the mass sorbed per unit mass of the sorbent ( $\mu g \, \mu g^{-1}$ ),  $K_q$  is the equilibrium partitioning coefficient ( $m^3 \, \mu g^{-1}$ ), and  $C_g$  is the gas-phase OC concentration ( $\mu g \, m^{-3}$ ). We assume that the sorptive characteristics of the gas-phase OC on quartz during a given 24-hour sampling period is described by a single, constant value of  $K_q$ . Also,  $K_q$  is assumed to be concentration independent over the 24-hour concentration range and insensitive to changes in the mixture of individual gas-phase compounds resulting from preferential sorption in the denuder or on the quartz filters. Based on these assumptions, the gas-phase concentration of quartz-sorbable OC in sampled air can be calculated from the ratio of OC collected on two sequential quartz filters (QFA = front filter and QFB = backup filter) as follows. Combination of mass balance equations on OC in the sampled air before and after it encounters each filter and the equilibrium isotherms (equation 2) for OC in the gas and quartz-sorbed phases on each filter gives the following system of four equations in four unknowns:

$$\frac{C_{QFA}V_{samp}}{M_f} = K_q C_{g,A}$$
 (3)

$$\frac{C_{QFB}V_{samp}}{M_f} = K_q C_{g,B}$$
 (4)

$$C_{g,0} = C_{OFA} + C_{g,A} \tag{5}$$

$$C_{g,A} = C_{OFB} + C_{g,B} \tag{6}$$

where  $C_{QFA}$  and  $C_{QFB}$  are the OC "concentrations" obtained by dividing the OC mass collected on filters QFA and QFB, respectively, by the sample volume  $\left(m_s/V_{samp}\right)$  ( $\mu g \, m^{-3}$ );  $V_{samp}$  is the sampled air volume  $(m^3)$ ;  $M_f$  is the mass of a quartz filter ( $\mu g$ ); and  $C_g$ ,  $C_{g,A}$ , and  $C_{g,B}$  are the gas phase concentrations in the sampled air before it encounters filter QFA, in equilibrium with (leaving) filter QFA, and in equilibrium with (leaving) filter QFB, respectively ( $\mu g \, m^{-3}$ ). Solution of equations 3-6 generates expressions for  $K_q$  and  $C_{g,0}$  in terms of the two known values  $C_{QFA}$  and  $C_{QFB}$ :

$$K_{q} = \frac{V_{\text{samp}}}{M_{f}} \begin{pmatrix} C_{\text{QFA}} / C_{\text{QFB}} - 1 \end{pmatrix}$$
 (7)

$$C_{g,0} = C_{QFA} \left( 1 + \frac{V_{samp}}{M_f K_q} \right)$$
 (8)

The gas-phase OC concentrations calculated using equations 7 and 8 can be used to estimate daily denuder efficiencies using equation 1 with  $C_{g,in} = C_{g,0}$  from the prefiltered, undenuded sampler and  $C_{g,out} = C_{g,0}$  from the prefiltered, denuded sampler. Because the denuder removes a substantial fraction of the gas-phase OC before it reaches the front quartz filter in the denuded sampler and the front quartz filter removes additional OC before the air stream encounters filter the backup filter, the denuded sampler QFB values are close to the lower quantifiable limit and the denuded sampler QFA/QFB ratio is very noisy compared to that for the undenuded sampler. To eliminate this difficulty, we calculate the equilibrium constant for both samplers using the undenuded sampler  $C_{QFA}/C_{QFB}$  in equation 7 and then calculate the  $C_{g,0}$  values for each sampler using the sampler-specific  $C_{QFA}$  data.

# Carbon Sampling

During the past two decades, many attempts have been made to account for the exchange of COCs between the gas and particle phases during collection and analysis of filter samples and to accurately quantify particle-phase organics in the undisturbed atmosphere. Figure 8 illustrates three commonly employed approaches to estimating particle-phase organic carbon concentrations and accounting for volatilization of particle-

phase OC and adsorption of gas-phase organics on the filter media. Sampler configurations (a) and (b) have been used to generate a large body of PM<sub>2.5</sub> carbon data. Both samplers employ a quartz filter (Q) as the primary collection medium for PM<sub>2.5</sub> carbon. The differences between the samplers lies in the methods used to estimate adsorption of gas-phase organics and/or volatilization losses of particle-phase OC collected on filter Q. Sampler (a) uses a parallel filter pack containing an additional quartz filter in series behind a Teflon filter. The Teflon filter collects effectively 100% of the particle phase but allows gas-phase organics to pass relatively undisturbed to the quartz filter (TQ) because of Teflon's low specific surface area (Turpin et al., 1994). Sampler (b) uses a backup quartz filter (QB) in series behind filter Q to estimate the impacts of gas-phase organic adsorption on Q. In these samplers, PM<sub>2.5</sub> OC is often estimated by subtracting OC measured on TQ or QB from Q. This estimation method assumes that 1) adsorption of gas-phase organics on TQ or QB is equal to that occurring on Q and 2) negligible particulate OC volatilizes from filter Q during sampling. As Turpin et al. (1999) note, this estimation method is not universally accepted. Chow et al., (1994, 1996, 1998) expressed uncertainty in the meaning of OC measurements from filters TQ or QB and assumed that adsorption and volatilization from the front filter are either negligible or equal and opposite. They used OC measured on filter Q to calculate PM<sub>2.5</sub> organics.

Other researchers have suggested that sampler (a) may more accurately estimate adsorption of gas-phase OC on filter Q. TQ backup filters have been found to collect 30% to 50% more carbon than a QB filter from a parallel sampler (McDow and Huntzicker, 1990; Turpin *et al.*, 1994). Turpin *et al.* (1999) note that this probably results from the smaller specific surface area of Teflon filters relative to quartz filters. Because quartz filters have surface areas approximately 5 times larger than Teflon filters, they are expected to adsorb substantially more gas-phase organic material than a Teflon prefilter. Thus, a TQ filter is exposed to a higher gas-phase OC concentration than a concurrently

sampled QB filter and would be expected to collect more OC. Based on this argument, sampler (a) would appear to provide the superior estimate of gas-phase adsorption on filter Q. However, many monitoring networks currently employ samplers configured like (b) in Figure 1, so characterization of the potential biases introduced by these samplers has significant value.

Sampler (c) is a modification of sampler (b) which incorporates a VOC denuder upstream of two quartz filters (DQ and DQB). A denuder exploits the several orders of magnitude slower diffusion rates of particles compared to gas molecules in air to selectively remove gas-phase compounds from an air stream. In a sampler configured like example (c), particle phase OC would be estimated as the sum of the organic mass collected on filters DQ and DQB. If the denuder is 100% efficient, no adsorption of gas-phase organics should occur on either quartz filter. However, removal of gas-phase organics from the air stream passing through DQ should enhance volatilization of particle-phase OC according to Le Châtelier's Principle. Addition of the OC mass collected on DQB to that collected on DQ partially accounts for this loss because some fraction of the volatilized OC from DQ would adsorb on DQB.

# **RESULTS**

### Sampler Intercomparisons

### **Sulfate**

Table 8 lists statistics for sulfate concentration data collected on the discrete samplers used in this study. Figures 9 to 31 compare sulfate data collected with the discrete samplers listed in Table 2. With a few exceptions all of the tested samplers, including the FRM-equivalent HI agree within the experimental and analytical uncertainty. Where there is a small but consistent disagreement between methods, for instance between the HEADS and HI in Figures 10 and 11, the results may be related to small flow calibration errors. Some of the samplers operated by BYU seem to have experienced quality assurance problems at Riverside which were corrected at Bakersfield. The most obvious issues occurred with the PC-BOSS as evidenced by a comparison of the –A, -R, and –B versions of Figures 15 to 17. At Riverside, Samplers A and B disagree on both the minor and major flow channels and when the two channels are summed to give total sulfate. Scatter is substantially smaller in the –B figures. This improvement may be due to improved flow control on the major flow channel at Bakersfield. Accurate characterization of the particle concentrator minor-major flow split is hindered if this ratio changes over the course of sample collection with increasing pressure drop as the major flow filter collects small particles. In addition, the PC-BOSS B sampler was modified several times during the Riverside study period to explore issues such as denuder breakthrough. These sampler modifications may have impacted reproducibility of the sampler performance. Collocated ADS and CSS samples showed less scatter in Bakersfield than Riverside and in general were in better agreement than the two BOSS-based samplers. At both sites, the Teflon filter quantitatively collected sulfate with the exception of a few days during the Bakersfield study.

Figures 18 to 31 intercompare the various sulfate samplers. In general, agreement between the samplers operated at both Riverside and Bakersfield improved at Bakersfield much as the agreement between collocated samplers improved. PC-BOSS results tended to underestimate those from other samplers in cases where data scatter was minimized.

This underestimation may be due to small (~5%) but consistent losses of particles from the air stream in the particle concentrator. HEADS sulfate concentrations significantly exceeded ADS and CSS results at Riverside but agreed more closely at Bakersfield. A similar trend occurred for the Big BOSS. At Riverside, HEADS measurements were larger (Figure 29), but at Bakersfield they were slightly smaller: the HEADS – Big BOSS slopes were less than one, although not significantly so, and the intercepts were equivalent to zero in Figure 29B. Finally, the PC-BOSS – HEADS comparisons in Figures 30 and 31 reveal similar characteristics to the other sampler inter-comparisons. However, HEADS concentrations routinely exceeded PC-BOSS measurements at both sites. Regressions on data from all sites as well as from Riverside and Bakersfield individually yield slopes significantly greater than 1. This indicates that the PC-BOSS loses sulfate relative to the HEADS systems, perhaps because of particle concentrator losses discussed above. The underestimate of sulfate is smaller at Riverside than at Bakersfield and smaller using the PC-BOSS minor flow Teflon filter than the minor flow quartz filter.

Figures 41 to 45 compare HEADS sampler sulfate with the BYU samplers. The HEADS – Annular Denuder Sampler and HEADS – ChemSpec correlations were very scattered at Riverside, but both improved markedly at Bakersfield (Figures 41 and 42) Both BYU samplers gave slightly lower sulfate concentrations than the HEADS on average. The Annular Denuder – HEADS slope at Riverside was not significantly different than 1, but both HEADS regressions were greater than 0.8 μg m<sup>-3</sup>. At Bakersfield, the slope was not significantly different than 1 and the intercept was equivalent to zero. The ChemSpec – HEADS correlations at the two cities were similar.

BIG BOSS sulfate results also mirror the trends observed for the BYU Teflon filter-based samplers. As Figure 43 shows, results at all sites are reasonably correlated  $(r_{pearson}) = 0.89$  but the scatter is substantial. The regression slope is 1.14, but this value is not significantly different than unity. Most of the observed scatter is in the Riverside data whose slope is not significantly different than one though there is are significant intercepts for both the Full and Nylon HEADS  $(0.63 \pm 0.44)$  and  $0.51 \pm 0.45$ .

#### **Nitrate**

A statistical summary of PM<sub>2.5</sub> nitrate data from the discrete samplers is given in Table 9. Our discussion of PM<sub>2.5</sub> nitrate results follows the same pattern as the preceding treatment of sulfate sampling results. Analogous observations for nitrate are shown in Figures 32 to 57 starting with comparisons of nitrate concentrations in co-located samplers and ending with sampler inter-comparisons between different samplers.

Total nitrate concentrations calculated from the total of front + backup filters on the two HEADS samplers differ slightly. The regression slope between the two samplers is  $1.14 \pm 0.03$  for all sites together with Full HEADS measuring a higher concentration. Figures 33A and 34A demonstrate that the Teflon filter in Nylon HEADS captures a significantly smaller fraction of the total front + back filter nitrate than that observed in the Full HEADS. Overall, the Full HEADS Teflon filter collected approximately  $0.73 \pm 0.05~\mu g~m^{-3}$  per  $\mu g~m^{-3}$  collected on both the front and backup filters while Nylon HEADS averaged only  $0.15 \pm 0.03~\mu g~m^{-3}$  per  $\mu g~m^{-3}$  collected on the front and backup filters. Though we have explored a few potential explanations for these results, we have not resolved the observed discrepancies in the Teflon filter nitrate collection efficiencies. Loss of nitrate from the Teflon front filter was greatest at the warmest site and lowest at the colder sites.

Figures 35 to 38 compare HEADS nitrate values with nitrate measured on the Harvard Impactor. The comparisons in Figures 35 and 36 show total nitrate data from front and backup filters of the Full and Nylon systems. As the figures show, data from all sites give a regression slope of  $0.91 \pm 0.05$  for Full HEADS and  $1.04 \pm 0.05$  for Nylon HEADS. Individual site regression lines for Full HEADS all have slopes below one except for Riverside indicating an apparently greater collection efficiency for nitrate on the HI than the HEADS. The Nylon HEADS individual site slopes are all closer to one except for Riverside whose slope was  $1.37 \pm 0.28$ . Intuitively, the Harvard Impactor should measure less nitrate than the HEADS samplers because it uses no backup filter to capture volatilized nitrate. The results indicate that nitrate losses from FRM-type samplers may be relatively small except in areas with high nitrate concentrations and high temperatures. The following two figures (37A and 38A) show the same comparisons as Figures 35 and 36, respectively, for all sites except the HEADS data

show only front filter values. In this case, both HEADS samplers collected much less nitrate than the HI. The lower HEADS nitrate values seen at all sites were expected because of the removal of gas-phase nitric acid from the sampling stream by the HEADS denuder. With the nitric acid removed, Le Châtelier's principle would cause large volatilization of nitrate from the HEADS front filters. Without removal of the nitric acid, nitrate collected on the HI seems more stable except under high nitrate, high temperature conditions such as those experienced at Riverside. In light of these results, two explanations for the HI – total HEADS nitrate comparisons discrepancies are possible: 1) the HI nitrate values are biased high due to the interference of gas-phase nitric acid or 2) volatilization of PM<sub>2.5</sub> nitrate from the undenuded HI was small compared to that which volatilized from the denuded HEADS Teflon filters and passed uncollected through the backup filters.

Figures 39 to 45 compare results from identical collocated samplers operated at Riverside and Bakersfield by BYU. For the ADS and CSS, the collocated samplers agreed with regression slopes near unity with the two sites taken together and almost exactly one for just Bakersfield data. This may be related to the similar trends observed in the sulfate data: sampler flow control problems at Riverside. Both of these samplers collected a larger fraction of total nitrate on their front Teflon filters than did the HEADS samplers. Figures 43 and 44 compare total nitrate results from collocated PC-BOSS samplers. The samplers agree with some scatter but regression slopes not significantly different than 1. The PC-BOSS nitrate data were less scattered than those for sulfate at Riverside. The following four figures (45A to 48A compare individual components of the PC-BOSS systems. Major flow nitrate values agree with some scatter (Pearson correlation of 0.84). The quartz and Teflon minor flow channels on PC-BOSS A have little scatter, but there is an apparent bias toward higher values on the Teflon channel (slope = 0.91). Figures 46 and 47 show nearly total collection of nitrate on the front (quartz or Teflon) filters in the minor flow path. This contrasts with the HEADS and even the ADS and CSS results, but may be attributable to the effects of the particle concentrator.

The remaining figures in this subsection show sampler nitrate intercomparisons. As Figure 49 demonstrates, the ADS/CSS regression slope for total nitrate is 0.89 with larger ADS values. This trend occurred at both study sites. PC-BOSS total nitrate (minor + major flow quartz filters + minor flow Empore) nitrate collection was significantly less than the Annular Denuder Sampler Teflon + nitrate collection filter at both Riverside and Bakersfield (Figure 50). Similar results were observed for PC-BOSS minor flow Teflon + major flow quartz + minor flow nylon nitrate (Figure 51): the regression slopes were 0.73 and 0.69, respectively for the quartz and Teflon minor flow channels. Similar results were observed for the CSS – PC-BOSS comparisons, but the regression slopes were closer to 1 as shown in Figures 52 and 53. This improved agreement is likely due to the lower levels of nitrate collected on CSS relative to ADS. The ADS/HEADS regressions shown in Figure 54 are relatively scattered in Figure 54R, but cleaner in Figure 54B. In both cases, the regression slope was less than one for Full HEADS (ADS larger) and greater than one for Nylon HEADS (ADS smaller). For CSS, Full HEADS agreed closely, but Nylon HEADS has a regression slope of 1.21 in Figure 55A. Comparisons of the HEADS samplers with total PC-BOSS nitrate (Figures 56 and 57) based on both the Teflon and quartz minor flow channels gives the same results observed above for the ADS and CS comparisons with PC-BOSS. Both HEADS samplers give significantly larger nitrate concentrations: based on the quartz minor flow channel, the all sites regression slopes for Full and Nylon HEADS are  $1.24 \pm 0.05$  and  $1.44 \pm 0.05$ , respectively. PC-BOSS Teflon minor flow channel-based regression slopes are slightly higher (1.29  $\pm$  0.05 and 1.50  $\pm$  0.06, respectively for Full and Nylon HEADS).

### **HEADS Ion Balances**

Ammonium concentrations at the study sites are summarized in Table 10. Figures 58 to 61 present ion balances from Full and Nylon HEADS samples on a daily basis at each of the sites. The ion balance for Full HEADS front filters (Figure 58) at all sites has a regression slope of  $0.99 \pm 0.02$  and a Pearson correlation coefficient of 0.98. The Nylon HEADS front filter ion balance (Figures 59) is slightly skewed toward extra cations: the slope is  $1.17 \pm 0.03$ . Only the HEADS ion balance for front + backup filters

and backup filters alone are shown (Figures 60 and 61) because Nylon HEADS does not include a backup filter for ammonium. Figures 60 and 61 demonstrate that backup filter collection in Full HEADS leave room for improvement. Correlation coefficients in both figures are low, and the regression slopes strongly favor cations (mainly ammonium) over anions (mainly nitrate). These difficulties may be linked to improper estimation of collected volatilized nitrate from the F2 and F3 filters in Full HEADS. The backup filter system on Full HEADS seems to fail to completely account for nitrate volatilized from the front filter since the ammonium / nitrate correlation on this filter is dramatically skewed toward higher ammonium concentrations as shown in Figure 61.

#### **HSPH Carbon Denuder Field Tests at Bakersfield**

Figures 62B and 63B show the differing collection rates of organic carbon on the front quartz filters of the denuded and undenuded samplers operated at Bakersfield with Teflon prefilters (DPF and UPF, respectively). Since the prefilter removes the particle phase, the differences in front filter OC collection between DEN and DPF (in Figure 62) and between UND and UPF (in Figure 63B) give a qualitative assessment of the denuder's ability to prevent gas-phase OC adsorption on a quartz filter. The regression slope in Figure 62B is  $0.12 \pm 0.06$  while that in Figure 63B is  $0.29 \pm 0.05$ . Similarly, in Figure 64B which compares Q<sub>a</sub> OC collection in DPF and UPF, the regression slope is  $0.52 \pm 0.11$  with UPF values larger. We used equations 7 and 8 to estimate both the gasfilter adsorption equilibrium constant for quartz and the denuder efficiency (E) on each study day. Figures 65B to 68B illustrate the impacts of changing temperature and relative humidity on calculated denuder efficiencies and equilibrium constants (K<sub>q</sub>), respectively. No clear effect of meteorological conditions on the calculated denuder efficiency can be discerned although denuder efficiency may increase slightly with increasing relative humidity. These results are not surprising because other factors such as changes in the daily composition of gas phase OC may confound identification of weather based effects. The increased denuder efficiency with humidity may be due to

increased capture of oxygenated organics in water sorbed on the denuder surfaces. The denuder efficiency estimates shown in Figures 67B and 68B average 68.2% with a median of 70.6%.

We close the discussion of our denuder efficiency tests by emphasizing that the foregoing analysis represents an explanation of denuder and quartz collection characteristics using unprecedented, yet empirical experiments. The results underscore the message that despite widespread and long-standing use of quartz filters (both with and without denuders) for sampling total particle-phase carbon, their sampling characteristics remain fraught with conjecture. The only way to definitively elucidate the sampling characteristics of quartz filters and denuders is to measure the molecular composition of what they sample (gas and particle phase) using techniques that can quantify compounds with a wide range of polarities.

#### Carbon

A statistical summary of PM<sub>2.5</sub> carbon data from the discrete samplers is given in Tables 11 and 12. Figures 69 to 74 compare the sampler results for elemental carbon at the study sites. As Figure 69 shows, the two Harvard carbon samplers operated at all sites agree closely. None of the sites had a regression slope significantly different than 1, though most sites had slopes slightly greater than 1 with UND concentrations being higher. This slight bias toward the undenuded sampler indicates the potential for small losses of EC in the denuder. Collocated Big BOSS and PC-BOSS total EC measurements showed more scatter than expected for a nonvolatile, relatively inert PM<sub>2.5</sub> constituent. The PC-BOSS Riverside correlation was the only single site comparison with a correlation coefficient greater than 0.5. It is possible that either the flow control problems highlighted in the inorganic ions section above or perhaps some analytical difficulties in distinguishing EC from total carbon contributed to these results.

As expected based on the scatter in the Big BOSS and PC-BOSS results, the Harvard Carbon Sampler / BOSS comparisons were very noisy as shown in Figures 73 and 74. The concentrations measured on the UND and DEN samplers were significantly lower than those on either Big BOSS or PC-BOSS (regression slopes for UND were  $0.62 \pm 0.21$  with Big BOSS higher and  $0.68 \pm 0.18$  with PC-BOSS higher. It is worth noting

that BYU and Harvard used different analytical techniques with different arbitrary thermal analysis cutpoints for defining EC, so the discrepancies shown in Figures 73 and 74 may not be sampler related.

Figures 75 to 83 show similar comparisons for these samplers' measurements of total carbon (TC). The UND sampler  $Q_a$  filter collected more TC than DEN (regression slope =  $1.09 \pm 0.04$ ) at all sites as shown in Figure 129. This is expected since the denuder in DEN removes some fraction of the gas-phase carbon that might otherwise sorb on  $Q_a$ . Additionally, the removal of gas-phase carbon may enhance volatilization of organics from DEN  $Q_a$  in the same manner as we discussed previously for nitrate in a denuded sampler. This expectation is consistent with the results shown in Figure 76.  $Q_b$  TC is larger for UND than DEN because DEN  $Q_b$  should be exposed mainly to volatilized OC from  $Q_a$  while UND  $Q_b$  is exposed to any gas-phase OC not sorbed by  $Q_a$ . Comparison of the three available methods of determining TC from the front and back filter measurements (corresponding to methods a, c, and d in Figure 8) shown in Figure 77 indicates that using the sum of  $Q_a$  and  $Q_b$  in the DEN sampler (method d) gives similar results to using only  $Q_a$  from UND (method a). Method b (UND  $Q_a - Q_b$ ) gives significantly smaller concentrations.

Analysis of collocated BIG BOSS TC data (Figure 78) reveals a significant bias at Bakersfield. Riverside data show relatively close agreement. Collocated PC-BOSS data are somewhat scattered but unbiased at both sites as shown in Figures 79 and 80. PC-BOSS results give lower TC concentrations than Big BOSS at all sites (regression slope =  $0.78 \pm 0.20$ ), but the data are scattered as shown in Figure 81. Comparison of the two BOSS samplers with UND and DEN (Figures 82 and 83) results in the same trend seen for EC above: the BYU samplers collected significantly more carbon. These results could be due to volatilization losses in the HSPH samplers or to positive errors in the BOSS data due to penetration of gas-phase OC through the denuder followed by essentially quantitative collection on the Empore filter. Our results presented here and in the previous subsection on denuder performance highlight the important need for improved analytical techniques for carbon in PM<sub>2.5</sub>. The greater than 50% variability in

estimates of PM<sub>2.5</sub> carbon could have substantial impacts on health risk assessments and design of effective concentration reduction strategies.

## Inorganic Gases

Tables 14, 15, and 16 summarize sulfur dioxide, nitric acid, and ammonia measurements, respectively made at the six study sites. Figure 84 compares HEADS denuder measurements of gas-phase nitric acid. At all sites except Bakersfield, the 24-h average nitric acid concentrations were below 5 ppb and the two HEADS systems were in close agreement. At Bakersfield, both samplers measured much higher nitric acid concentrations – a peak of more than 300 ppb for Full HEADS and slightly less than 200 ppb for Nylon HEADS. Though the sampler agreement was poor, there was a reasonable correlation between the measurements at Bakersfield indicating possible fractional breakthrough on the Nylon HEADS denuder. We are unsure of the origin of the elevated nitric acid concentrations here. The time series reveals several very high concentration episodes which may be correlated to precipitation or other meteorological events. Oil pumps in the area are generally powered by small natural gas generators which may contribute significant nitrogen oxide concentrations.

Figures 85 and 86 present gas-particle partitioning of nitric acid and PM<sub>2.5</sub> nitrate based on denuder and front + backup filter HEADS measurements. In general, there was very little correlation between gas-phase nitric acid and PM<sub>2.5</sub> nitrate at any of the sampling sites. Gas-phase nitric acid concentrations were lower than PM<sub>2.5</sub> nitrate at all sites except Riverside and Bakersfield. At Riverside, the average concentrations were similar, but the data exhibit significant scatter. At Bakersfield, the aforementioned large nitric acid concentrations were one to two orders of magnitude larger than the PM<sub>2.5</sub> nitrate values.

Table 15 summarizes ammonia measurements in this study. Figure 87 compares HEADS denuder measurements of gas-phase ammonia. With the exception of a few days at Bakersfield, the 24-h average ammonia concentrations measured by the two HEADS systems were in close agreement. At Bakersfield, the Nylon system detected four near-zero concentration days.

Figure 105 present gas-particle partitioning of ammonia and PM<sub>2.5</sub> ammonium based on denuder and front + backup filter Full HEADS measurements. The Nylon HEADS had no backup filter for ammonium, so its data are not reported here. In general, the gas-particle correlations were closer to one for ammonia than for nitrate, although the ammonia correlation was also very scattered in Dallas and Chicago where concentrations were very low. Gas-phase ammonia concentrations were higher than PM<sub>2.5</sub> ammonium at all sites where a significant correlation existed. The largest ammonia concentrations were measured at Riverside and Bakersfield which is not surprising in light of the agricultural activities near these sites.

### Continuous Sampler Tests

#### PM2.5 Mass

Figure 89 compares  $PM_{2.5}$  mass measurements by CAMM and Harvard Impactor (HI). The samplers agree closely. CAMM and HI are correlated with  $r_{pearson}$  and  $r_{spearman}$  both greater than 0.91 at all study sites. CAMM measurements averaged 6% greater than HI mass measurements at all sites (based on the zero-intercept regression slope). The average offset (y-intercept with CAMM on the y-axis) was only slightly larger than its 95% confidence interval. The zero-intercept slope was less than 1 (0.99) only at Phoenix which was also the only site with a significant y-intercept.

#### **Nitrate**

Figure 90R compares HEADS nitrate with 23.5-h average concentrations from the ADI nitrate sampler for 15 days at Riverside. Pearson correlations between ADI and HEADS are greater than 0.96. The Full HEADS total nitrate vs. ADI regression line slope was significantly less than one with a non-zero intercept, but the nylon HEADS slope was equivalent to one with a zero intercept. The time series shows close replication of the nitrate peaks and valleys during the sampling period. Figures 91R and 92R compare averaged ADI results with the BYU discrete nitrate samplers. As with HEADS, ADS, CSS, and PC-BOSS are closely correlated with the ADI data. However, all three BYU samplers underpredict nitrate concentrations relative to the ADI sampler. This

result is consistent with the disagreements between HEADS and these samplers noted above in the discrete sampler testing section.

#### Carbon

Figure 93 compares front filter EC from the UND HSPH carbon sampler with 24-h average black carbon concentrations from the aethalometer. Combination of the data from all sites gives a Pearson correlation coefficient of 0.97 and a regression slope of  $1.26 \pm 0.05$  for the undenuded sampler. Individual sampling site regression slopes fall within the 95% confidence interval for the entire data set with the exception of Dallas where the slope was significantly steeper. The concentrations observed at Dallas were somewhat lower than the other sites, and the data are more scattered, so this result may be a sampling artifact.

### **Light Scattering**

The nephelometer-HI comparison in Figure 94 shows substantial scatter the study overall. However, at each individual site the correlation coefficients for HI mass and the scattering coefficient were somewhat closer to one. Significant differences in the regression slopes occurred between Riverside and both Chicago and Bakersfield. Phoenix was not significantly different than Riverside or the other sites. Dallas had an extremely low regression slope with a significant y-intercept. These observations may be linked to the low PM<sub>2.5</sub> concentrations that occurred during the study period at this site.

### Continuous PM<sub>2.5</sub> Sampler Correlations

Figures 95 and 96 intercompare hourly averages of data from the continuous samplers. Figure 95 show the correlation between CAMM PM<sub>2.5</sub> mass and aethalometer black carbon (and ADI nitrate at Riverside). Correlation coefficients ( $r_{pearson}$ ) for the aethalometer-CAMM comparisons in Figure 95 vary between a low of 0.32 at Riverside and a high of 0.75 at Phoenix. Riverside and Bakersfield had the smallest fractions of PM<sub>2.5</sub> mass attributable to black carbon. As Figure 96 illustrates, 1-hour average CAMM mass and nephelometer  $b_{scat}$  measurements were correlated with  $r_{pearson}$  greater than 0.7 at all sites except Dallas. As discussed above, Dallas presented extremely low particle concentrations throughout our study period. The individual site Deming regression

slopes on these plots vary between approximately 0.04 and 0.2 for CAMM-aethalometer data and between approximately 2.5 and greater than 9 for the CAMM-nephelometer correlation. All sites except Phoenix had slopes lower than 0.1. It appears unlikely that a coherent correlation between light scattering or PM<sub>2.5</sub> black carbon and CAMM mass would exist over longer periods or for combined data collected under different geographical or seasonal conditions.

# PM<sub>2.5</sub> Speciation

Figures 97 to 104 illustrate the differences in PM<sub>2.5</sub> composition between the sampling sites using the four different algorithms for calculating the reconstructed mass described in the footnotes to Table 16 which also summarizes our PM<sub>2.5</sub> measurements at the six sites. In many cases (particularly at Riverside and occasionally at Dallas), the daily sum of the chemical constituents was significantly greater than the Harvard Impactor total PM<sub>2.5</sub> mass, sometimes by a factor of two or more. In contrast, the sum of the speciated masses at Chicago, Bakersfield, Phoenix, and Philadelphia were predominantly lower than the HI mass. The reconstructed PM<sub>2.5</sub> mass at Philadelphia omits crustal and other trace element contributions because XRF data were not available. Bakersfield and Phoenix both had very small sulfate concentrations but some of the largest negative differences between reconstructed mass and HI measured mass. This is somewhat counterintuitive since sulfate in PM<sub>2.5</sub> is nonvolatile and thus reproducibly measured by both the HI and the speciated samplers. Similarly, Phoenix PM<sub>2.5</sub> was on average more than 50% organics and 15% nitrate, both volatile species expected to be underrepresented by an FRM-like sampler such as the HI. Bakersfield had even larger nitrate concentrations and similar organic concentrations.

It is possible that the effects of relatively cool, damp weather conditions at these sites cancelled out those of the relatively volatile chemical composition of the  $PM_{2.5}$  during the study periods. The final four sets of figures (105 to 108) show relationships between average and peak 1-h temperature and relative humidity And the relative disagreements between HI and reconstructed mass based on algorithm 4 (Table 16 footnote). We also explored correlations between individual  $PM_{2.5}$  component concentrations and the HI-recon4 value, but found none that were statistically significant.

Based on the results in Figures 105 to 108, there may be a negative correlation between temperature and the "unidentified" mass and a slightly stronger positive correlation with relative humidity. Both results are intuitively reasonable since increasing humidity is expected to increase the  $PM_{2.5}$  mass that would not be accounted for by chemical speciation analysis. Increasing temperature is likely to enhance volatilization of organics and nitrate form the HI and thus lead to a more negative difference between the HI and reconstructed masses.

## **CONCLUSIONS**

This study provides "snapshot" data on PM<sub>2.5</sub> mass and chemical component concentrations in 6 U.S. cities for approximately one month at each site. In addition, the PM<sub>2.5</sub> speciation sampler inter-comparisons generate important topics for discussion and hopefully future improvement of PM<sub>2.5</sub> sampling techniques. Finally, analysis and comparison of data from the various samplers allows estimation of the potential errors associated with PM sampling based on single Teflon filter technology.

PM<sub>2.5</sub> speciation data based on HSPH sampler measurements at the study sites challenge some widely held paradigms regarding particulate matter composition in the United States. Sulfate is typically assumed to account for about one third of the mass of PM<sub>2.5</sub>. The results of studies, such as SEAVS, in rural areas of the United States have reinforced this assumption. Furthermore, these studies reported a significantly lower fraction of particle-phase organics – approximately 13% in SEAVS – and negligible contributions from nitrate. In contrast to the rural PM<sub>2.5</sub> data, the largest sulfate fraction measured was 36% at Philadelphia, but the next highest fractions were 19% at Chicago, 15% at Dallas, and 13% at Riverside. The other western cities (Bakersfield and Phoenix) had sulfate fractions smaller than 6%. Organics comprised a much larger fraction of PM<sub>2.5</sub> at all sites sampled, ranging from 36% at Chicago to 54% at Phoenix and Philadelphia. Nitrate was also a more dominant PM<sub>2.5</sub> component: about 12% in Dallas; more than 15% in Riverside, Chicago, Philadelphia, and Phoenix; and almost 29% in Bakersfield. Only Philadelphia had a trivial contribution from nitrate: 2.9%.

The increased relative importance of potentially volatile PM<sub>2.5</sub> components (nitrate and organics) observed in this study highlights the potential pitfalls of PM<sub>2.5</sub> mass samplers which rely on a single, undenuded Teflon filter with no backup filter. Such samplers are suspected to lose a substantial fraction of PM<sub>2.5</sub> nitrate during sampling and equilibration of the filters prior to weighing. We observed losses of nitrate from the HI of less than 10% on a whole study average of the nitrate collected on the Nylon HEADS. The largest losses (approximately 35% of the Nylon HEADS nitrate) were observed in Riverside where nitrate concentrations were relatively high and ambient temperatures

were elevated. The other sites experienced little or no nitrate loss on the HI. Thus, In sites where the nitrate fraction is substantial and temperatures are higher, it is possible that this volatilization could lead to errors on the order of 10% in the quantification of PM<sub>2.5</sub> mass and relative contribution of other components to the total mass observed. Loss of organics from Teflon filters is less well understood. Teflon has a low adsorption capacity for most organics (relative to quartz of carbon impregnated filters). Thus, Teflon filters are not likely to significantly trap organic compounds which volatilize from collected particles. For the same reason, they are also unlikely to capture much gas phase organic material during sampling. Some loss of PM<sub>2.5</sub> OC is likely while the filter is equilibrated in preparation for weighing, but this effect has not been quantified.

This study also highlights PM<sub>2.5</sub> sampling issues which merit additional research. Foremost among these is the sampling of organic compounds. Our investigation of denuder efficiency in Bakersfield reveals that carbon-impregnated filter paper denuders may not be as efficient as originally thought at removing gas-phase organics from the sampled air stream before they encounter the filter media. This observation highlights the need for a more robust sampling system for carbon in airborne particles that measures the gas-particle partitioning as it exists in an unperturbed air parcel. In currently employed sampling systems, uncertainties in denuder efficiency for removing gas-phase organics and in collection efficiency of quartz or other filter media for particle-phase organics severely hinder accurate characterization of OC in PM<sub>2.5</sub>. OC quantification depends strongly upon the sampler configuration and the assumptions used to infer a "total" particle-phase OC concentration. In the published literature, different investigators tend to use different assumptions which may lead to markedly varied results. Our work indicates that the best available sampling technology for OC may be an undenuded quartz filter. In such a sampling system, volatilization of PM<sub>2.5</sub> OC during sampling should be minimized because the gas-particle equilibrium present in ambient air is not perturbed during sampling by removing the gas phase in a denuder. Adsorption of gas-phase OC on the undenuded quartz filter may introduce an error leading to over estimation of particle-phase OC. However, this effect could be accounted for using a quartz filter following a Teflon pre-filter (Turpin et al., 1994). The Teflon filter would

remove particle-phase OC, so any OC measured on the following quartz could be attributed to gas-phase adsorption and thus subtracted from the OC measured on the undenuded quartz filter without a prefilter.

Revision of our understanding of the composition of PM<sub>2.5</sub> has additional implications beyond accurate sampling of the airborne aerosol mass. Because the various components of PM<sub>2.5</sub> have different dominant sources, accurate characterization of aerosol composition is necessary to design effective emission reduction strategies.

In summary, our results indicate that EPA's FRM for PM<sub>2.5</sub> sampling does have significant limitations. It cannot assess the chemical composition of the collected aerosol and it may be susceptible to sampling errors based on gas-particle partitioning of volatile organics and nitrate under certain conditions. In high nitrate areas, a significant potential for underestimation of PM<sub>2.5</sub> mass concentrations exists. Additionally, if chemical speciation were performed on FRM samples in an effort to identify sources of elevated PM levels, the loss of volatile material is likely to lead overestimation of the importance of nonvolatile components such as sulfate and elemental carbon while underestimating organics and nitrate. Clearly, care must be taken in interpreting FRM PM<sub>2.5</sub> sampling data and using them to design and implement effective and rational PM mitigation strategies.

## REFERENCES

- Allen, G.; Lawrence, J.; Koutrakis, P. Field validation of a semi-continuous method for aerosol black carbon (aethalometer) and temporal patterns of summertime hourly black carbon measurements in Southwestern PA, *Atmospheric Environment*, 1999, 33, 817-823.
- Chow, J.C.; Watson, J.G.; Pritchett, L.C.; Pierson, W.R.; Frazier, C.A.; Purcell, R.G.
  The DRI thermal/optical reflectance carbon analysis system: description, evaluation
  and applications in U.S. air quality studies, *Atmospheric Environment*, 1993, 27A,
  1185-1201.
- Chow, J.C.; Watson, J.G.; Fujita, E.M.; Lu, Z.; Lawson, D.R.; Ashbaugh, L.L.
   Temporal and spatial variations of PM<sub>2.5</sub> and PM<sub>10</sub> aerosol in the Southern California Air Quality Study, *Atmospheric Environment*, 1994, 28, 2061-2080.
- Chow, J.C.; Watson, J.G.; Lu, Z.; Lowenthal, D.H.; Frazier, C.A.; Solomon, P.A.; Thullier, R.H.; Magliano, K.L. Descriptive analysis of PM<sub>2.5</sub> and PM<sub>10</sub> at regionally representative locations during SJVAQS/AUSPEX, *Atmospheric Environment*, 1996, 30, 2079-2112.
- Chow, J.C.; Zielinska, B.; Watson, J.G.; Fujita, E.; Richards, H.W.; Neff, W.; Dietrich, D.; Hering, S. Northern Front Range Air Quality Study, Volume A: Ambient Measurements, DRIU Document No. 6580-685-8750.2F2, Desert Research Institute: Reno, Prepared for Colorado State University and EPRI, 1998.
- Cui, W.; Eatough, D.J.; Eatough, N.L. Fine particulate organic material in the Los Angeles basin – I: assessment of the High-Volume Brigham Young University organic Sampling System, BIG BOSS, *Journal of the Air and Waste Management* Association, 1998, 48, 1024-1037.
- 7. Deming, W.E. *Statistical Adjustment of Data*, John Wiley and Sons, New York, **1943**.

- 8. Eatough, D.J.; Sedar, B.; Lewis, L.; Hansen, L.D.; Lewis, E.A.; Farber, R.J. Determination semivolatile organic compounds in particles in the Grand Canyon area, *Aerosol Science and Technology*, **1989**, *10*, 438-439.
- 9. Eatough, D.J.; Aghdaie, N.; Cottam, M.; Gammon, T.; Hansen, L.D.; Lewis, E.A.; Farber, R.J. Loss of semivolatile organic compounds from particles during sampling on filters, in *Transactions, Visibility and Fine Particles*, Matthai, C.V., ed.; Air and Waste Management Association: Pittsburgh, PA, **1990**, pp. 146-156.
- 10. Eatough, D.J.; Tang, H.; Cui, W.; Machir, J. Determination of the size distribution and chemical composition of fine particulate semivolatile organic material in urban environments using denuder diffusion technology, *Inhalation Toxicology*, **1995**, *7*, 691-710.
- 11. Eatough, D.J.; Obeidi, F.; Pang, Y.; Ding, Y.; Eatough, N.L.; Wilson, W.E. Integrated and real-time diffusion denuder sampler for PM<sub>2.5</sub>, *Atmospheric Environment*, **1999**, *33*, 2835-2844.
- 12. Ellestad, T.J.; *et al.* Acid aerosol measurement intercomparisons: an outdoor smog chamber study, in: *Proceedings of the 1991 USEPA/AWMA International Symposium on Measurement of Toxic and Related Air Pollutants*, USEPA report # EPA/600/9-91/018, **1991**.
- 13. Goss, K.-U. Adsorption of organic vapors on ice and quartz sand at temperatures below 0 °C, *Environmental Science and Technology*, **1993**, 27, 2826-2830.
- 14. Gundel, L.A.; Dod, R.L.; Rosen, H.; Novakov, T. The relationship between optical attenuation and black carbon concentration for ambient and source particles, *Science of the Total Environment*, **1984**, *36*, 197-202.
- 15. Hansen, A.D.A.; Rosen, H. Individual measurements of the emission factor of aerosol black carbon in automobile plumes, *Journal of the Air and Waste Management Association*, **1990**, *40*, 1654-1657.

- 16. Hansen A.D.A.; Rosen, H.; Novakov, T. The aethalometer an instrument for the real-time measurement of optical absorption by aerosol particles, *Science of the Total Environment*, **1984**, *36*, 191-196.
- 17. Hering, S.; Stolzenburg, M.; Kreisberg, N. *Automated Nitrate and PM*<sub>2.5</sub> *FRM Measurements for Method Evaluation and Secondary Aerosol Characterization during SCOS'97*, Final Report for EPRI Contract WO915203/CRC Contract A-22, Aerosol Dynamics Inc.: Berkeley, CA, **1999**.
- 18. Hering, S.; Friedlander, S.K. Origins of Sulfur Size Distributions in the Los Angeles Basin, *Atmospheric Environment*, **1982**, *16*, 2647-2656.
- 19. Koutrakis, P.; Wolfson, J.M.; Slater, J.L. Evaluation of an annular denuder/filter pack system to collect acidic aerosols and gases." *Environmental Science and Technology*, **1988**, 22, 1463-1468.
- 20. Lioy, P.J., Wainman, T. An intercomparison of the indoor air sampling impactor and the dichotomous sampler for a 10μm cut size, *Journal of the Air Pollution Control Association*, **1988**, *38*, 668-669.
- 21. Marple, V.A.; Rubow, K.L.; Turner, W. Low flow rate sharp cut impactors for indoor air sampling: design and calibration, *Journal of the Air Pollution Control Association*, **1987**, *37*, 1303-1307.
- 22. Marple, V.A., Liu, B.Y.H., Burton, R.M. High-volume impactor for sampling fine and coarse particles, *Journal of the Air and Waste Management Association*, **1990**, 40, 762-767.
- 23. McDow, S.R.; Huntzicker, J.J. Vapor adsorption artifact in the sampling of organic aerosol: face velocity effects, *Atmospheric Environment*, **1990**, *24A*, 2563-2571.
- 24. Office of Research and Development, USEPA. *Determination of the Strong Acidity of Atmospheric fine-particles* (<2.5 μm) using Annular Denuder Technology, Produced by the AREAL, ORD, USEPA, RTP, NC. Revision 0. Report # EPA/600/R-93/037, **1992**.

- 25. Saxena, P.; Hildemann, L.M. Water–soluble organics in atmospheric particles: a critical review of the literature and application of thermodynamics to identify candidate compounds, *Journal of Atmospheric Chemistry*, **1996**, *24*, 57-109.
- 26. Sioutas, C.; Koutrakis, P.; Burton, R.M. A high-volume small cutpoint virtual impactor for separation of atmospheric particulate from gaseous pollutants, *Particulate Science and Technology*, **1994**, *12*, 207-221.
- 27. Storey, J.M.E.; Luo, W.; Isabelle, L.M.; Pankow, J.F. Gas/solid partitioning of semi-volatile organic compounds to model atmospheric solid surfaces as a function of relative humidity 1. Clean quartz, *Environmental Science and Technology*, **1995**, 29, 2420-2428.
- 28. Turpin, B.J.; Huntzicker, J.J.; Hering, S.V. Investigation of organic aerosol sampling artifacts in the Los Angeles basin, *Atmospheric Environment*, **1994**, 28, 3061-3071.
- 29. Turpin, B.J.; Saxena, P.; Andrews, E. Measuring and simulating particulate organics in the atmosphere, *Atmospheric Environment* **1999**, submitted July, 1999.
- 30. Wolff, G.T. Particulate elemental carbon in the atmosphere, *Journal of the Air Pollution Control Association*, **1981**, *31*, 935-938.
- 31. Yamamoto M.; Kosaka H. Determination of nitrate in deposited aerosol particles by thermal decomposition and chemiluminesence, *Analytical Chemistry*, **1994**, *66*, 362-367.

## **APPENDIX: DEMING REGRESSION**

Linear regression compares data from two sets of observations and determines the slope and y-axis intercept of the best fit line through the data. When comparing data obtained from two methods of measuring a single observable, the slope give information about the relative error between the methods while the intercept provides insight into any constant offset between them. Standard linear regression analyses determine best-fit line parameters by minimizing the sum of the squared differences (residuals) between observed data points and the line in the vertical (y-axis) direction. This method relies on two assumptions 1) one of the methods (that plotted on the x-axis) has no associated error in its measurements (i.e. it is a reference method) and 2) the residuals are randomly distributed (independent of the x and y values). If the method designated as the reference method is changed (x and y values are swapped), the calculated best-fit relationship between the variables will change.

A more appropriate approach to determining regression coefficients in cases where neither data set is free of experimental errors (i.e. there is no absolute reference method) is to minimize the distance between each data point and the regression line in the direction perpendicular to the best fit line. A method for this approach was described by Deming (1943). The slope of the best fit line is

$$m = \frac{S + \sqrt{S + S_{xy}^2}}{S_{xy}}$$

and the intercept is

$$b = \langle y \rangle - m \langle m \rangle$$

where

$$S = \frac{S_y - S_x}{2}$$

<y> and <x> are the means of the two data sets, <y $^2>$  and <x $^2>$  are the averages of the squared data given by

$$\left\langle \mathbf{y}^{2}\right\rangle =\frac{1}{n}\sum \mathbf{y}_{i}^{2}$$

$$\langle x^2 \rangle = \frac{1}{n} \sum x_i^2$$

and  $S_y,\,S_x,\,$  and  $S_{xy}$  are the data set variances given by

$$\mathbf{S}_{\mathbf{y}} = \left\langle \mathbf{y}^2 \right\rangle - \left\langle \mathbf{y} \right\rangle$$

$$\mathbf{S}_{\mathbf{x}} = \langle \mathbf{x}^2 \rangle - \langle \mathbf{x} \rangle$$

$$S_y = \langle xy \rangle - \langle y \rangle \langle x \rangle$$

The slope of the line passing through the origin (b = 0) is given by

$$m = \frac{T + \sqrt{T + \langle xy \rangle^2}}{\langle xy \rangle}$$

where

$$T = \frac{\left\langle y^2 \right\rangle - \left\langle x^2 \right\rangle}{2}$$

and

$$\langle xy \rangle = \frac{1}{n} \sum x_i y_i$$

## **TABLES**

 Table 1
 Summary of sampling dates and sampling locations for the 6 study sites.

Site	Sampling Dates	Site Location	Approx. Sampler Height <sup>a</sup> , m	Site Surroundings Details
Riverside	8/16/97 to	Univ. of CA	5	On top of a shelter building
	9/22/97	Agricultural. Operations Field		situated in a dirt field
Chicago	10/10/97 to 11/16/97	Illinois Institute of Technology Campus	18	Roof of 4-story building at corners of 33 <sup>rd</sup> St. and S. Michigan Ave.
Dallas	12/5/97 to 1/21/98	Fire Station #25: 4607 South Lancaster Road	8	On the roof of the firehouse approximately 20 m from Lancaster Road.
Phoenix	12/14/97 to 1/26/98	Arizona Department of Environmental Protection "Supersite": 4530 N. 17 <sup>th</sup> Avenue	4	Residential neighborhood approximately 2.5 km NW of downtown
Bakersfield	2/4/98 to 3/26/98	CARB Monitoring Station at 5558 California Street	5	On top of 1 story building in a shopping plaza
Philadelphia	8/8/98 to 8/25/98	City of Philadelphia Water Treatment Plant	5	6 km E-NE of downtown, 100 m from lightly traveled, 4 lane state road, and 400 m from Interstate 90

<sup>&</sup>lt;sup>a</sup> Elevation above surrounding ground level

 Table 2
 Summary of discrete particle-phase sulfate samplers.

Instrument	Prefilters/ Denuders	Primary Collection Media	Secondary Collection Media	Invest-	Sites Used <sup>a</sup>
Harvard Impactor	N/A	Teflon Impactor Surface	Media	HSPH	All
F-HEADS	Na <sub>2</sub> CO <sub>3</sub> - coated and citric acid- coated denuder	Teflon filter (F1)	N/A	HSPH	R, C, D, P, B
N-HEADS	Na <sub>2</sub> CO <sub>3</sub> - coated and citric acid- coated denuder	Teflon filter (F1)	N/A	HSPH	All
ADS	Na <sub>2</sub> CO <sub>3</sub> - coated and citric acid- coated denuder	Teflon filter	Nylon filter	BYU	R, B
CSS	Na <sub>2</sub> CO <sub>3</sub> - coated and citric acid- coated denuder	Teflon filter	Nylon filter	BYU	R, B
Big BOSS	Carbon- impregnated filter paper denuder	Quartz filter	Carbon impreg- nated filter	BYU	R, B
PC-BOSS	Particle concentrator <sup>b</sup> + carbon-impregnated filter paper denuder	Quartz filter	Carbon impreg- nated filter	BYU	R, B
PC-BOSS	Particle concentrator <sup>b</sup> + carbon-impregnated filter paper denuder	Teflon filter	Nylon filter	BYU	R, B

<sup>\*</sup> All samples were analyzed by ion chromatography

<sup>&</sup>lt;sup>a</sup> All = All sites, R = Riverside, C = Chicago, D = Dallas, P = Phoenix, B = Bakersfield

 $<sup>^{</sup>b}$  Particle concentrator has an approximate particle diameter cutpoint of 0.1  $\mu$ m.

 Table 3
 Summary of discrete particle-phase nitrate samplers.

	Prefilters/	Primary Collection	Secondary Collection	Invest-	Sites
Instrument	Denuders	Media	Media	igator	Used <sup>a</sup>
Harvard Impactor	N/A	Teflon Impactor Surface	N/A	HSPH	All
F-HEADS	Na <sub>2</sub> CO <sub>3</sub> - coated and citric acid- coated denuder	Teflon filter (F1)	Na <sub>2</sub> CO <sub>3</sub> impreg- nated filter	HSPH	R, C, D, P, B
N-HEADS	Na <sub>2</sub> CO <sub>3</sub> - coated and citric acid- coated denuder	Teflon filter (F1)	Nylon filter	HSPH	All
ADS	Na <sub>2</sub> CO <sub>3</sub> - coated and citric acid- coated denuder	Teflon filter	Nylon filter	BYU	R, B
CSS	Na <sub>2</sub> CO <sub>3</sub> - coated and citric acid- coated denuder	Teflon filter	Nylon filter	BYU	R, B
Big BOSS	Carbon- impregnated filter paper denuder	Quartz filter	Carbon impreg- nated filter	BYU	R, B
PC-BOSS	Particle concentrator <sup>b</sup> + carbon-impregnated filter paper denuder	Quartz filter	Carbon impreg- nated filter	BYU	R, B
PC-BOSS	Particle concentrator <sup>b</sup> + carbon-impregnated filter paper denuder	Teflon filter	Nylon filter	BYU	R, B

<sup>\*</sup> All samplers except were analyzed by ion chromatography

<sup>&</sup>lt;sup>a</sup> All = All sites, R = Riverside, C = Chicago, D = Dallas, P = Phoenix, B = Bakersfield

 $<sup>^{</sup>b}$  Particle concentrator has an approximate particle diameter cutpoint of 0.1  $\mu$ m.

Table 4 Summary of discrete particle-phase ammonium samplers

Instrument	Prefilters/ Denuders	Primary Collection Media	Secondary Collection Media	Invest-	Sites Used <sup>a</sup>
F-HEADS	Na <sub>2</sub> CO <sub>3</sub> - coated and citric acid- coated denuders	Teflon filter (F1)	Citric acid impreg-nated filter	HSPH	R, C, D, P, B
N-HEADS	Na <sub>2</sub> CO <sub>3</sub> - coated and citric acid- coated denuders	Teflon filter (F1)	N/A	HSPH	All

All samples were analyzed by ion chromatography
All = All sites, R = Riverside, C = Chicago, D = Dallas, P = Phoenix, B = Bakersfield, F = Philadelphia

 Table 5
 Summary of particle-phase carbon samplers.

	Denuders/	Primary Collection	Secondary Collection	Invest-	Sites
Instrument	Prefilters	Media	Media	igator <sup>a</sup>	Used <sup>b</sup>
Harvard Carbon Sampler: UND	N/A	Quartz filter	Quartz filter	HSPH	All
Harvard Carbon Sampler: DEN	Carbon- impregnated filter paper denuder	Quartz filter	Quartz filter	HSPH	R, B, C, D, P, B
Harvard Carbon Sampler: UPF	Teflon filter	Quartz filter	Quartz filter	HSPH	В
Harvard Carbon Sampler: DPF	Teflon filter + Carbon- impregnated filter paper denuder	Quartz filter	Quartz filter	HSPH	В
Big BOSS	Carbon- impregnated filter paper denuder	Quartz filter	Carbon impreg- nated filter	BYU	R, B
PC-BOSS	Particle concentrator <sup>c</sup> + carbon-impregnated filter paper denuder	Quartz filter	Carbon impreg- nated filter	BYU	R, B

<sup>&</sup>lt;sup>a</sup> BYU samples were analyzed using BYU's thermal-optical analysis method. HSPH samples were analyzed by TOR at DRI (Chow *et al.*, 1993).

b All = All sites, R = Riverside, C = Chicago, D = Dallas, P = Phoenix, B = Bakersfield

 $<sup>^{</sup>c}$  Particle concentrator has an approximate particle diameter cutpoint of 0.1  $\mu$ m.

**Table 6** Summary of temperature data for all study sites except Philadelphia.

Site	Average	Median	Standard Deviation	Minimum	Maximum
Riverside	26.4	26.6	2.4	21.4	31.2
Chicago	7.1	7.3	5.9	-5.3	23.3
Dallas	8.0	7.7	4.0	-0.4	17.1
Phoenix	11.6	11.4	2.3	7.1	17.5
Bakersfield	13.1	12.1	3.3	8.2	21.3

statistics are based on 24-h averages (approximately 10:00 am to 10:00 pm local time)

 Table 7
 Summary of relative humidity data for all study sites except Philadelphia.

			Standard		
Site	Average	Median	Deviation	Minimum	Maximum
Riverside	54.3	53.1	10.5	30.2	76.8
Chicago	68.7	68.5	11.1	43.2	89.2
Dallas	75.4	78.2	17.5	43.7	99.6
Phoenix	59.5	54.5	12.0	43.2	84.4
Bakersfield	73.3	72.8	8.9	49.6	94.2

statistics are based on 24-h averages (approximately 10:00 am to 10:00 pm local time)

Table 8 $PM_{2.5}$  sulfate concentration statistics for the six study sites.

				Standard		
Site	Sampler	Average	Median	Deviation	Minimum	Maximum
Riverside	HI	3.0	2.7	1.0	1.3	5.2
	F-HEADS <sup>a</sup>	2.8	2.6	0.9	1.2	4.7
	N-HEADS <sup>b</sup>	2.8	2.5	1.0	1.2	4.8
	$ADS^{c}$	2.2	2.0	1.0	0.5	4.7
	$CSS^d$	2.5	2.4	1.0	1.0	4.6
	Big BOSS <sup>e</sup>	2.6	2.5	1.1	0.5	4.8
	PC-BOSS <sup>f</sup>	2.2	2.2	0.7	0.9	4.6
	PC-BOSS <sup>g</sup>	2.3	2.1	0.8	0.9	4.7
Chicago	HI	3.2	2.9	1.9	0.6	9.3
	F-HEADS <sup>a</sup>	3.0	2.7	1.8	0.8	8.7
	N-HEADS <sup>b</sup>	2.8	2.6	1.7	0.6	8.9
Dallas	HI	1.7	1.4	1.1	0.3	4.5
	F-HEADS <sup>a</sup>	1.8	1.4	1.2	0.6	4.7
	N-HEADS <sup>b</sup>	1.8	1.5	1.1	0.5	4.4
Phoenix	HI	0.7	0.7	0.3	0.1	1.7
	F-HEADS <sup>a</sup>	0.6	0.6	0.4	0.0	1.8
	N-HEADS <sup>b</sup>	0.7	0.6	0.4	0.1	1.8

Table 8 Continued

Site	Sampler	Average	Median	Standard Deviation	Minimum	Maximum
Bakersfield	HI	1.2	1.0	0.8	0.2	4.2
	F-HEADS <sup>a</sup>	1.0	0.9	0.7	0.2	3.3
	N-HEADS <sup>b</sup>	1.0	0.9	0.7	0.2	3.4
	$ADS^{c}$	1.0	0.9	0.7	0.1	3.3
	$CSS^d$	0.9	0.7	0.7	0.1	3.4
	Big BOSS <sup>e</sup>	0.9	0.8	0.6	0.0	2.7
	PC-BOSS <sup>f</sup>	0.8	0.7	0.5	0.2	2.2
	PC-BOSS <sup>g</sup>	0.9	0.7	0.5	0.1	2.3
Philadelphia	HI	8.0	4.9	7.7	1.5	28.4
	N-HEADS <sup>b</sup>	7.7	4.6	7.7	1.4	28.8

All concentrations are in µg m<sup>-3</sup>

Full HEADS Teflon filter

Nylon HEADS Teflon filter

BYU Annular Denuder sampler Teflon filter

BYU ChemSpec Sampler Teflon filter

Big BOSS quartz filter

PC-BOSS minor flow quartz + major flow quartz filters PC-BOSS minor flow Teflon + major flow quartz filters f

**Table 9** PM<sub>2.5</sub> nitrate concentration statistics for the six study sites

				Standard		
Site	Sampler	Average	Median	Deviation	Minimum	Maximum
Riverside	HI	2.6	1.7	2.7	0.3	13.2
	F-HEADS <sup>a</sup>	3.8	2.8	2.9	1.2	14.6
	N-HEADS <sup>b</sup>	4.4	3.3	3.6	1.3	19.0
	$ADS^{c}$	3.8	2.9	3.2	1.0	15.7
	$CSS^d$	3.9	3.4	2.5	1.4	12.9
	PC-BOSS <sup>e</sup>	3.1	2.3	2.6	0.7	14.8
	PC-BOSS <sup>f</sup>	2.6	2.1	2.0	0.7	10.5
Chicago	HI	3.2	2.6	2.4	0.2	8.0
	F-HEADS <sup>a</sup>	2.5	1.8	1.9	0.2	6.2
	N-HEADS <sup>b</sup>	3.1	2.7	2.0	0.5	7.7
Dallas	HI	1.9	1.5	1.4	0.1	4.8
	F-HEADS <sup>a</sup>	1.5	1.2	1.1	0.2	3.8
	N-HEADS <sup>b</sup>	2.1	1.9	1.3	0.4	4.7
Phoenix	HI	4.1	3.7	3.7	0.1	14.9
	F-HEADS <sup>a</sup>	3.1	2.5	2.5	0.2	9.4
	N-HEADS <sup>b</sup>	3.9	3.4	3.1	0.5	13.2
Bakersfield	HI	5.3	3.9	5.0	0.5	22.3
	F-HEADS <sup>a</sup>	4.5	3.0	4.7	0.4	20.1
	N-HEADS <sup>b</sup>	5.5	4.0	5.3	0.5	25.0
	$ADS^{c}$	5.3	3.9	5.2	0.8	24.2
	$CSS^d$	4.6	3.3	4.6	0.2	21.3
	PC-BOSS <sup>e</sup>	4.4	3.7	3.8	0.6	15.8
	PC-BOSS <sup>f</sup>	4.4	3.4	3.7	0.7	16.5
Philadelphia	HI	0.4	0.2	0.3	0.0	0.9
	N-HEADS <sup>b</sup>	0.6	0.4	0.5	0.1	1.6

<sup>\*</sup> All concentrations are in µg m<sup>-3</sup>

<sup>&</sup>lt;sup>a</sup> Full HEADS Teflon filter + difference of two Na<sub>2</sub>CO<sub>3</sub>-impregnated backup filters

b Nylon HEADS Teflon filter + nylon backup filter

c BYU Annular Denuder sampler Teflon filter + nylon backup filter

d BYU ChemSpec Sampler Teflon filter + nylon backup filter

e PC-BOSS minor flow quartz + minor flow Empore backup + major flow quartz filters

<sup>&</sup>lt;sup>f</sup> PC-BOSS minor flow Teflon + minor flow nylon backup + major flow quartz filters

Table 10  $\ensuremath{\text{PM}_{2.5}}$  ammonium concentration statistics for the six study sites.

				Standard		
Site	Sampler	Average	Median	Deviation	Minimum	Maximum
Riverside	F-HEADS <sup>a</sup>	4.0	3.6	2.5	1.0	10.7
	N-HEADS <sup>b</sup>	0.9	0.8	0.4	0.3	2.1
Chicago	F-HEADS <sup>a</sup>	2.4	2.3	1.0	0.8	4.3
	N-HEADS <sup>b</sup>	1.3	1.2	0.7	0.3	3.1
Dallas	F-HEADS <sup>a</sup>	1.4	1.3	0.7	0.5	3.0
	N-HEADS <sup>b</sup>	0.8	0.7	0.6	0.2	2.2
Phoenix	F-HEADS <sup>a</sup>	1.5	1.5	0.9	0.4	3.9
	N-HEADS <sup>b</sup>	0.3	0.3	0.2	0.1	1.3
Bakersfield	F-HEADS <sup>a</sup>	1.4	0.9	1.4	0.1	5.6
	N-HEADS <sup>b</sup>	0.6	0.4	0.7	0.0	3.5
Philadelphia	N-HEADS <sup>b</sup>	2.7	1.6	2.5	0.6	9.1

All concentrations are in µg m<sup>-3</sup>
Full HEADS Teflon filter + citric acid impregnated filter
Nylon HEADS Teflon filter

PM<sub>2.5</sub> elemental carbon concentration statistics for the six study sites. Table 11

				Standard		
Site	Sampler	Average	Median	Deviation	Minimum	Maximum
Riverside	$DEN^a$	1.8	1.8	0.7	0.6	3.6
	$UND^{\mathrm{a}}$	1.9	1.9	0.6	0.7	3.6
	Aethalometer <sup>b</sup>	1.6	1.5	0.6	0.6	3.2
	Big BOSS <sup>c</sup>	2.7	2.7	0.7	1.7	3.8
	PC-BOSS <sup>d</sup>	3.0	3.2	0.7	1.8	4.0
Chicago	DEN <sup>a</sup>	1.4	1.1	0.9	0.3	3.9
	$\mathrm{UND}^{\mathrm{a}}$	1.5	1.2	1.0	0.3	3.8
	Aethalometer <sup>b</sup>	1.2	1.0	0.8	0.2	3.3
Dallas	DEN <sup>a</sup>	1.3	1.1	0.8	0.4	3.9
	$\mathrm{UND}^{\mathrm{a}}$	1.3	1.1	0.8	0.4	3.9
	Aethalometer <sup>b</sup>	0.8	0.7	0.5	0.3	2.7
Phoenix	DEN <sup>a</sup>	3.8	3.7	1.7	0.6	7.1
	$\mathrm{UND}^{\mathrm{a}}$	3.9	3.6	1.8	0.5	7.2
	Aethalometer <sup>b</sup>	3.0	3.0	1.3	0.6	5.6
Bakersfield	DEN <sup>a</sup>	1.4	1.3	0.7	0.5	4.1
	$\mathrm{UND}^{\mathrm{a}}$	1.5	1.4	0.7	0.5	4.0
	Aethalometer <sup>b</sup>	1.1	1.0	0.5	0.5	2.2
	Big BOSS <sup>c</sup>	2.7	2.7	0.7	1.7	3.8
	PC-BOSS <sup>d</sup>	3.0	3.2	0.7	1.8	4.0
Philadelphia	UND <sup>a</sup>	1.5	1.4	1.0	0.2	4.2
	Aethalometer <sup>b</sup>	1.1	1.1	0.6	0.2	2.8

All concentrations are in  $\mu g \ m^{-3}$ 

All DEN and UND elemental carbon concentrations are based on  $Q_a$  filter measurements. Aethalometer concentrations are based on a factor of  $\_\_\_$  to convert light absorbance to black carbon concentration.

Big BOSS elemental carbon concentrations are based on quartz filter measurements

PC-BOSS elemental carbon concentrations are based on minor flow quartz + major flow quartz filter measurements.

**Table 12** Organic carbon concentration statistics for the six study sites.

				Standard		
Site	Sampler	Average	Median	Deviation	Minimum	Maximum
Riverside	DEN $Q_a + Q_b^{\ a}$	6.5	6.8	1.4	3.7	10.0
	UND Q <sub>a</sub> b	5.7	5.7	1.3	2.9	8.5
	UND $Q_a - Q_b^c$	4.1	4.0	1.1	1.6	6.3
	Big BOSS <sup>d</sup>	9.6	9.4	4.0	3.4	19.3
	PC-BOSS <sup>e</sup>	7.6	6.7	2.8	4.0	13.1
Chicago	$DEN\ Q_a + {Q_b}^a$	3.8	3.6	1.7	0.9	7.8
	UND Qa b	3.8	3.8	1.7	1.1	8.3
	UND $Q_a$ - $Q_b^c$	3.2	3.0	1.4	0.9	6.7
Dallas	$DEN \ Q_a + Q_b^{\ a}$	3.9	3.4	1.9	0.6	10.0
	$UND\ {Q_a}^b$	3.9	3.4	2.1	1.1	9.9
	UND $Q_a$ - $Q_b^c$	3.1	2.6	1.7	0.5	8.0
Phoenix	$DEN\;Q_a+{Q_b}^a$	7.7	8.2	2.9	1.9	15.8
	UND Qa b	7.8	8.0	2.7	2.5	13.4
	UND $Q_a - Q_b^c$	6.1	6.1	2.2	2.3	11.9
Bakersfield	$DEN\;Q_a+{Q_b}^a$	4.8	4.6	1.5	1.2	7.9
	UND Q <sub>a</sub> <sup>b</sup>	4.3	4.4	1.4	1.5	6.9
	UND $Q_a$ - $Q_b^{\ c}$	3.4	3.6	1.1	1.1	5.4
	Big BOSS <sup>d</sup>	9.6	9.4	4.0	3.4	19.3
	PC-BOSS <sup>e</sup>	7.6	6.7	2.8	4.0	13.1
Philadelphia	UND Qa b	4.3	4.4	1.4	1.5	6.9

<sup>\*</sup> All concentrations are in μg m<sup>-3</sup>

<sup>&</sup>lt;sup>a</sup> DEN QFA + QFB organic carbon concentrations are based on front + back filter measurements from the denuded sampler

b UND QFA organic carbon concentrations are based on front filter measurements from the undenuded sampler

<sup>&</sup>lt;sup>c</sup> UND QFA - QFB organic carbon concentrations are based on front - back filter measurements from the undenuded sampler

Big BOSS organic carbon concentrations are based on the sum of the quartz and Empore filter measurements. Quartz filter measurements are adjusted to account for adsorption by gasphase carbon which may have penetrated the denuder as described in the text.

e PC-BOSS organic carbon concentrations are based on the sum of the minor quartz and Empore filter + major flow quartz measurements. The major flow quartz filter measurements are adjusted to account for adsorption by gas-phase carbon as described in the text. Air flowing through the major flow filter is not denuded.

 Table 13
 Gas-phase nitric acid concentration statistics for the six study sites.

				Standard		
Site	Sampler	Average	Median	Deviation	Minimum	Maximum
Riverside	F-HEADS	1.0	1.0	0.4	0.3	2.1
	N-HEADS	1.0	1.0	0.4	0.2	2.1
Chicago	F-HEADS	7.2	5.7	4.7	0.5	21.7
	N-HEADS	7.9	6.6	5.3	0.8	22.1
Dallas	F-HEADS	1.3	0.9	1.0	0.3	4.1
	N-HEADS	1.3	0.9	1.1	0.3	4.6
Phoenix	F-HEADS	0.8	0.7	0.5	0.2	2.2
	N-HEADS	0.8	0.7	0.6	0.2	2.4
Bakersfield	F-HEADS	0.4	0.3	0.2	0.0	1.1
	N-HEADS	0.4	0.4	0.2	0.2	1.2
Philadelphia	N-HEADS	5.3	2.7	5.6	0.1	21.2

All concentrations are determined from ion chromatography on the HEADS sodium carbonate denuders. Concentrations are in ppb<sub>v</sub>.

 Table 14
 Gas-phase sulfur dioxide concentration statistics for the six study sites.

				Standard		
Site	Sampler	Average	Median	Deviation	Minimum	Maximum
Riverside	F-HEADS	1.0	1.0	0.4	0.3	2.1
	N-HEADS	1.0	1.0	0.4	0.2	2.1
Chicago	F-HEADS	7.2	5.7	4.7	0.5	21.7
	N-HEADS	7.9	6.6	5.3	0.8	22.1
Dallas	F-HEADS	1.3	0.9	1.0	0.3	4.1
	N-HEADS	1.3	0.9	1.1	0.3	4.6
Phoenix	F-HEADS	0.8	0.7	0.5	0.2	2.2
	N-HEADS	0.8	0.7	0.6	0.2	2.4
Bakersfield	F-HEADS	0.4	0.3	0.2	0.0	1.1
	N-HEADS	0.4	0.4	0.2	0.2	1.2
Philadelphia	N-HEADS	5.3	2.7	5.6	0.1	21.2

All concentrations are determined from ion chromatography on the HEADS sodium carbonate denuders. Concentrations are in ppb<sub>v</sub>.

 Table 15
 Gas-phase ammonia concentration statistics for the six study sites.

				Standard		
Site	Sampler	Average	Median	Deviation	Minimum	Maximum
Riverside	F-HEADS	1.0	1.0	0.4	0.3	2.1
	N-HEADS	1.0	1.0	0.4	0.2	2.1
Chicago	F-HEADS	7.2	5.7	4.7	0.5	21.7
	N-HEADS	7.9	6.6	5.3	0.8	22.1
Dallas	F-HEADS	1.3	0.9	1.0	0.3	4.1
	N-HEADS	1.3	0.9	1.1	0.3	4.6
Phoenix	F-HEADS	0.8	0.7	0.5	0.2	2.2
	N-HEADS	0.8	0.7	0.6	0.2	2.4
Bakersfield	F-HEADS	0.4	0.3	0.2	0.0	1.1
	N-HEADS	0.4	0.4	0.2	0.2	1.2
Philadelphia	N-HEADS	5.3	2.7	5.6	0.1	21.2

ullet All concentrations are determined from ion chromatography on the HEADS citric acid denuders. Concentrations are in ppb<sub>v</sub>.

Table 16  $PM_{2.5}$  mass concentration statistics for the six study sites.

				Standard		
Site	Sampler	Average	Median	Deviation	Minimum	Maximum
Riverside	HI	18.4	15.7	6.7	9.0	38.8
	CAMM $(24-h)^a$	20.3	18.8	6.5	10.2	42.0
	Reconstructed 1 <sup>b</sup>	23.0	21.6	7.7	11.5	43.8
	Reconstructed 2 <sup>c</sup>	21.9	20.1	7.5	10.5	41.1
	Reconstructed 3 <sup>d</sup>	20.7	19.1	6.2	11.4	39.7
	Reconstructed 4 <sup>e</sup>	19.6	18.5	6.0	10.4	37.0
Chicago	HI	16.8	16.2	7.3	5.1	32.5
	CAMM $(24-h)^a$	17.8	16.3	8.4	5.8	34.1
	Reconstructed 1 <sup>b</sup>	15.3	16.1	6.1	4.2	29.0
	Reconstructed 2 <sup>c</sup>	15.3	15.2	6.0	4.1	30.4
	Reconstructed 3 <sup>d</sup>	14.7	15.7	5.6	4.1	27.9
	Reconstructed 4 <sup>e</sup>	14.6	15.3	5.5	4.1	29.3
Dallas	HI	11.7	11.2	4.9	2.9	22.4
	CAMM $(24-h)^a$	12.2	11.8	5.0	3.6	22.6
	Reconstructed 1 <sup>b</sup>	12.3	11.2	4.3	4.1	23.5
	Reconstructed 2 <sup>c</sup>	12.3	11.2	4.6	4.1	23.3
	Reconstructed 3 <sup>d</sup>	12.1	11.2	4.3	3.5	22.1
	Reconstructed 4 <sup>e</sup>	12.0	11.1	4.5	4.2	22.0
Phoenix	HI	22.5	22.2	10.3	5.7	41.8
	CAMM $(24-h)^a$	23.1	23.8	8.5	7.9	37.9
	Reconstructed 1 <sup>b</sup>	20.7	19.7	7.9	7.6	32.5
	Reconstructed 2 <sup>c</sup>	20.8	19.8	7.8	8.3	31.7
	Reconstructed 3 <sup>d</sup>	20.2	19.6	7.7	7.5	32.3
	Reconstructed 4 <sup>e</sup>	20.4	19.1	7.7	8.3	35.0

Table 16 Continued

				Standard		
Site	Sampler	Average	Median	Deviation	Minimum	Maximum
Bakersfield	HI	18.4	16.4	10.9	5.8	54.2
	CAMM $(24-h)^a$	20.6	18.0	11.5	5.5	54.8
	Reconstructed 1 <sup>b</sup>	15.4	13.6	8.1	3.5	40.7
	Reconstructed 2 <sup>c</sup>	14.9	12.8	8.0	4.0	39.6
	Reconstructed 3 <sup>d</sup>	15.6	14.4	8.0	3.9	42.8
	Reconstructed 4 <sup>e</sup>	15.1	13.3	7.9	4.4	41.7
Philadelphia	HI	21.1	16.1	16.0	6.2	63.8
	CAMM $(24-h)^a$	21.8	18.5	13.0	8.3	57.4
	Reconstructed 4 <sup>e</sup>	20.9	15.1	14.2	8.0	57.5

<sup>\*</sup> All concentrations are in µg m<sup>-3</sup>

- Continuous CAMM data averaged over nominal 24-h periods to coincide with HI sampling periods
- b PM<sub>2.5</sub> mass reconstruction based on the sum of sulfate, nitrate, and ammonium from F-HEADS; elemental and organic carbon from HSPH DEN sampler, and crustal and non-crustal elements from XRF analysis of HEADS Teflon filters. A factor of 1.4 was used to convert organic carbon from TOR analysis to PM<sub>2.5</sub> hydrocarbon mass.
- PM<sub>2.5</sub> mass reconstruction based on the sum of sulfate, nitrate, and ammonium from F-HEADS; elemental and organic carbon from HSPH UND sampler, and crustal and non-crustal elements from XRF analysis of HEADS Teflon filters. A factor of 1.4 was used to convert organic carbon from TOR analysis to PM<sub>2.5</sub> hydrocarbon mass.
- d PM<sub>2.5</sub> mass reconstruction based on the sum of sulfate, nitrate, and ammonium from N-HEADS; elemental and organic carbon from HSPH DEN sampler, and crustal and non-crustal elements from XRF analysis of HEADS Teflon filters. A factor of 1.4 was used to convert organic carbon from TOR analysis to PM<sub>2.5</sub> hydrocarbon mass.
- e PM<sub>2.5</sub> mass reconstruction based on the sum of sulfate, nitrate, and ammonium from N-HEADS; elemental and organic carbon from HSPH UND sampler, and crustal and non-crustal elements from XRF analysis of HEADS Teflon filters. A factor of 1.4 was used to convert organic carbon from TOR analysis to PM<sub>2.5</sub> hydrocarbon mass.

## **FIGURES**

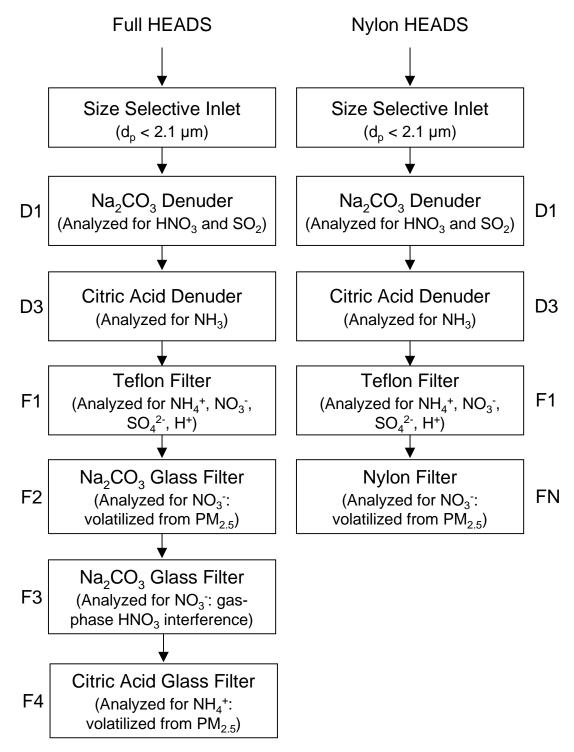


Figure 1 Harvard – EPA Annular Denuder Sampler (HEADS) schematic.

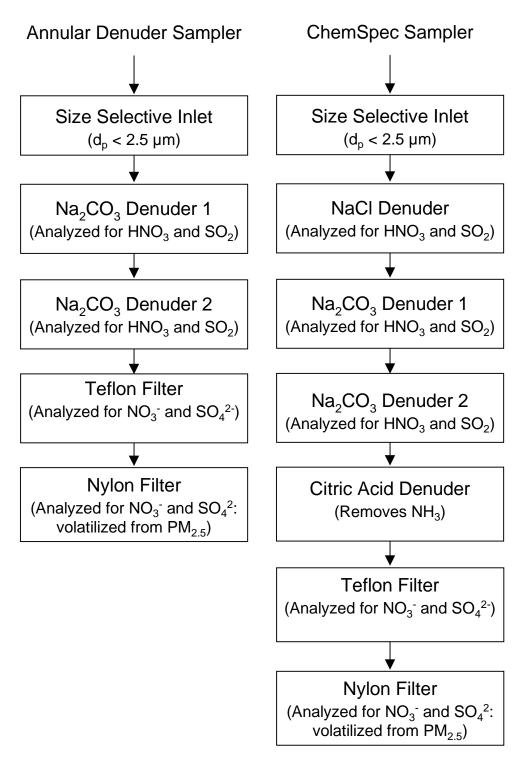


Figure 2 BYU Annular Denuder and ChemSpec Sampler schematics.

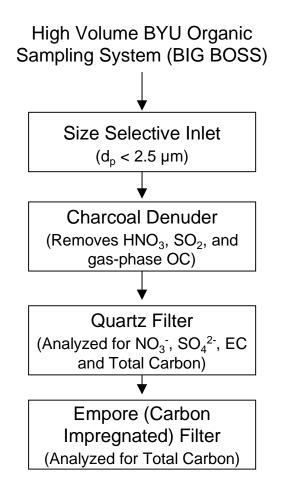
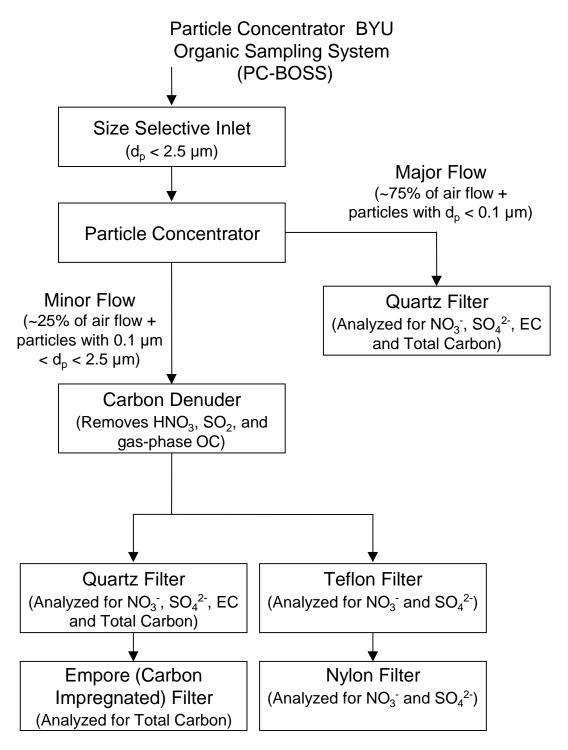


Figure 3 High Volume BYU Organic Sampler System (BIG BOSS) schematic.



**Figure 4** Particle Concentrator -- BYU Organic Sampler System (PC-BOSS) schematic.

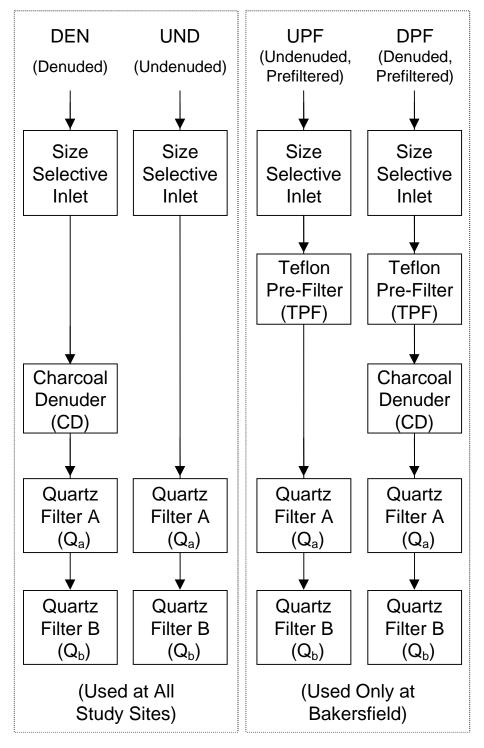


Figure 5 Schematic of HSPH Carbon Samplers.

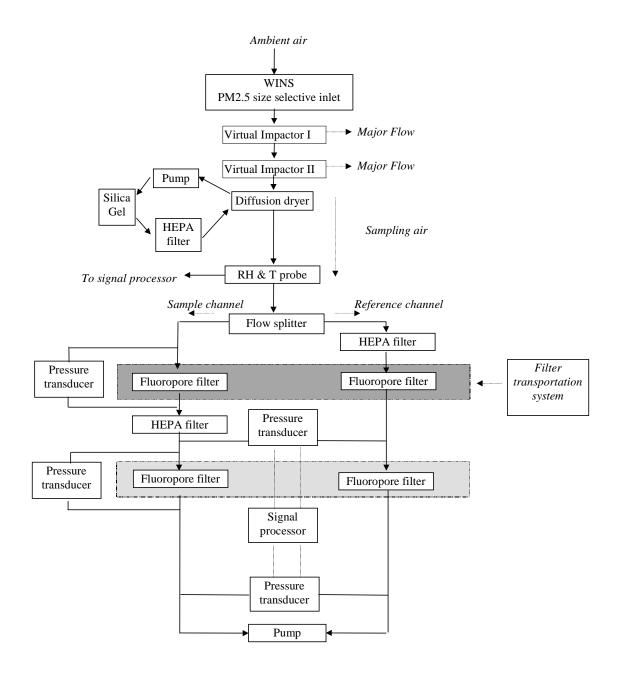


Figure 6 Schematic of the Continuous Ambient Mass Monitor (CAMM)

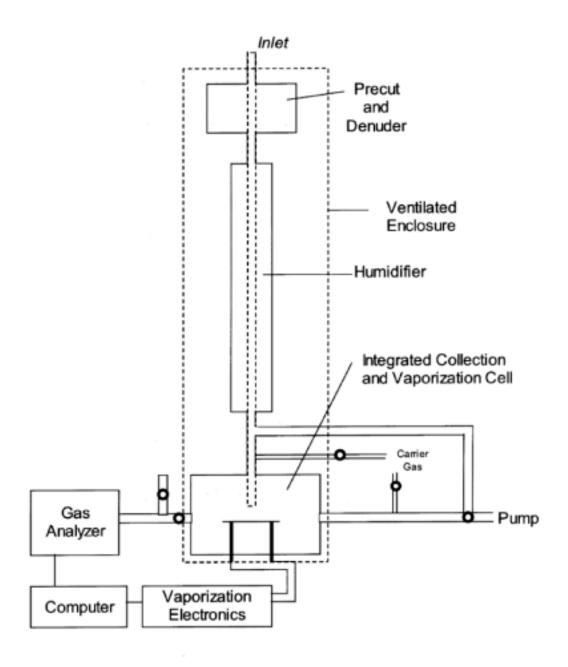


Figure 7 Schematic of the Aerosol Dynamics Inc. Continuous Nitrate Monitor (ACNM)

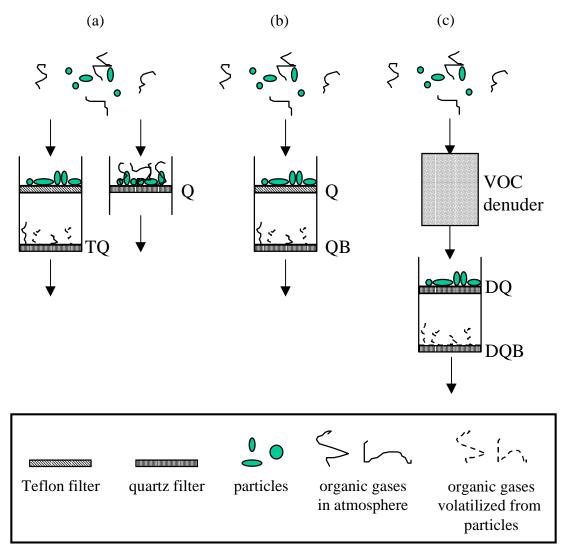
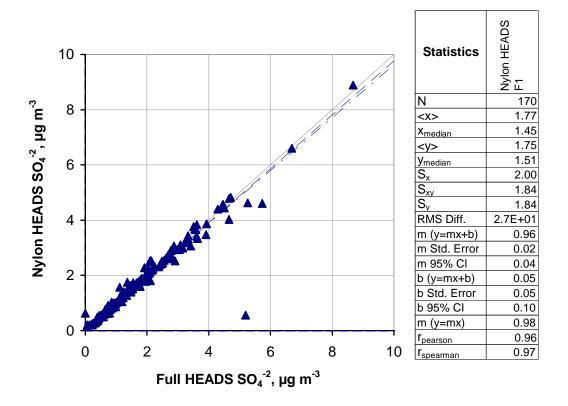


Figure 8 Schematic diagrams of commonly used  $PM_{2.5}$  carbon samplers.



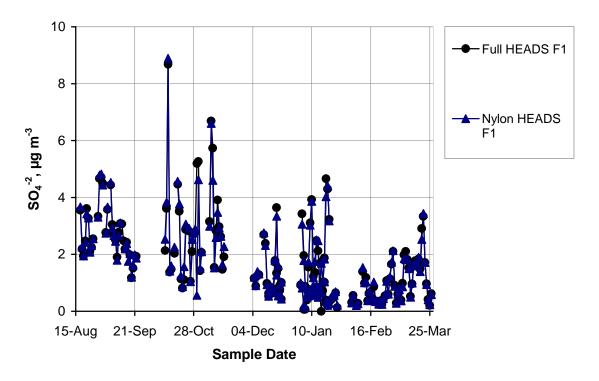
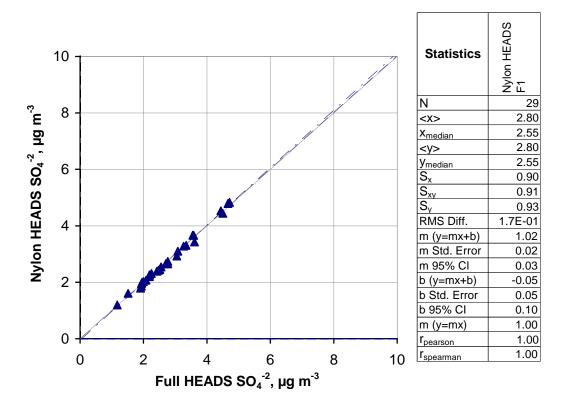


Figure 9A Sulfate: Full HEADS F1 vs. Nylon HEADS F1 (Teflon) filter at all sites.



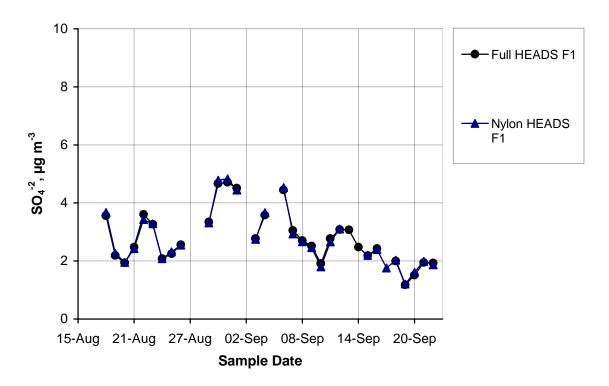
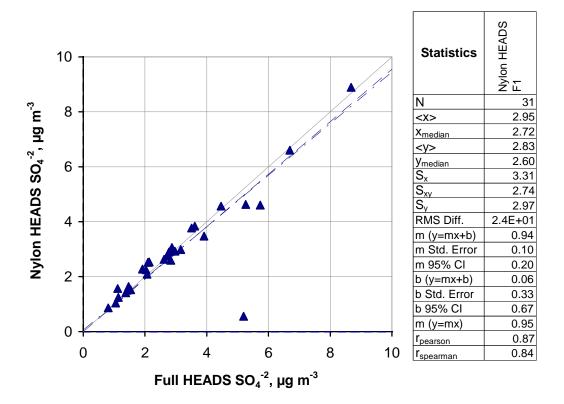


Figure 9R Sulfate: Full HEADS F1 vs. Nylon HEADS F1 (Teflon) filter at Riverside.



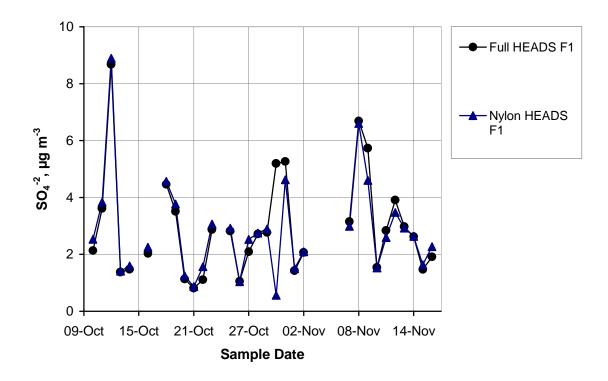
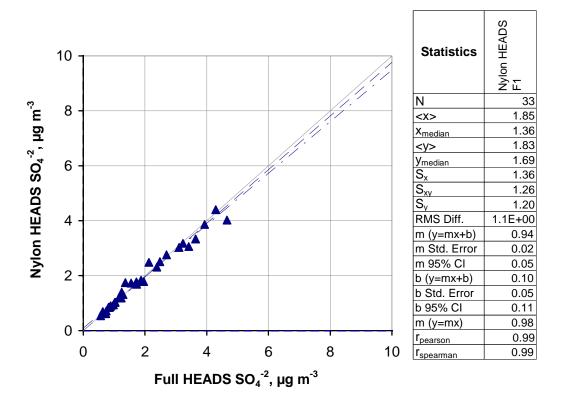
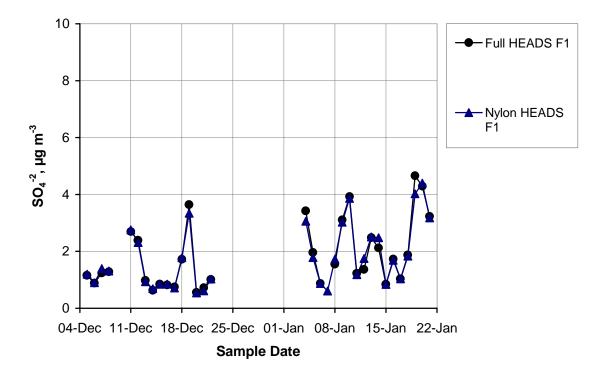
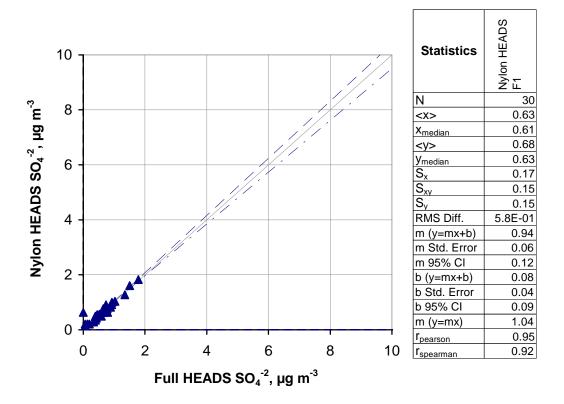


Figure 9C Sulfate: Full HEADS F1 vs. Nylon HEADS F1 (Teflon) filter at Chicago.





**Figure 9D** Sulfate: Full HEADS F1 vs. Nylon HEADS F1 (Teflon) filter at Dallas.



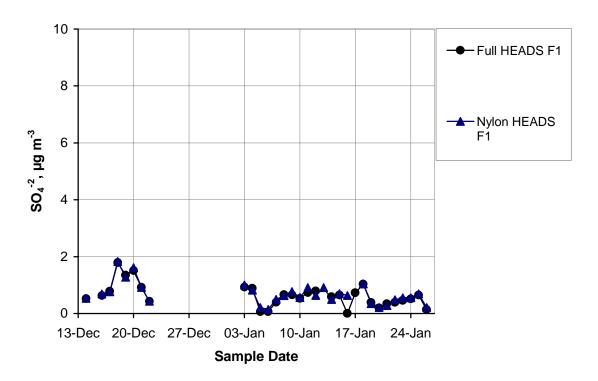
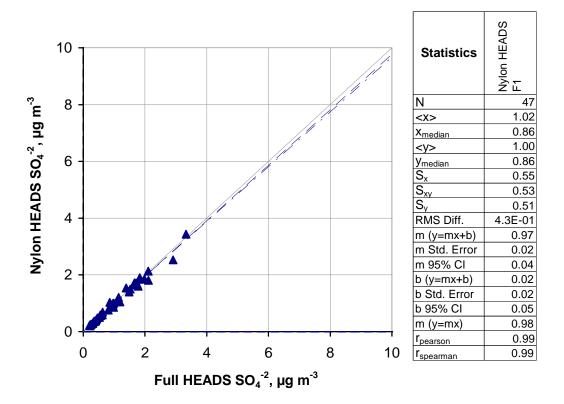
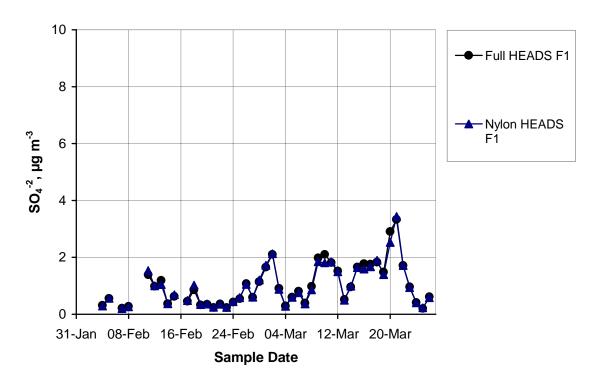
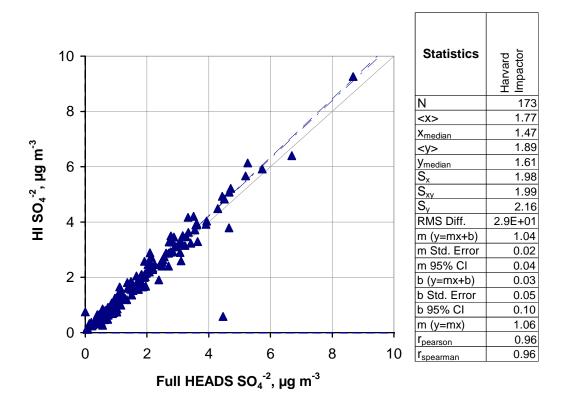


Figure 9P Sulfate: Full HEADS F1 vs. Nylon HEADS F1 (Teflon) filter at Phoenix.





**Figure 9B** Sulfate: Full HEADS F1 vs. Nylon HEADS F1 (Teflon) filter at Bakersfield.



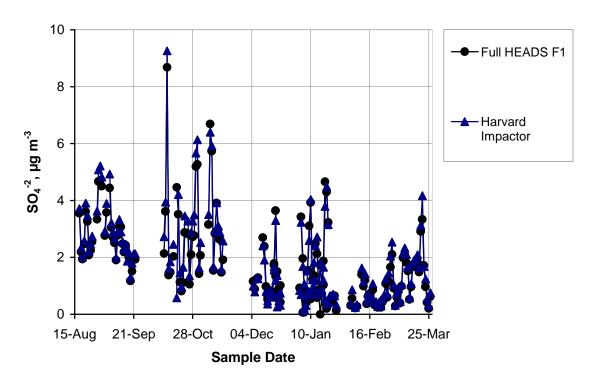
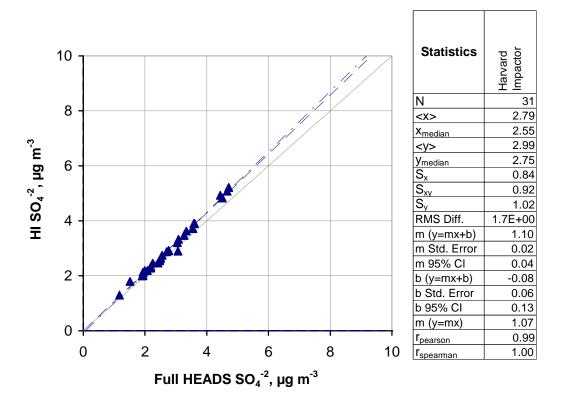


Figure 10A Sulfate: Harvard Impactor vs. Full HEADS F1 (Teflon) filter at all sites.



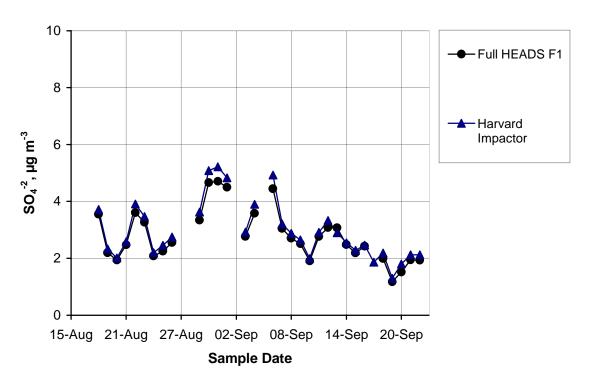
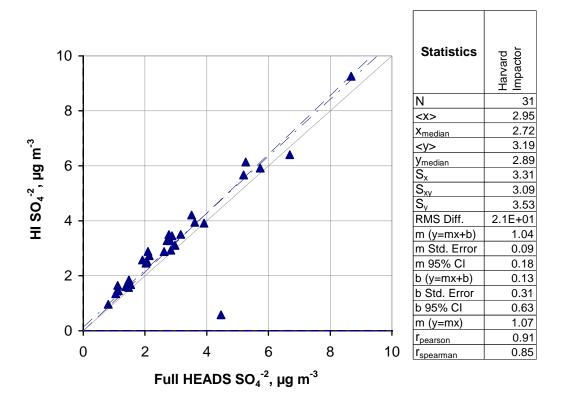


Figure 10R Sulfate: Harvard Impactor vs. Full HEADS F1 (Teflon) filter at Riverside.



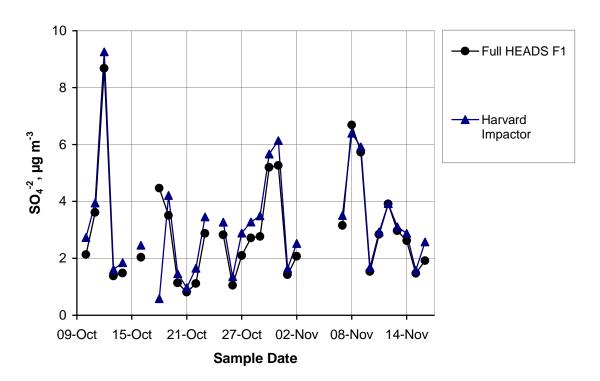
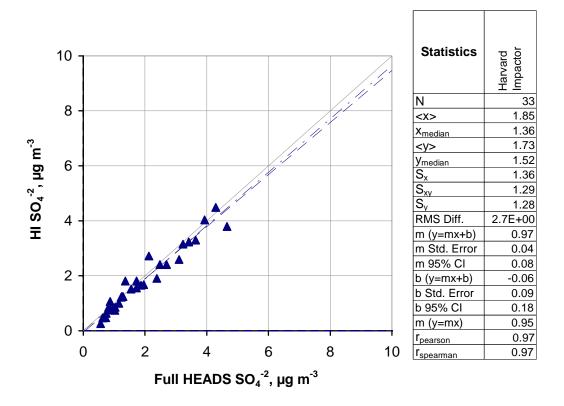


Figure 10C Sulfate: Harvard Impactor vs. Full HEADS F1 (Teflon) filter at Chicago.



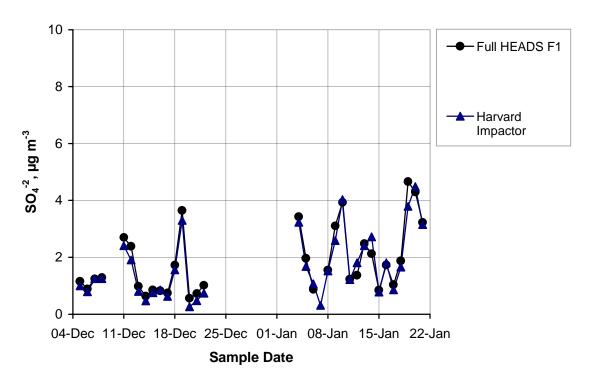
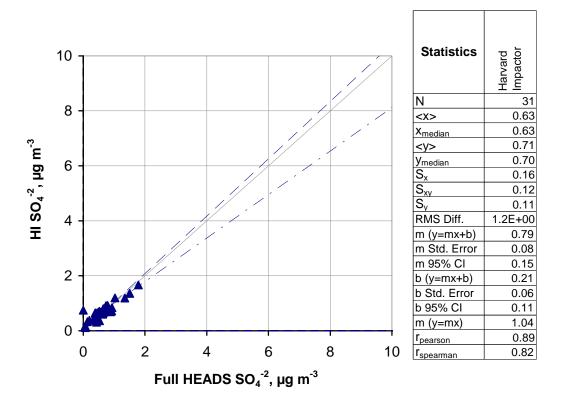
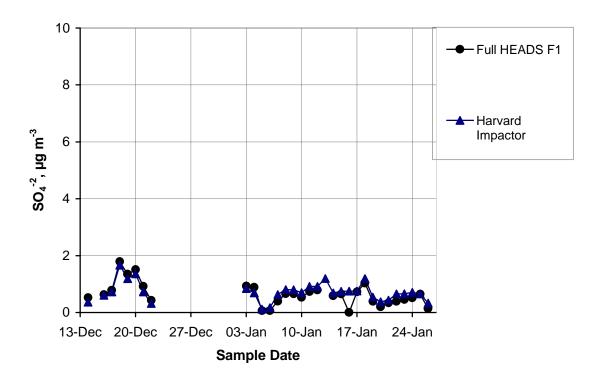
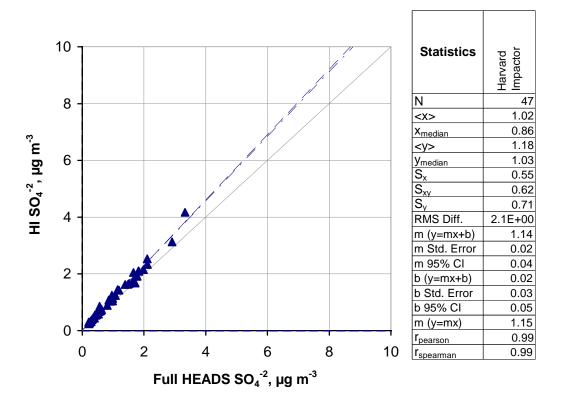


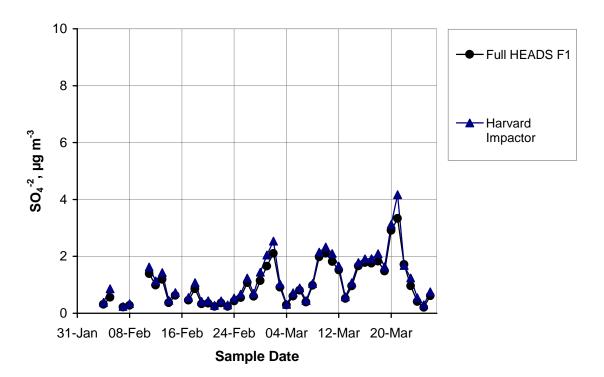
Figure 10D Sulfate: Harvard Impactor vs. Full HEADS F1 (Teflon) filter at Dallas.



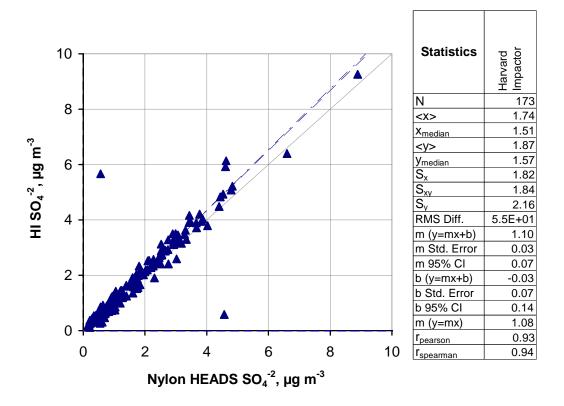


**Figure 10P** Sulfate: Harvard Impactor vs. Full HEADS F1 (Teflon) filter at Phoenix.





**Figure 10B** Sulfate: Harvard Impactor vs. Full HEADS F1 (Teflon) filter at Bakersfield.



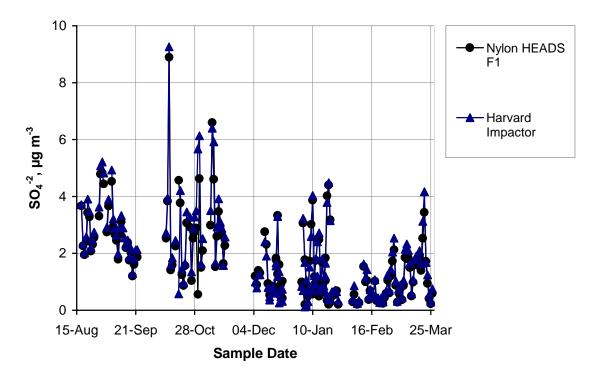
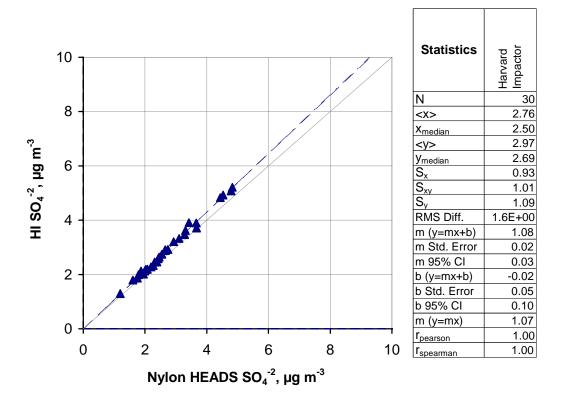
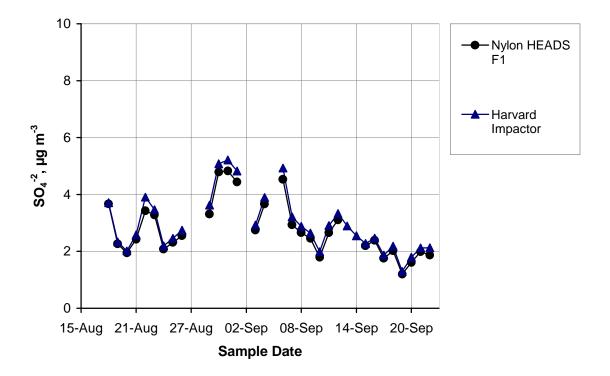
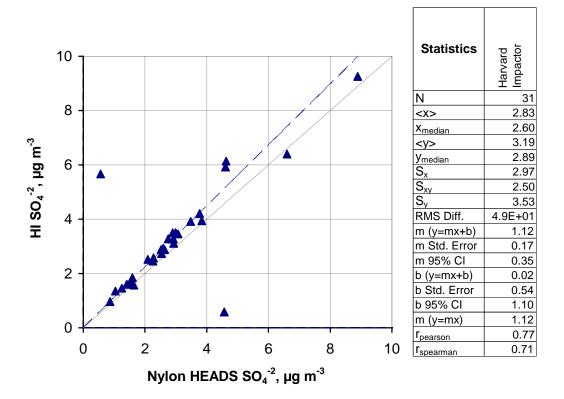


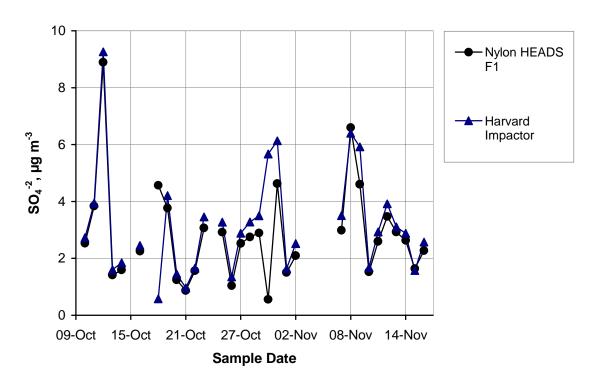
Figure 11A Sulfate: Harvard Impactor vs. Nylon HEADS F1 (Teflon) filter at all sites.



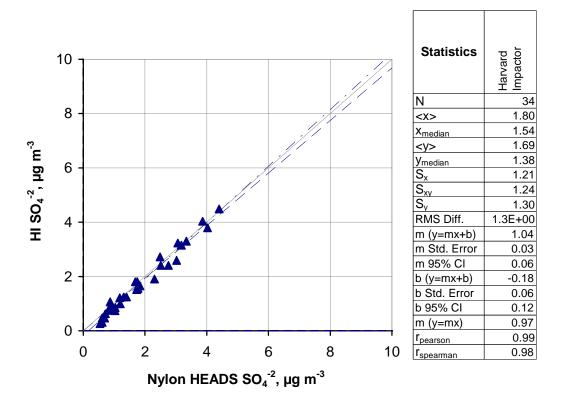


**Figure 11R** Sulfate: Harvard Impactor vs. Nylon HEADS F1 (Teflon) filter at Riverside.





**Figure 11C** Sulfate: Harvard Impactor vs. Nylon HEADS F1 (Teflon) filter at Chicago.



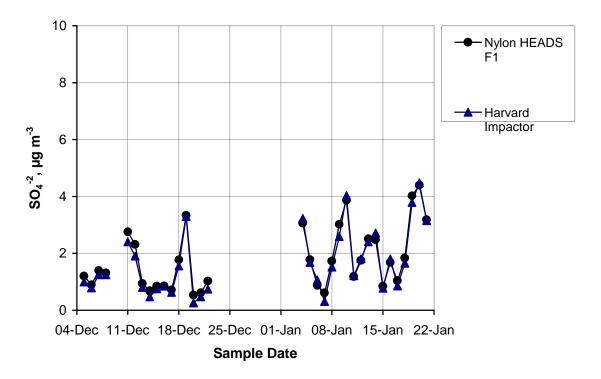
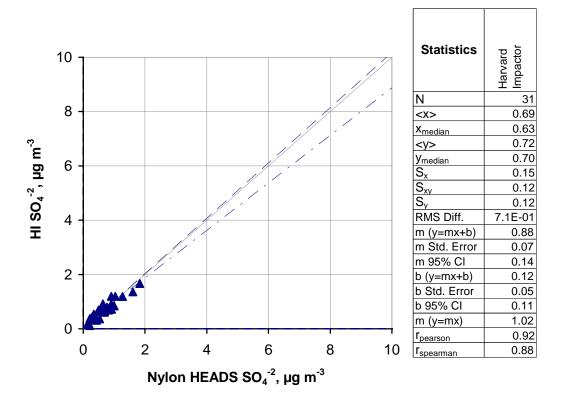
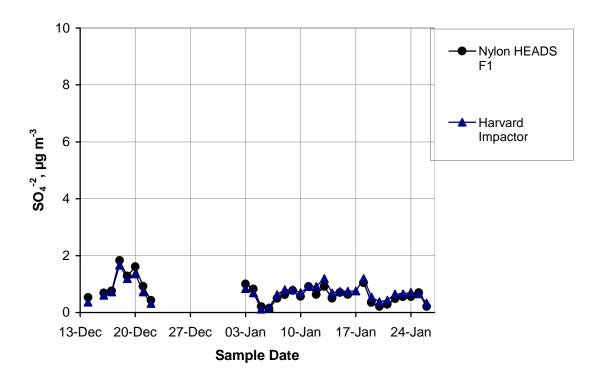
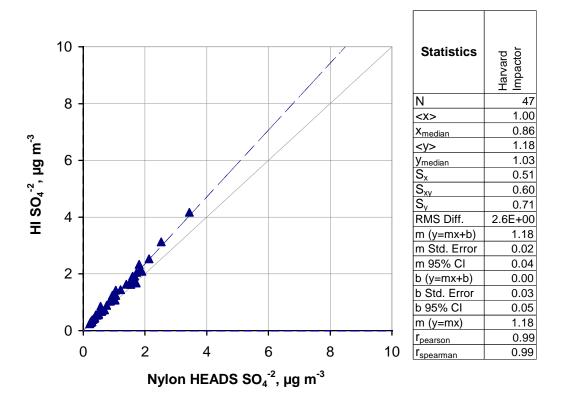


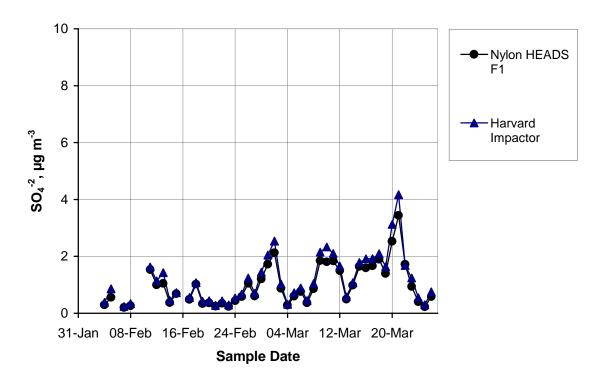
Figure 11D Sulfate: Harvard Impactor vs. Nylon HEADS F1 (Teflon) filter at Dallas.



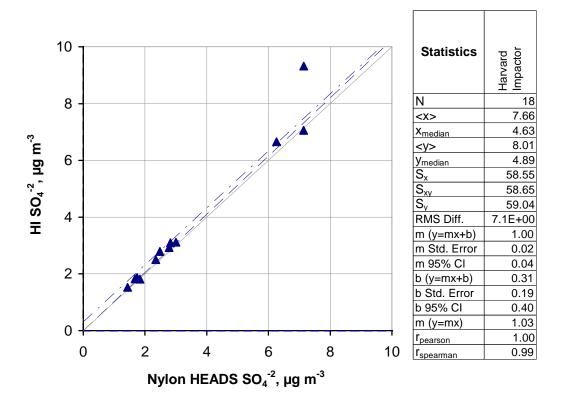


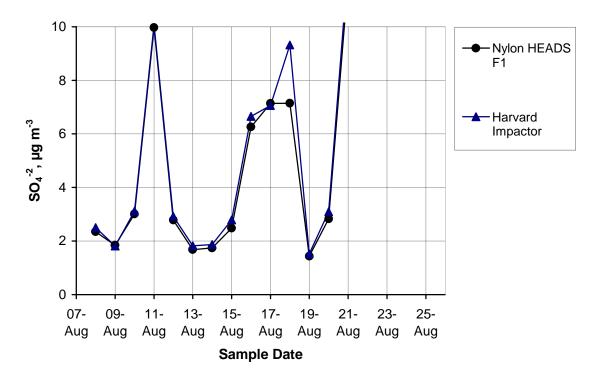
**Figure 11P** Sulfate: Harvard Impactor vs. Nylon HEADS F1 (Teflon) filter at Phoenix.



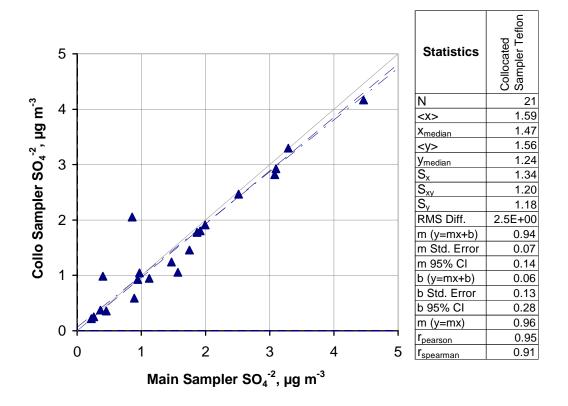


**Figure 11B** Sulfate: Harvard Impactor vs. Nylon HEADS F1 (Teflon) filter at Bakersfield.





**Figure 11F** Sulfate: Harvard Impactor vs. Nylon HEADS F1 (Teflon) filter at Philadelphia.



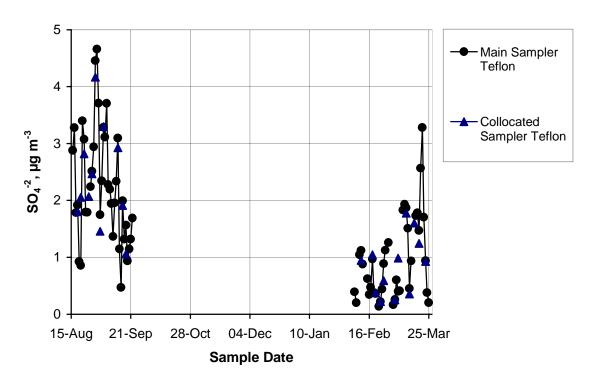
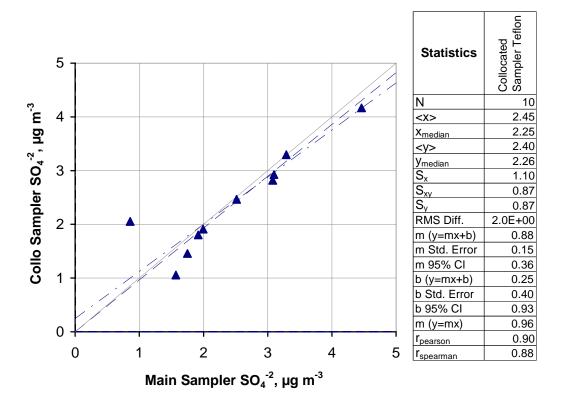


Figure 12A Sulfate: Collocated Annular Denuder Sampler Teflon filters at all sites.



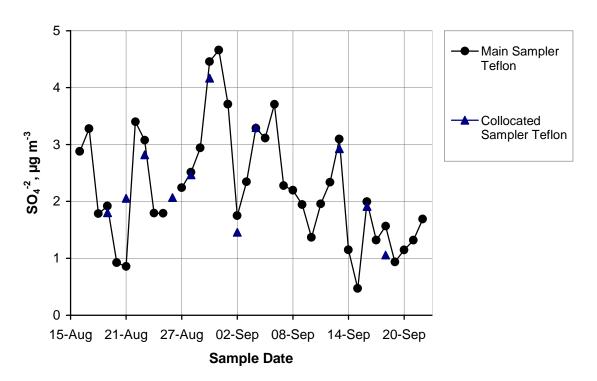
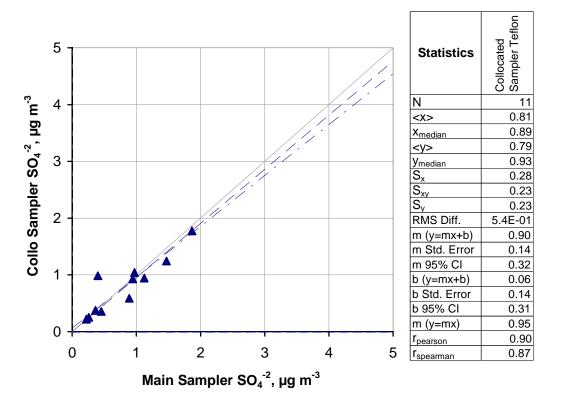
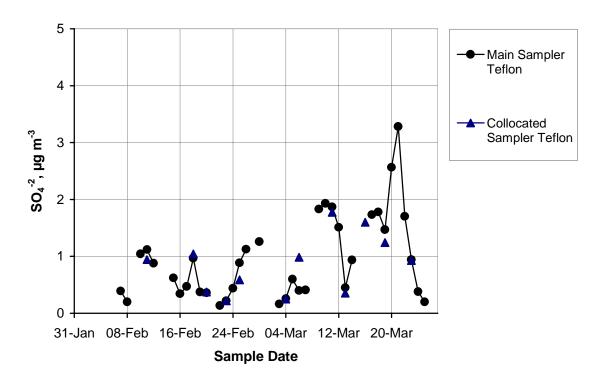
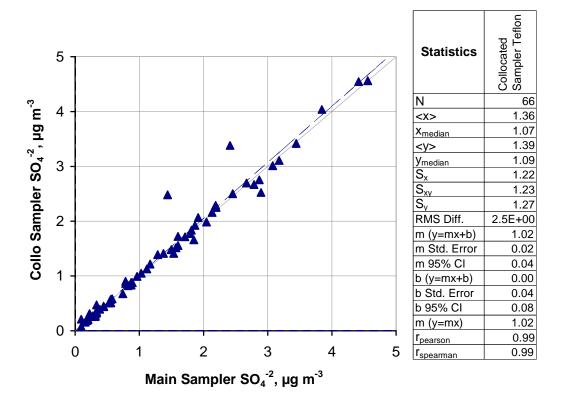


Figure 12R Sulfate: Collocated Annular Denuder Sampler Teflon filters at Riverside.





**Figure 12B** Sulfate: Collocated Annular Denuder Sampler Teflon filters at Bakersfield.



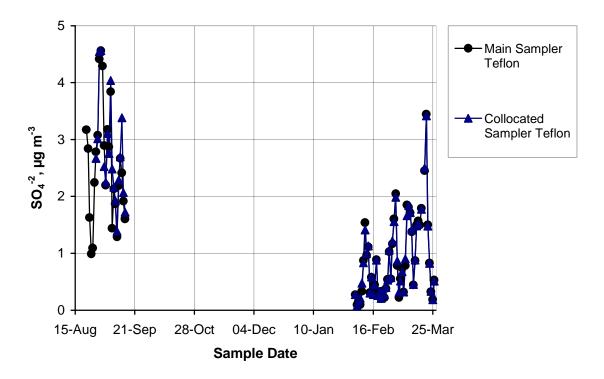
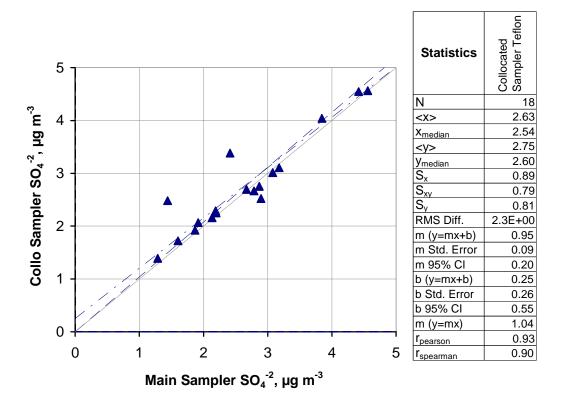


Figure 13A Sulfate: Collocated ChemSpec Sampler Teflon filters at all sites.



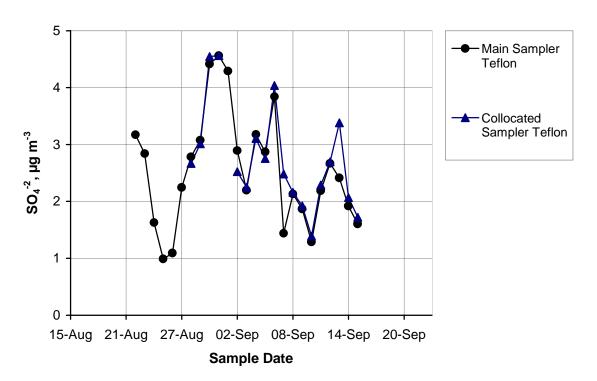
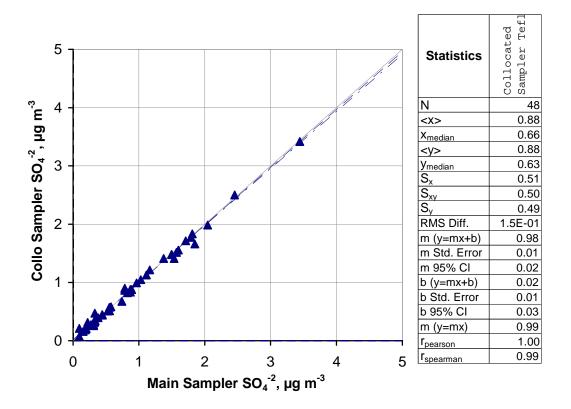


Figure 13R Sulfate: Collocated ChemSpec Sampler Teflon filters at Riverside.



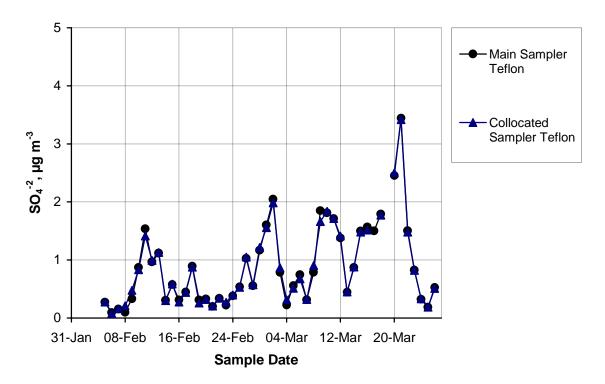
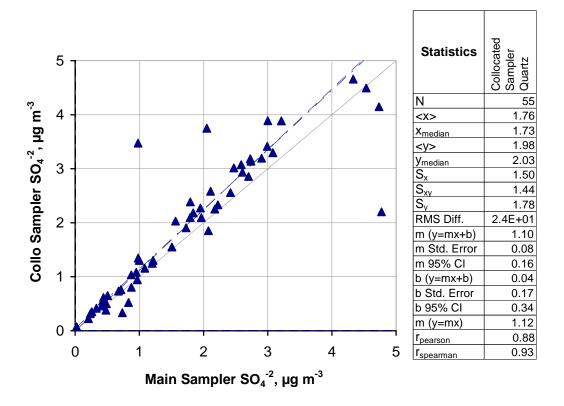


Figure 13B Sulfate: Collocated ChemSpec Sampler Teflon filters at Bakersfield.



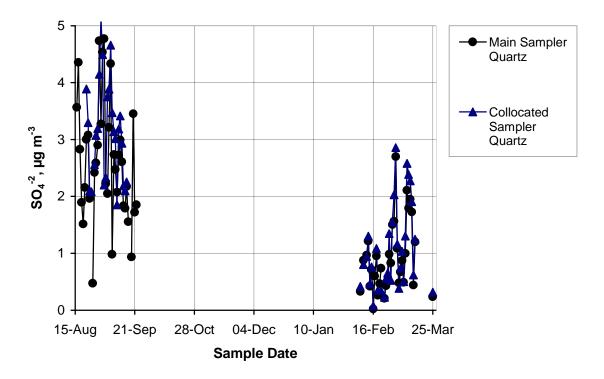
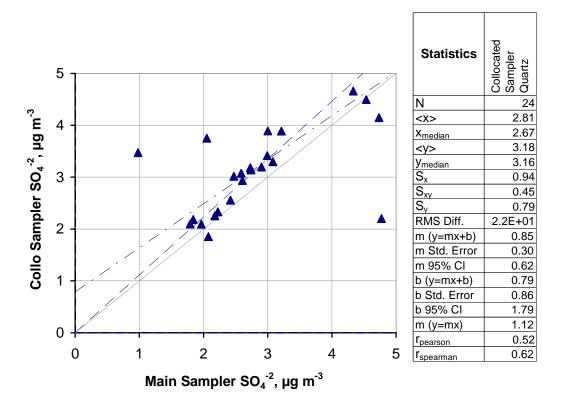


Figure 14A Sulfate: Collocated Big BOSS quartz filters at all sites.



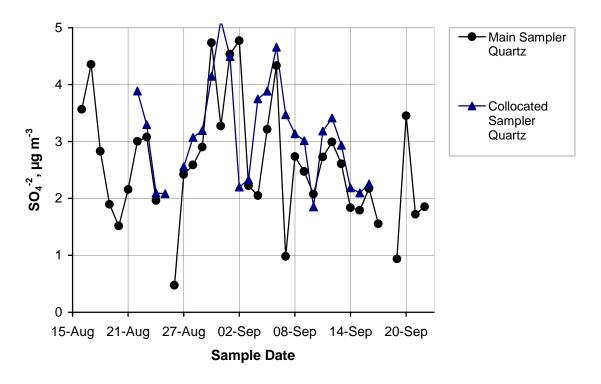
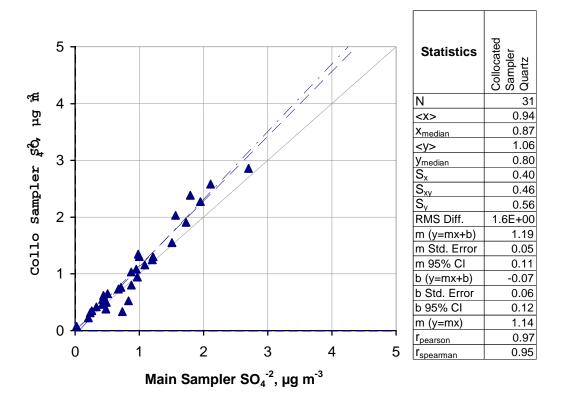


Figure 14R Sulfate: Collocated Big BOSS quartz filters at Riverside.



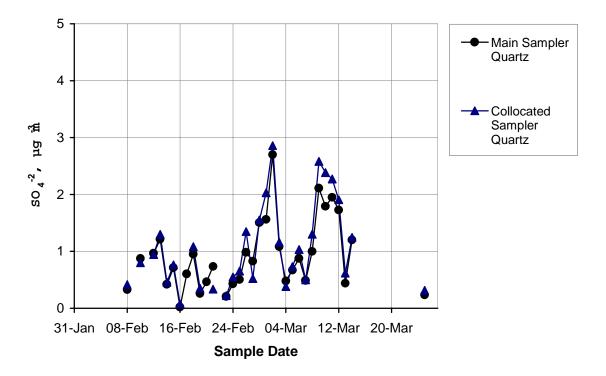
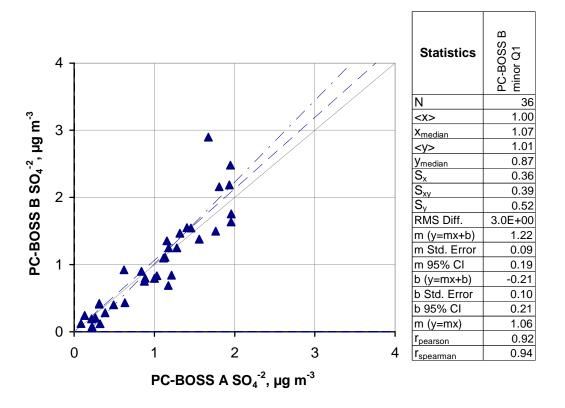


Figure 14B Sulfate: Collocated Big BOSS quartz filters at Bakersfield.



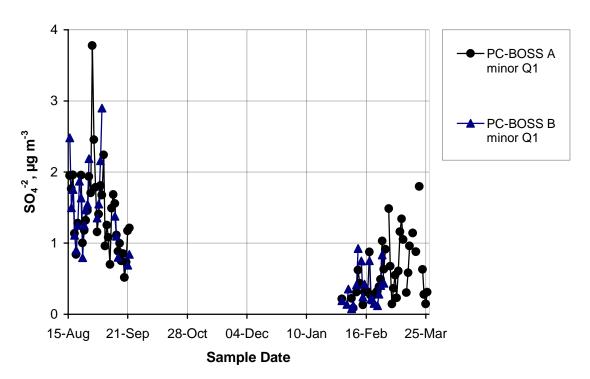


Figure 15A Sulfate: Collocated PC-BOSS minor flow quartz filters at all sites.

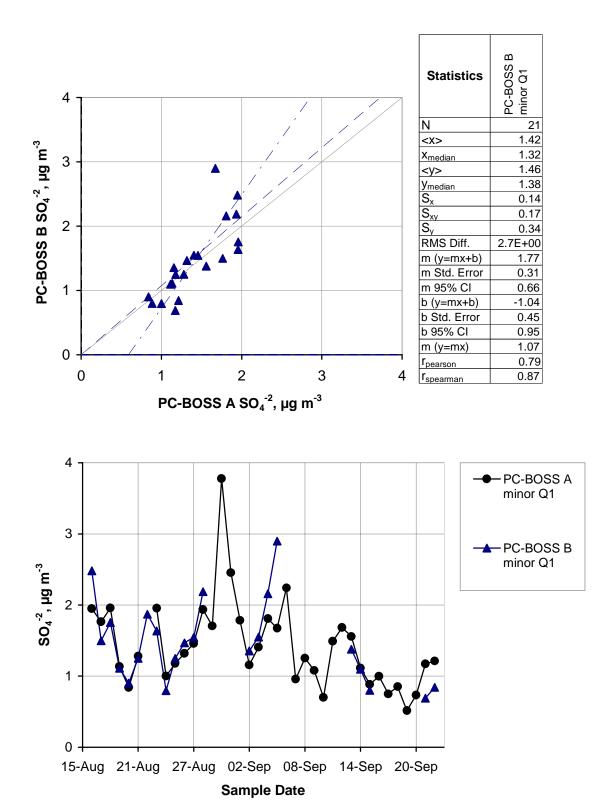
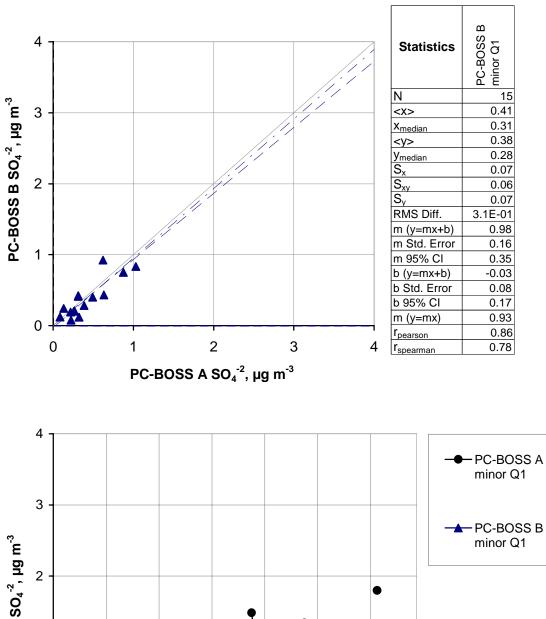
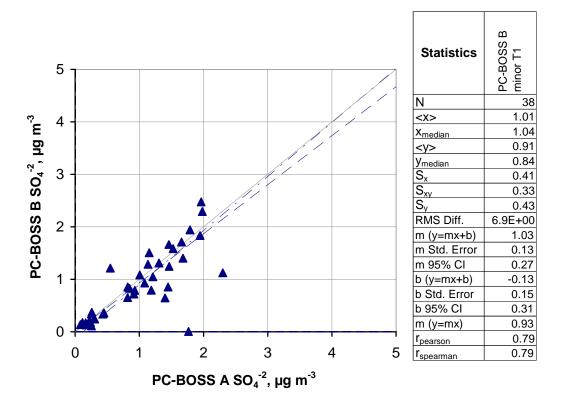


Figure 15R Sulfate: Collocated PC-BOSS minor flow quartz filters at Riverside.



31-Jan 08-Feb 16-Feb 24-Feb 04-Mar 12-Mar 20-Mar Sample Date

Figure 15B Sulfate: Collocated PC-BOSS minor flow quartz filters at Bakersfield.



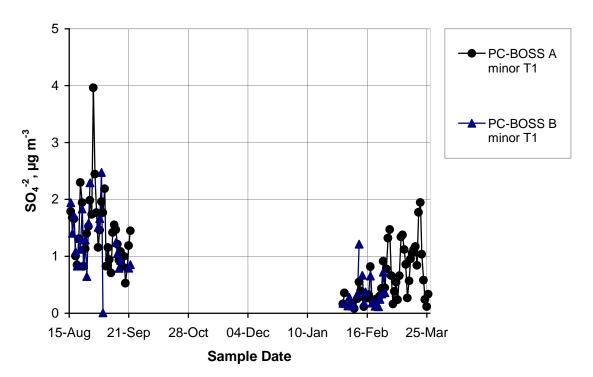
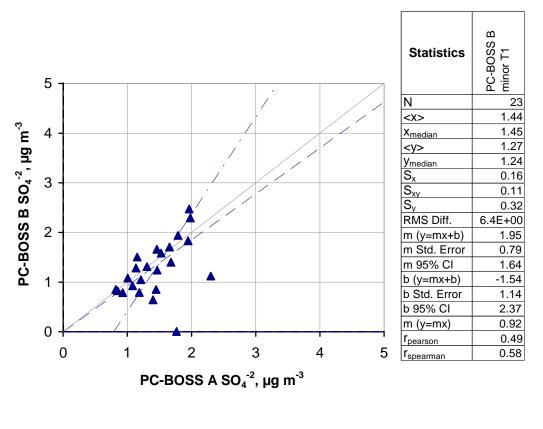


Figure 16A Sulfate: Collocated PC-BOSS minor flow Teflon filters at all sites.



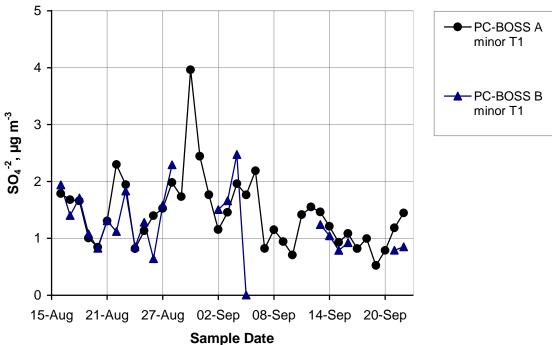
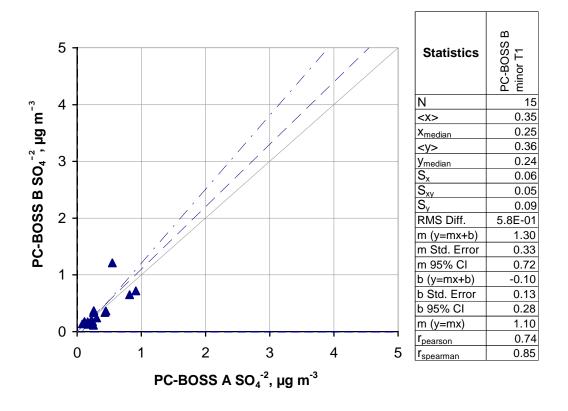


Figure 16R Sulfate: Collocated PC-BOSS minor flow Teflon filters at Riverside.



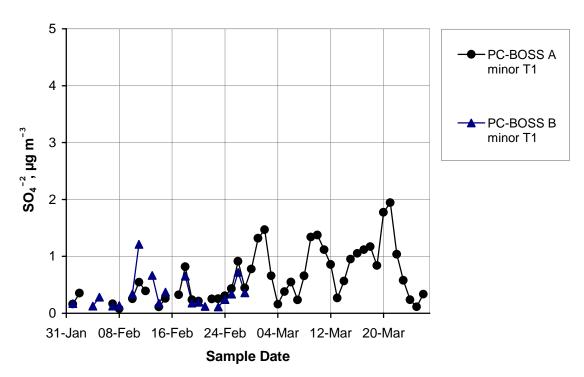
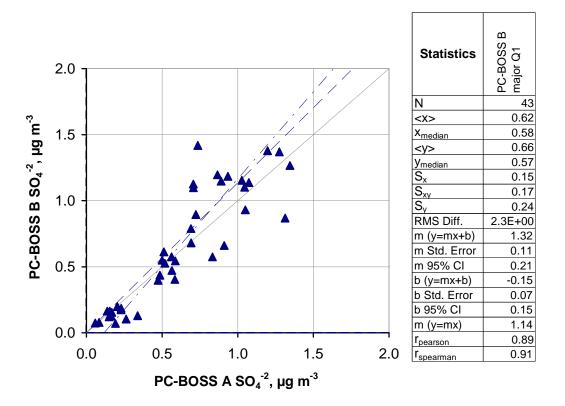


Figure 16B Sulfate: Collocated PC-BOSS minor flow Teflon filters at Bakersfield.



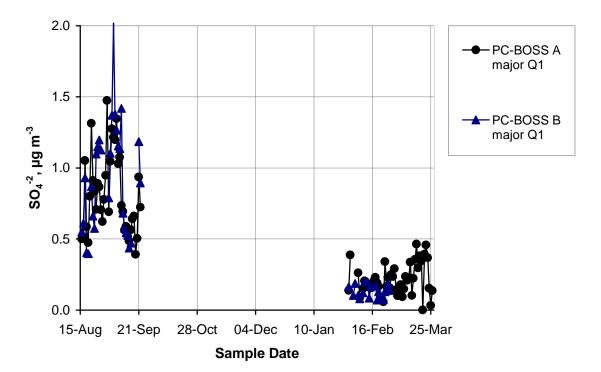
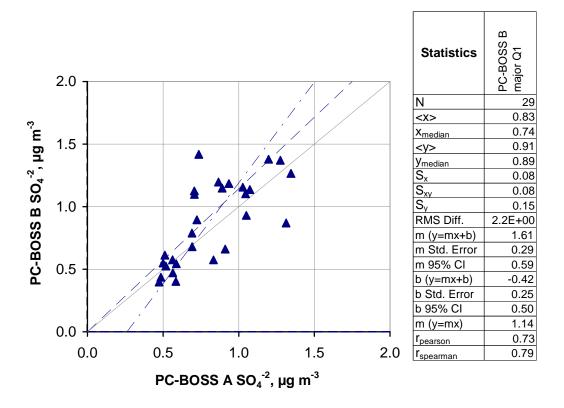


Figure 17A Sulfate: Collocated PC-BOSS major flow quartz filters at all sites.



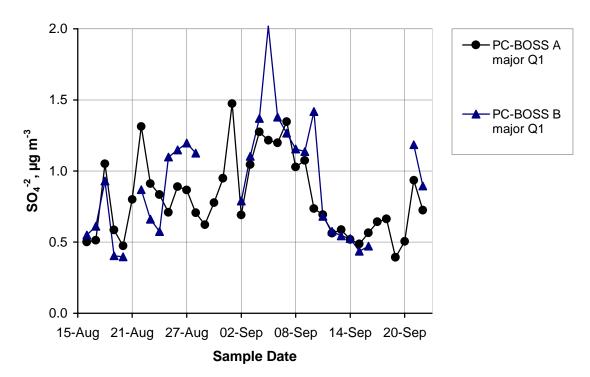
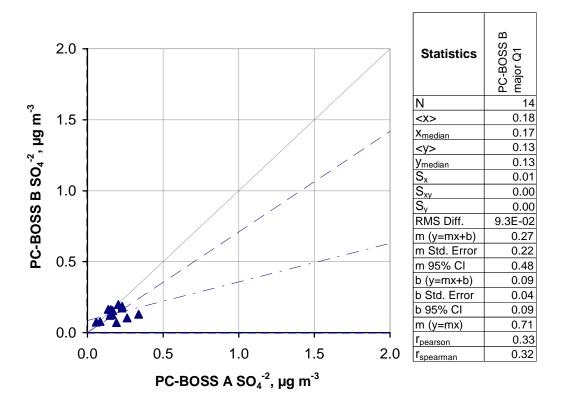


Figure 17R Sulfate: Collocated PC-BOSS major flow quartz filters at Riverside.



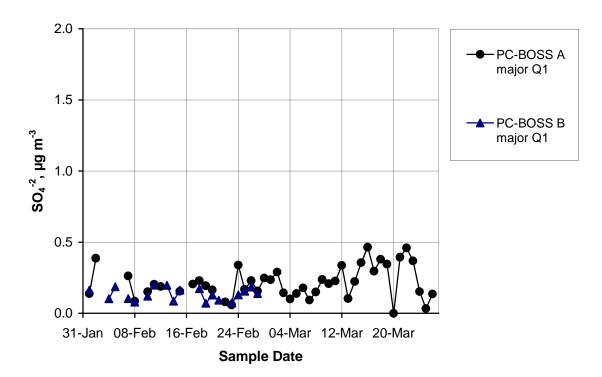
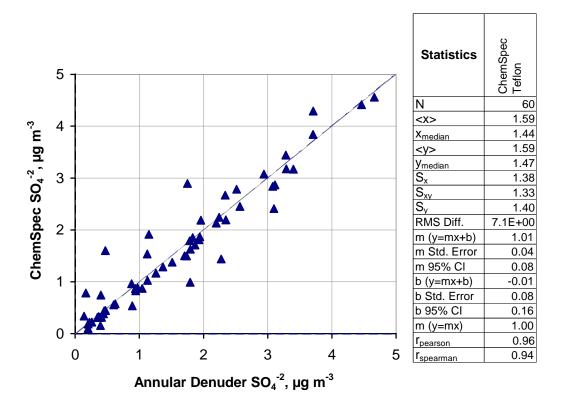
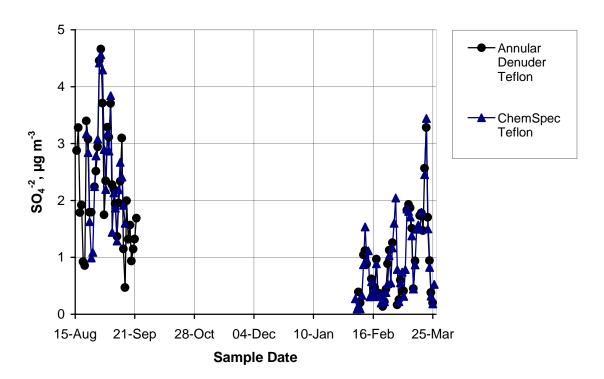
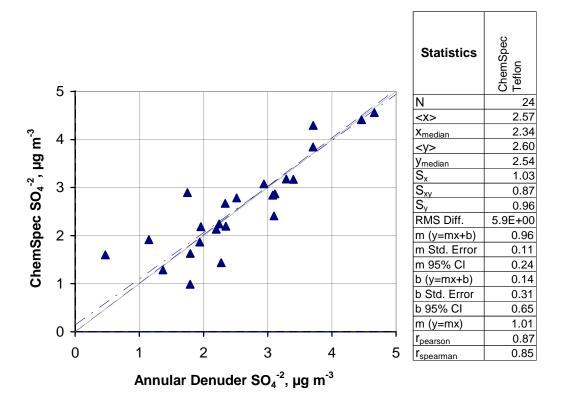


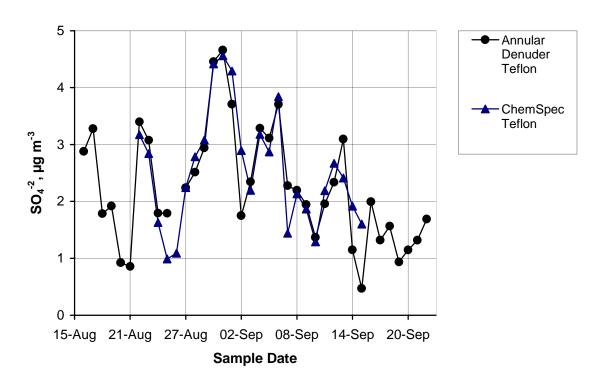
Figure 17B Sulfate: Collocated PC-BOSS major flow quartz filters at Bakersfield.



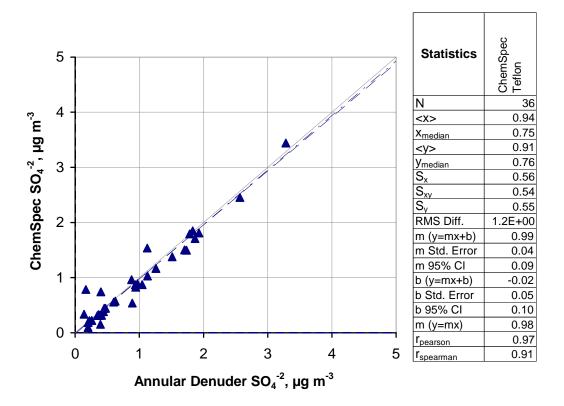


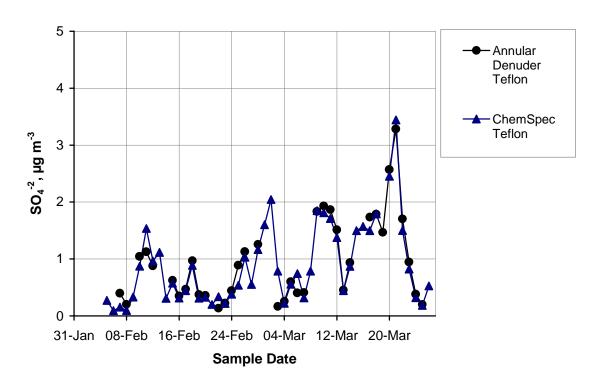
**Figure 18A** Sulfate: Annular Denuder Sampler vs. ChemSpec sampler Teflon filters at all sites.



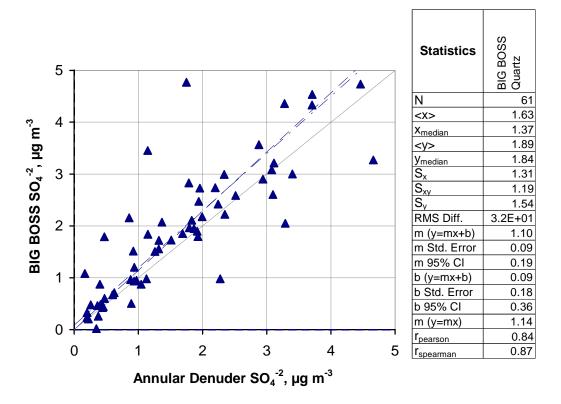


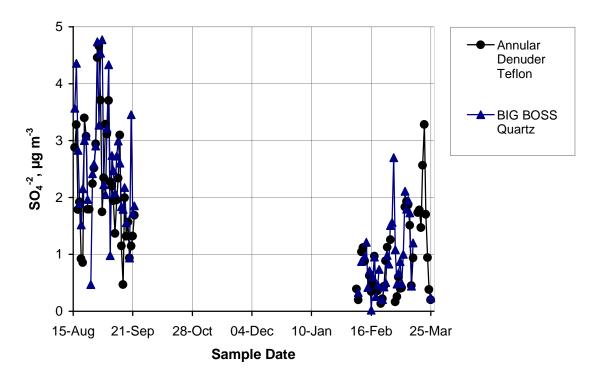
**Figure 18R** Sulfate: Annular Denuder Sampler vs. ChemSpec sampler Teflon filters at Riverside.



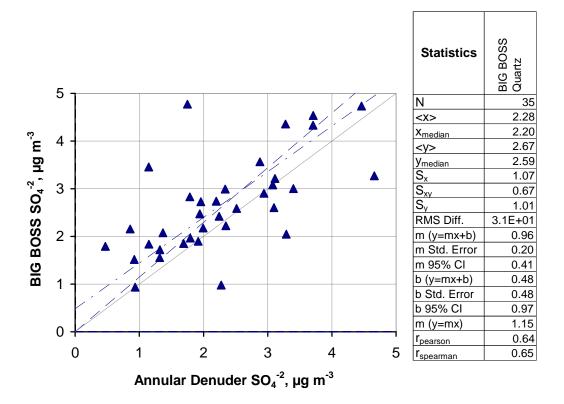


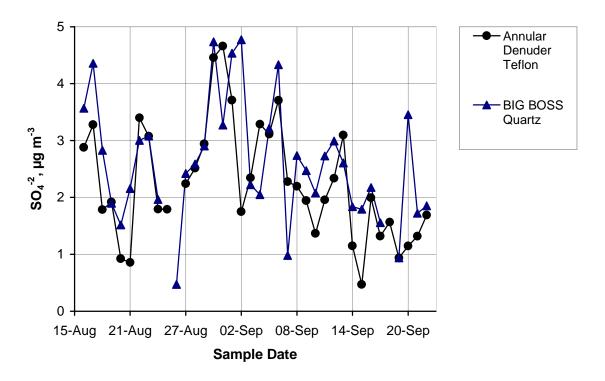
**Figure 18B** Sulfate: Annular Denuder Sampler vs. ChemSpec sampler Teflon filters at Bakersfield.



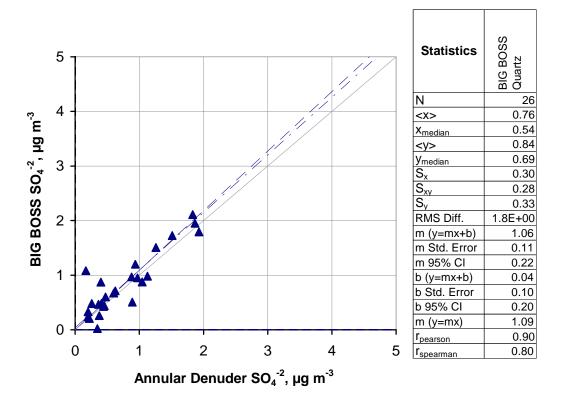


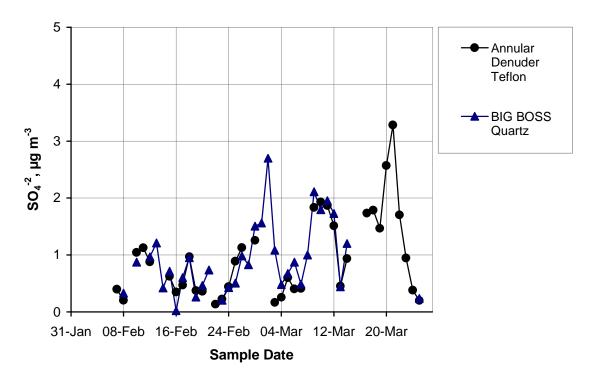
**Figure 19A** Sulfate: Annular Denuder Sampler Teflon filter vs. Big BOSS quartz filter at all sites.



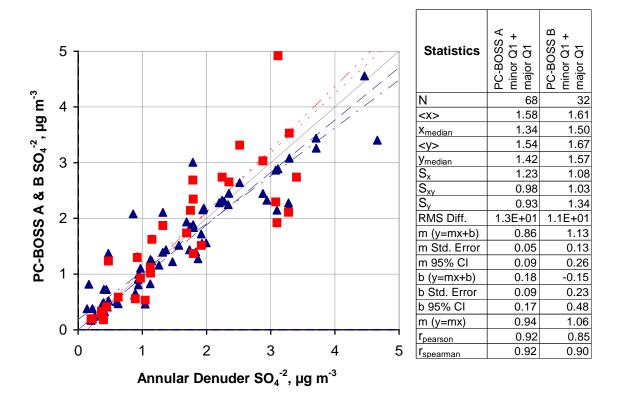


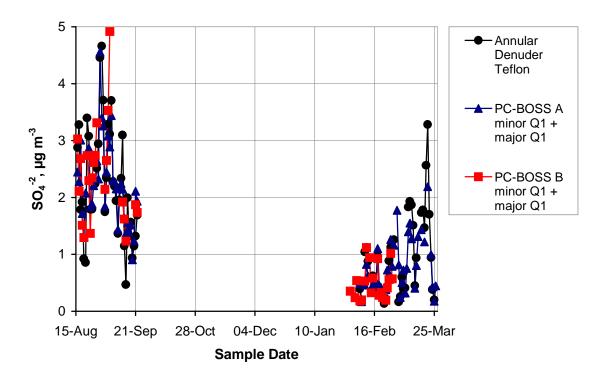
**Figure 19R** Sulfate: Annular Denuder Sampler Teflon filter vs. Big BOSS quartz filter at Riverside.



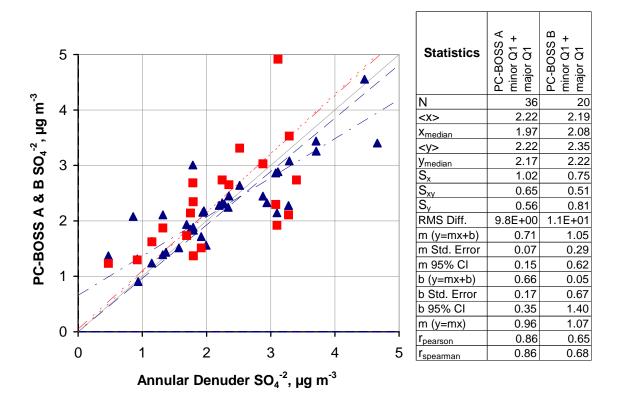


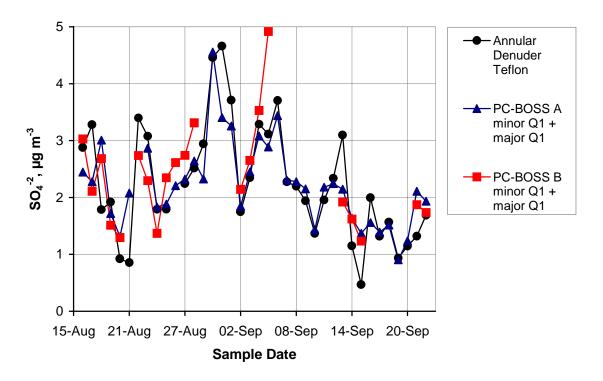
**Figure 19B** Sulfate: Annular Denuder Sampler Teflon filter vs. Big BOSS quartz filter at Bakersfield.



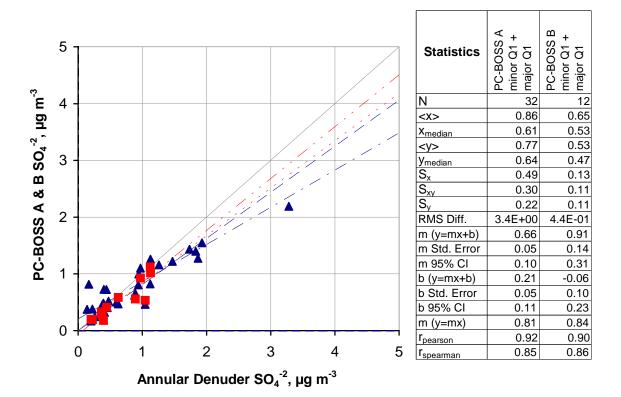


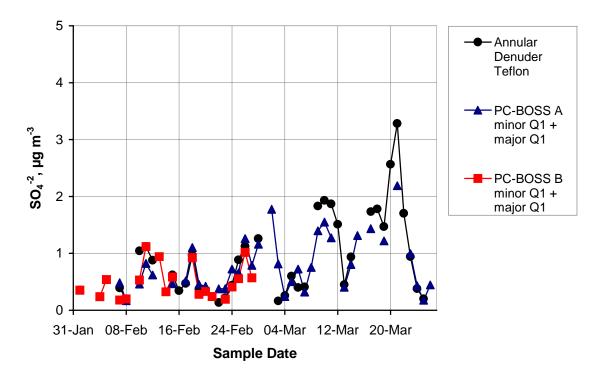
**Figure 20A** Sulfate: Annular Denuder Sampler Teflon filter vs. PC-BOSS A and B minor + major quartz filters at all sites.



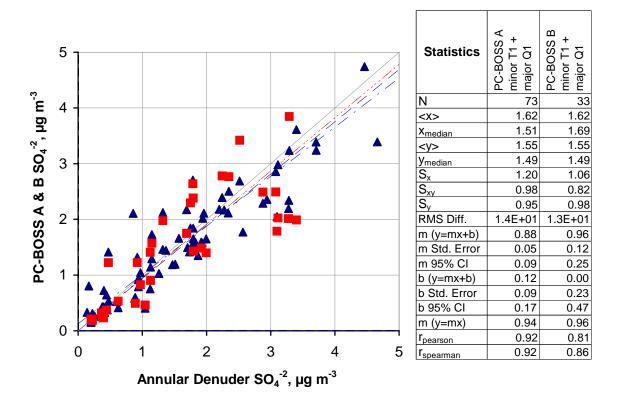


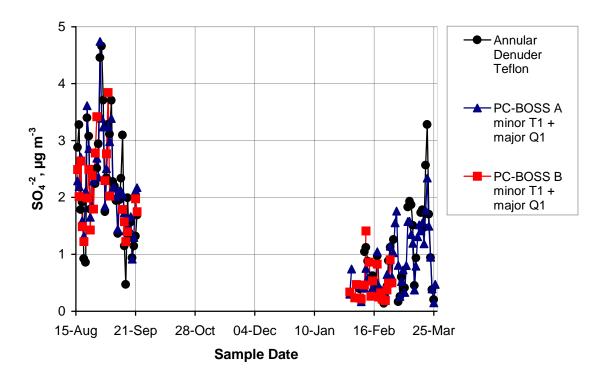
**Figure 20R** Sulfate: Annular Denuder Sampler Teflon filter vs. PC-BOSS A and B minor + major quartz filters at Riverside.



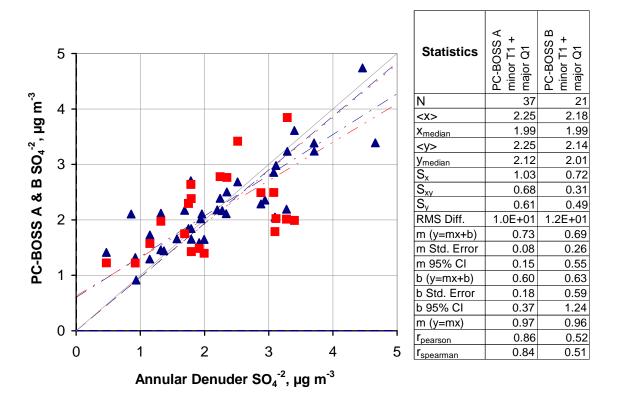


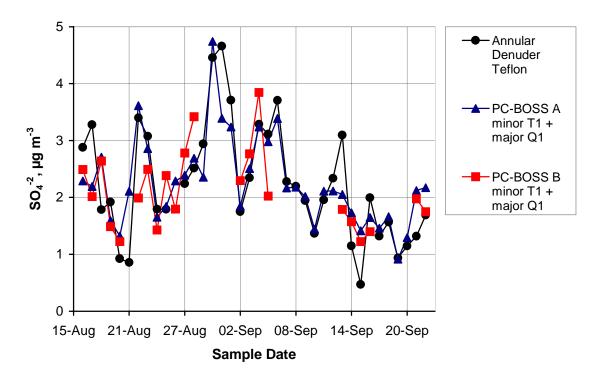
**Figure 20B** Sulfate: Annular Denuder Sampler Teflon filter vs. PC-BOSS A and B minor + major quartz filters at Bakersfield.



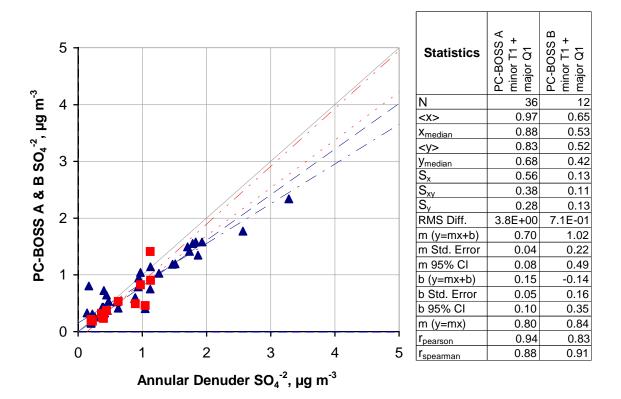


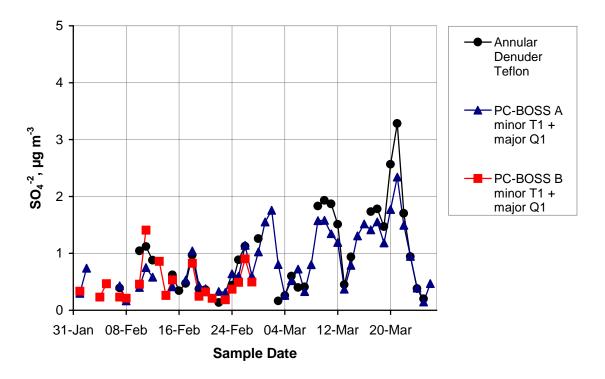
**Figure 21A** Sulfate: Annular Denuder Sampler Teflon filter vs. PC-BOSS A and B minor Teflon + major quartz filters at all sites.



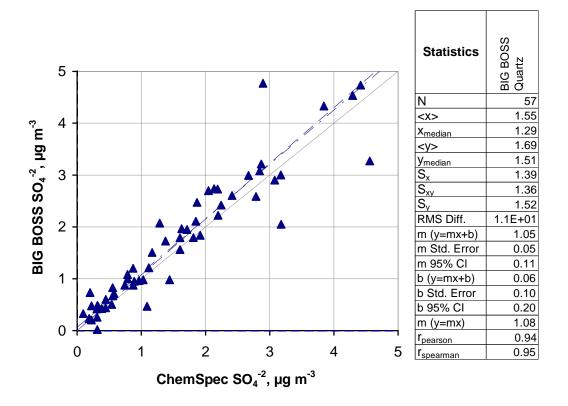


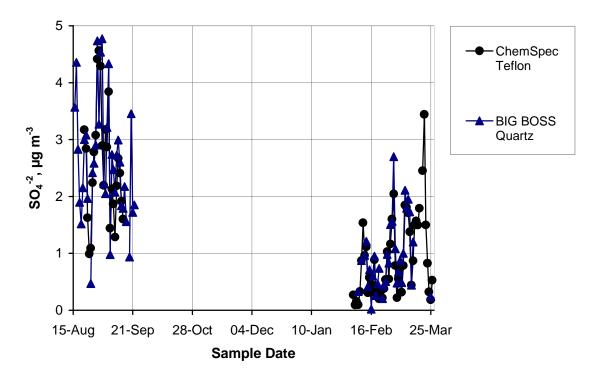
**Figure 21R** Sulfate: Annular Denuder Sampler Teflon filter vs. PC-BOSS A and B minor Teflon + major quartz filters at Riverside.



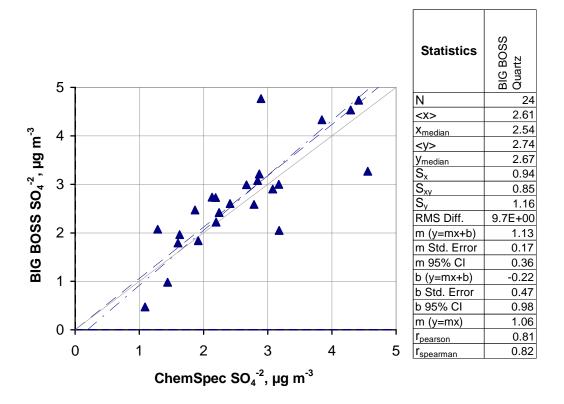


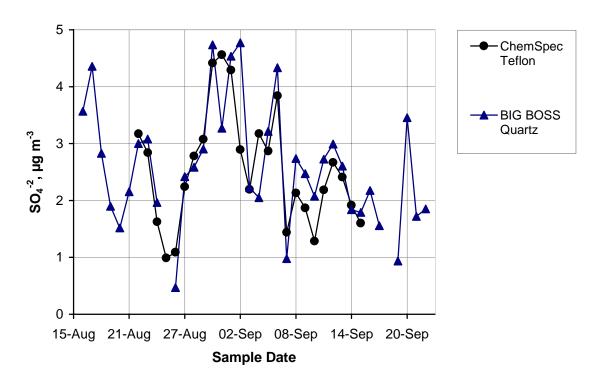
**Figure 21B** Sulfate: Annular Denuder Sampler Teflon filter vs. PC-BOSS A and B minor Teflon + major quartz filters at Bakersfield.



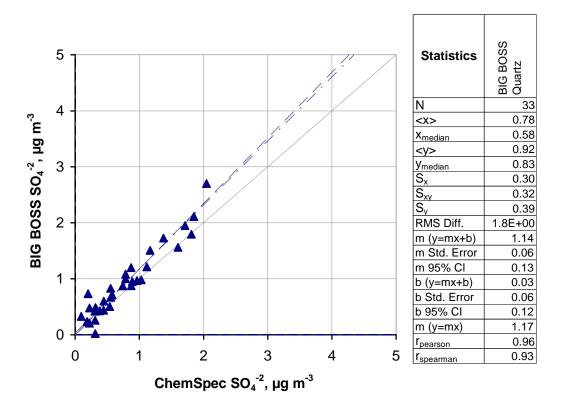


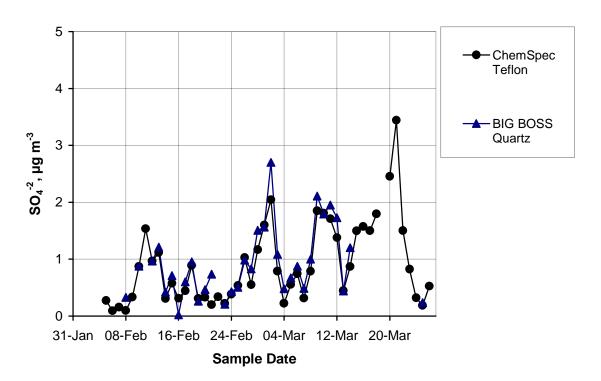
**Figure 22A** Sulfate: ChemSpec Sampler Teflon filter vs. Big BOSS quartz filter at all sites.



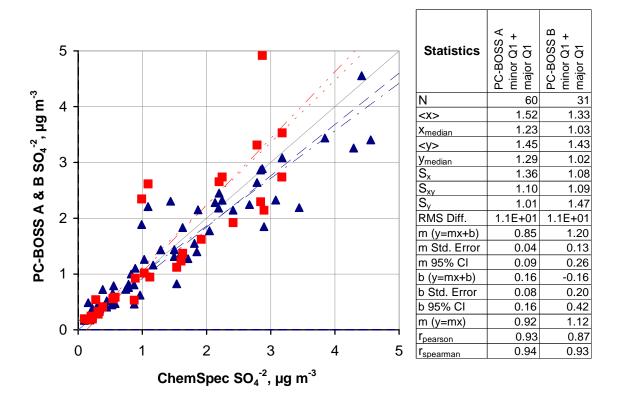


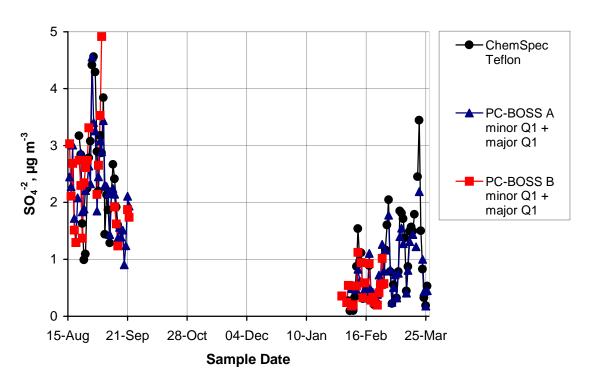
**Figure 22R** Sulfate: ChemSpec Sampler Teflon filter vs. Big BOSS quartz filter at Riverside.



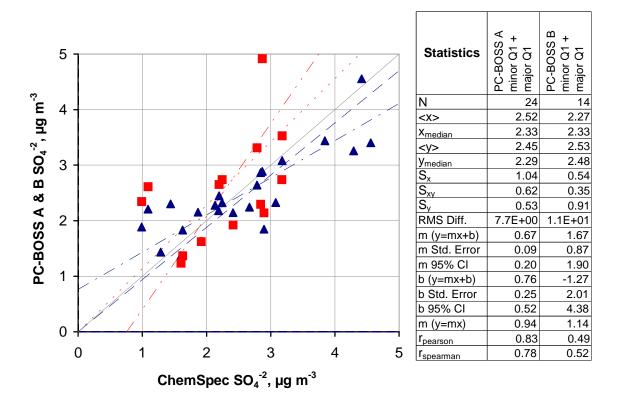


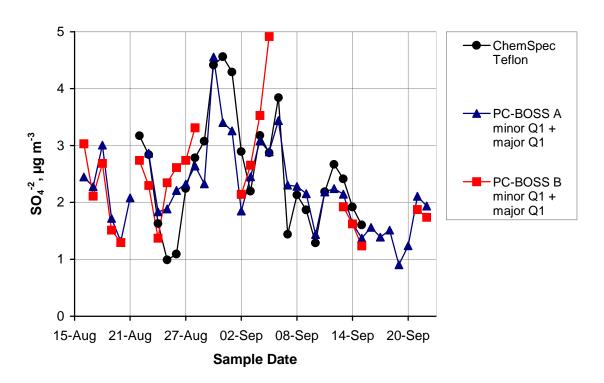
**Figure 22B** Sulfate: ChemSpec Sampler Teflon filter vs. Big BOSS quartz filter at Bakersfield.



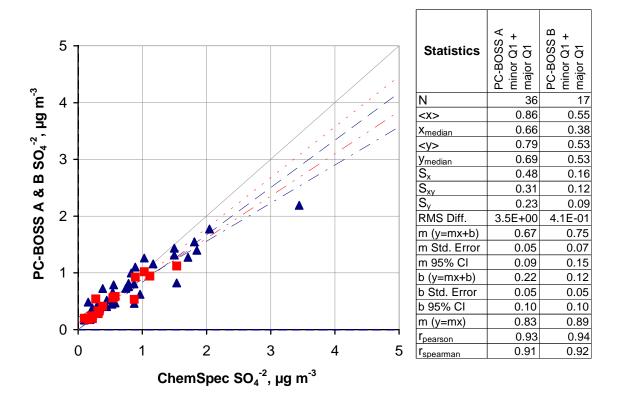


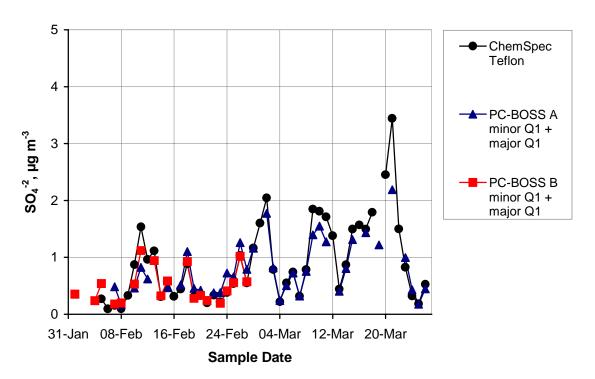
**Figure 23A** Sulfate: ChemSpec Sampler Teflon filter vs. PC-BOSS A and B minor + major quartz filters at all sites.



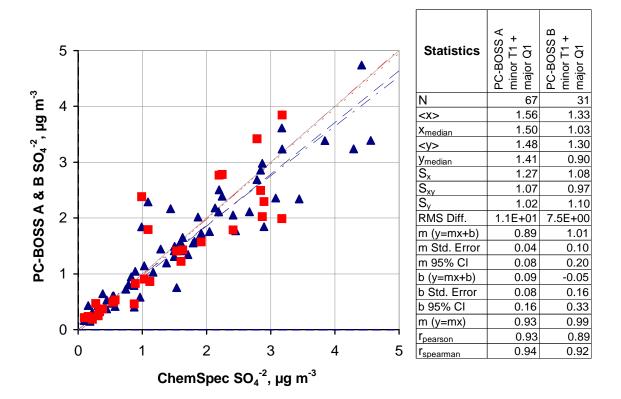


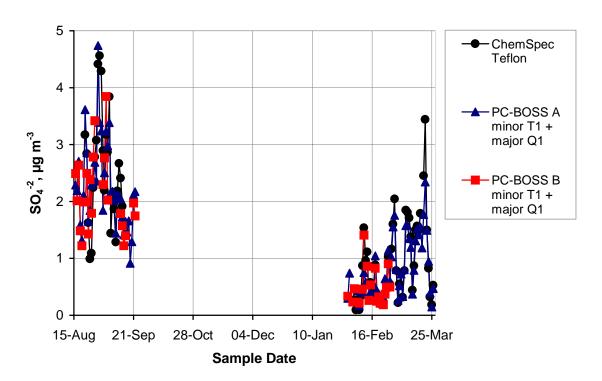
**Figure 23R** Sulfate: ChemSpec Sampler Teflon filter vs. PC-BOSS A and B minor + major quartz filters at Riverside.



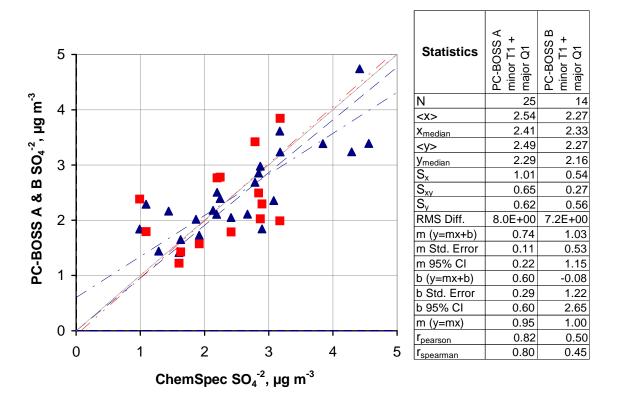


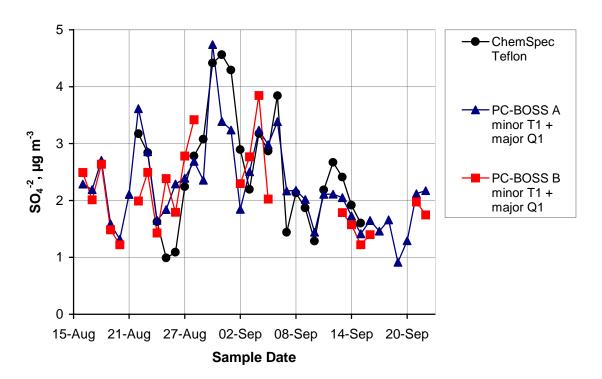
**Figure 23B** Sulfate: ChemSpec Sampler Teflon filter vs. PC-BOSS A and B minor + major quartz filters at Bakersfield.



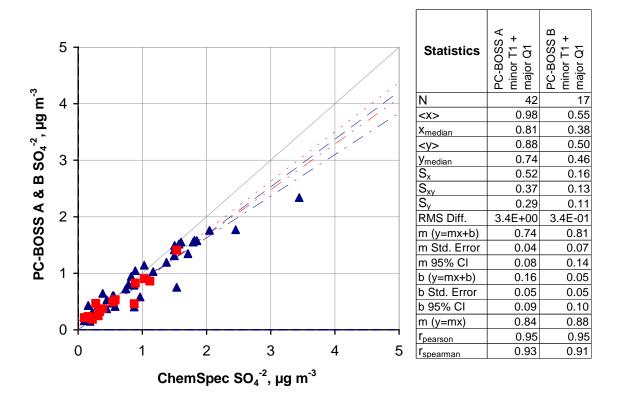


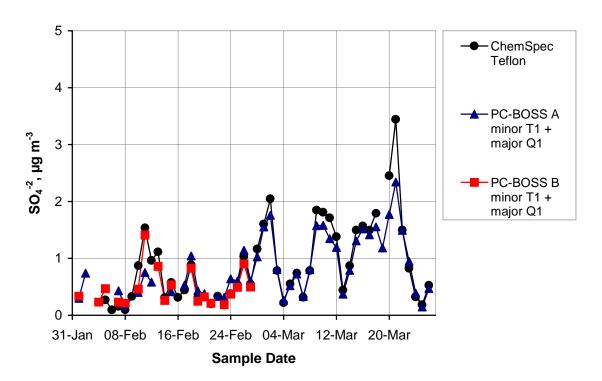
**Figure 24A** Sulfate: ChemSpec Sampler Teflon filter vs. PC-BOSS A and B minor Teflon + major quartz filters at all sites.



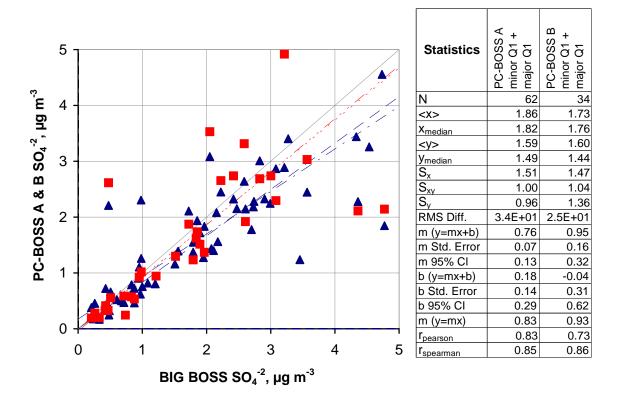


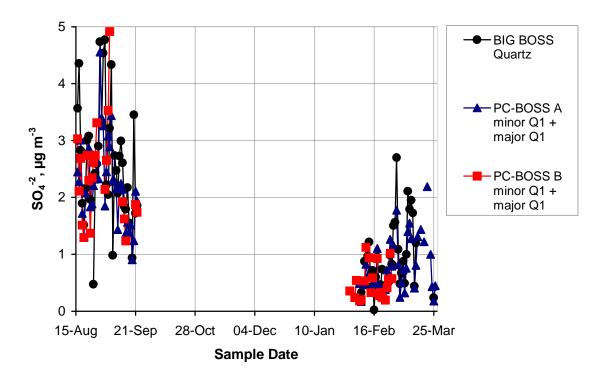
**Figure 24R** Sulfate: ChemSpec Sampler Teflon filter vs. PC-BOSS A and B minor Teflon + major quartz filters at Riverside.



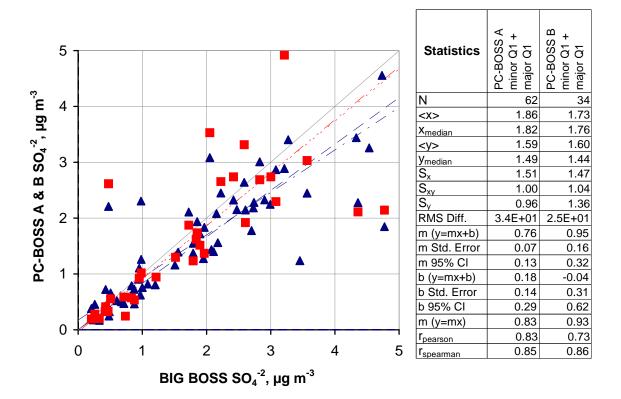


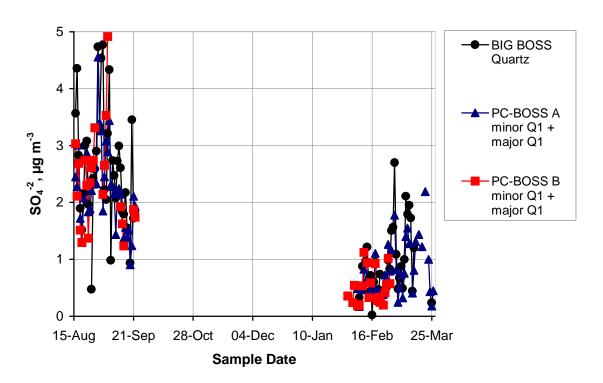
**Figure 24B** Sulfate: ChemSpec Sampler Teflon filter vs. PC-BOSS A and B minor Teflon + major quartz filters at Bakersfield.



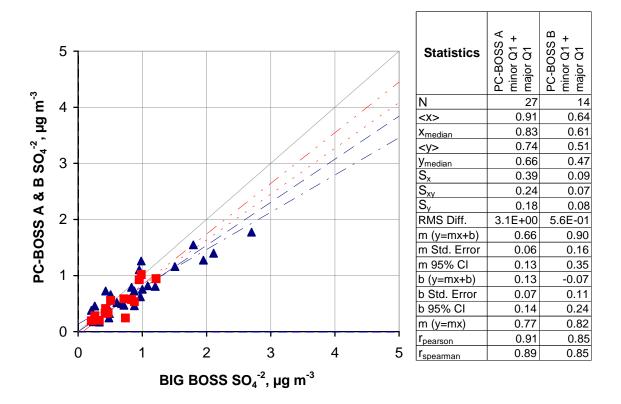


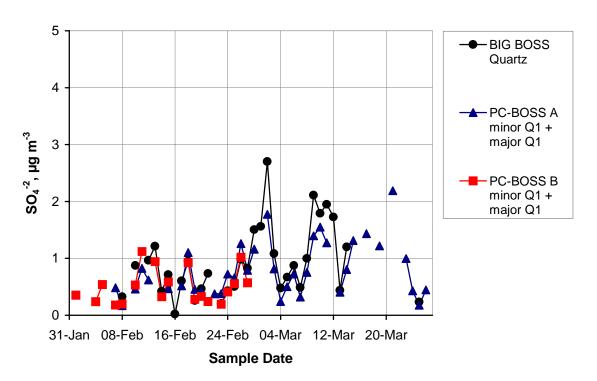
**Figure 25A** Sulfate: Big BOSS quartz filter vs. PC-BOSS A and B minor + major quartz filters at all sites.



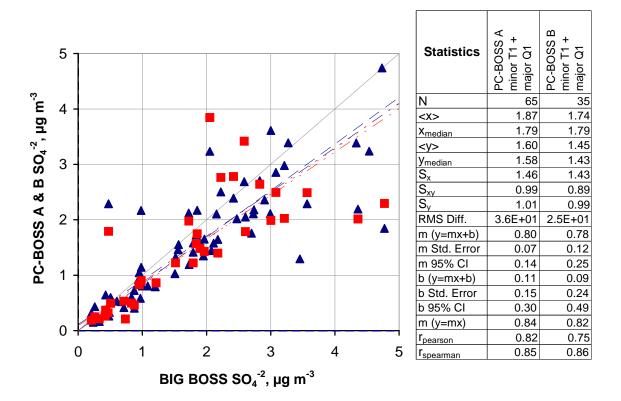


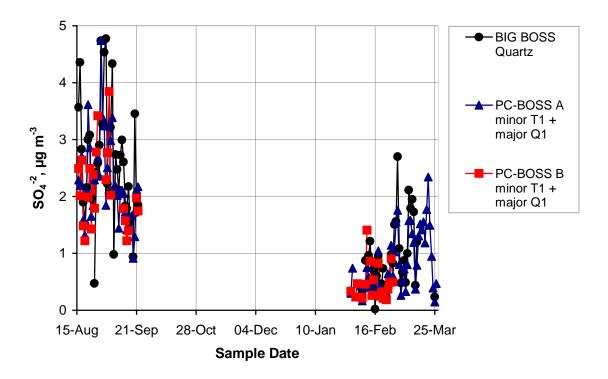
**Figure 25R** Sulfate: Big BOSS quartz filter vs. PC-BOSS A and B minor + major quartz filters at Riverside.



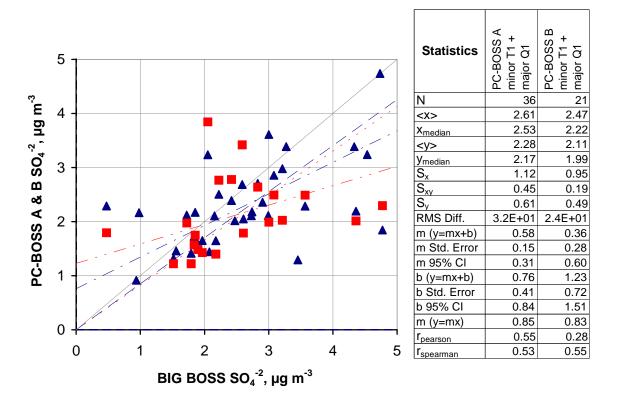


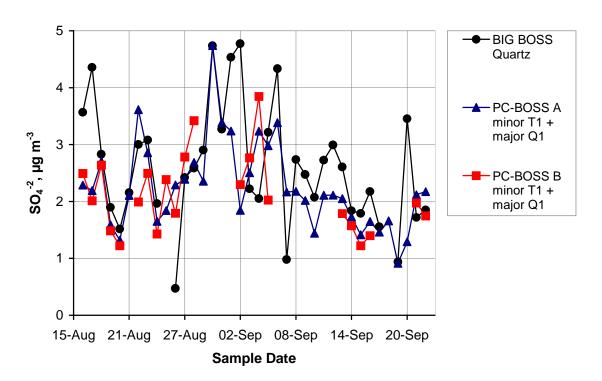
**Figure 25B** Sulfate: Big BOSS quartz filter vs. PC-BOSS A and B minor + major quartz filters at Bakersfield.



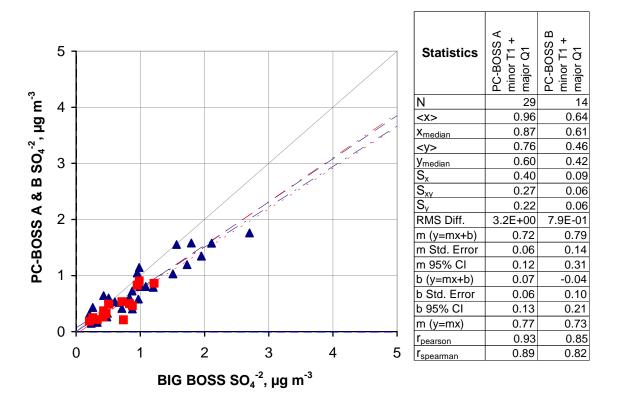


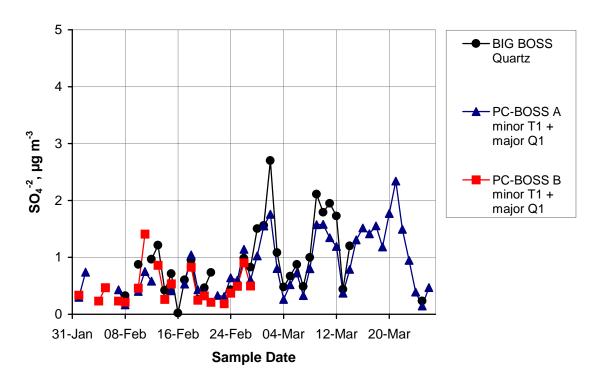
**Figure 26A** Sulfate: Big BOSS quartz filter vs. PC-BOSS A and B minor Teflon + major quartz filters at all sites.



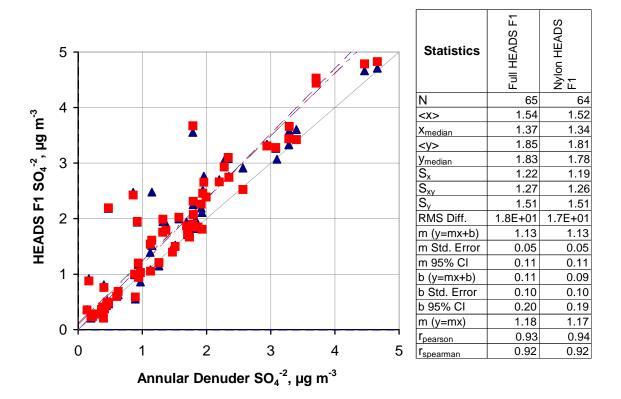


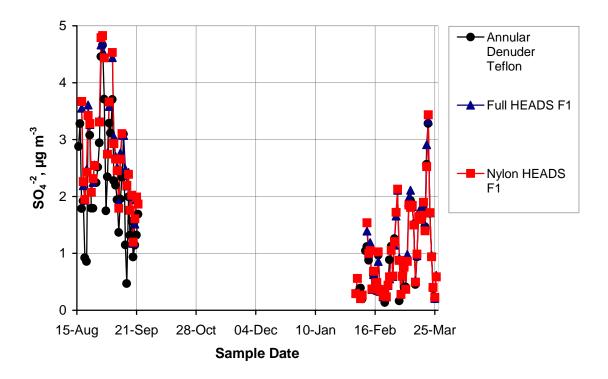
**Figure 26R** Sulfate: Big BOSS quartz filter vs. PC-BOSS A and B minor Teflon + major quartz filters at Riverside.



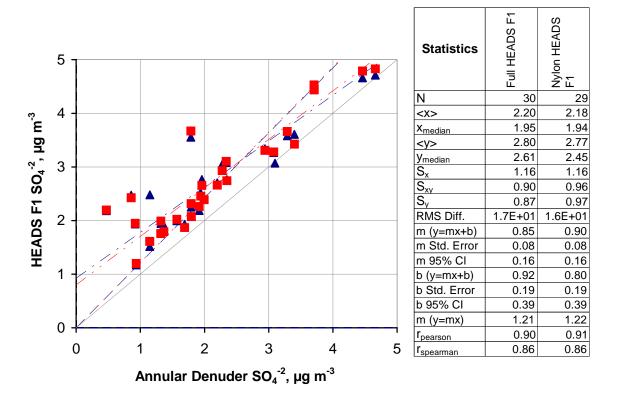


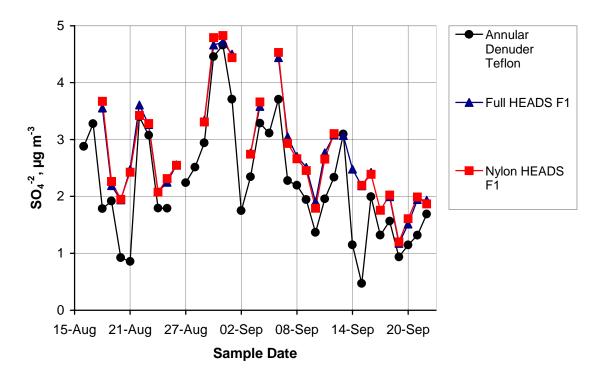
**Figure 26B** Sulfate: Big BOSS quartz filter vs. PC-BOSS A and B minor Teflon + major quartz filters at Bakersfield.



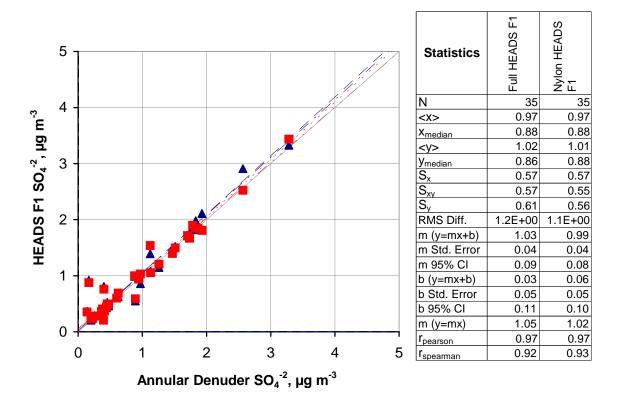


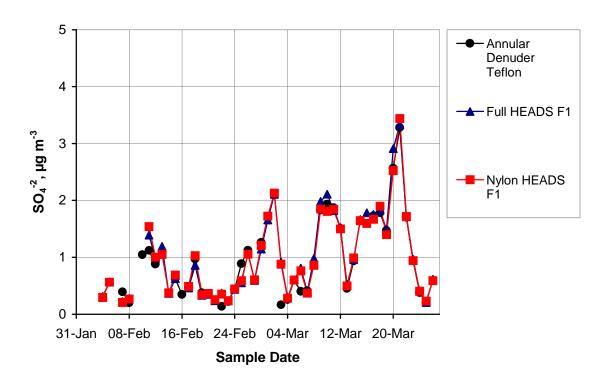
**Figure 27A** Sulfate: Full and Nylon HEADS F1 (Teflon) filter vs. Annular Denuder Sampler Teflon filter at all sites.



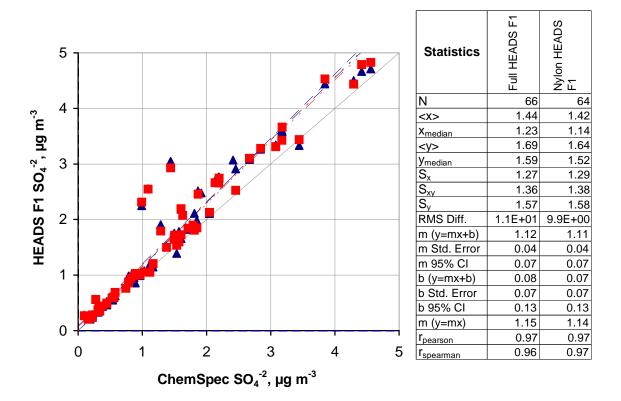


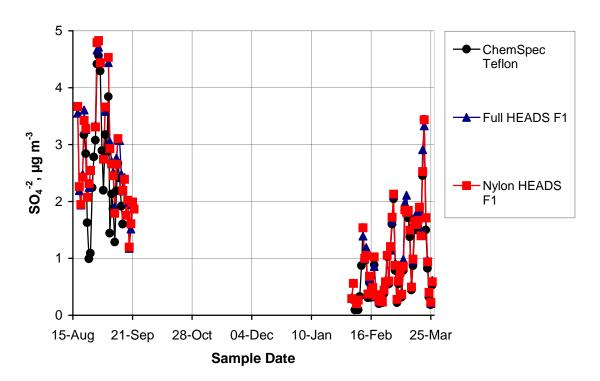
**Figure 27R** Sulfate: Full and Nylon HEADS F1 (Teflon) filter vs. Annular Denuder Sampler Teflon filter at Riverside.



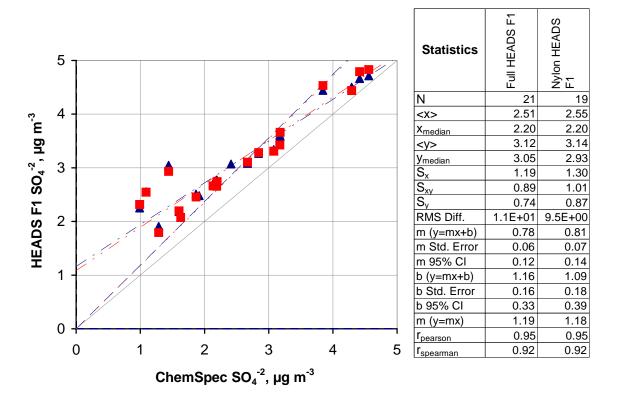


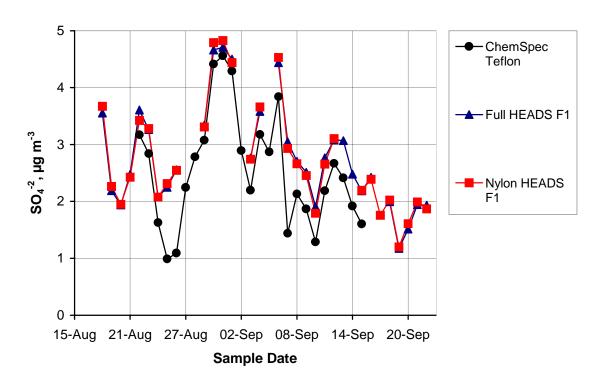
**Figure 27B** Sulfate: Full and Nylon HEADS F1 (Teflon) filter vs. Annular Denuder Sampler Teflon filter at Bakersfield.



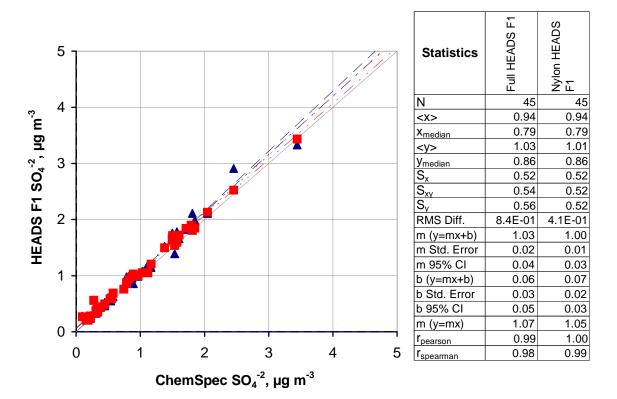


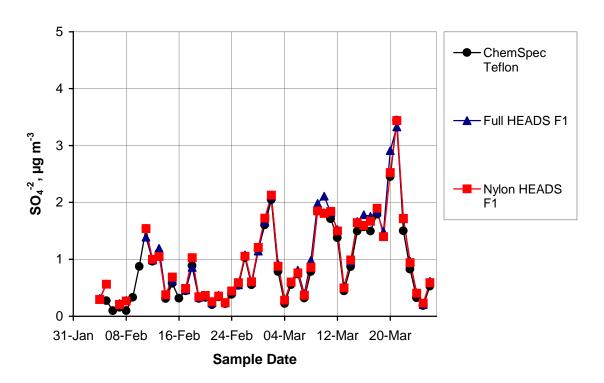
**Figure 28A** Sulfate: Full and Nylon HEADS F1 (Teflon) filter vs. ChemSpec Sampler Teflon filter at all sites.



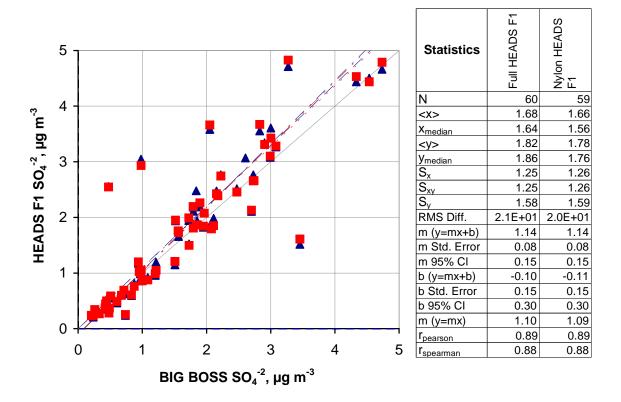


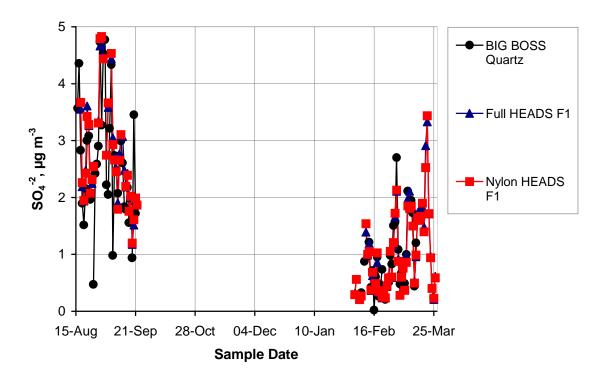
**Figure 28R** Sulfate: Full and Nylon HEADS F1 (Teflon) filter vs. ChemSpec Sampler Teflon filter at Riverside.



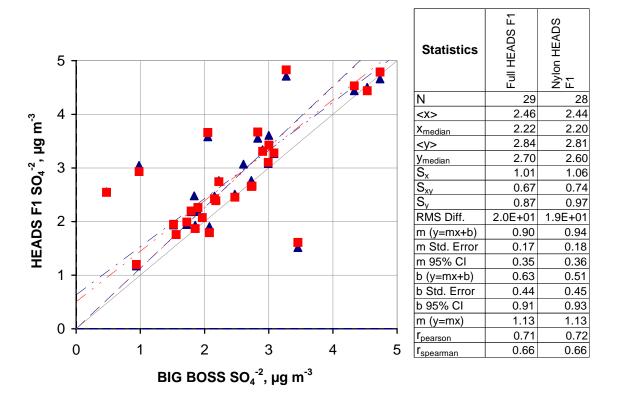


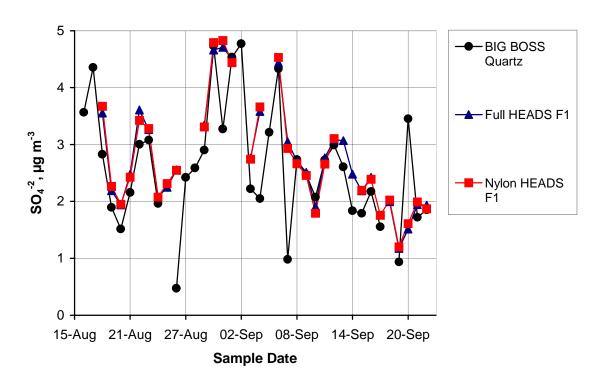
**Figure 28B** Sulfate: Full and Nylon HEADS F1 (Teflon) filter vs. ChemSpec Sampler Teflon filter at Bakersfield.



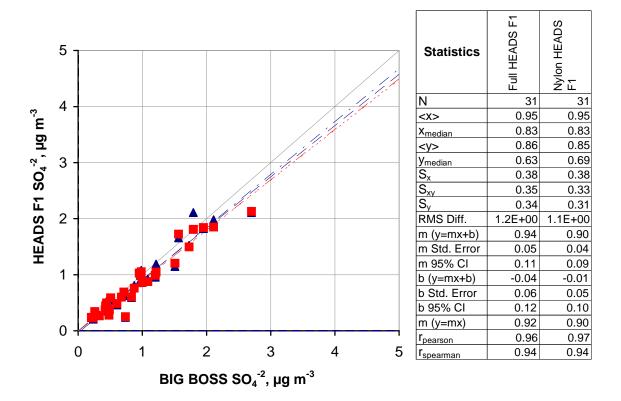


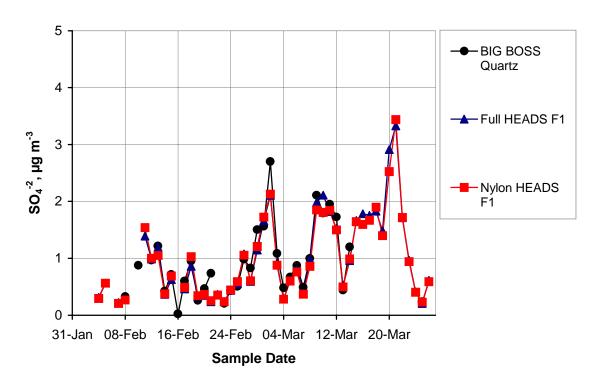
**Figure 29A** Sulfate: Full and Nylon HEADS F1 (Teflon) filter vs. Big BOSS quartz filter at all sites.



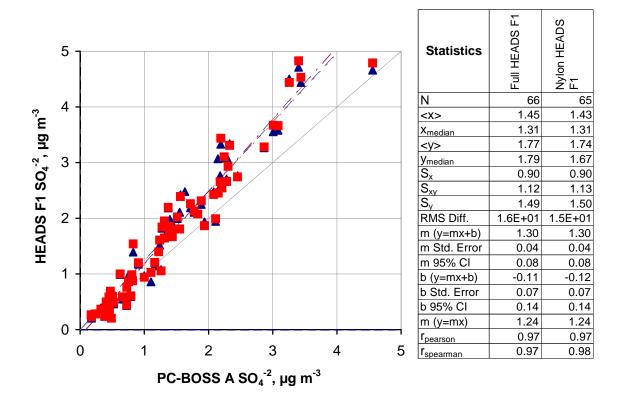


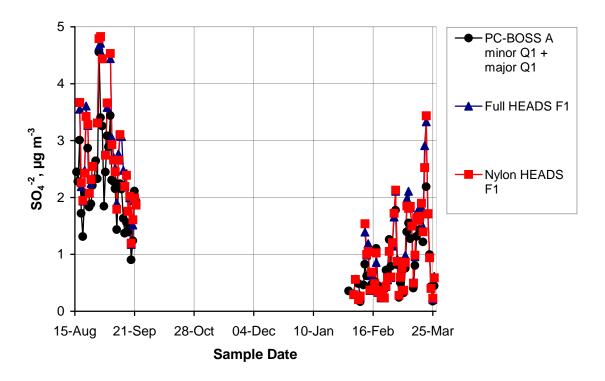
**Figure 29R** Sulfate: Full and Nylon HEADS F1 (Teflon) filter vs. Big BOSS quartz filter at Riverside.



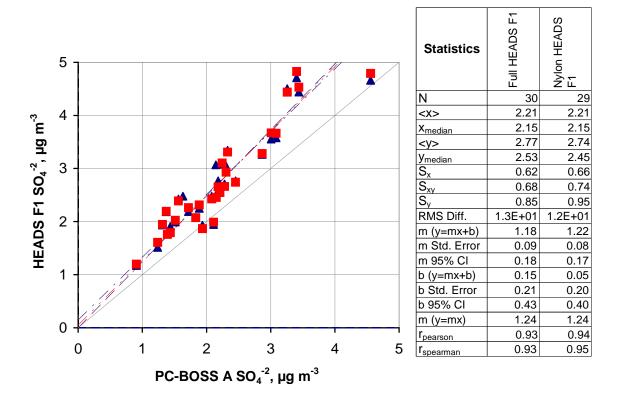


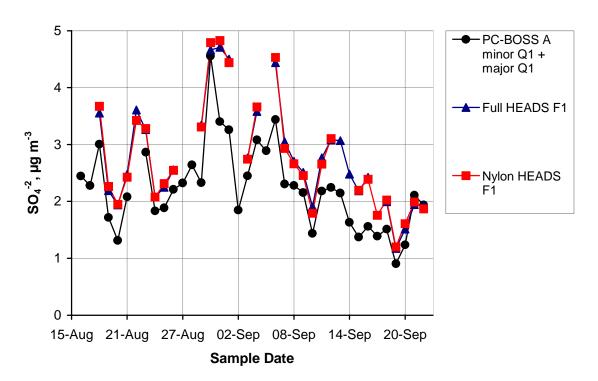
**Figure 29B** Sulfate: Full and Nylon HEADS F1 (Teflon) filter vs. Big BOSS quartz filter at Bakersfield.



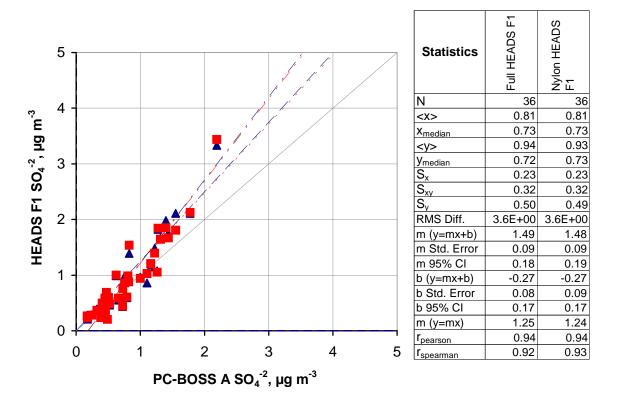


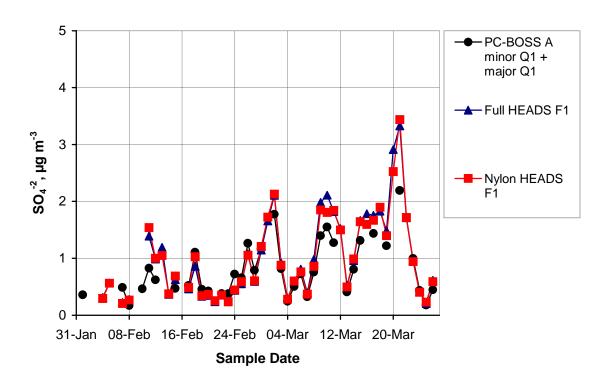
**Figure 30A** Sulfate: Full and Nylon HEADS F1 (Teflon) filter vs. PC-BOSS minor + major quartz filters at all sites.



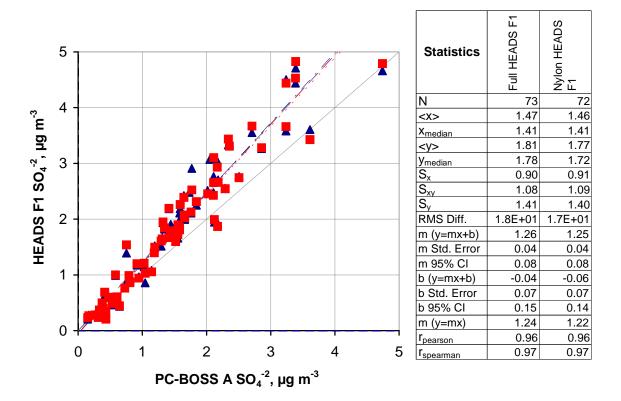


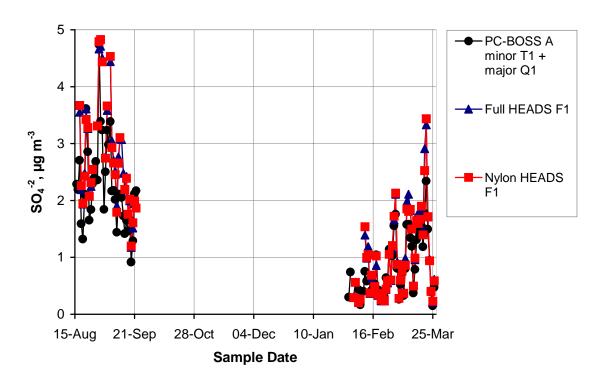
**Figure 30R** Sulfate: Full and Nylon HEADS F1 (Teflon) filter vs. PC-BOSS minor + major quartz filters at Riverside.



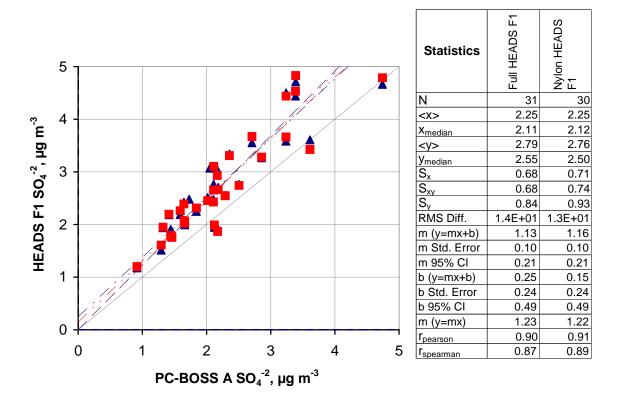


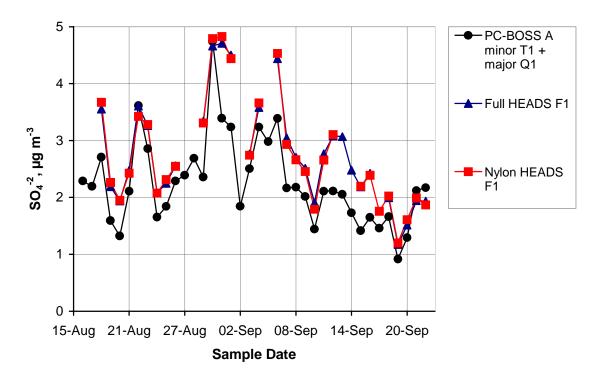
**Figure 30B** Sulfate: Full and Nylon HEADS F1 (Teflon) filter vs. PC-BOSS minor + major quartz filters at Bakersfield.



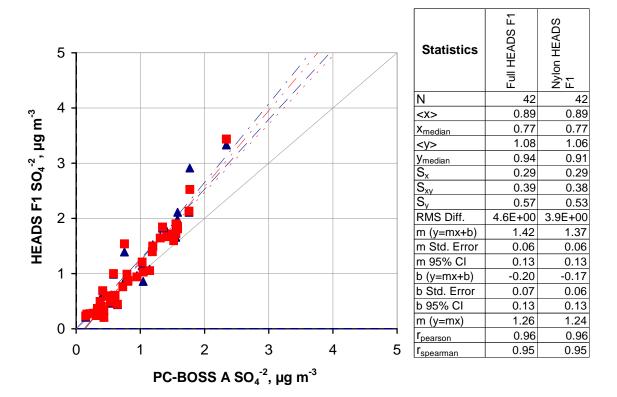


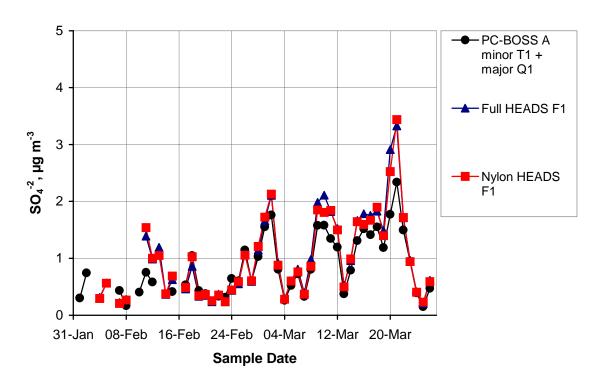
**Figure 31A** Sulfate: Full and Nylon HEADS F1 (Teflon) filter vs. PC-BOSS minor Teflon + major quartz filters at all sites.



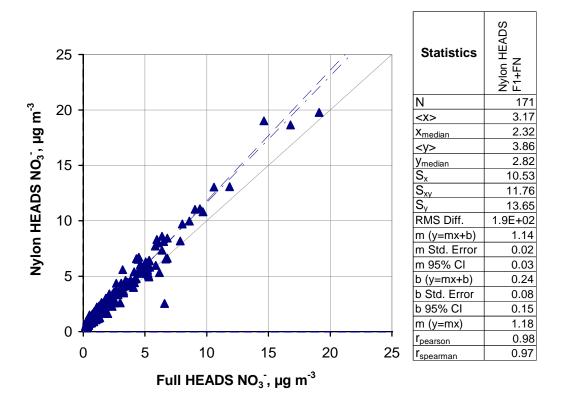


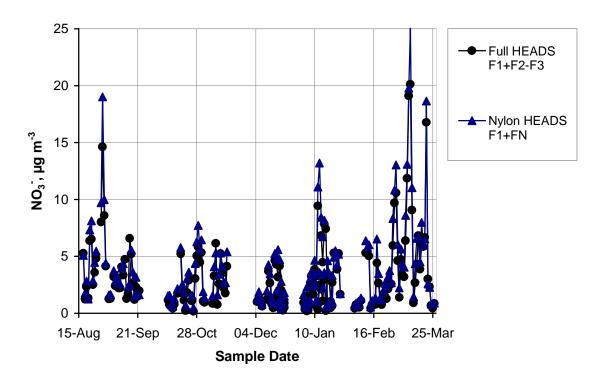
**Figure 31R** Sulfate: Full and Nylon HEADS F1 (Teflon) filter vs. PC-BOSS minor Teflon + major quartz filters at Riverside.



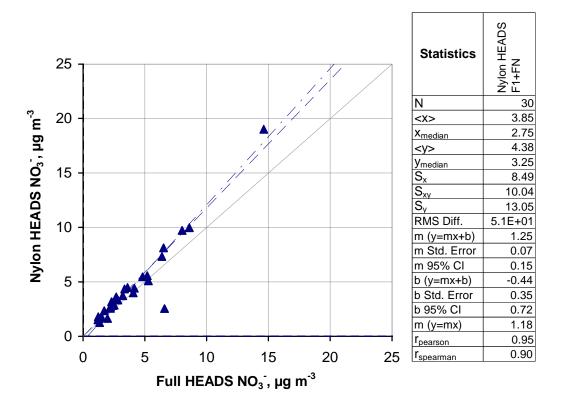


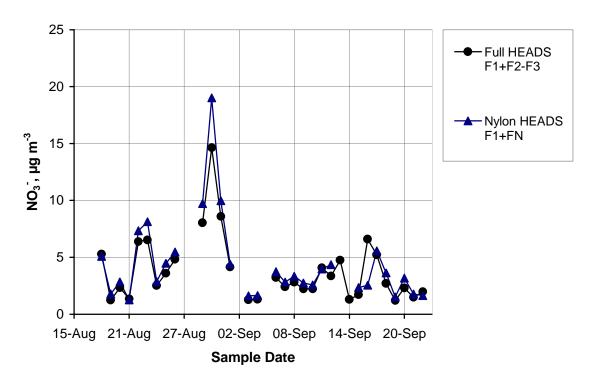
**Figure 31B** Sulfate: Full and Nylon HEADS F1 (Teflon) filter vs. PC-BOSS minor Teflon + major quartz filters at Bakersfield.



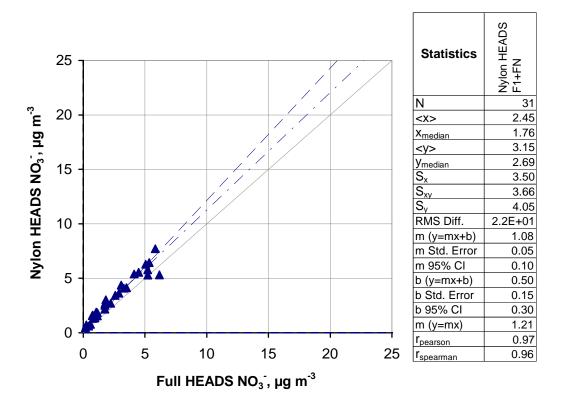


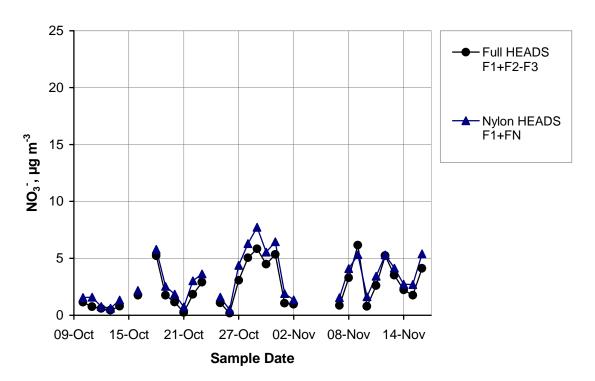
**Figure 32A** Nitrate: Full HEADS F1 + F2 – F3 filters vs. Nylon HEADS F1 + FN filters at all sites.



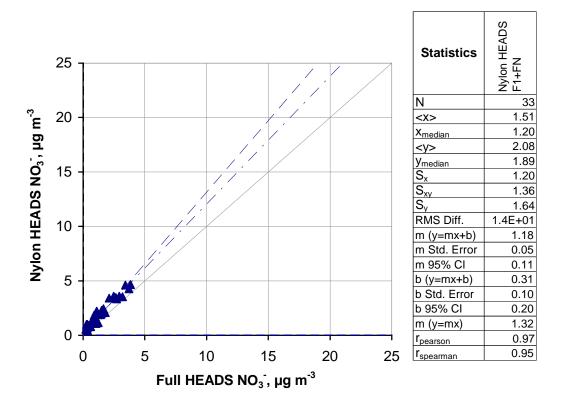


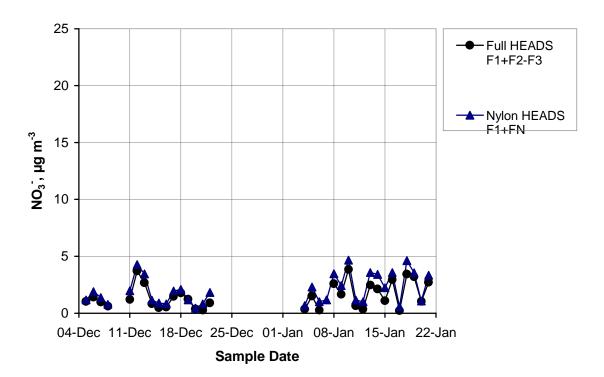
**Figure 32R** Nitrate: Full HEADS F1 + F2 – F3 filters vs. Nylon HEADS F1 + FN filters at Riverside.



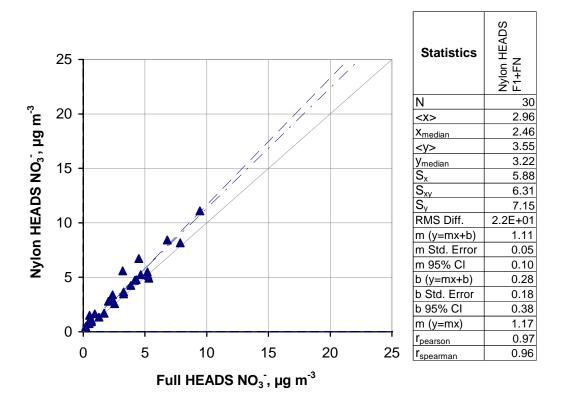


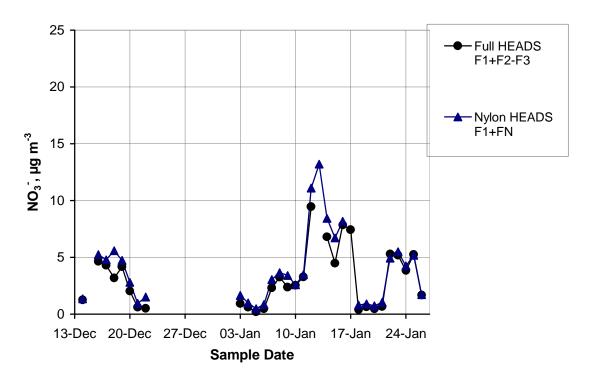
**Figure 32C** Nitrate: Full HEADS F1 + F2 – F3 filters vs. Nylon HEADS F1 + FN filters at Chicago.



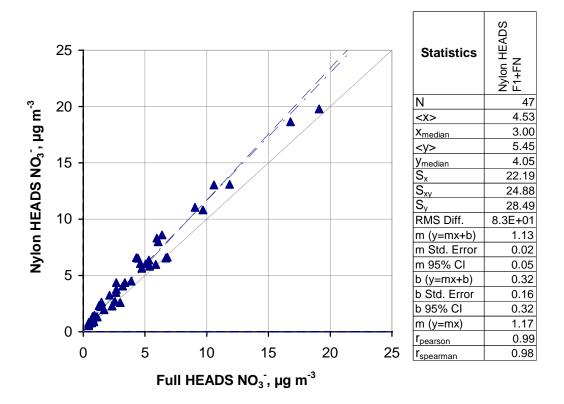


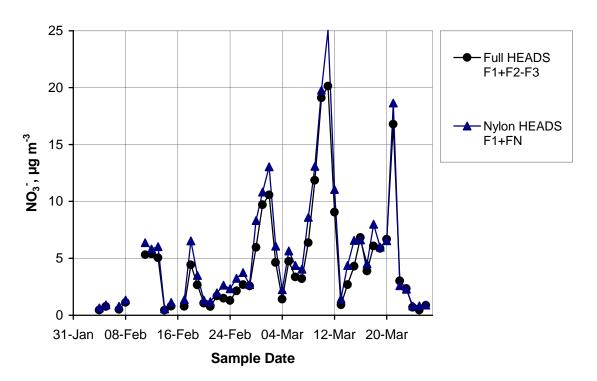
**Figure 32D** Nitrate: Full HEADS F1 + F2 – F3 filters vs. Nylon HEADS F1 + FN filters at Dallas.



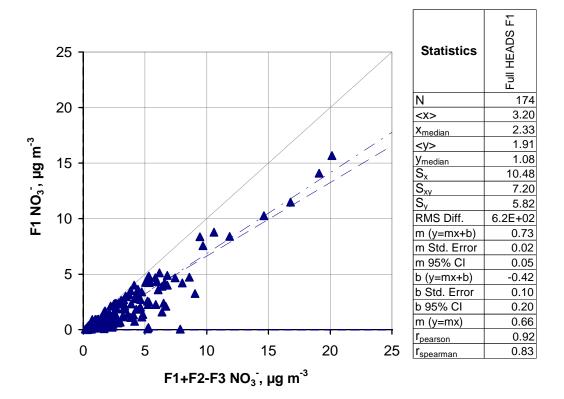


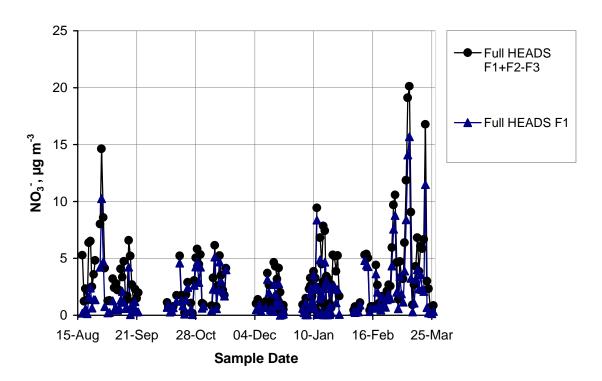
**Figure 32P** Nitrate: Full HEADS F1 + F2 – F3 filters vs. Nylon HEADS F1 + FN filters at Phoenix.



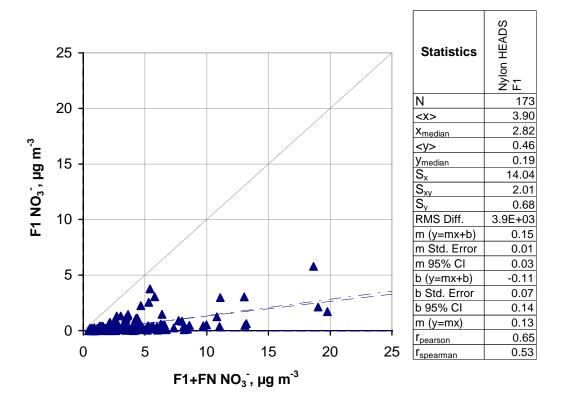


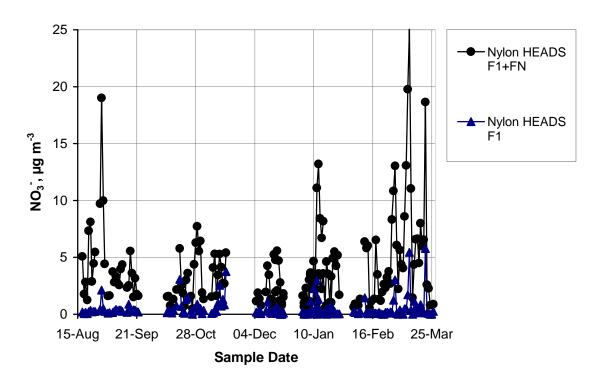
**Figure 32B** Nitrate: Full HEADS F1 + F2 – F3 filters vs. Nylon HEADS F1 + FN filters at Bakersfield.



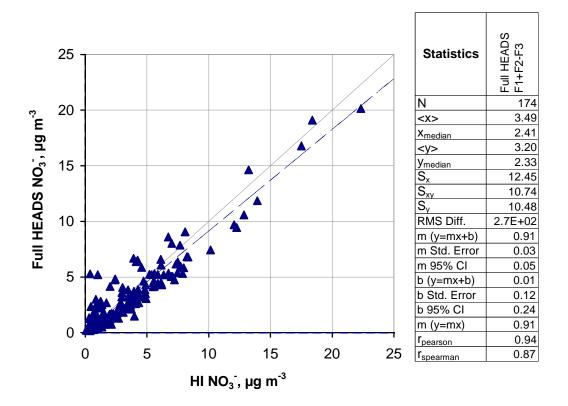


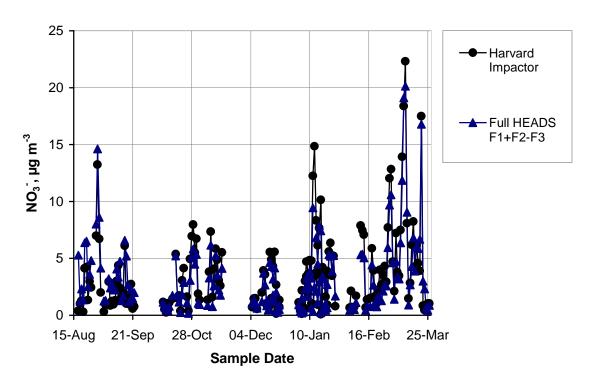
**Figure 33A** Nitrate: Full HEADS F1 (Teflon) filter vs. F1 (Teflon) + F2 – F3 (sodium carbonate) filters at all sites.



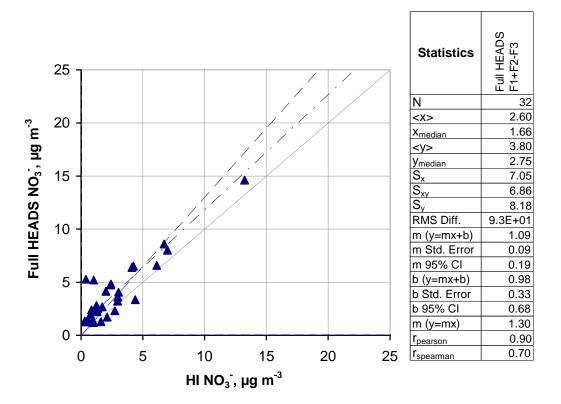


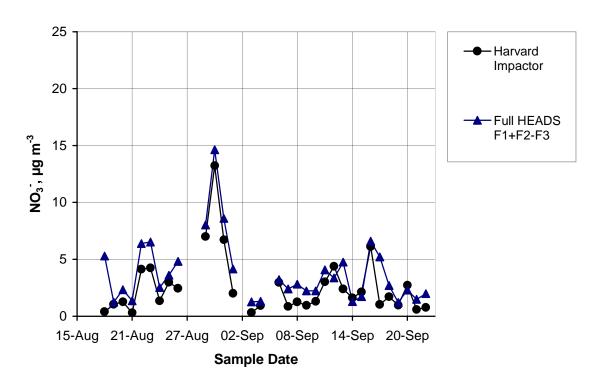
**Figure 34A** Nitrate: Nylon HEADS F1 (Teflon) filter vs. F1 (Teflon) + FN (nylon) filters at all sites.



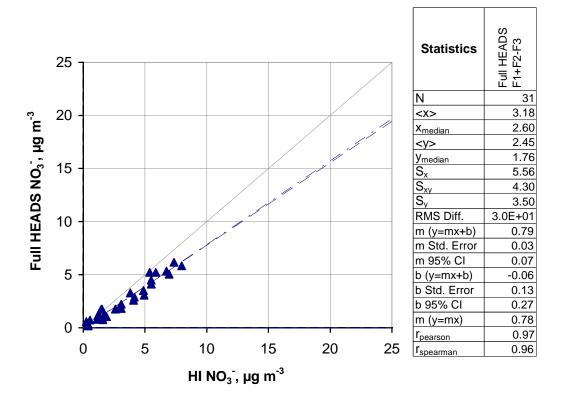


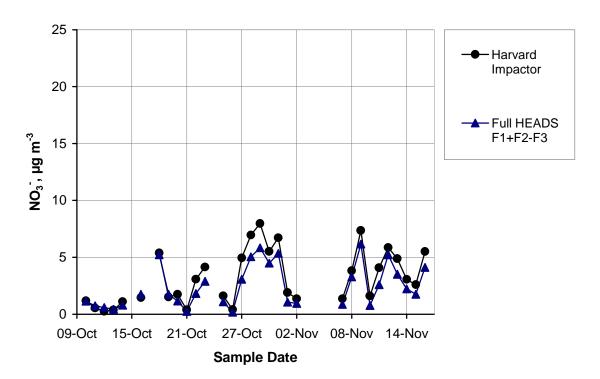
**Figure 35A** Nitrate: Harvard Impactor vs. Full HEADS F1 + F2 – F3 filters at all sites.



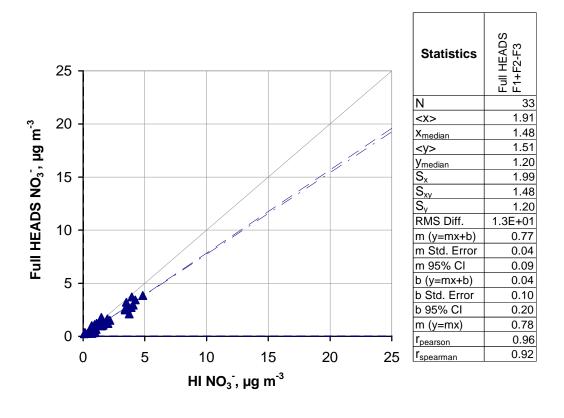


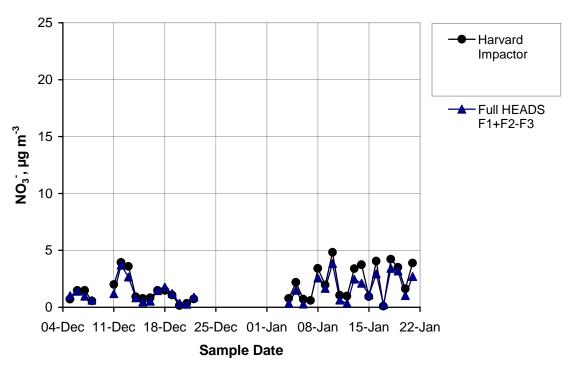
**Figure 35R** Nitrate: Harvard Impactor vs. Full HEADS F1 + F2 – F3 filters at Riverside.



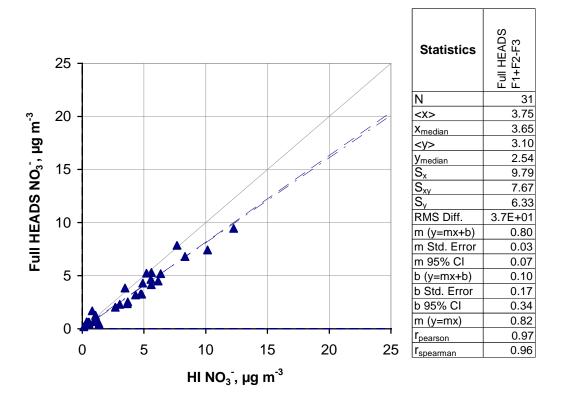


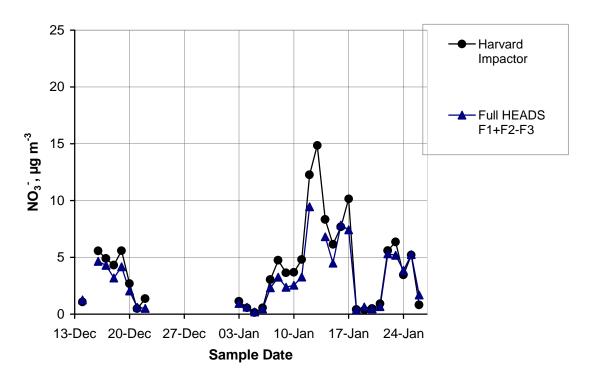
**Figure 35C** Nitrate: Harvard Impactor vs. Full HEADS F1 + F2 – F3 filters at Chicago.



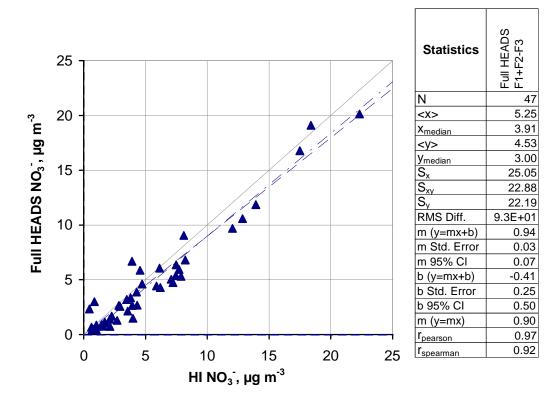


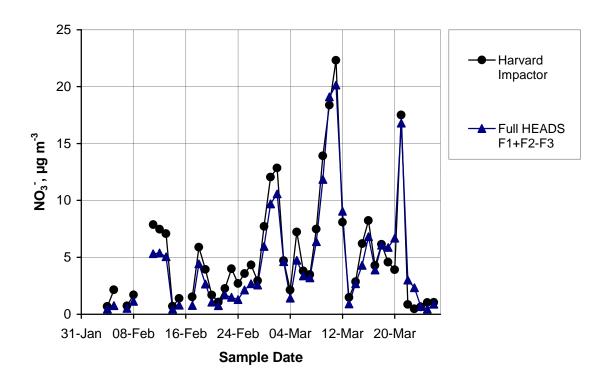
**Figure 35D** Nitrate: Harvard Impactor vs. Full HEADS F1 + F2 – F3 filters at Dallas.



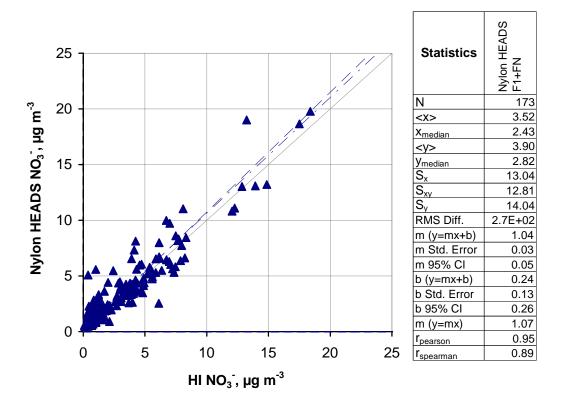


**Figure 35P** Nitrate: Harvard Impactor vs. Full HEADS F1 + F2 – F3 filters at Phoenix.





**Figure 35B** Nitrate: Harvard Impactor vs. Full HEADS F1 + F2 – F3 filters at Bakersfield.



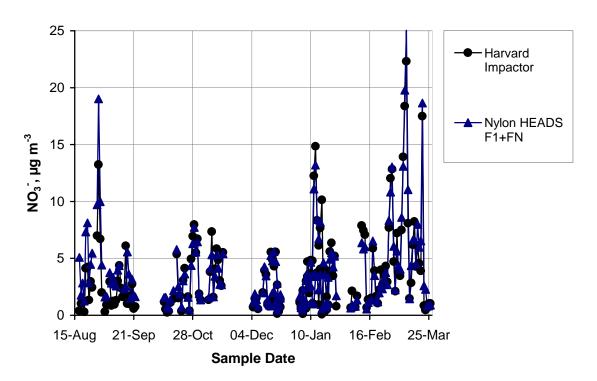
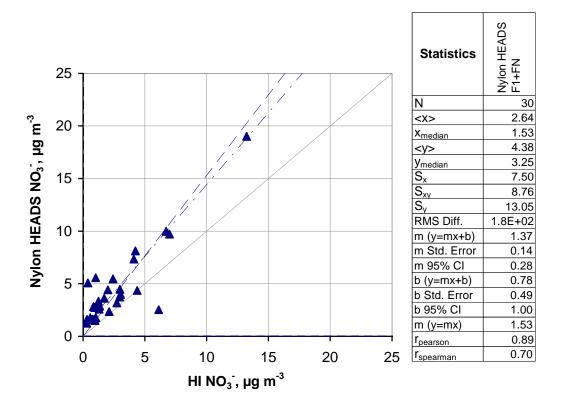


Figure 36A Nitrate: Harvard Impactor vs. Nylon HEADS F1 + FN filters at all sites.



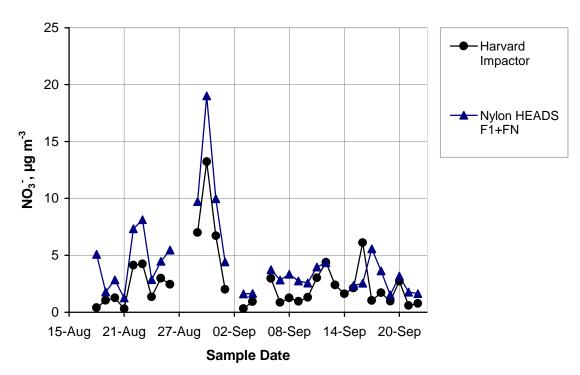
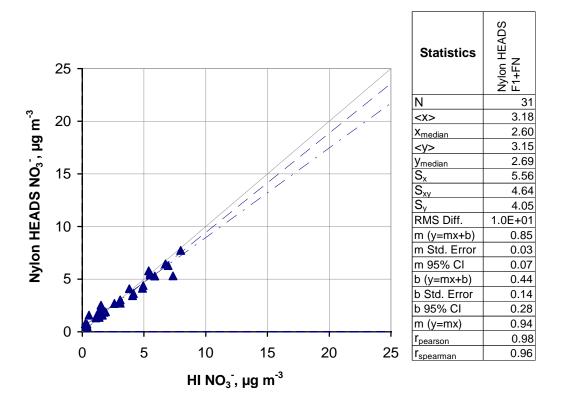
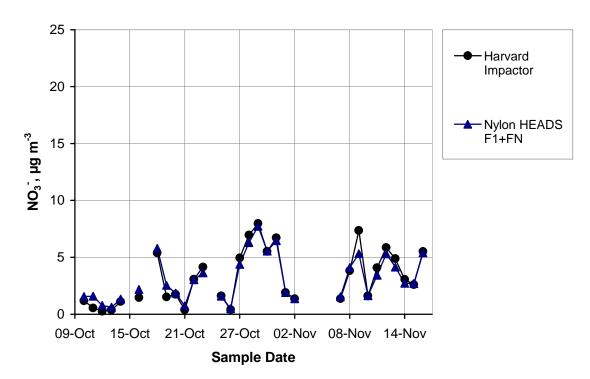
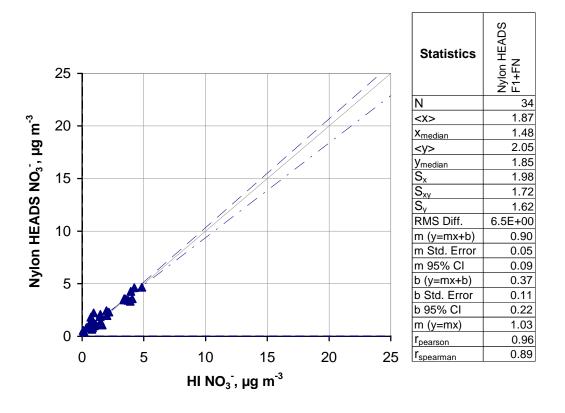


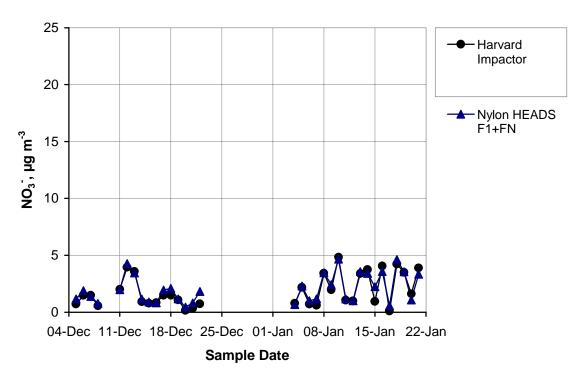
Figure 36R Nitrate: Harvard Impactor vs. Nylon HEADS F1 + FN filters at Riverside.



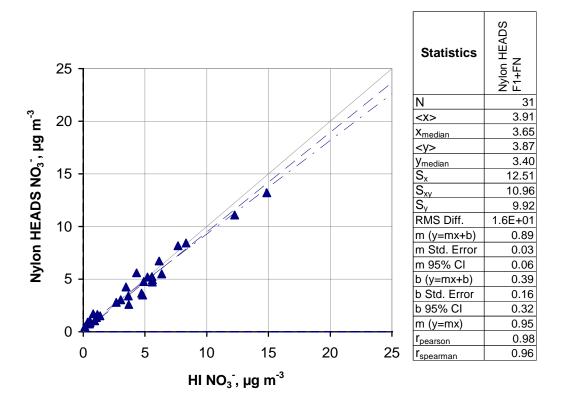


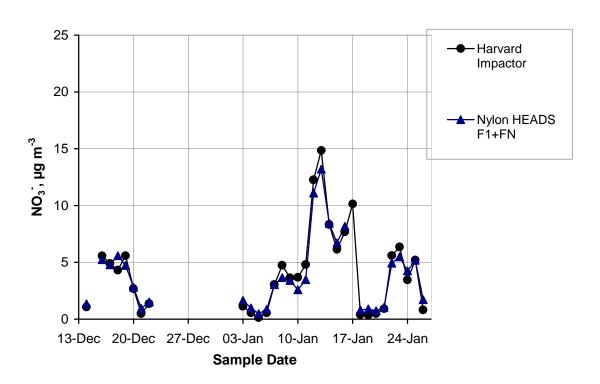
**Figure 36C** Nitrate: Harvard Impactor vs. Nylon HEADS F1 + FN filters at Chicago.



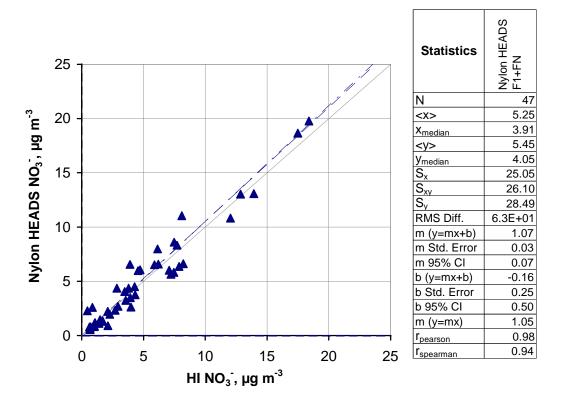


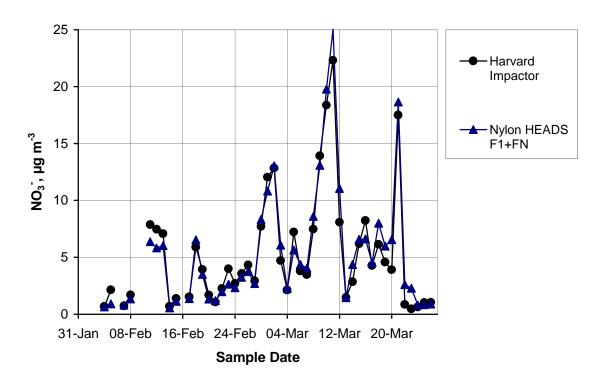
**Figure 36D** Nitrate: Harvard Impactor vs. Nylon HEADS F1 + FN filters at Dallas.



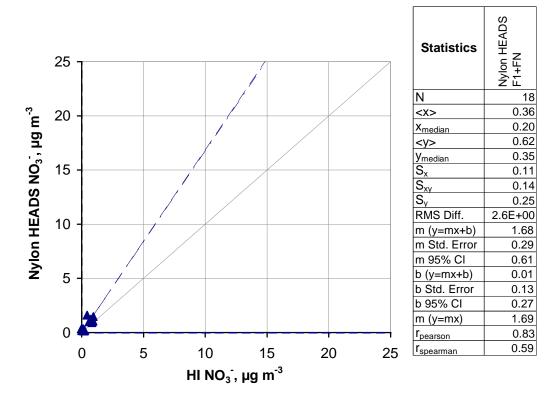


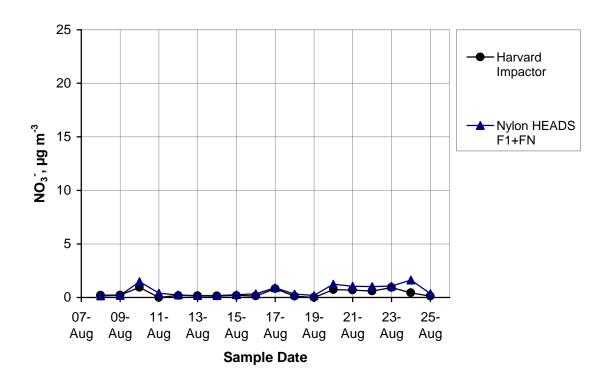
**Figure 36P** Nitrate: Harvard Impactor vs. Nylon HEADS F1 + FN filters at Phoenix.



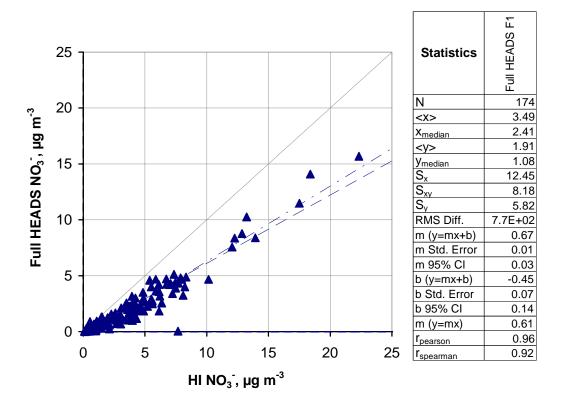


**Figure 36B** Nitrate: Harvard Impactor vs. Nylon HEADS F1 + FN filters at Bakersfield.





**Figure 36F** Nitrate: Harvard Impactor vs. Nylon HEADS F1 + FN filters at Philadelphia.



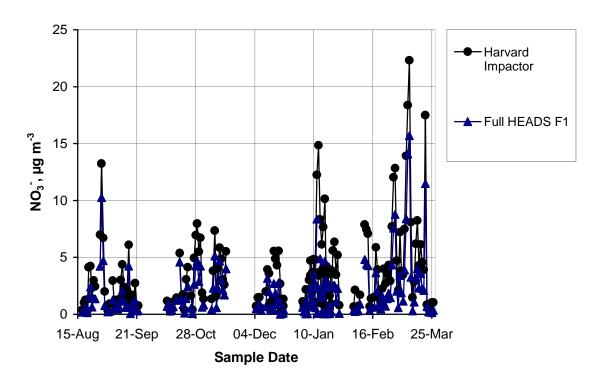
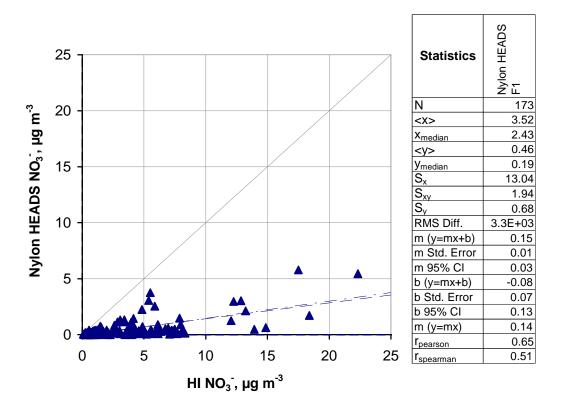


Figure 37A Nitrate: Harvard Impactor vs. Full HEADS F1 filter at all sites.



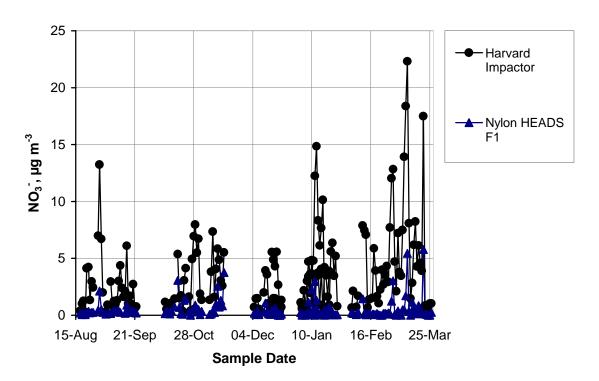
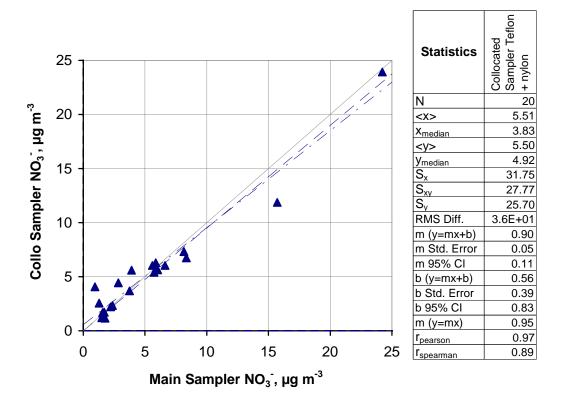
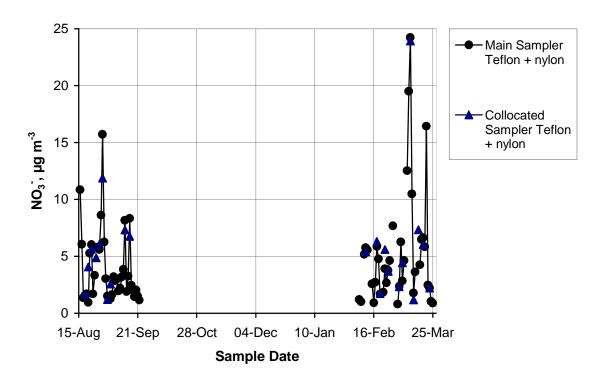
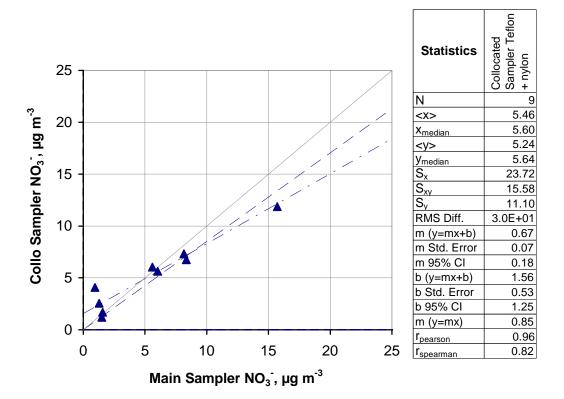


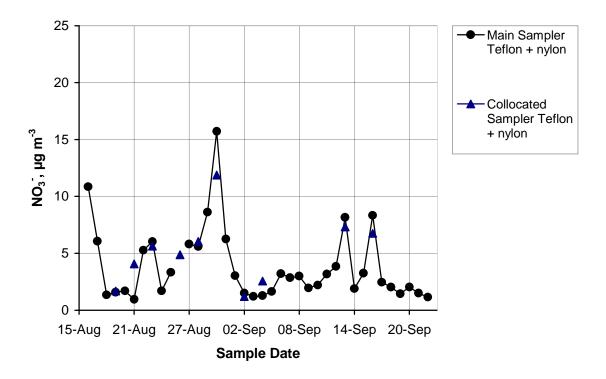
Figure 38A Nitrate: Harvard Impactor vs. Nylon HEADS F1 filter at all sites.



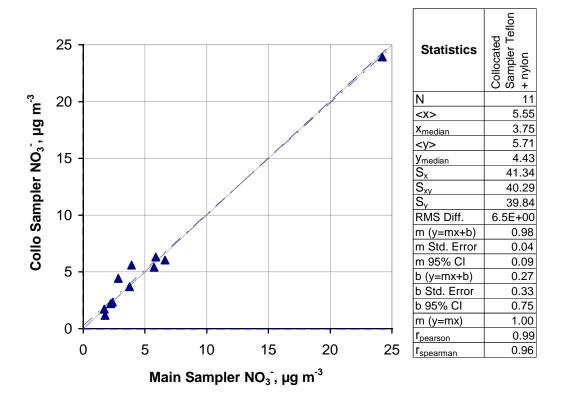


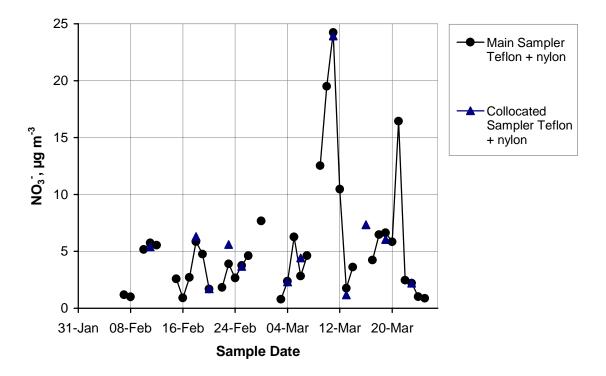
**Figure 39A** Nitrate: Collocated Annular Denuder Sampler Teflon + nylon filters at all sites.



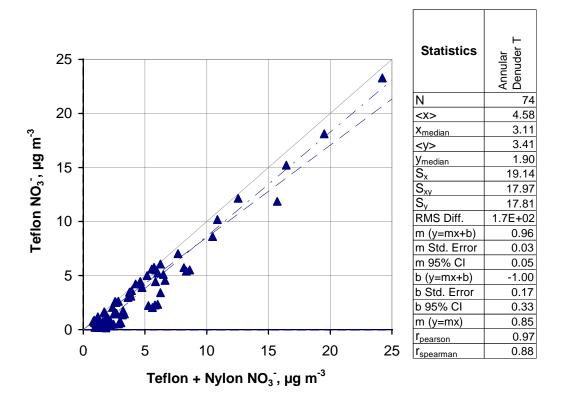


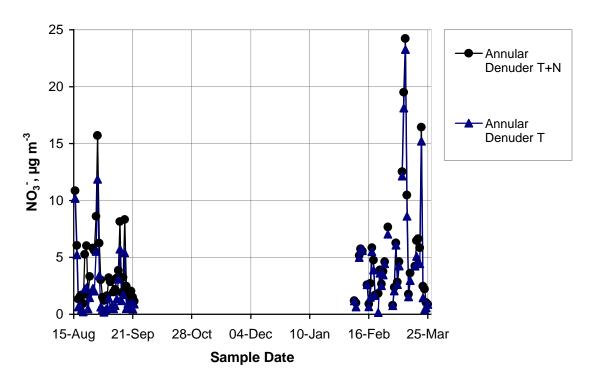
**Figure 39R** Nitrate: Collocated Annular Denuder Sampler Teflon + nylon filters at Riverside.



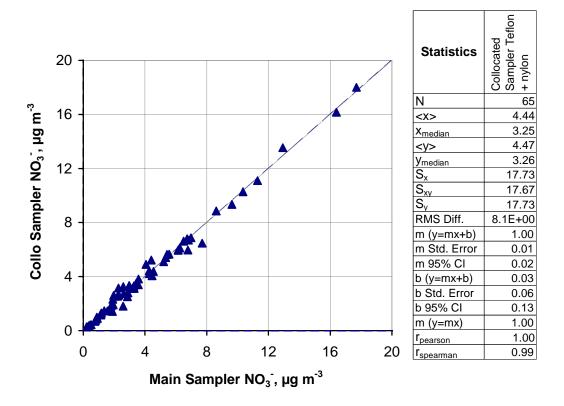


**Figure 39B** Nitrate: Collocated Annular Denuder Sampler Teflon + nylon filters at Bakersfield.





**Figure 40A** Nitrate: Annular Denuder Sampler Teflon filter vs. Teflon + nylon filters at all sites.



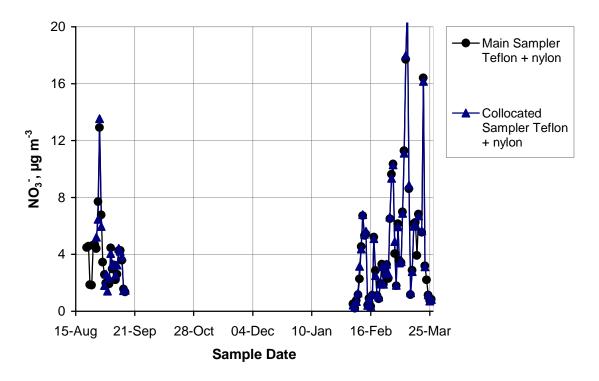
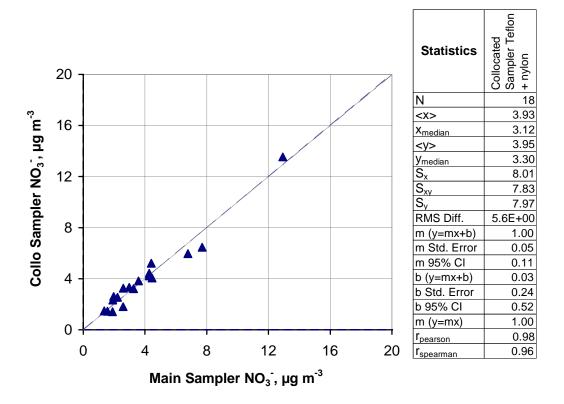


Figure 41A Nitrate: Collocated ChemSpec Sampler Teflon + nylon filters at all sites.



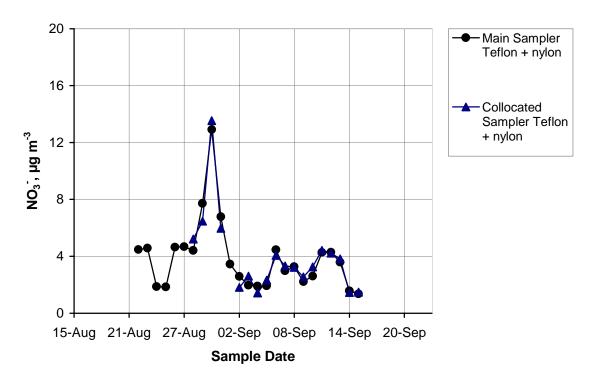
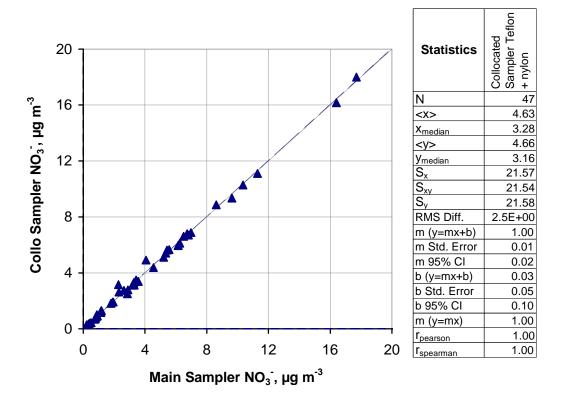
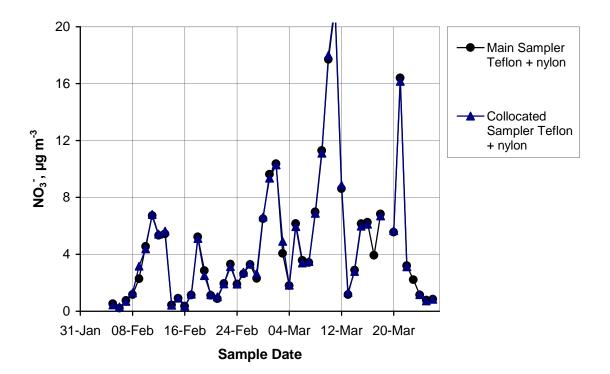
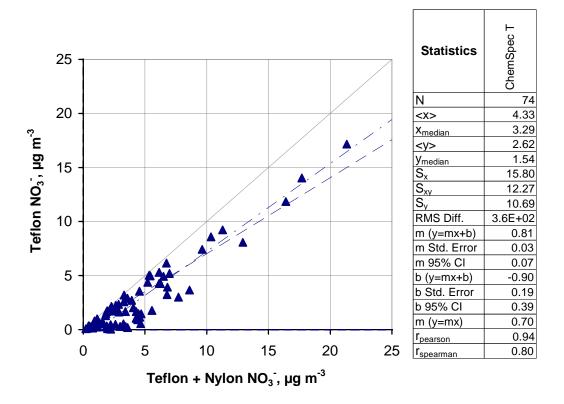


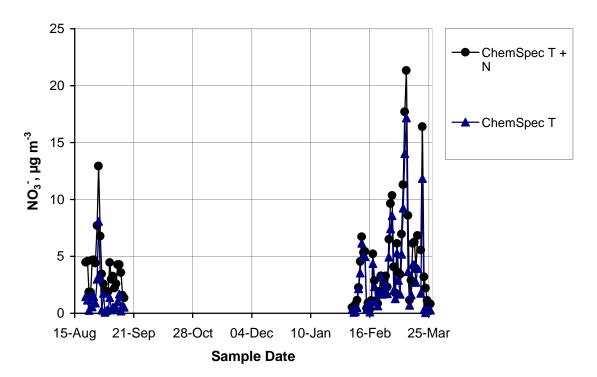
Figure 41R Nitrate: Collocated ChemSpec Sampler Teflon + nylon filters at Riverside.



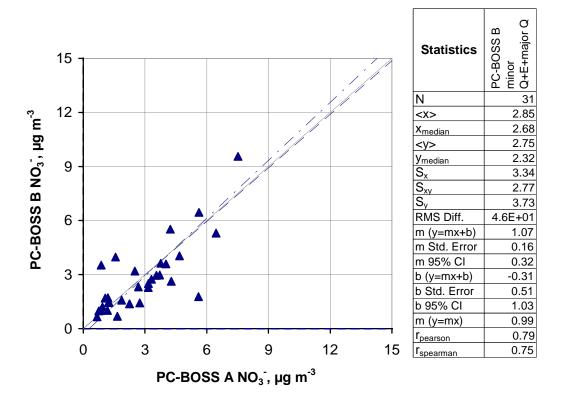


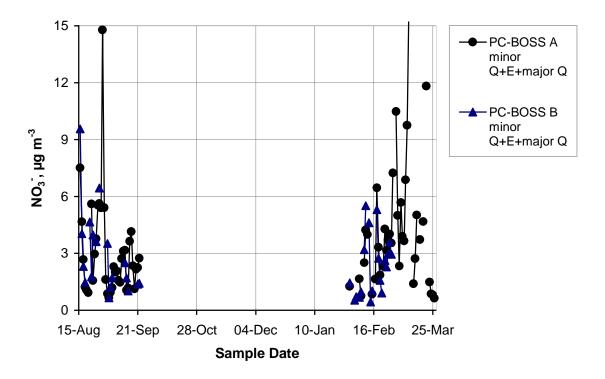
**Figure 41B** Nitrate: Collocated ChemSpec Sampler Teflon + nylon filters at Bakersfield.



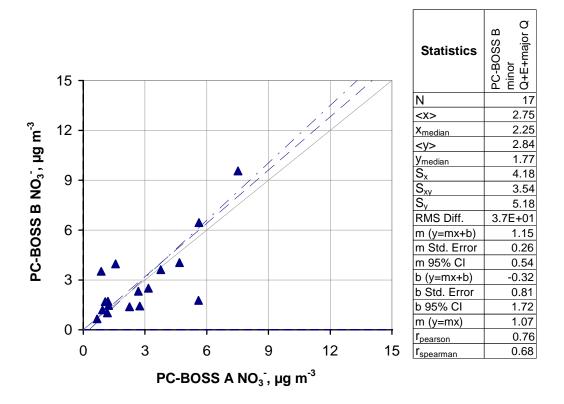


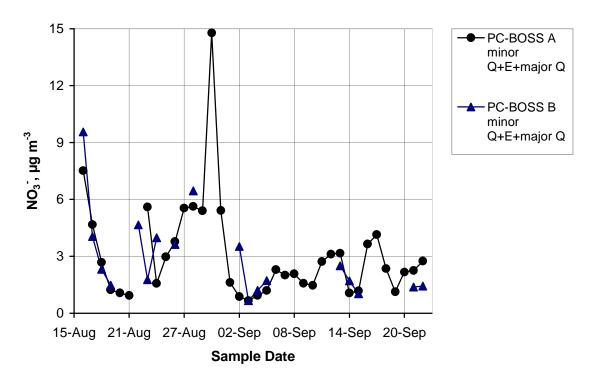
**Figure 42A** Nitrate: ChemSpec Sampler Teflon filter vs. Teflon + nylon filters at all sites.



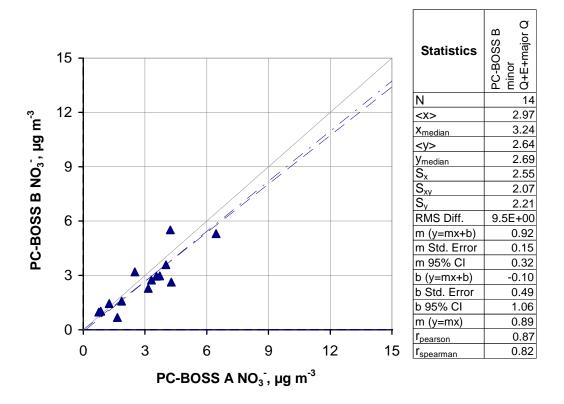


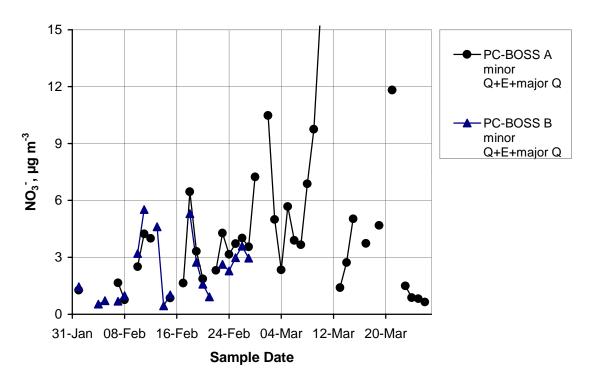
**Figure 43A** Nitrate: Collocated PC-BOSS minor flow quartz + Empore + major flow quartz filters at all sites.



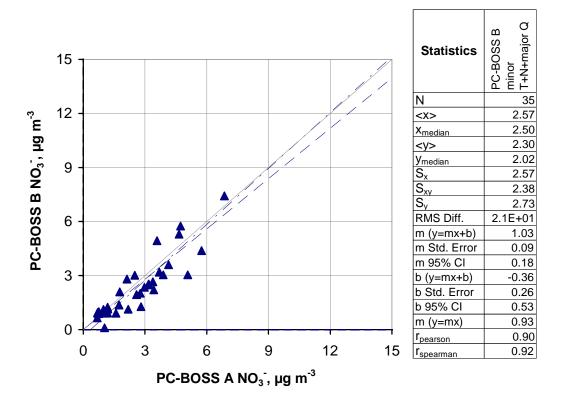


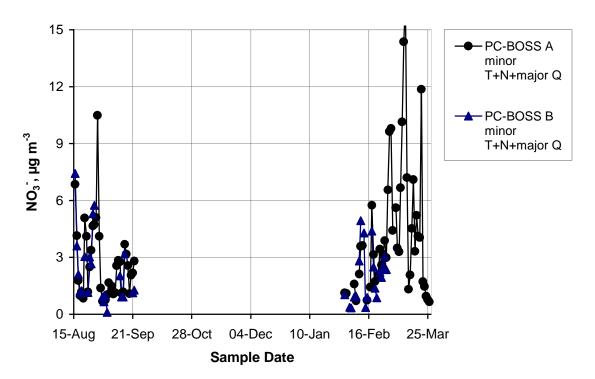
**Figure 43R** Nitrate: Collocated PC-BOSS minor flow quartz + Empore + major flow quartz filters at Riverside.



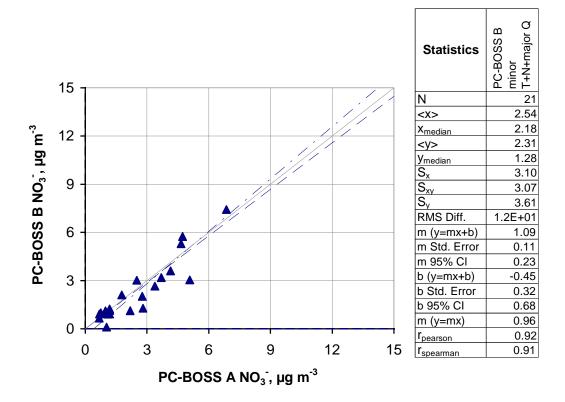


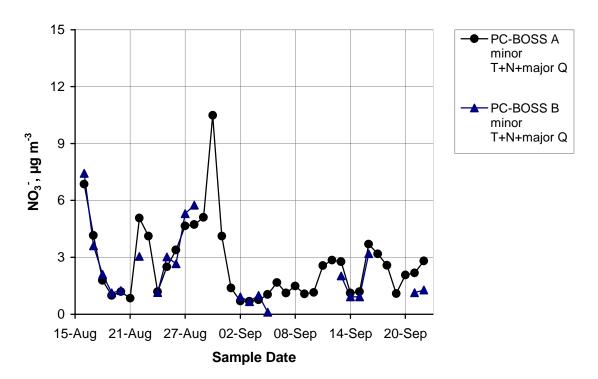
**Figure 43B** Nitrate: Collocated PC-BOSS minor flow quartz + Empore + major flow quartz filters at Bakersfield.



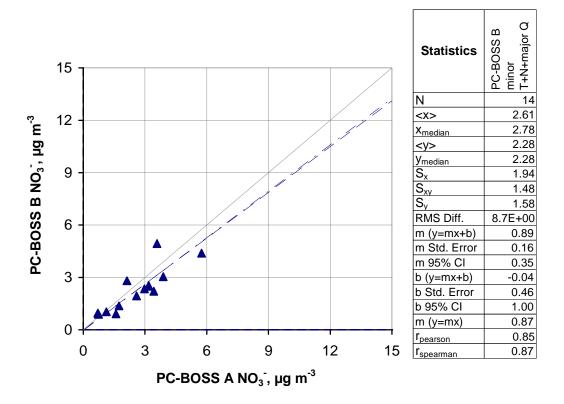


**Figure 44A** Nitrate: Collocated PC-BOSS minor flow Teflon + nylon + major flow quartz filters at all sites.





**Figure 44R** Nitrate: Collocated PC-BOSS minor flow Teflon + nylon + major flow quartz filters at Riverside.



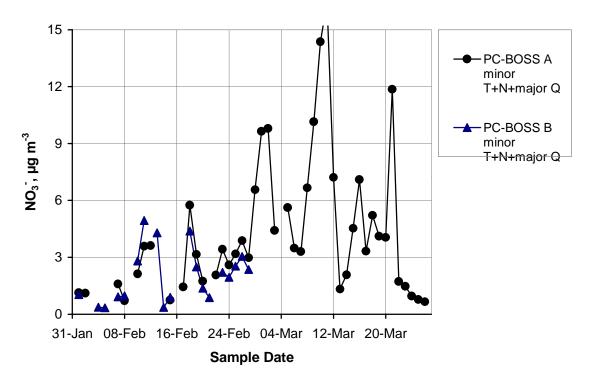


**Figure 44B** Nitrate: Collocated PC-BOSS minor flow Teflon + nylon + major flow quartz filters at Bakersfield.

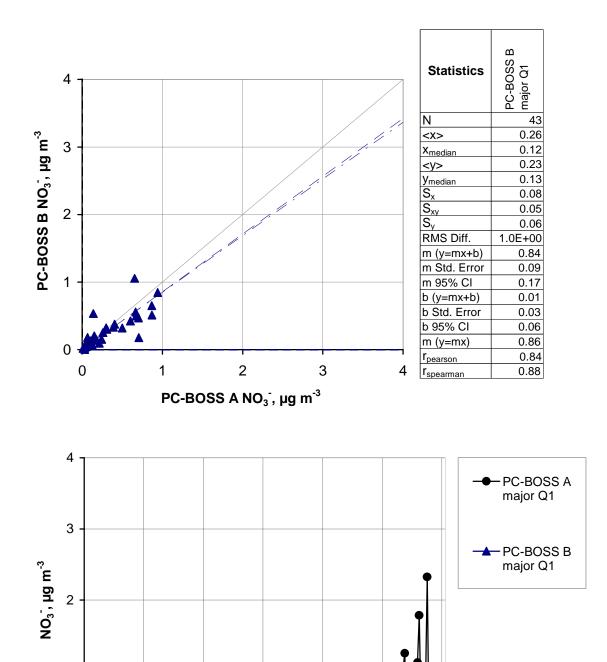


Figure 45A Nitrate: Collocated PC-BOSS major flow quartz filters at all sites.

04-Dec

**Sample Date** 

21-Sep

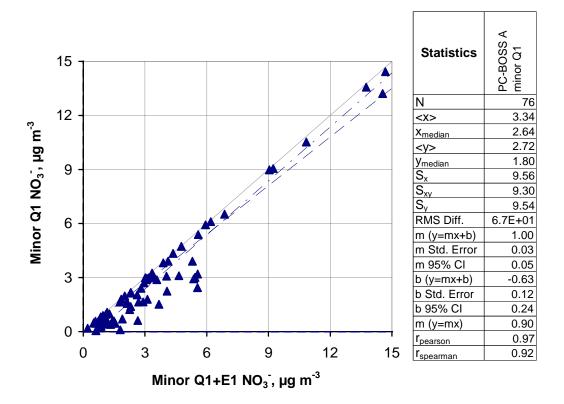
28-Oct

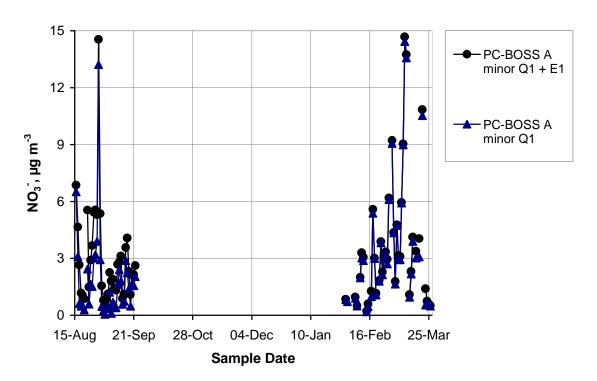
15-Aug

10-Jan

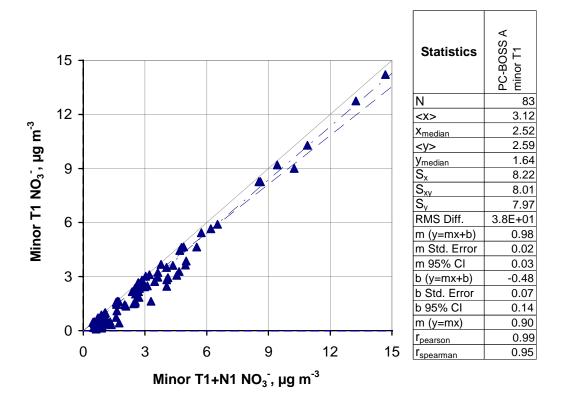
16-Feb

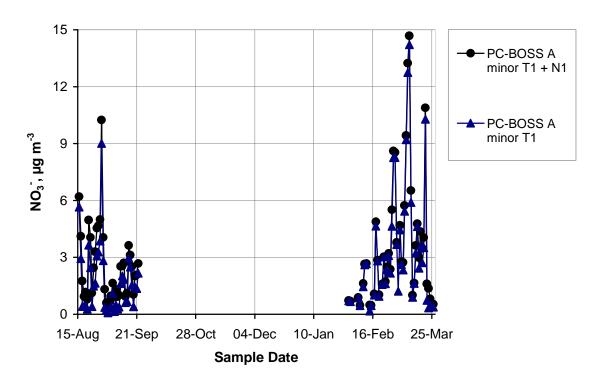
25-Mar



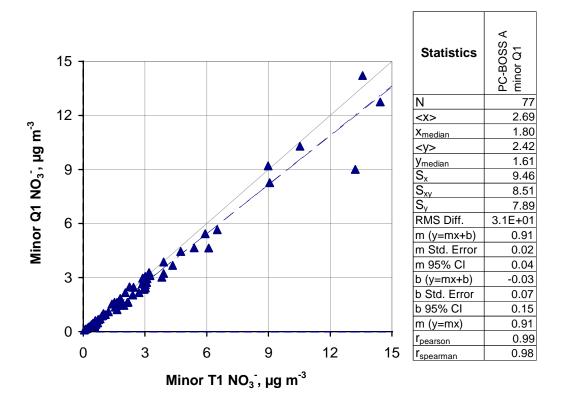


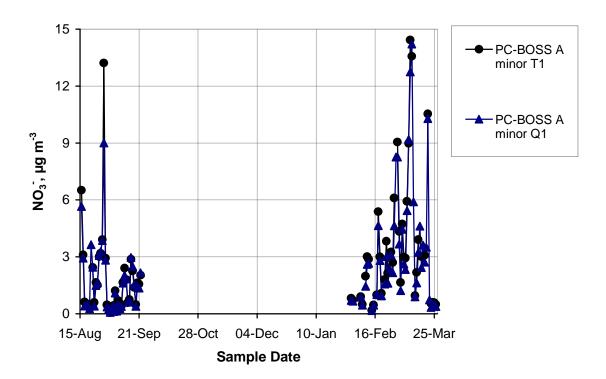
**Figure 46A** Nitrate: PC-BOSS minor flow quartz filter vs. minor flow quartz + Empore filters at all sites.



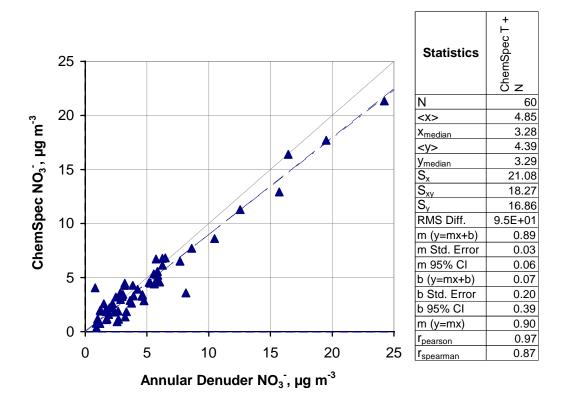


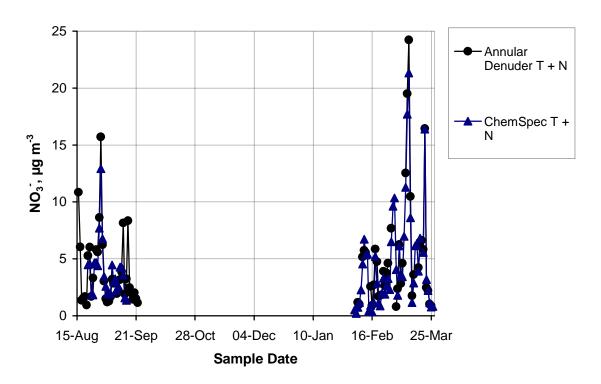
**Figure 47A** Nitrate: PC-BOSS minor flow Teflon filter vs. minor flow Teflon + nylon filters at all sites.



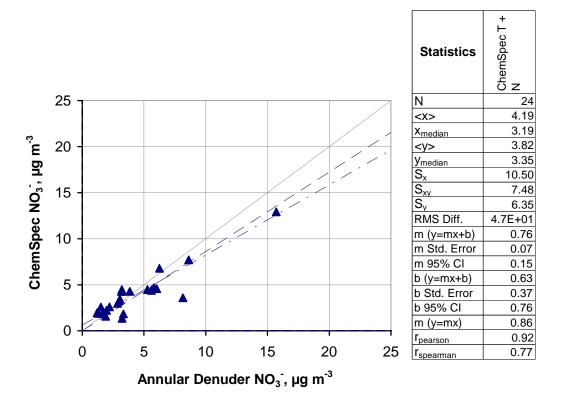


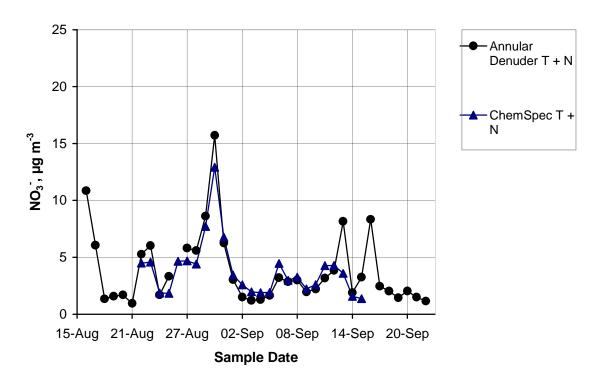
**Figure 48A** Nitrate: PC-BOSS minor flow quartz vs. minor flow Teflon filters at all sites.



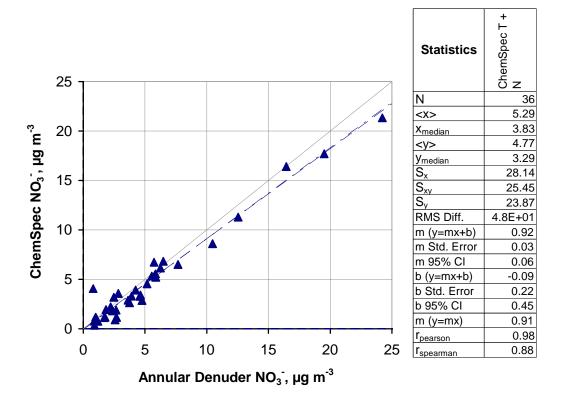


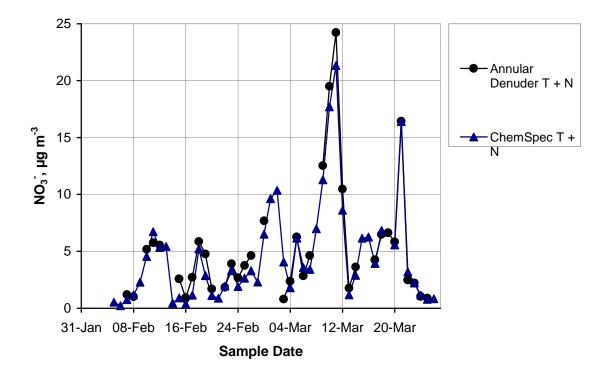
**Figure 49A** Nitrate: Annular Denuder Sampler Teflon + nylon filters vs. ChemSpec Sampler Teflon + nylon filters at all sites.



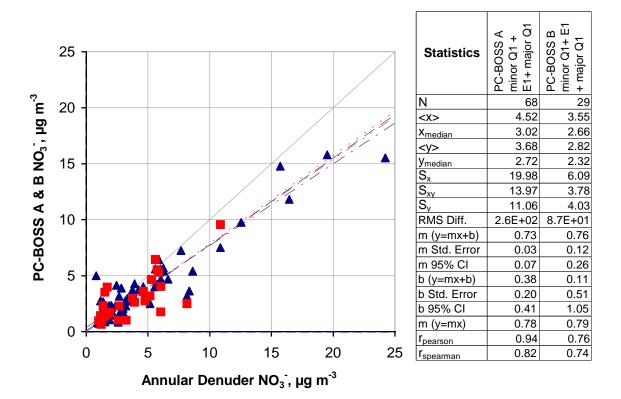


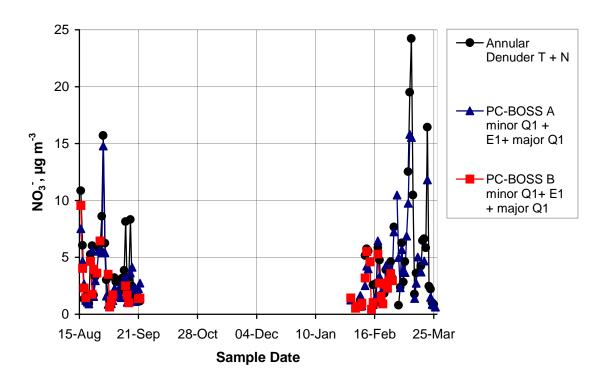
**Figure 49R** Nitrate: Annular Denuder Sampler Teflon + nylon filters vs. ChemSpec Sampler Teflon + nylon filters at Riverside.



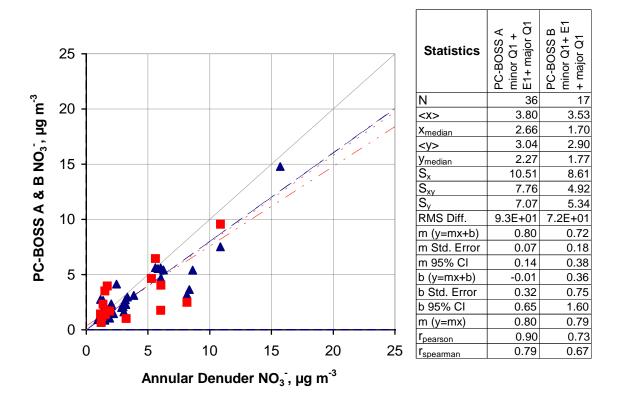


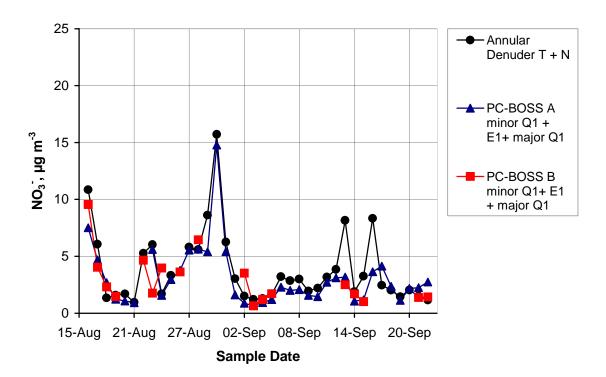
**Figure 49B** Nitrate: Annular Denuder Sampler Teflon + nylon filters vs. ChemSpec Sampler Teflon + nylon filters at Bakersfield.



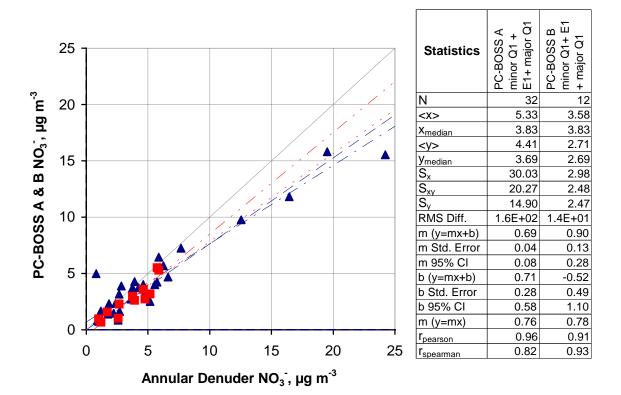


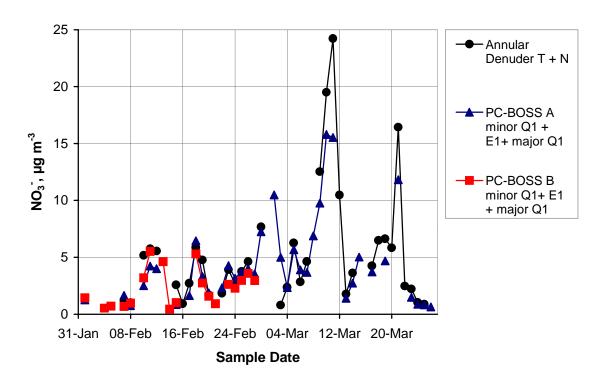
**Figure 50A** Nitrate: Annular Denuder Sampler Teflon + nylon filters vs. PC-BOSS A and B minor flow quartz + Empore + major flow quartz filters at all sites.



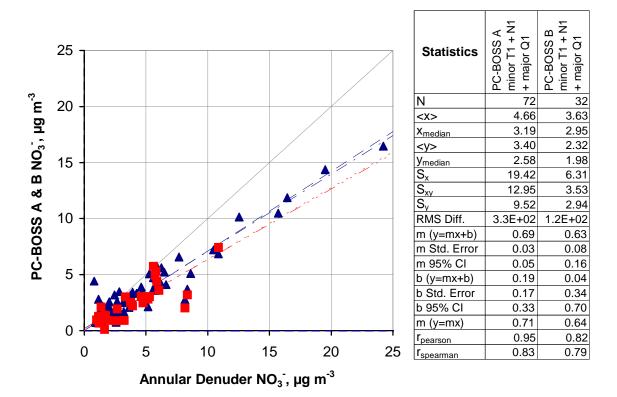


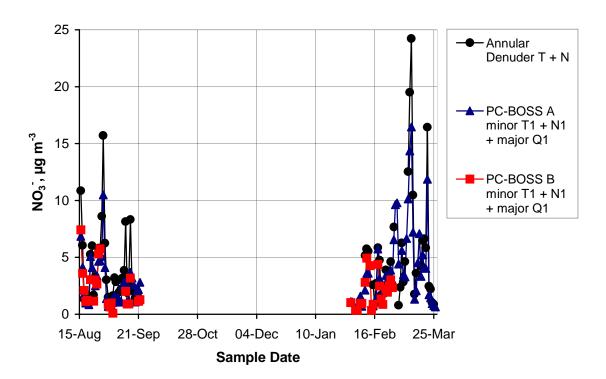
**Figure 50R** Nitrate: Annular Denuder Sampler Teflon + nylon filters vs. PC-BOSS A and B minor flow quartz + Empore + major flow quartz filters at Riverside.



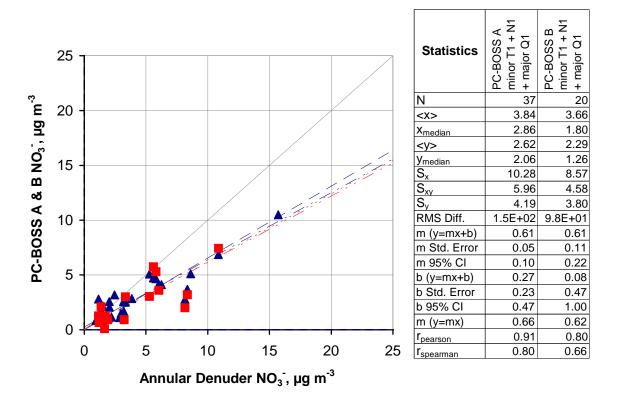


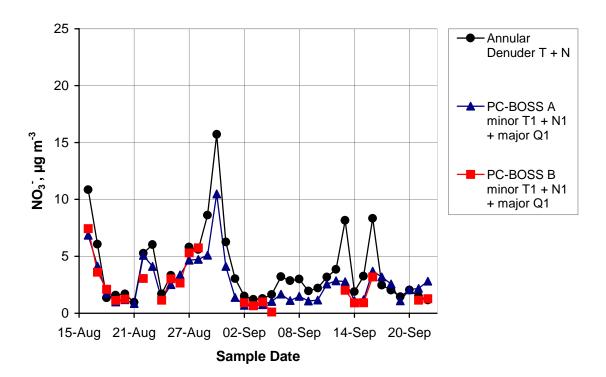
**Figure 50B** Nitrate: Annular Denuder Sampler Teflon + nylon filters vs. PC-BOSS A and B minor flow quartz + Empore + major flow quartz filters at Bakersfield.



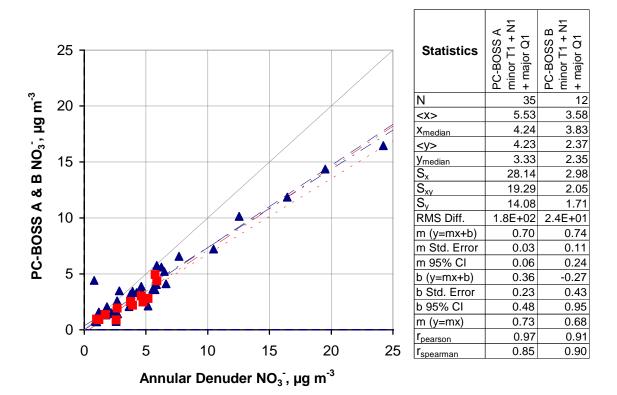


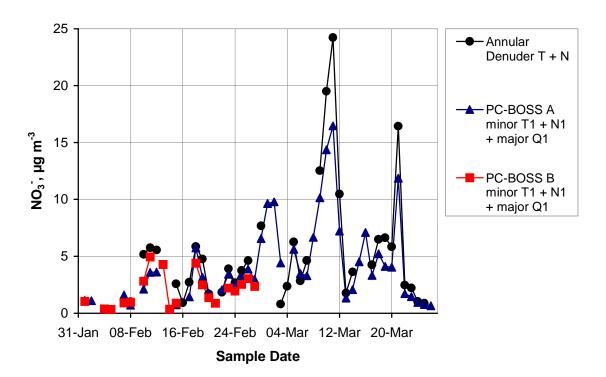
**Figure 51A** Nitrate: Annular Denuder Sampler Teflon + nylon filters vs. PC-BOSS A and B minor flow Teflon + nylon + major flow quartz filters at all sites.



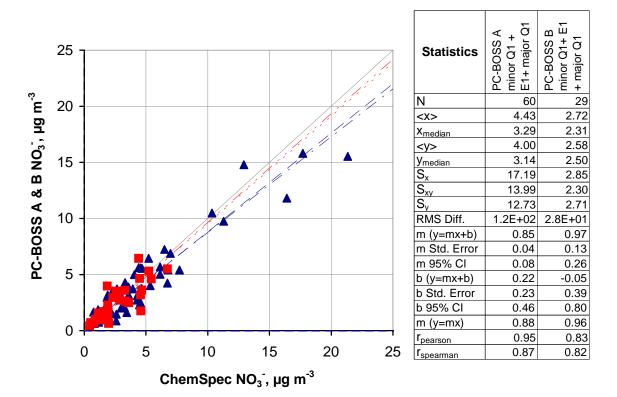


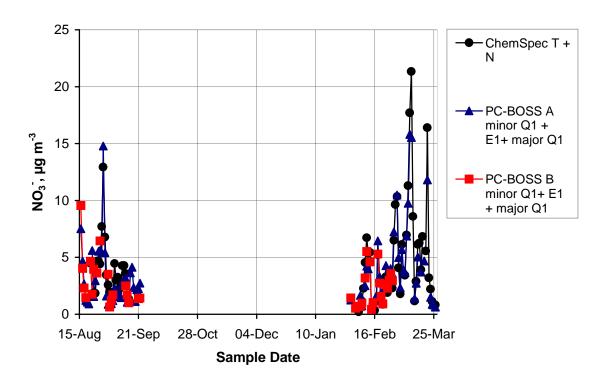
**Figure 51R** Nitrate: Annular Denuder Sampler Teflon + nylon filters vs. PC-BOSS A and B minor flow Teflon + nylon + major flow quartz filters at Riverside.



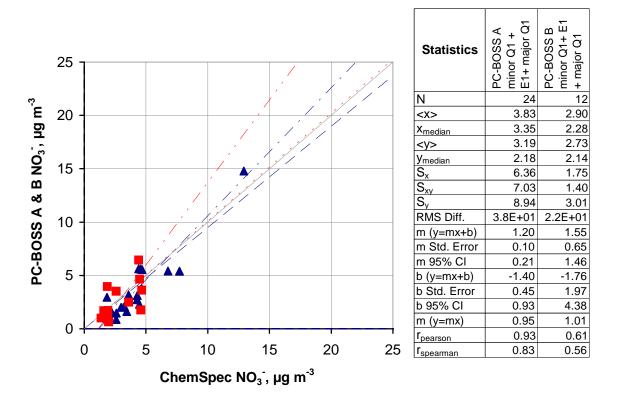


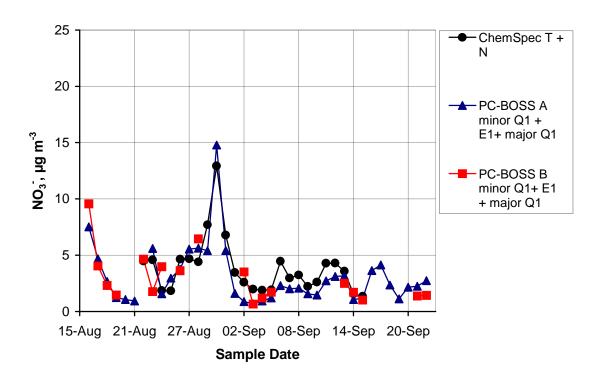
**Figure 51B** Nitrate: Annular Denuder Sampler Teflon + nylon filters vs. PC-BOSS A and B minor flow Teflon + nylon + major flow quartz filters at Bakersfield.



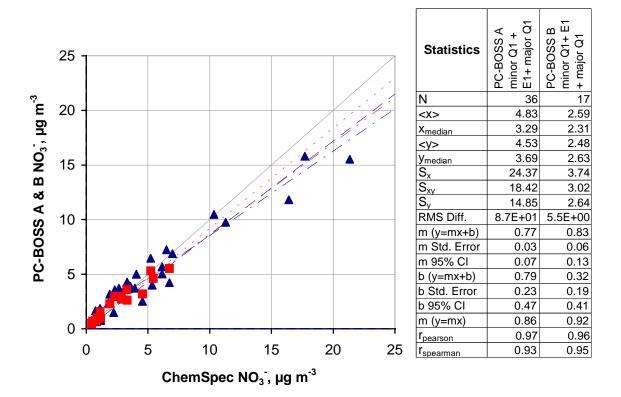


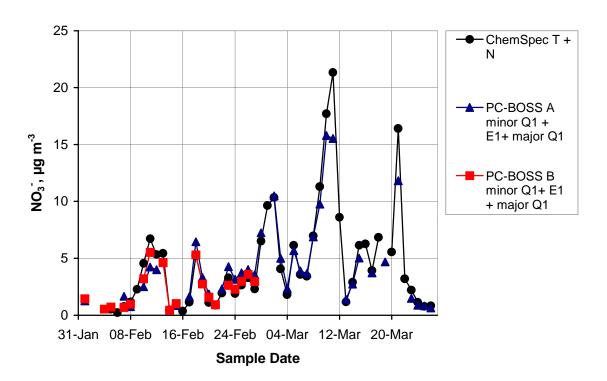
**Figure 52A** Nitrate: ChemSpec Sampler Teflon + nylon filters vs. PC-BOSS A and B minor flow quartz + Empore + major flow quartz filters at all sites.



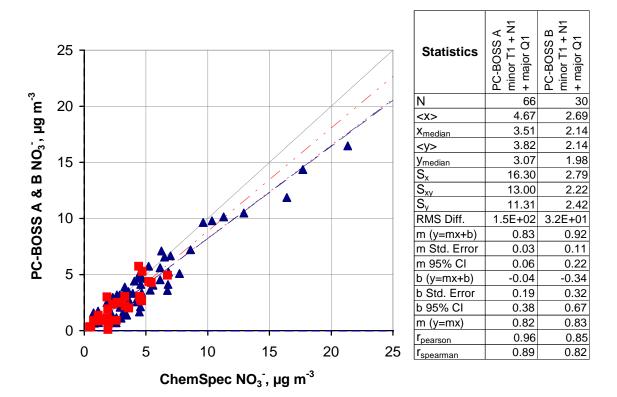


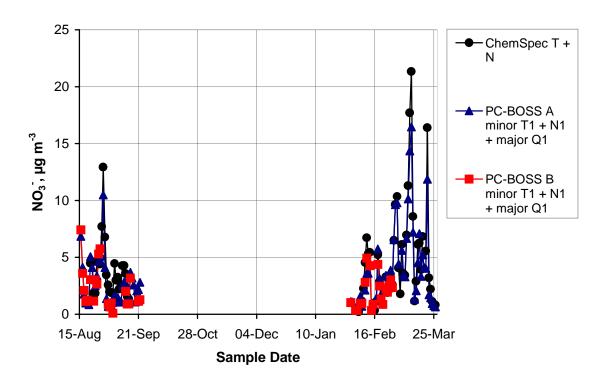
**Figure 52R** Nitrate: ChemSpec Sampler Teflon + nylon filters vs. PC-BOSS A and B minor flow quartz + Empore + major flow quartz filters at Riverside.



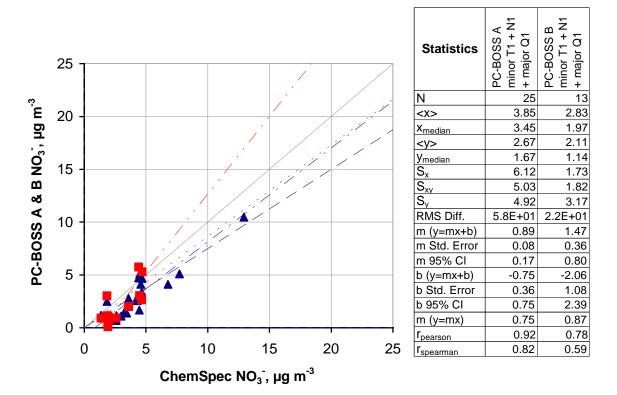


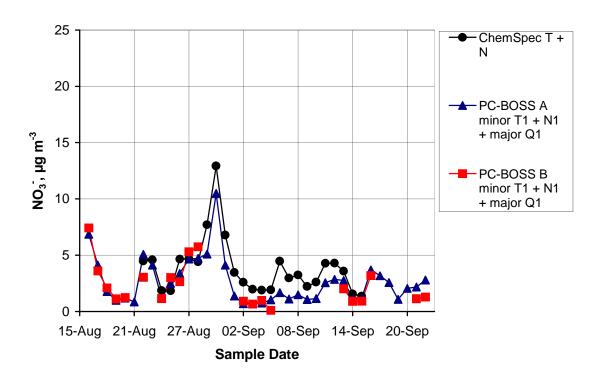
**Figure 52B** Nitrate: ChemSpec Sampler Teflon + nylon filters vs. PC-BOSS A and B minor flow quartz + Empore + major flow quartz filters at Bakersfield.



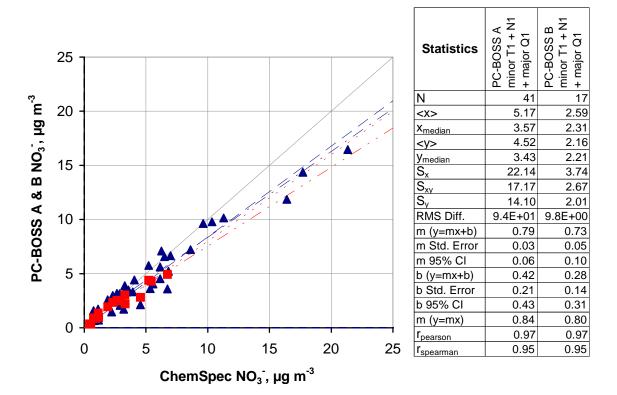


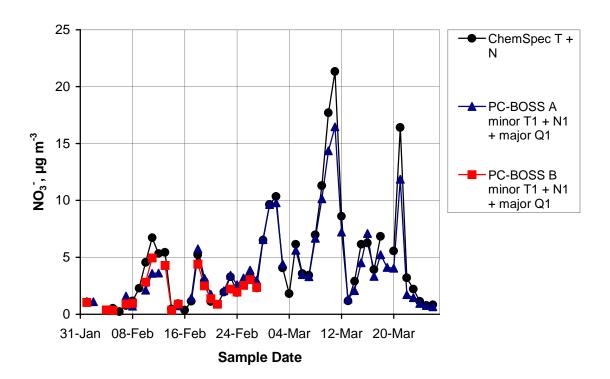
**Figure 53A** Nitrate: ChemSpec Sampler Teflon + nylon filters vs. PC-BOSS A and B minor flow Teflon + nylon + major flow quartz filters at all sites.



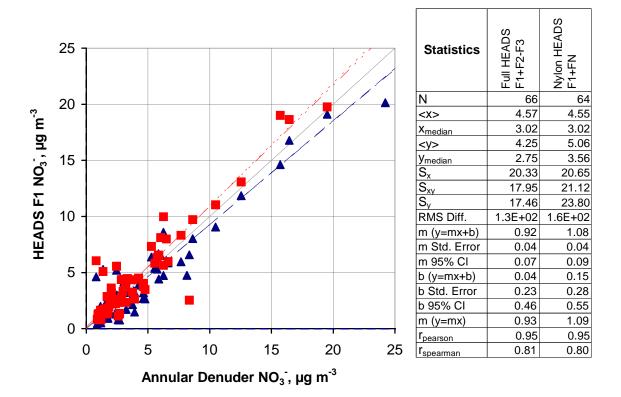


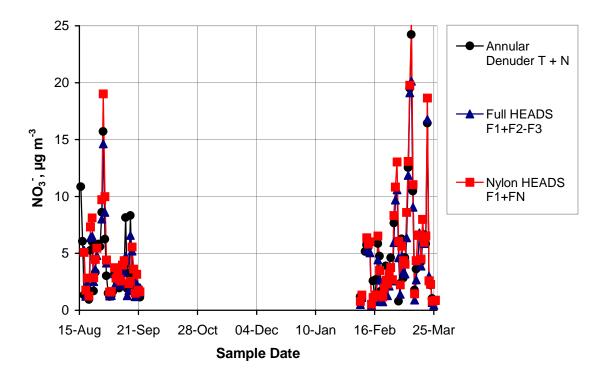
**Figure 53R** Nitrate: ChemSpec Sampler Teflon + nylon filters vs. PC-BOSS A and B minor flow Teflon + nylon + major flow quartz filters at Riverside.



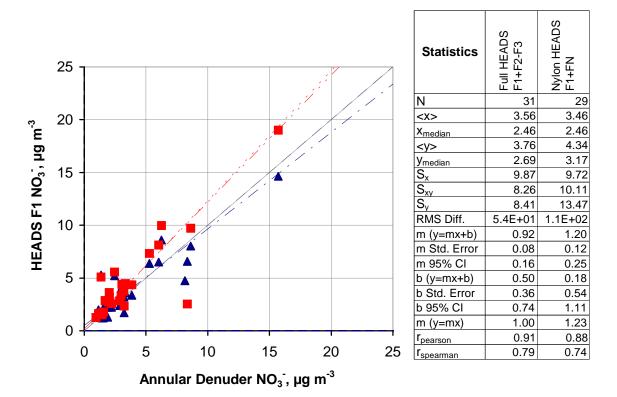


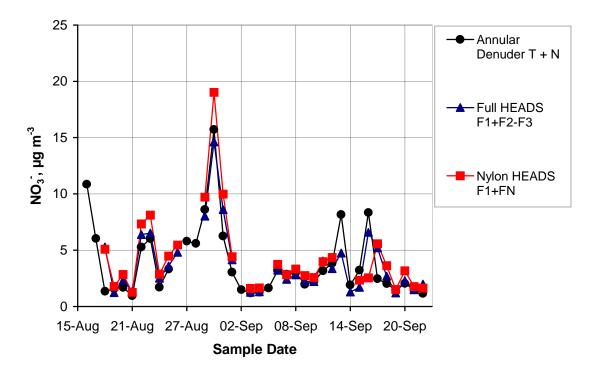
**Figure 53B** Nitrate: ChemSpec Sampler Teflon + nylon filters vs. PC-BOSS A and B minor flow Teflon + nylon + major flow quartz filters at Bakersfield.



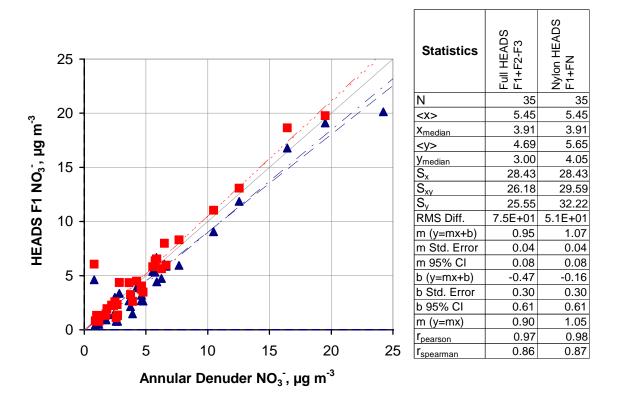


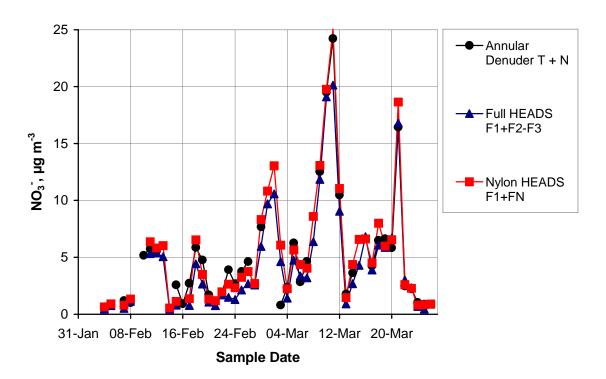
**Figure 54A** Nitrate: Full HEADS F1 + F2 – F3 and Nylon HEADS F1 + FN filters vs. Annular Denuder Sampler Teflon + nylon filters at all sites.



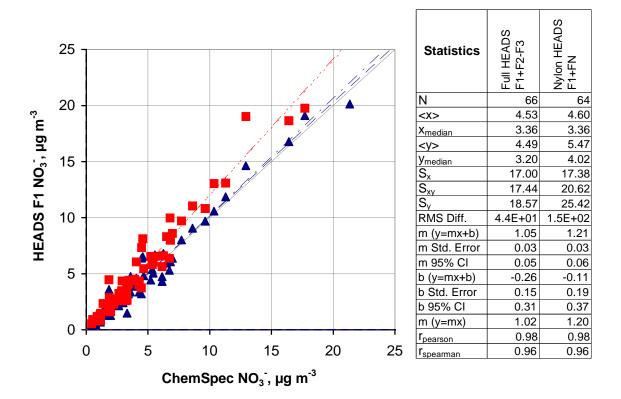


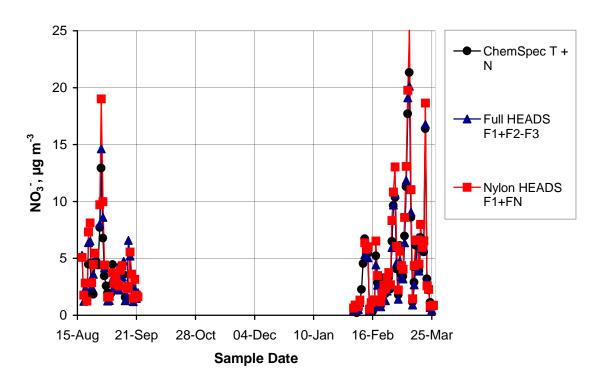
**Figure 54R** Nitrate: Full HEADS F1 + F2 – F3 and Nylon HEADS F1 + FN filters vs. Annular Denuder Sampler Teflon + nylon filters at Riverside.



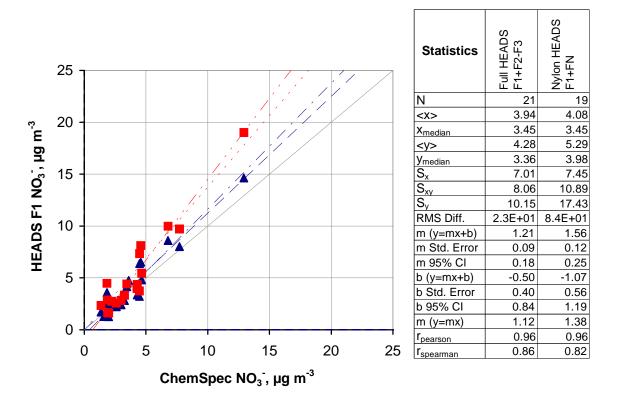


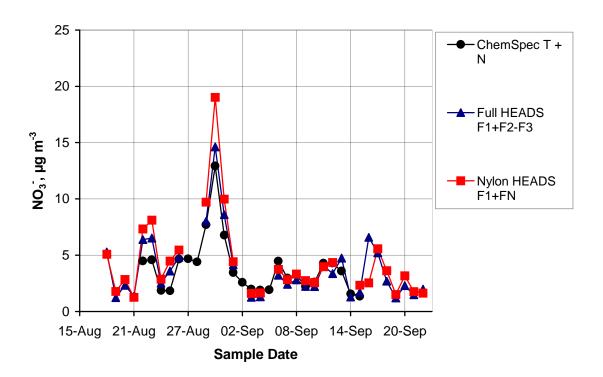
**Figure 54B** Nitrate: Full HEADS F1 + F2 – F3 and Nylon HEADS F1 + FN filters vs. Annular Denuder Sampler Teflon + nylon filters at Bakersfield.



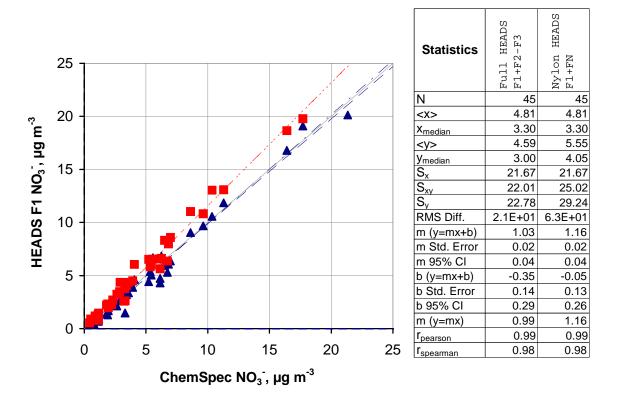


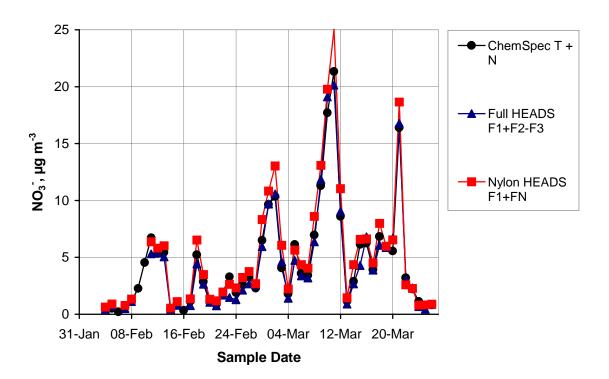
**Figure 55A** Nitrate: Full HEADS F1 + F2 – F3 and Nylon HEADS F1 + FN filters vs. ChemSpec Sampler Teflon + nylon filters at all sites.



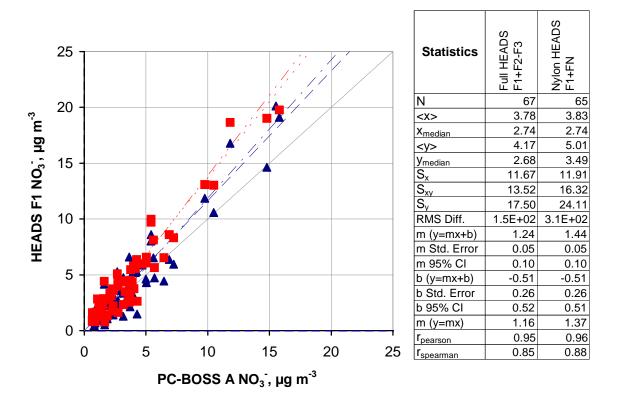


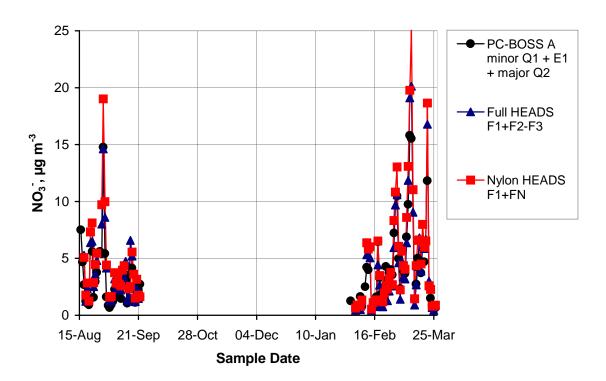
**Figure 55R** Nitrate: Full HEADS F1 + F2 – F3 and Nylon HEADS F1 + FN filters vs. ChemSpec Sampler Teflon + nylon filters at Riverside.



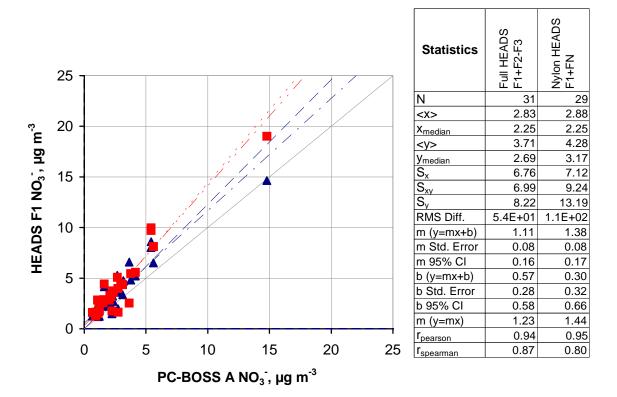


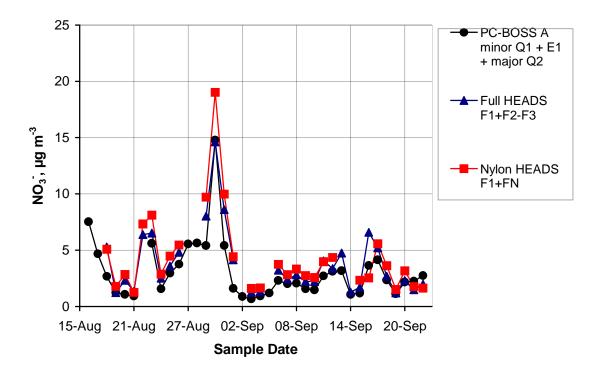
**Figure 55B** Nitrate: Full HEADS F1 + F2 – F3 and Nylon HEADS F1 + FN filters vs. ChemSpec Sampler Teflon + nylon filters at Bakersfield.



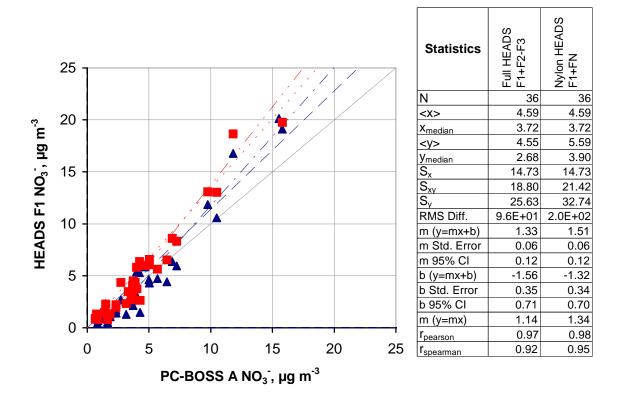


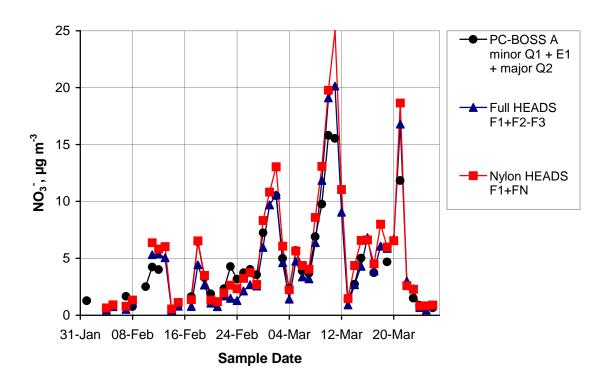
**Figure 56A** Nitrate: Full HEADS F1 + F2 – F3 and Nylon HEADS F1 + FN filters vs. PC-BOSS A minor flow quartz + Empore + major flow quartz filters at all sites.



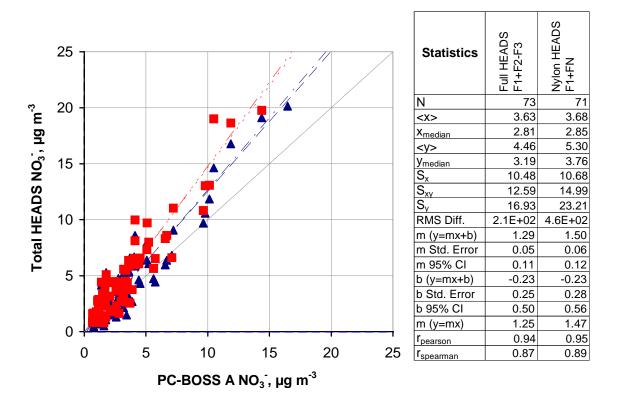


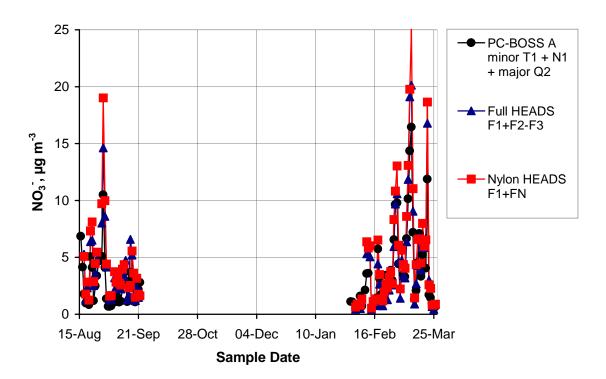
**Figure 56R** Nitrate: Full HEADS F1 + F2 – F3 and Nylon HEADS F1 + FN filters vs. PC-BOSS A minor flow quartz + Empore + major flow quartz filters at Riverside.



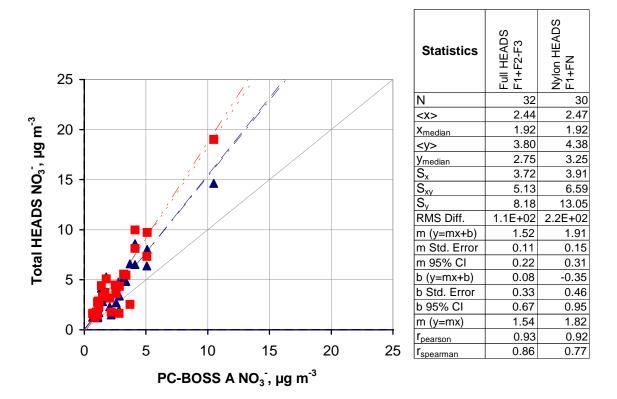


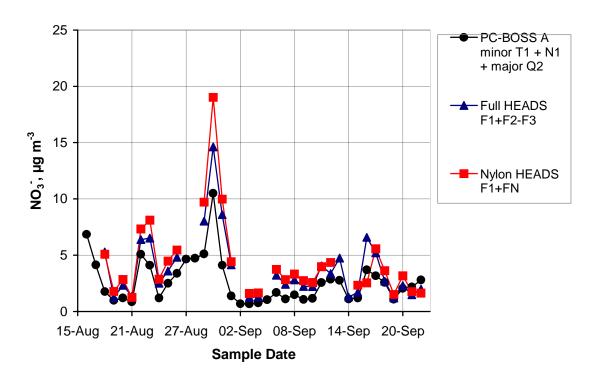
**Figure 56B** Nitrate: Full HEADS F1 + F2 – F3 and Nylon HEADS F1 + FN filters vs. PC-BOSS A minor flow quartz + Empore + major flow quartz filters at Bakersfield.



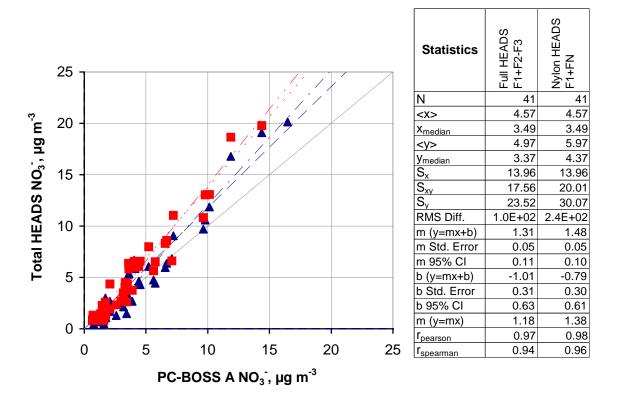


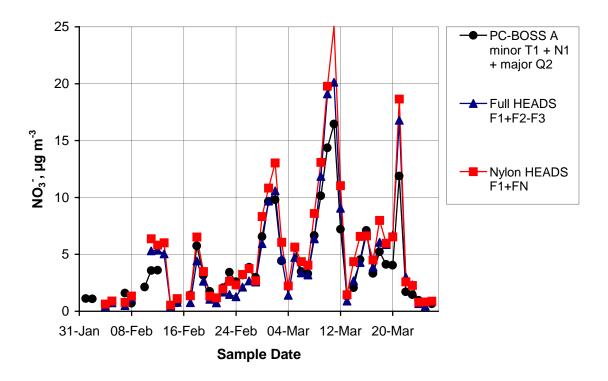
**Figure 57A** Nitrate: Full HEADS F1 + F2 – F3 and Nylon HEADS F1 + FN filters vs. PC-BOSS A minor flow Teflon + nylon + major flow quartz filters at all sites.



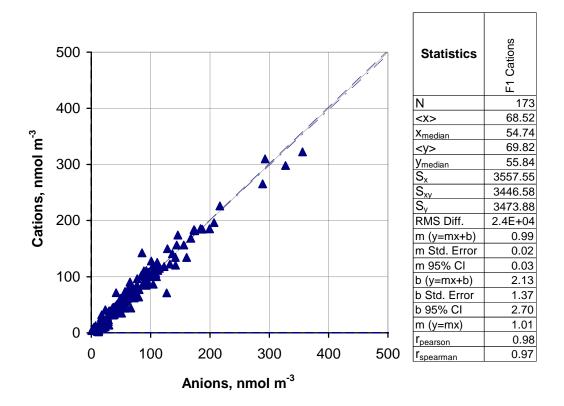


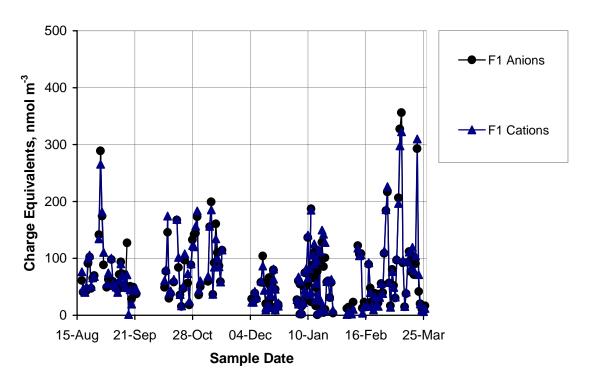
**Figure 57R** Nitrate: Full HEADS F1 + F2 – F3 and Nylon HEADS F1 + FN filters vs. PC-BOSS A minor flow Teflon + nylon + major flow quartz filters at Riverside.



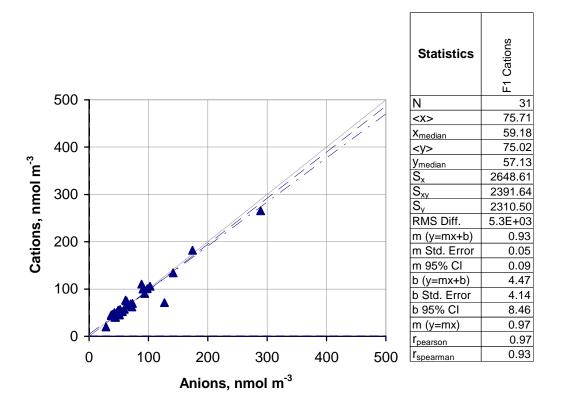


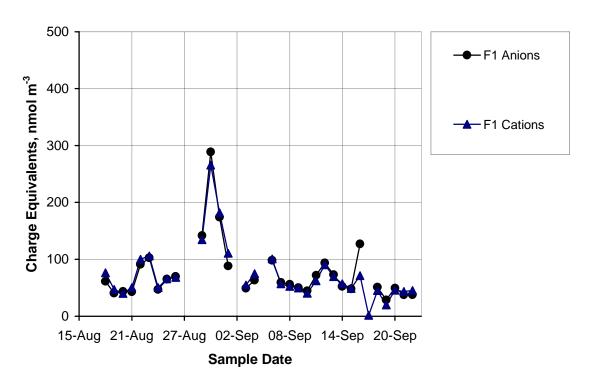
**Figure 57B** Nitrate: Full HEADS F1 + F2 – F3 and Nylon HEADS F1 + FN filters vs. PC-BOSS A minor flow Teflon + nylon + major flow quartz filters at Bakersfield.



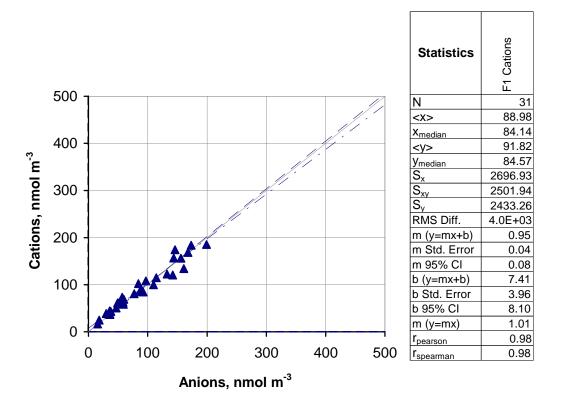


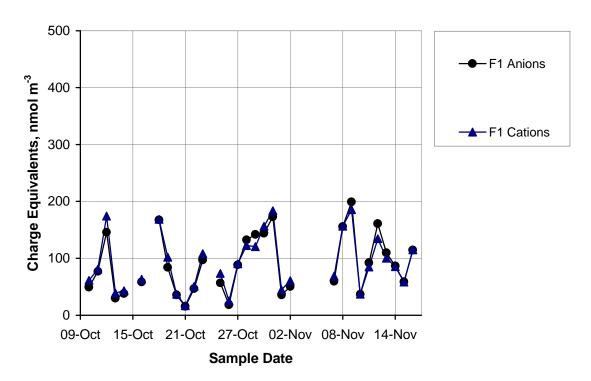
**Figure 58A** Ion Balance: Anion vs. cation equivalents for ammonium, acidity, nitrate, and sulfate collected on Full HEADS F1 (Teflon) filter at all sites.



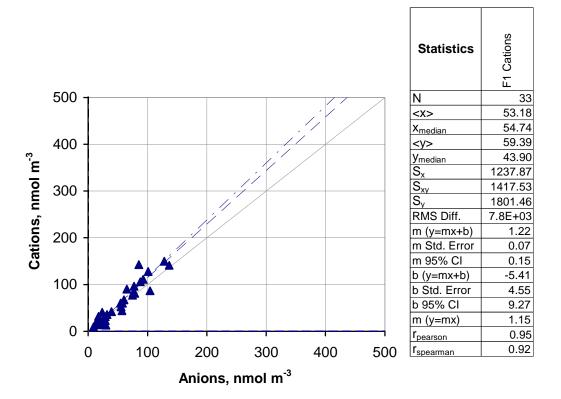


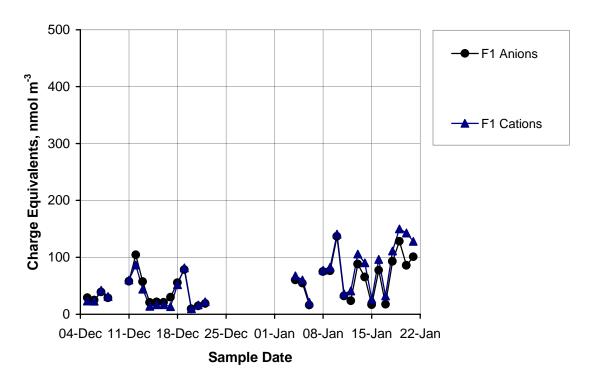
**Figure 58R** Ion Balance: Anion vs. cation equivalents for ammonium, acidity, nitrate, and sulfate collected on Full HEADS F1 (Teflon) filter at Riverside.



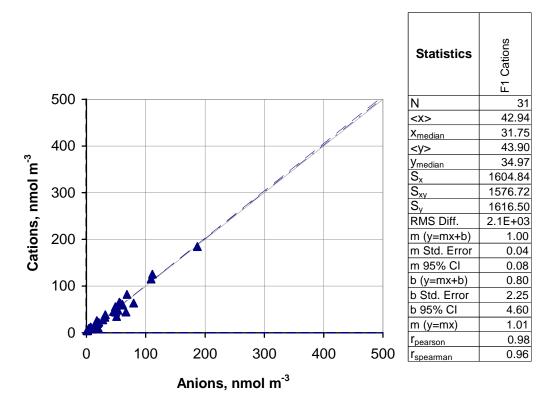


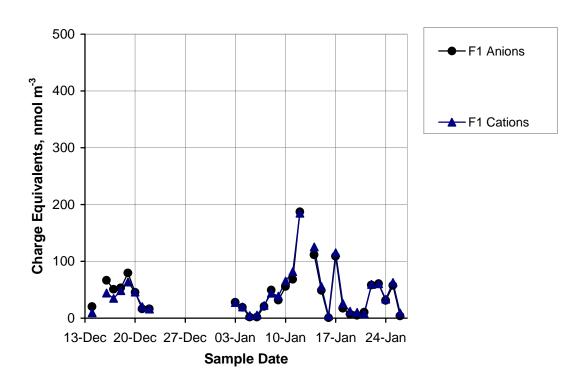
**Figure 58C** Ion Balance: Anion vs. cation equivalents for ammonium, acidity, nitrate, and sulfate collected on Full HEADS F1 (Teflon) filter at Chicago.



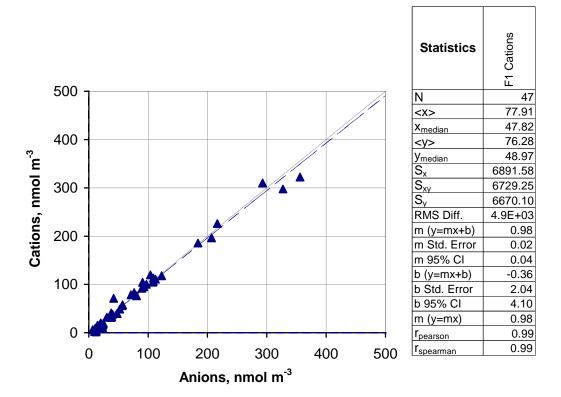


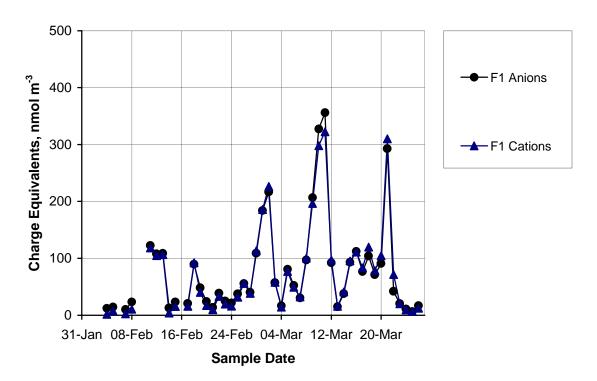
**Figure 58D** Ion Balance: Anion vs. cation equivalents for ammonium, acidity, nitrate, and sulfate collected on Full HEADS F1 (Teflon) filter at Dallas.



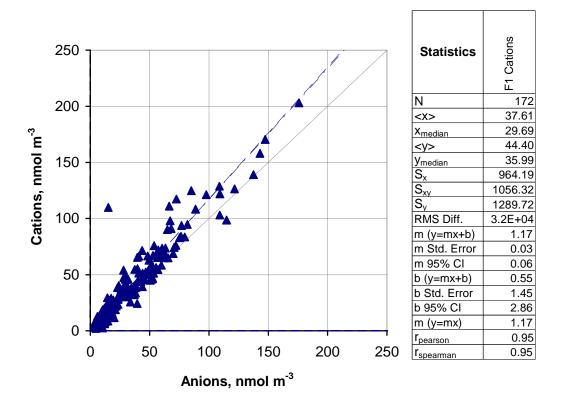


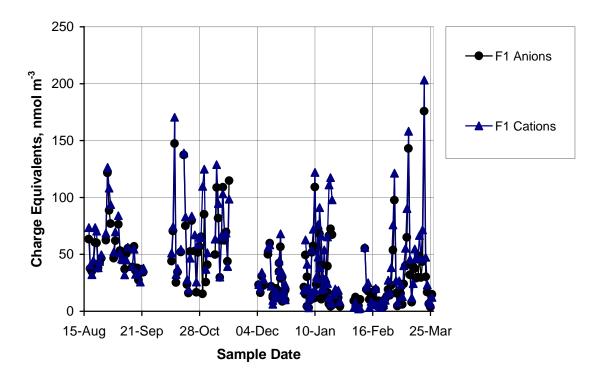
**Figure 58P** Ion Balance: Anion vs. cation equivalents for ammonium, acidity, nitrate, and sulfate collected on Full HEADS F1 (Teflon) filter at Phoenix.



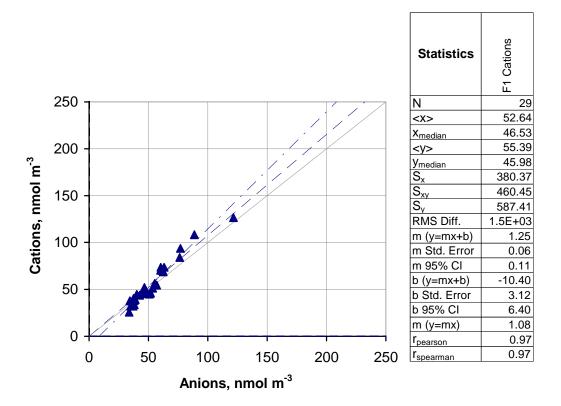


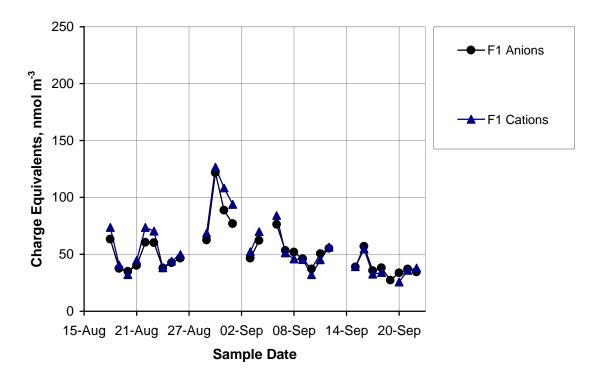
**Figure 58B** Ion Balance: Anion vs. cation equivalents for ammonium, acidity, nitrate, and sulfate collected on Full HEADS F1 (Teflon) filter at Bakersfield.



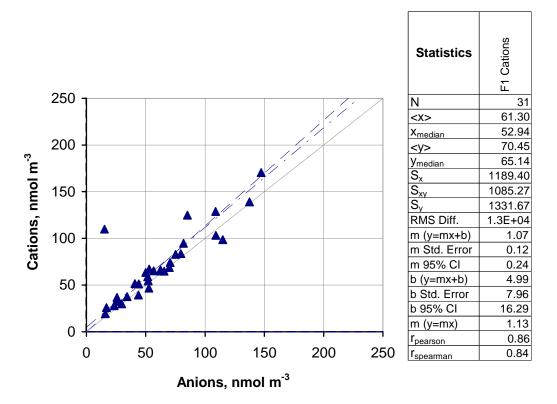


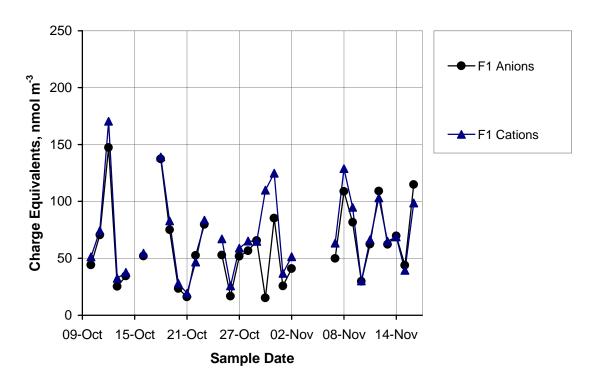
**Figure 59A** Ion Balance: Anion vs. cation equivalents for ammonium, acidity, nitrate, and sulfate collected on Nylon HEADS F1 (Teflon) filter at all sites.



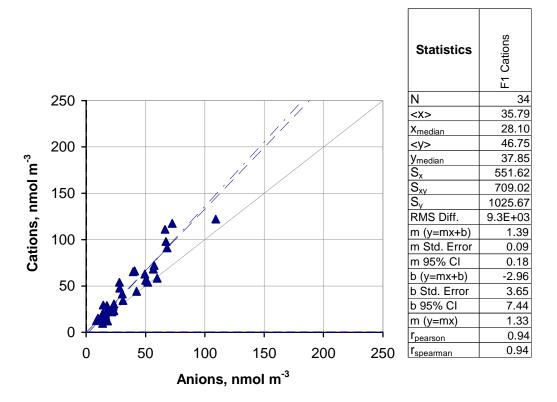


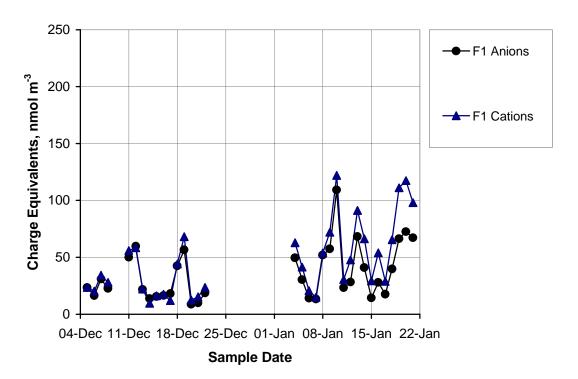
**Figure 59R** Ion Balance: Anion vs. cation equivalents for ammonium, acidity, nitrate, and sulfate collected on Nylon HEADS F1 (Teflon) filter at Riverside.



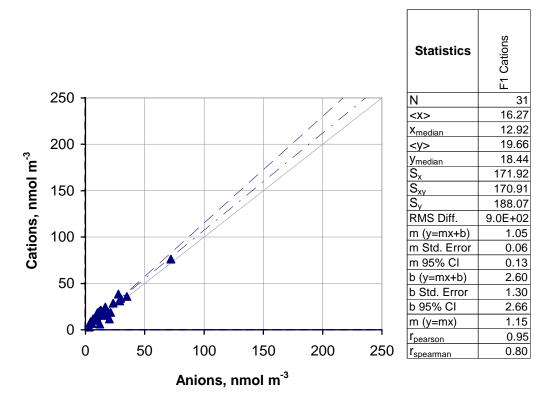


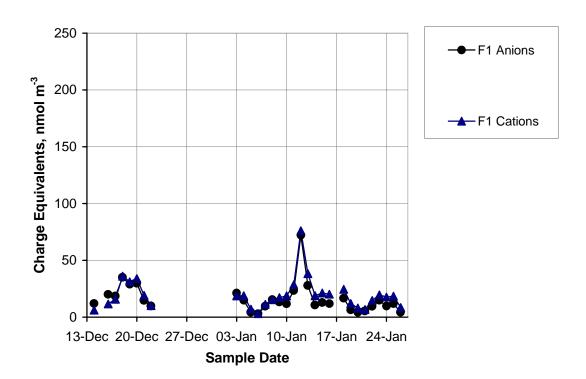
**Figure 59C** Ion Balance: Anion vs. cation equivalents for ammonium, acidity, nitrate, and sulfate collected on Nylon HEADS F1 (Teflon) filter at Chicago.



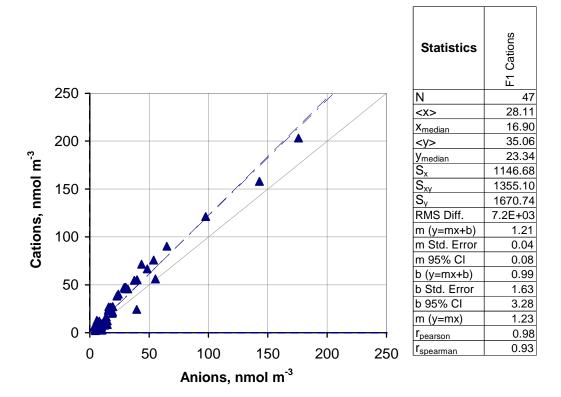


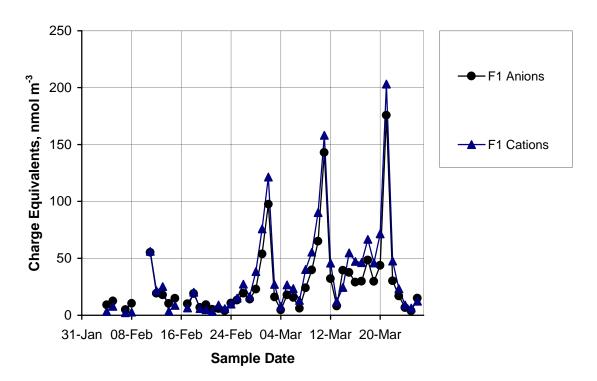
**Figure 59D** Ion Balance: Anion vs. cation equivalents for ammonium, acidity, nitrate, and sulfate collected on Nylon HEADS F1 (Teflon) filter at Dallas.



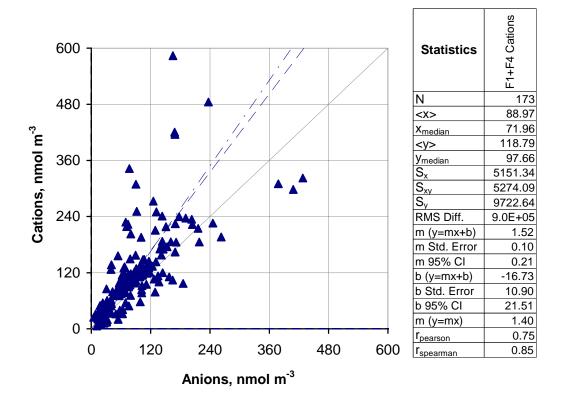


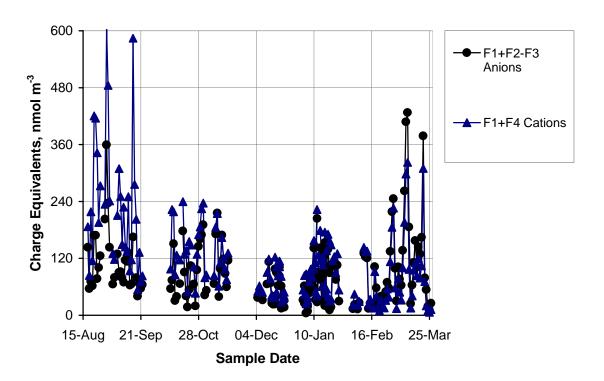
**Figure 59P** Ion Balance: Anion vs. cation equivalents for ammonium, acidity, nitrate, and sulfate collected on Nylon HEADS F1 (Teflon) filter at Phoenix.



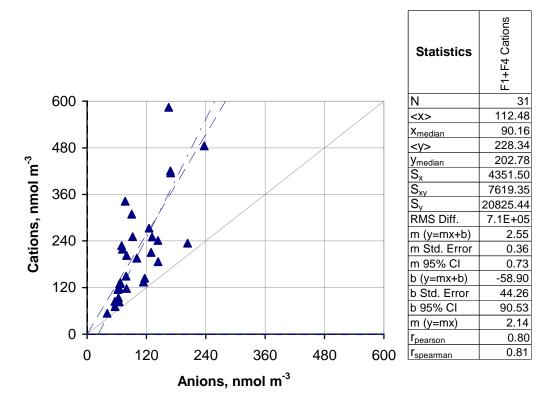


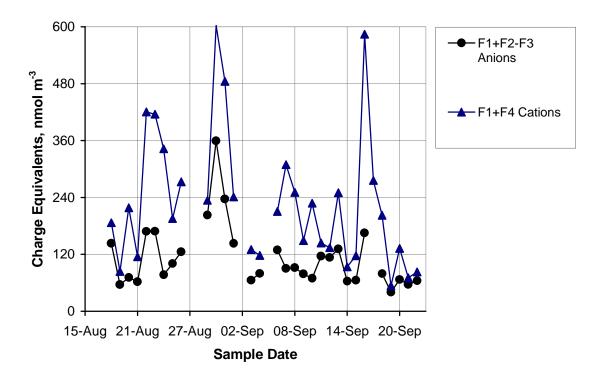
**Figure 59B** Ion Balance: Anion vs. cation equivalents for ammonium, acidity, nitrate, and sulfate collected on Nylon HEADS F1 (Teflon) filter at Bakersfield.



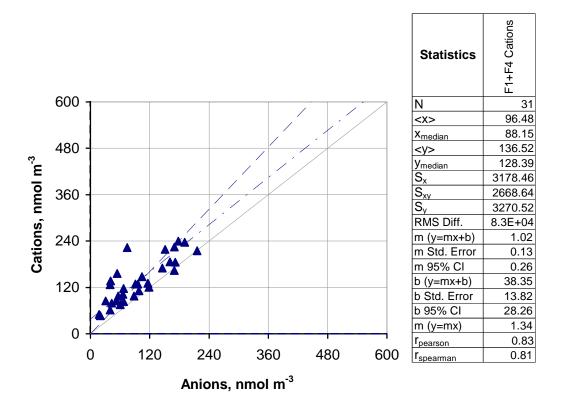


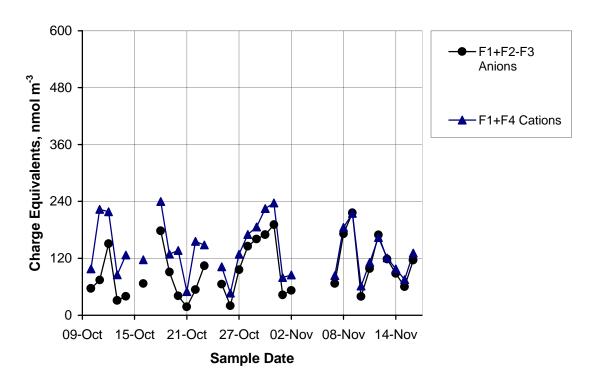
**Figure 60A** Ion Balance: Anion vs. cation equivalents for ammonium, acidity, nitrate, and sulfate collected on Full HEADS F1 (Teflon) + backup filters at all sites.



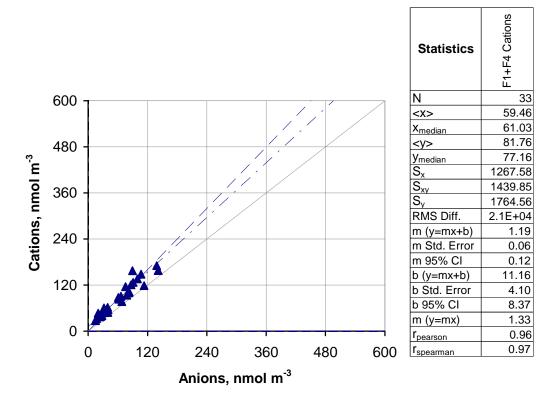


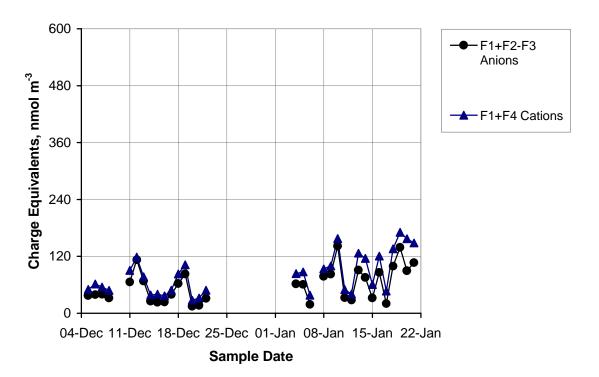
**Figure 60R** Ion Balance: Anion vs. cation equivalents for ammonium, acidity, nitrate, and sulfate collected on Full HEADS F1 (Teflon) + backup filters at Riverside.



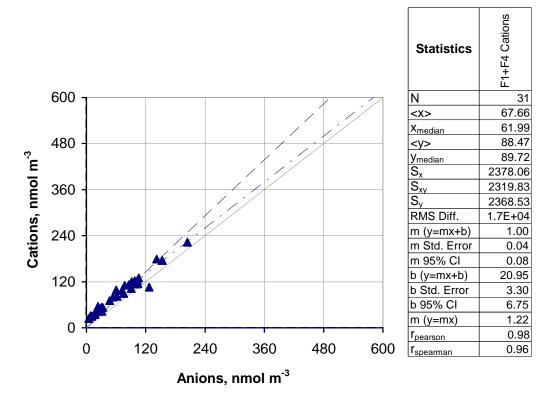


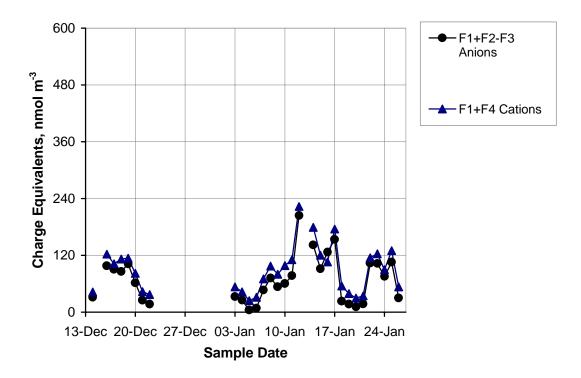
**Figure 60C** Ion Balance: Anion vs. cation equivalents for ammonium, acidity, nitrate, and sulfate collected on Full HEADS F1 (Teflon) + backup filters at Chicago.



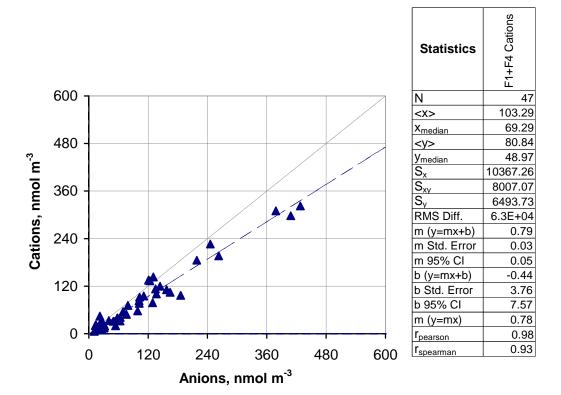


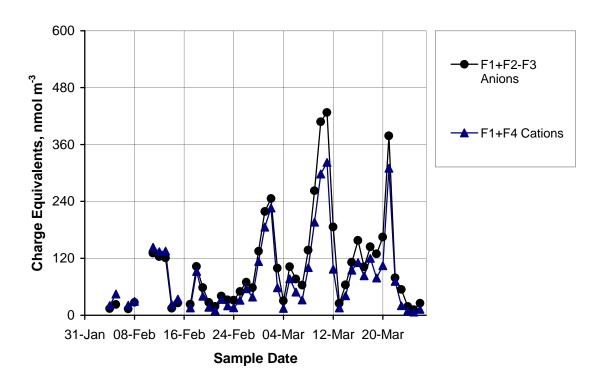
**Figure 60D** Ion Balance: Anion vs. cation equivalents for ammonium, acidity, nitrate, and sulfate collected on Full HEADS F1 (Teflon) + backup filters at Dallas.



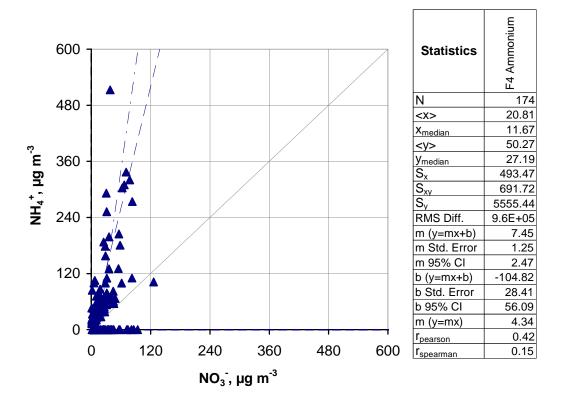


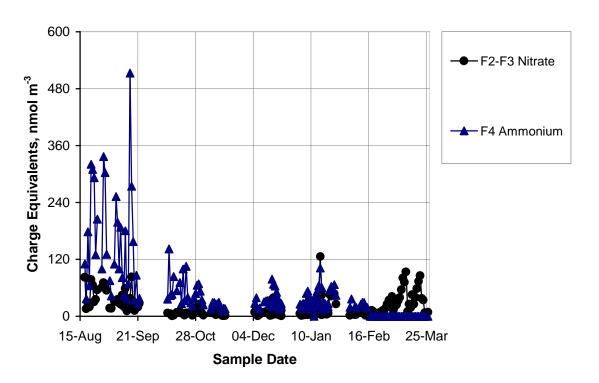
**Figure 60P** Ion Balance: Anion vs. cation equivalents for ammonium, acidity, nitrate, and sulfate collected on Full HEADS F1 (Teflon) + backup filters at Phoenix.



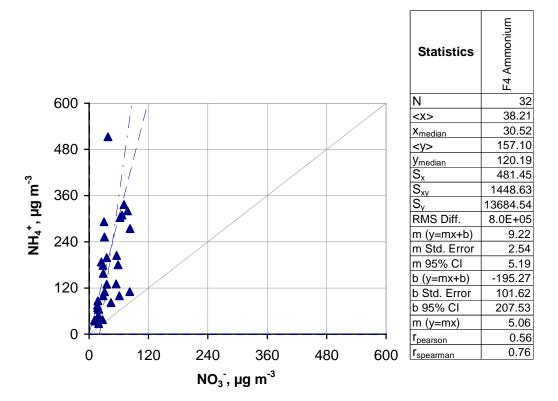


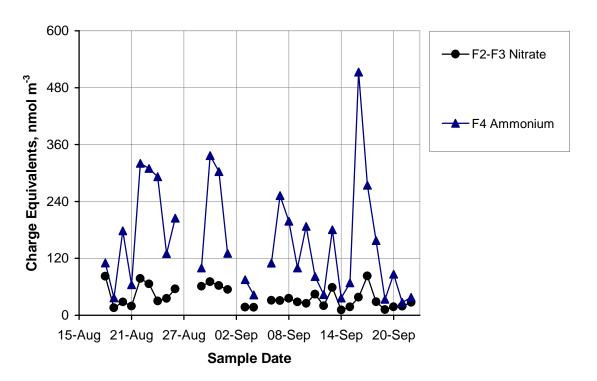
**Figure 60B** Ion Balance: Anion vs. cation equivalents for ammonium, acidity, nitrate, and sulfate collected on Full HEADS F1 (Teflon) + backup filters at Bakersfield.



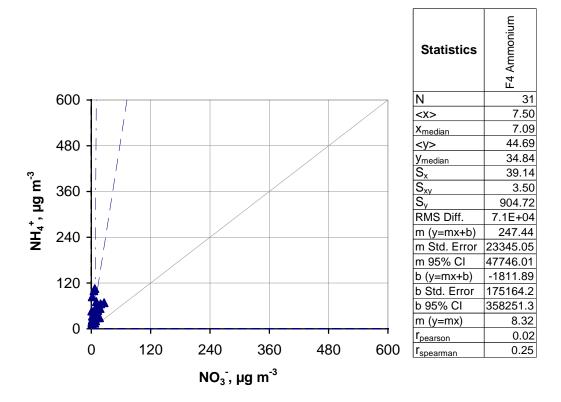


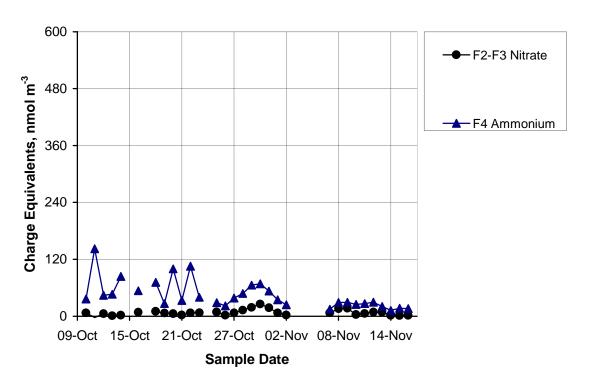
**Figure 61A** Ion Balance: Anion vs. cation equivalents for ammonium, acidity, nitrate, and sulfate collected on Full HEADS backup filters (F2 – F3 and F4) at all sites.



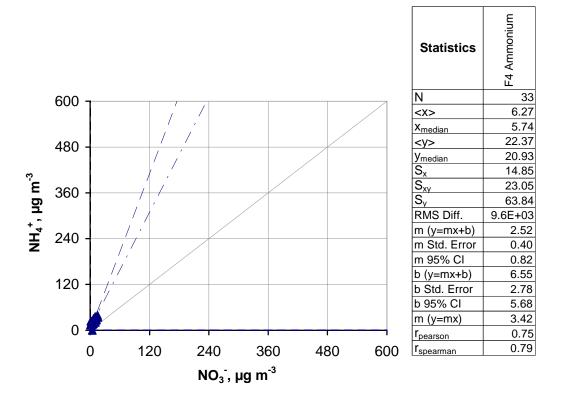


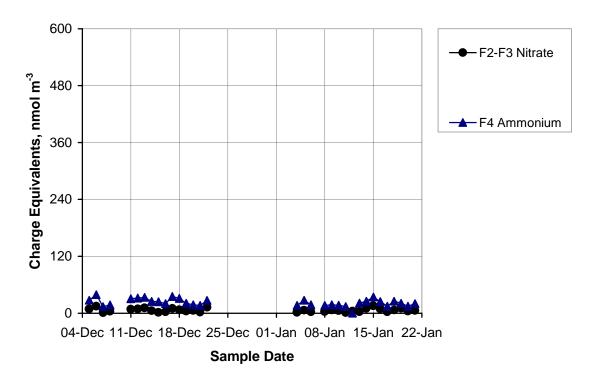
**Figure 61R** Ion Balance: Anion vs. cation equivalents for ammonium, acidity, nitrate, and sulfate collected on Full HEADS backup filters (F2 – F3 and F4) at Riverside.



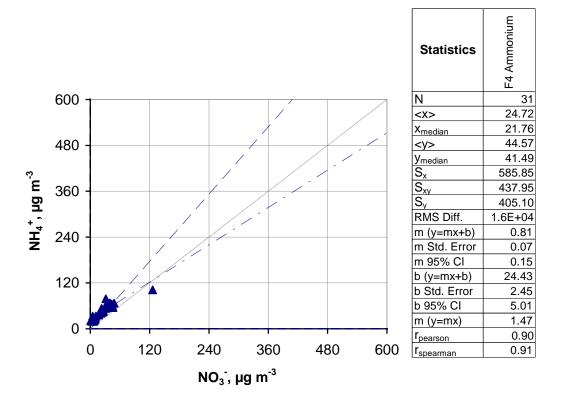


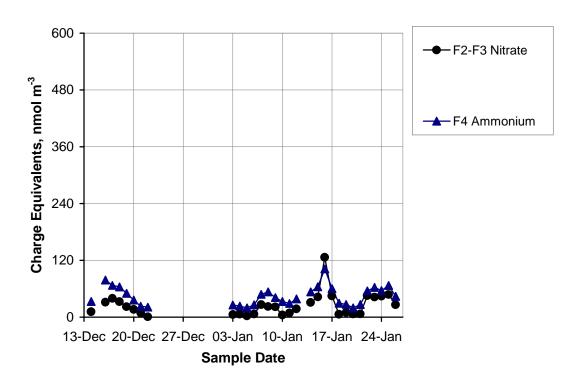
**Figure 61C** Ion Balance: Anion vs. cation equivalents for ammonium, acidity, nitrate, and sulfate collected on Full HEADS backup filters (F2 – F3 and F4) at Chicago.



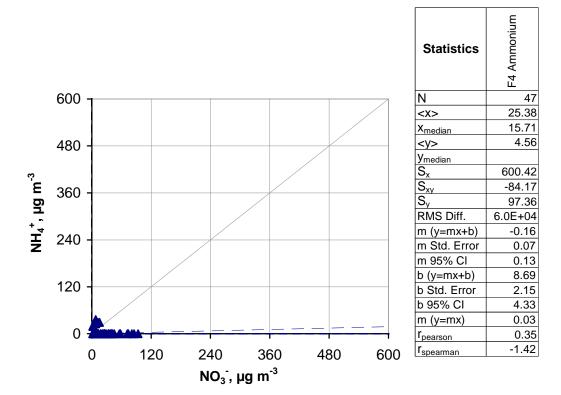


**Figure 61D** Ion Balance: Anion vs. cation equivalents for ammonium, acidity, nitrate, and sulfate collected on Full HEADS backup filters (F2 – F3 and F4) at Dallas.





**Figure 61P** Ion Balance: Anion vs. cation equivalents for ammonium, acidity, nitrate, and sulfate collected on Full HEADS backup filters (F2 – F3 and F4) at Phoenix.



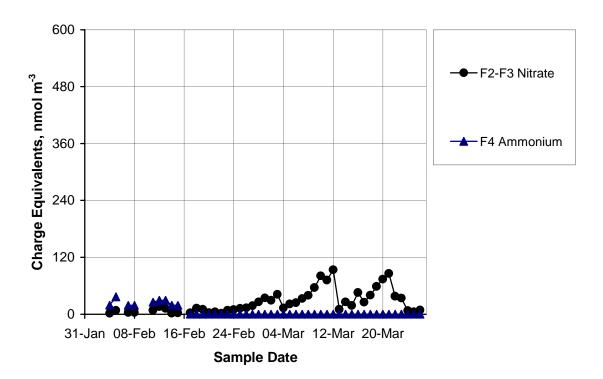
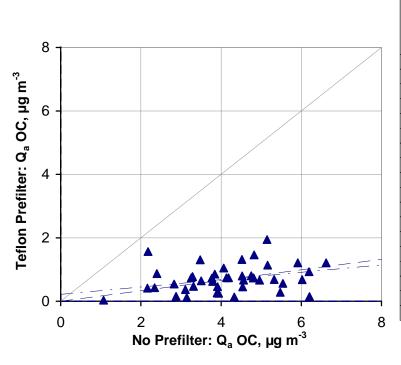


**Figure 61B** Ion Balance: Anion vs. cation equivalents for ammonium, acidity, nitrate, and sulfate collected on Full HEADS backup filters (F2 – F3 and F4) at Bakersfield.



Statistics	Denuded Qa OC (PF)
Ν	44
<x></x>	4.13
X <sub>median</sub>	4.10
<y></y>	0.70
<b>y</b> <sub>median</sub>	0.69
S <sub>v</sub>	1.52
S <sub>xy</sub>	0.16
$S_{v}$	0.18
RMS Diff.	5.8E+02
m (y=mx+b)	0.12
m Std. Error	0.06
m 95% CI	0.12
b (y=mx+b)	0.22
b Std. Error	0.25
b 95% CI	0.50
m (y=mx)	0.16
r <sub>pearson</sub>	0.30
r <sub>spearman</sub>	0.31

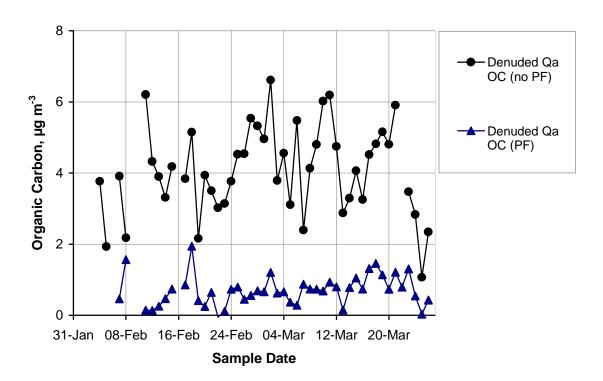
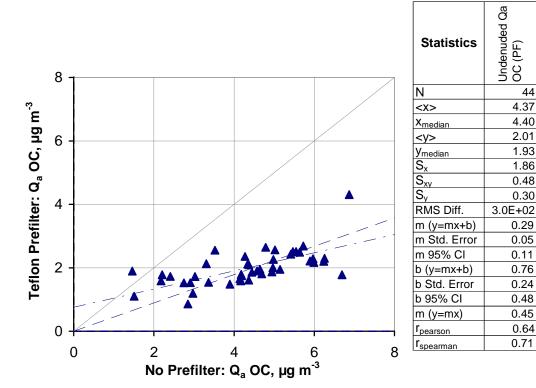


Figure 62B Carbon denuder test: organic carbon on front quartz filter  $(Q_a)$  of denuded sampler without prefilter (DEN) vs. denuded sampler with Teflon prefilter (DPF) at Bakersfield.



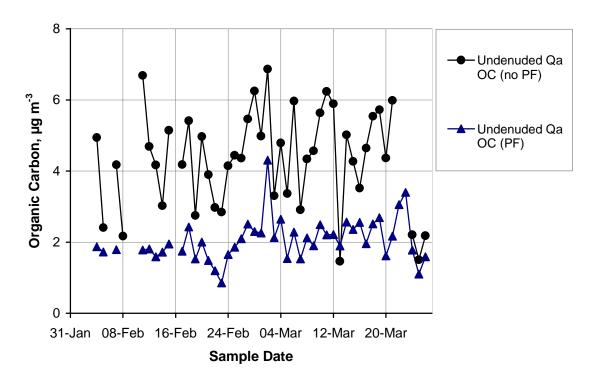
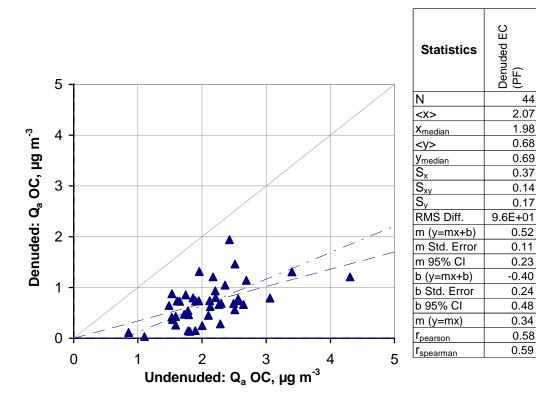


Figure 63B Carbon denuder test: organic carbon on front quartz filter  $(Q_a)$  of undenuded sampler without prefilter (UND) vs. undenuded sampler with Teflon prefilter (UPF) at Bakersfield.



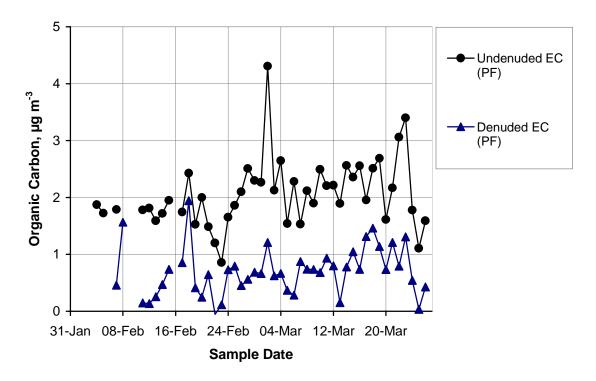
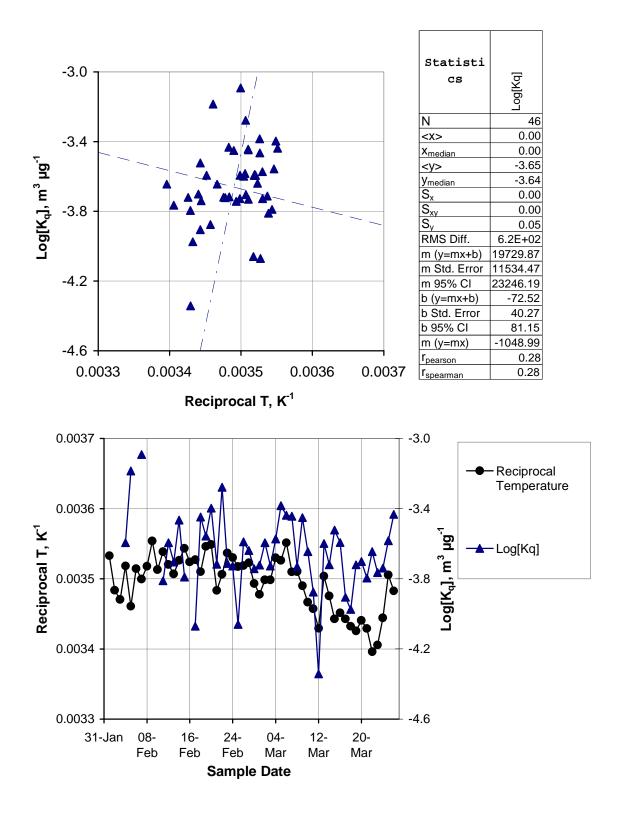
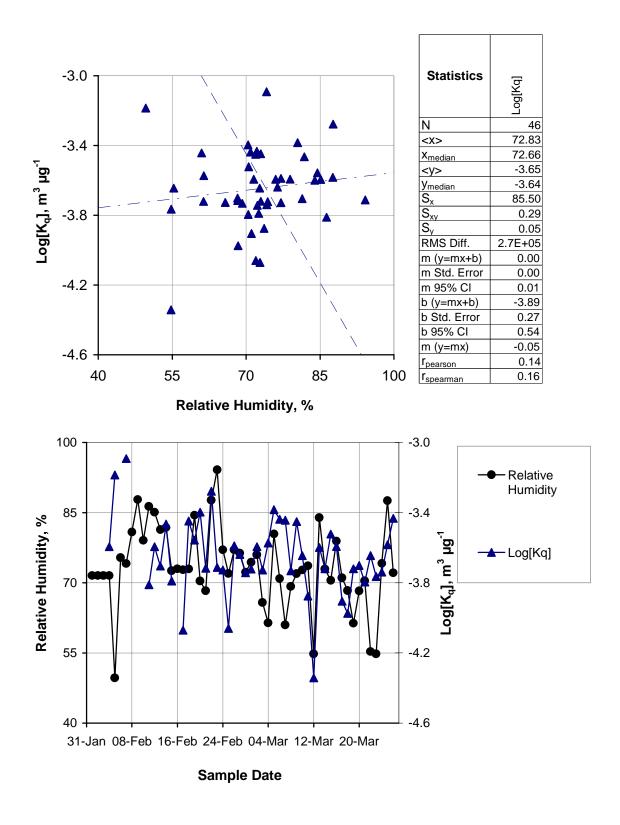


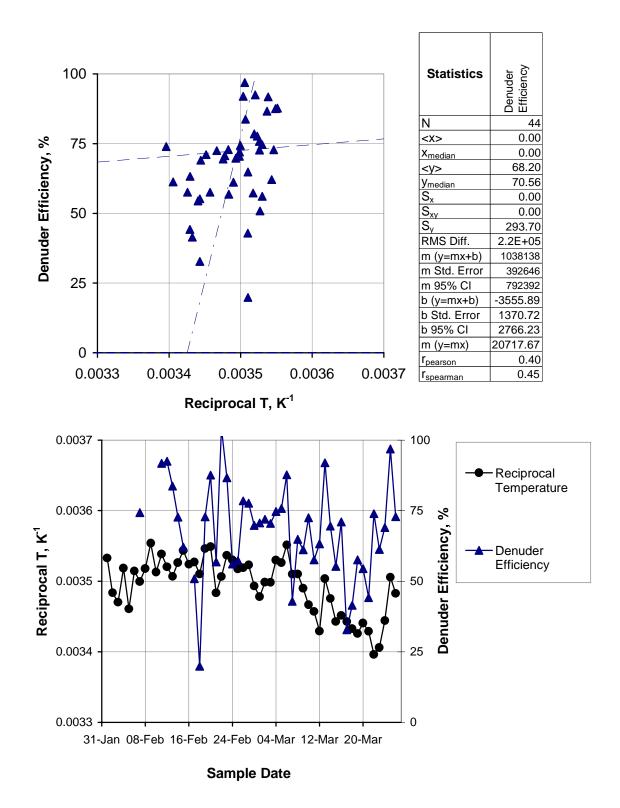
Figure 64B Carbon denuder test: organic carbon on front quartz filter  $(Q_a)$  of denuded sampler with Teflon prefilter (DPF) vs. undenuded sampler with Teflon prefilter (UPF) at Bakersfield.



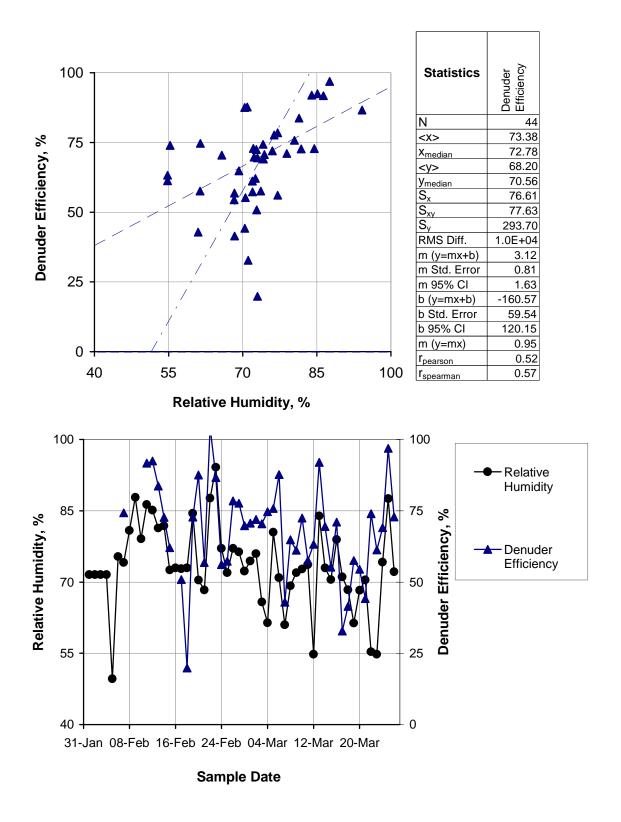
**Figure 65B** Carbon denuder test: calculated gas-quartz filter adsorption equilibrium constant vs. 23-h average reciprocal Kelvin temperature at Bakersfield.



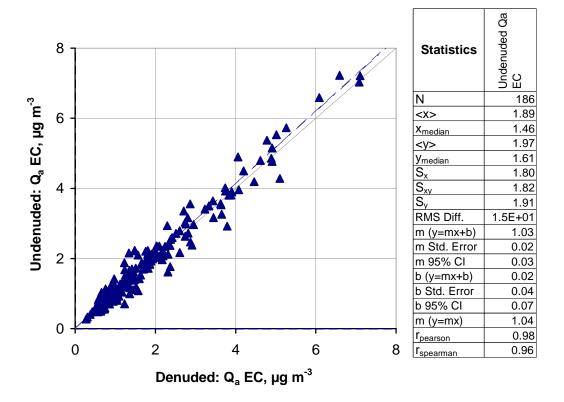
**Figure 66B** Carbon denuder test: calculated gas-quartz filter adsorption equilibrium constant vs. 23-h average relative humidity at Bakersfield.



**Figure 67B** Carbon denuder test: calculated denuder efficiency vs. 23-h average reciprocal Kelvin temperature at Bakersfield.



**Figure 68B** Carbon denuder test: calculated denuder efficiency vs. 23-h average relative humidity at Bakersfield.



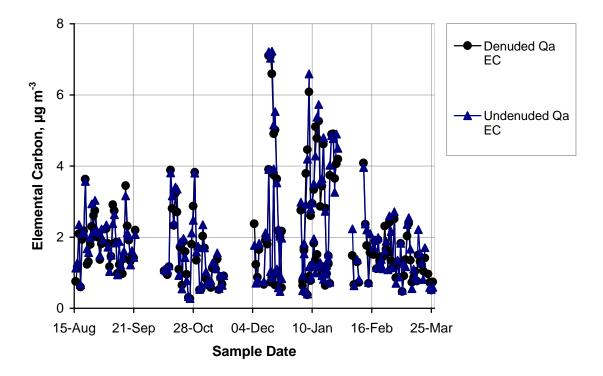
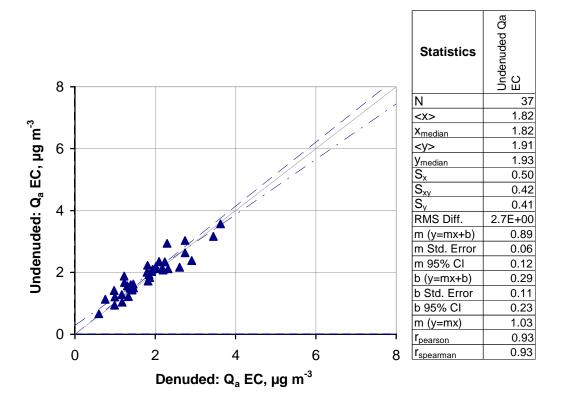


Figure 69A Elemental carbon: denuded (DEN) vs. undenuded (UND) Harvard carbon Sampler front quartz filter  $(Q_a)$  at all sites.



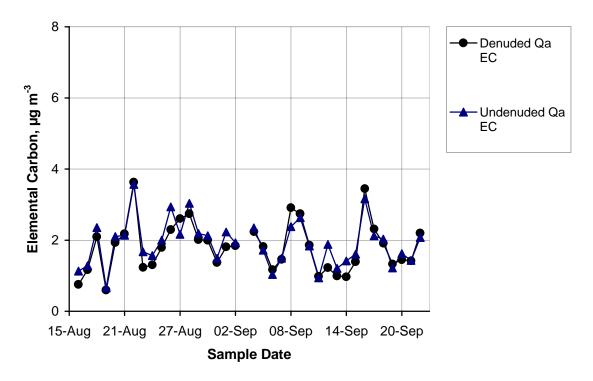
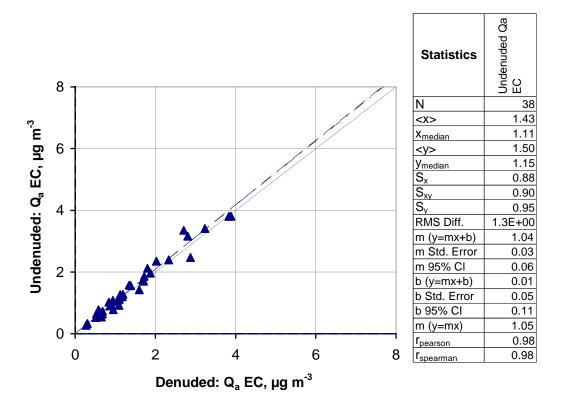


Figure 69R Elemental carbon: denuded (DEN) vs. undenuded (UND) Harvard carbon Sampler front quartz filter  $(Q_a)$  at Riverside.



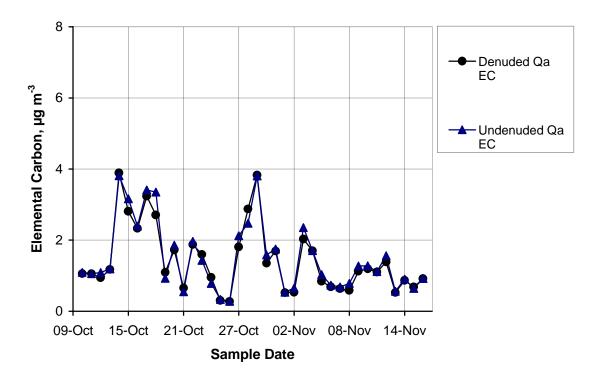
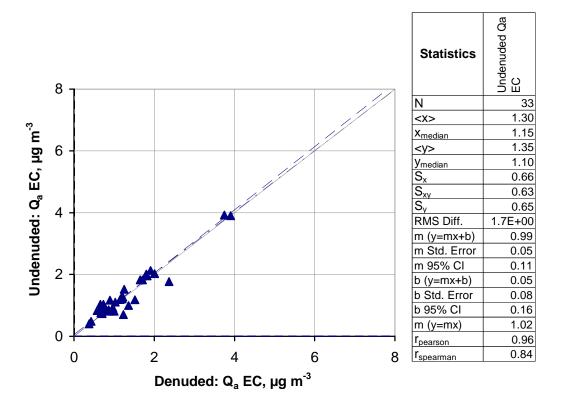
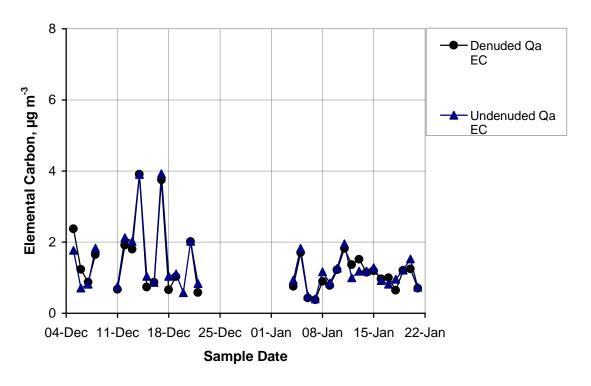
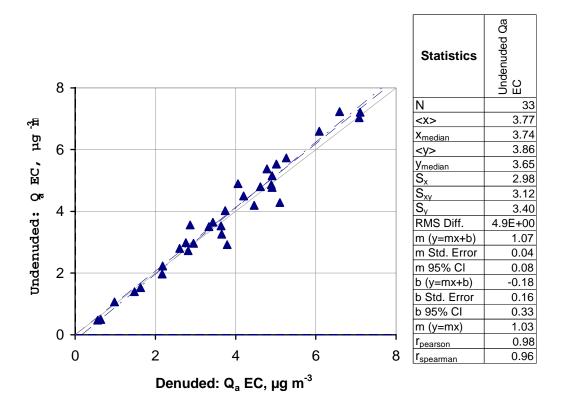


Figure 69C Elemental carbon: denuded (DEN) vs. undenuded (UND) Harvard carbon Sampler front quartz filter  $(Q_a)$  at Chicago.





 $\begin{tabular}{ll} \textbf{Figure 69D} & Elemental carbon: denuded (DEN) vs. undenuded (UND) Harvard carbon \\ & Sampler front quartz filter (Q_a) at Dallas. \end{tabular}$ 



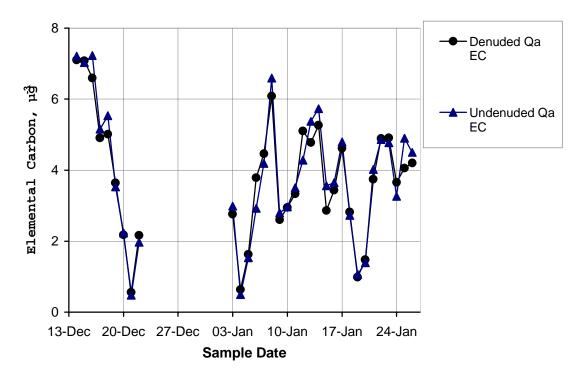
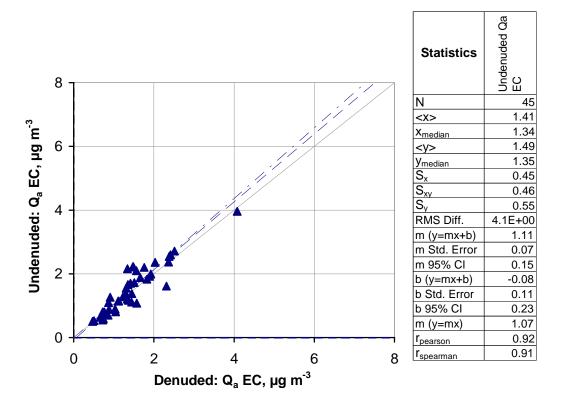
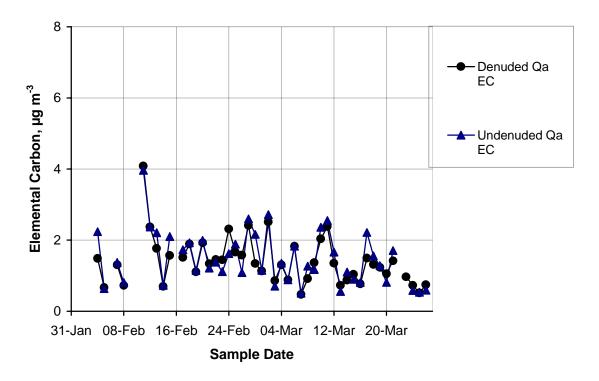
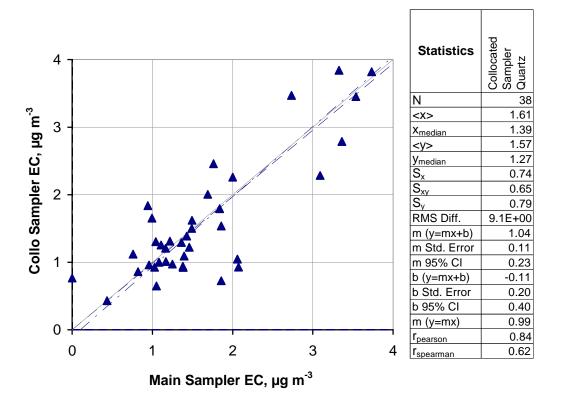


Figure 69P Elemental carbon: denuded (DEN) vs. undenuded (UND) Harvard carbon Sampler front quartz filter  $(Q_a)$  at Phoenix.





 $\begin{tabular}{ll} \textbf{Figure 69B} & Elemental carbon: denuded (DEN) vs. undenuded (UND) Harvard carbon \\ & Sampler front quartz filter (Q_a) at Bakersfield. \\ \end{tabular}$ 



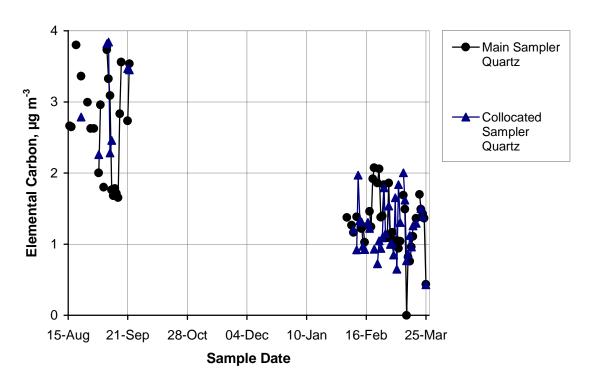
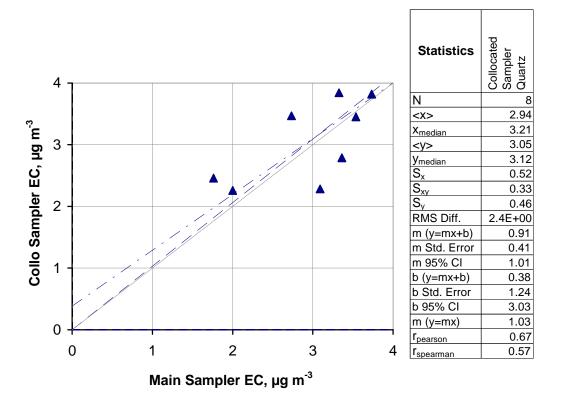


Figure 70A Elemental carbon: collocated Big BOSS quartz filter at all sites.



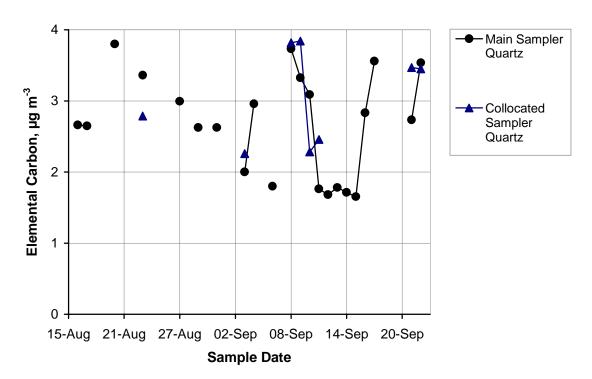
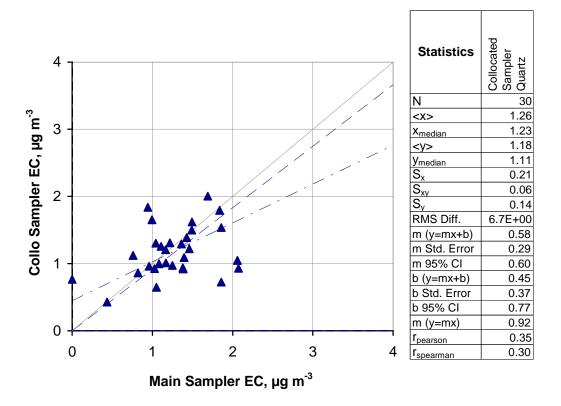


Figure 70R Elemental carbon: collocated Big BOSS quartz filter at Riverside.



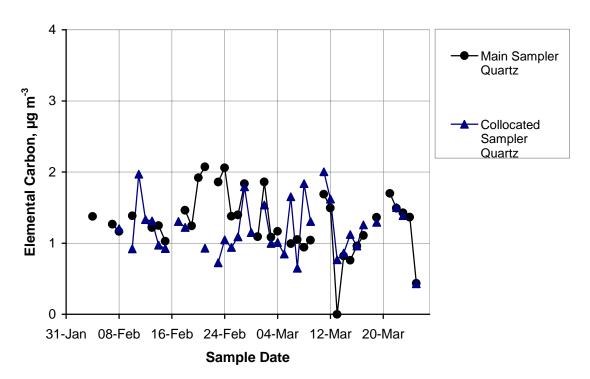
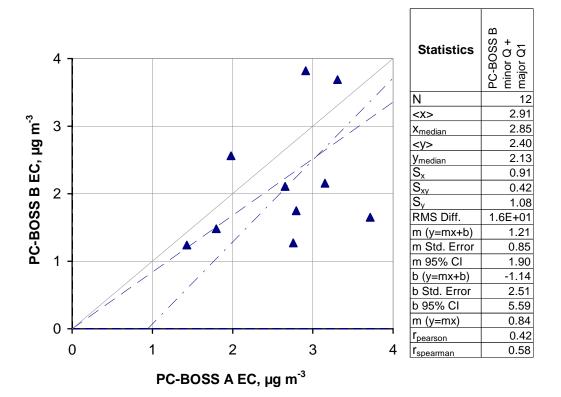
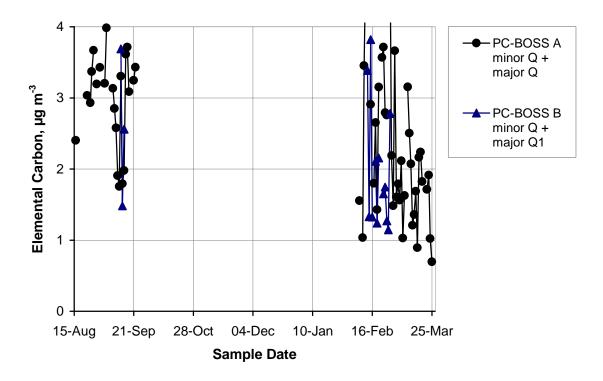
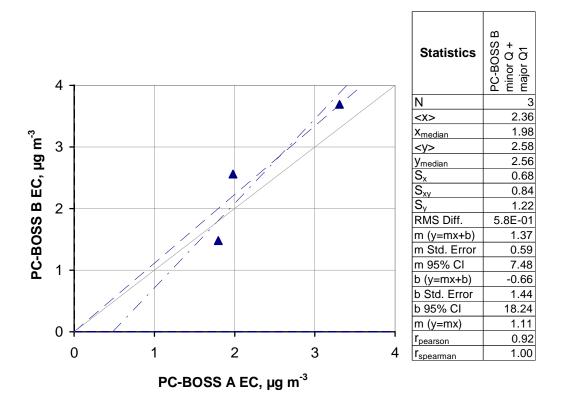


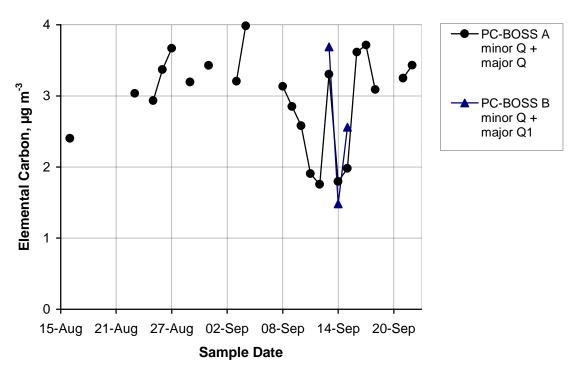
Figure 70B Elemental carbon: collocated Big BOSS quartz filter at Bakersfield.



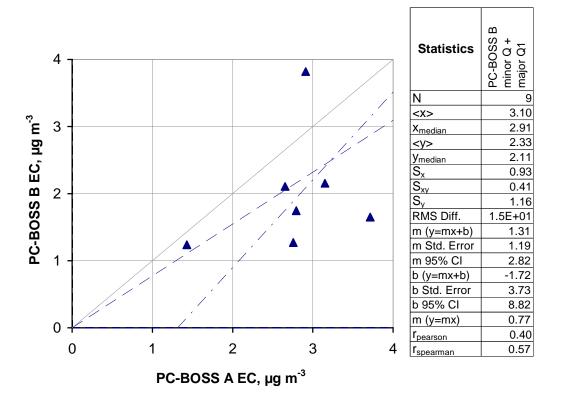


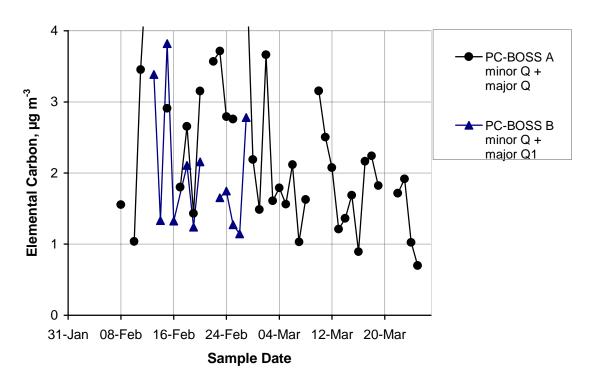
**Figure 71A** Elemental carbon: collocated PC-BOSS minor + major flow quartz filters at all sites.



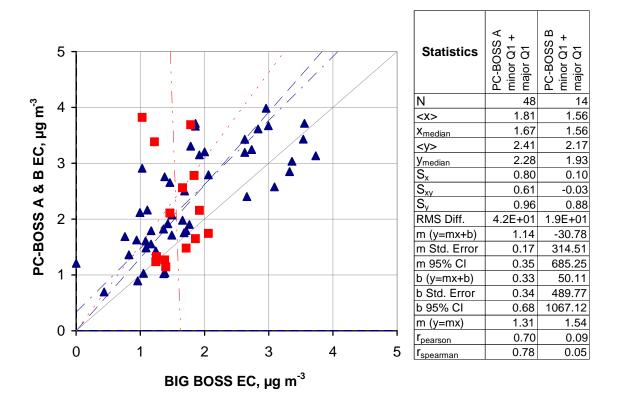


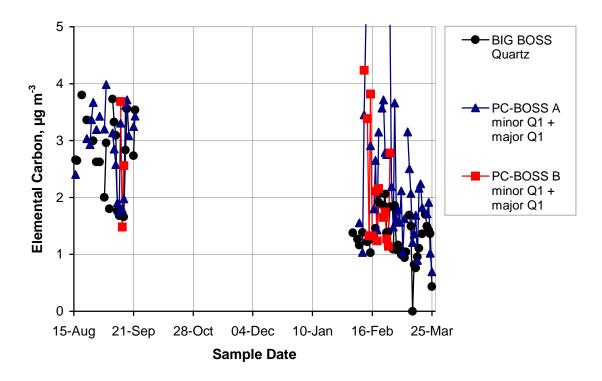
**Figure 71R** Elemental carbon: collocated PC-BOSS minor + major flow quartz filters at Riverside.



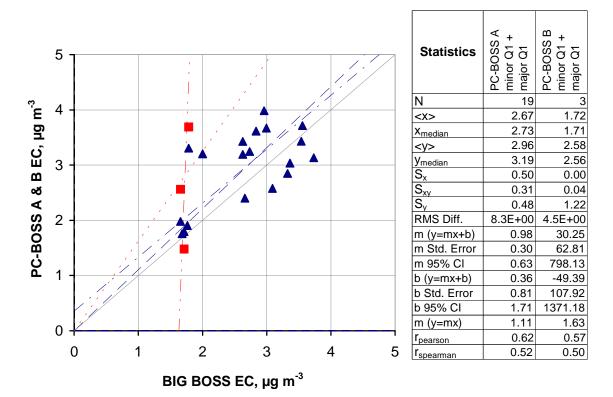


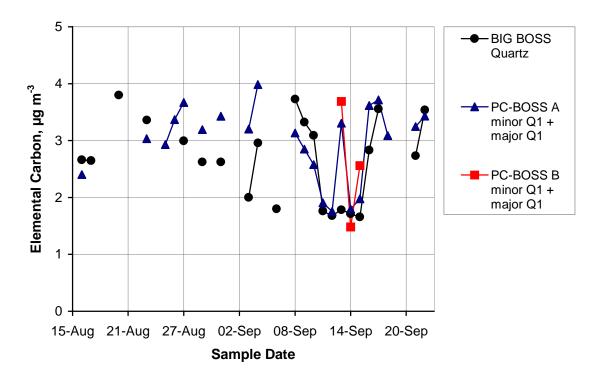
**Figure 71B** Elemental carbon: collocated PC-BOSS minor + major flow quartz filters at Bakersfield.



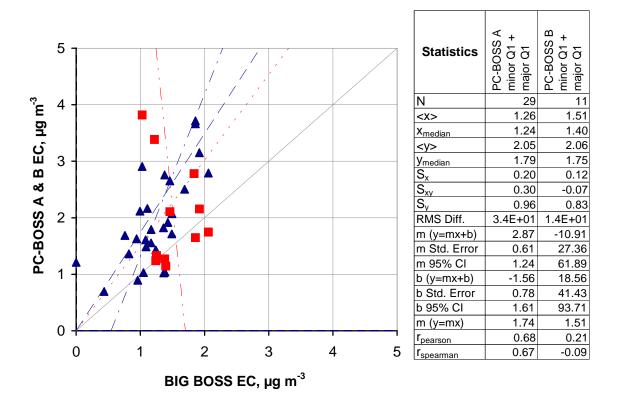


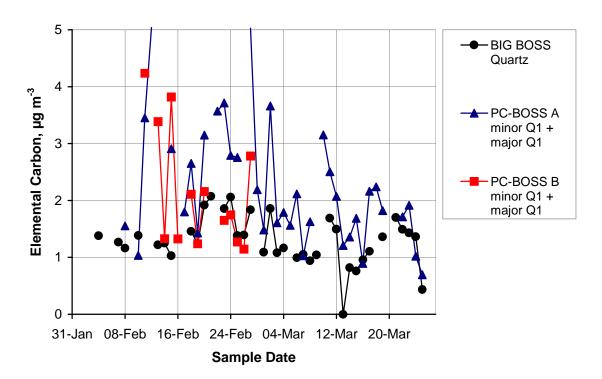
**Figure 72A** Elemental carbon: Big BOSS quartz filter vs. PC-BOSS A minor + major flow quartz filters at all sites.



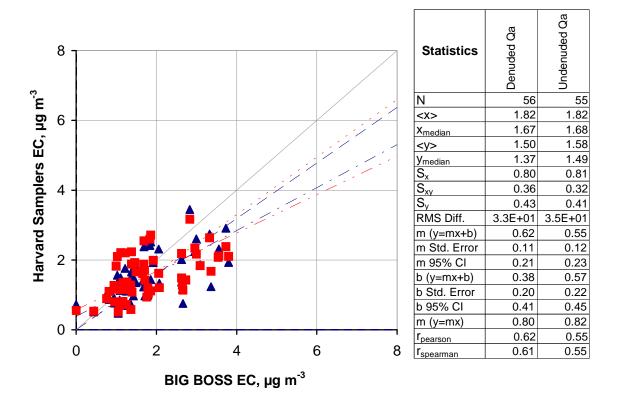


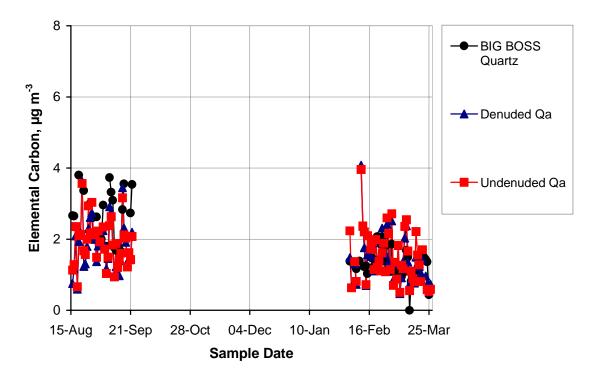
**Figure 72R** Elemental carbon: Big BOSS quartz filter vs. PC-BOSS A minor + major flow quartz filters at Riverside.



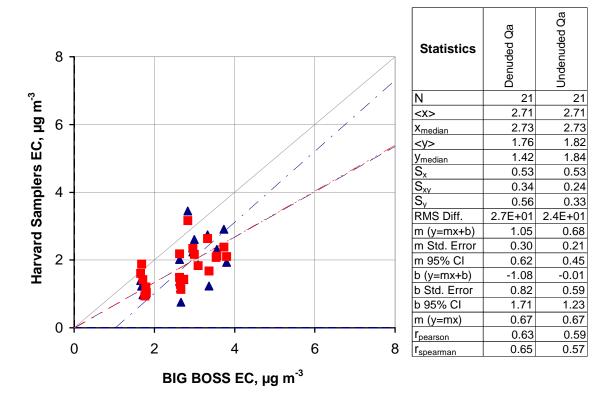


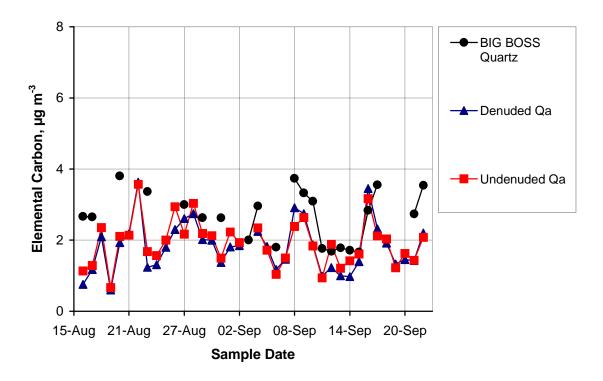
**Figure 72B** Elemental carbon: Big BOSS quartz filter vs. PC-BOSS A minor + major flow quartz filters at Bakersfield.



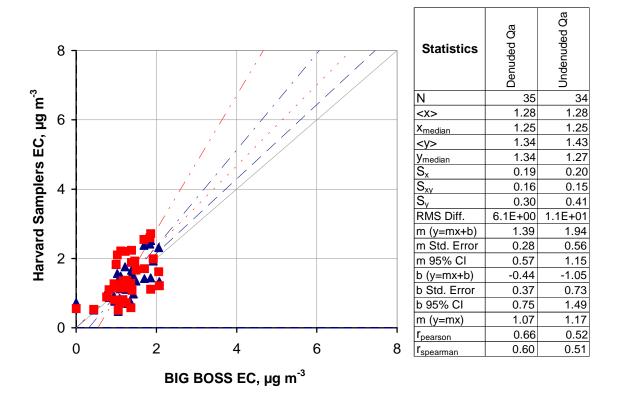


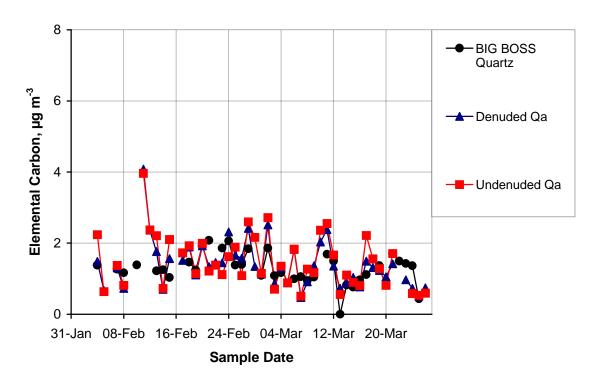
 $\begin{array}{ll} \textbf{Figure 73A} & \text{Elemental carbon: denuded (DEN) and undenuded (UND) Harvard} \\ & \text{Carbon Sampler front filters } (Q_a) \text{ vs. Big BOSS quartz filter at all sites.} \end{array}$ 



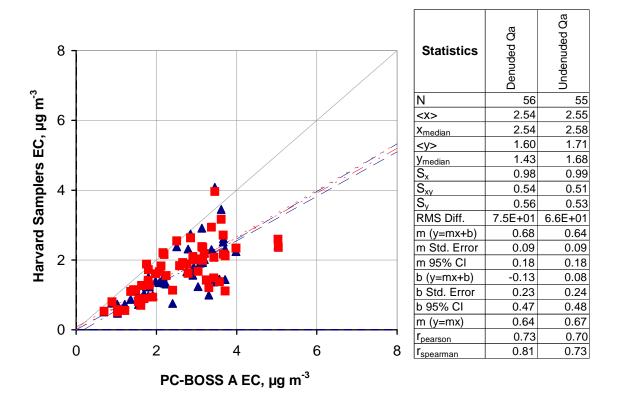


 $\label{eq:Figure 73R} \begin{array}{ll} \textbf{Elemental carbon: denuded (DEN) and undenuded (UND) Harvard} \\ \textbf{Carbon Sampler front filters } (Q_a) \ vs. \ Big \ BOSS \ quartz \ filter \ at \ Riverside. \\ \end{array}$ 





 $\label{eq:Figure 73B} \begin{array}{ll} \text{Elemental carbon: denuded (DEN) and undenuded (UND) Harvard} \\ \text{Carbon Sampler front filters } (Q_a) \text{ vs. Big BOSS quartz filter at} \\ \text{Bakersfield.} \end{array}$ 



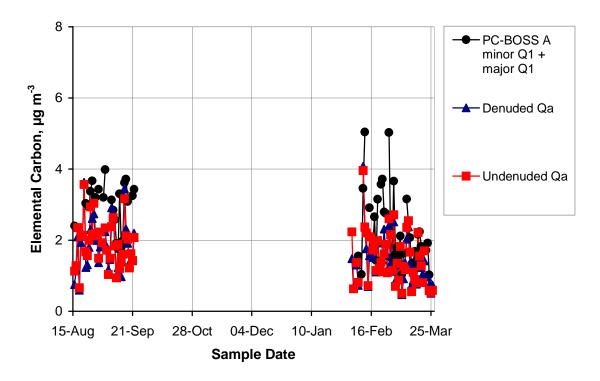
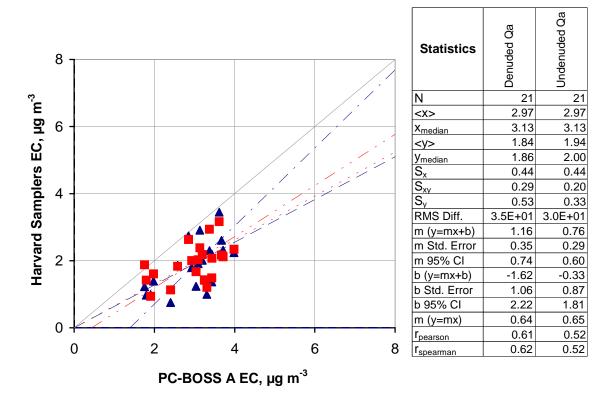
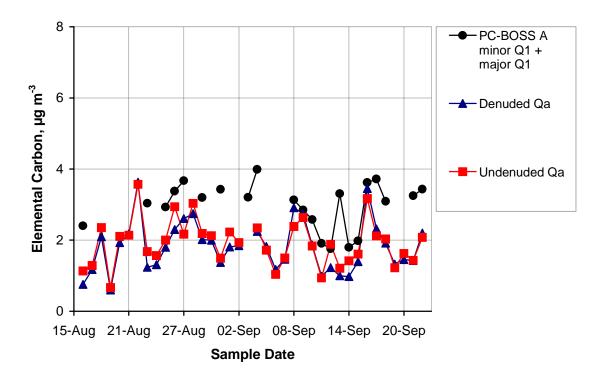
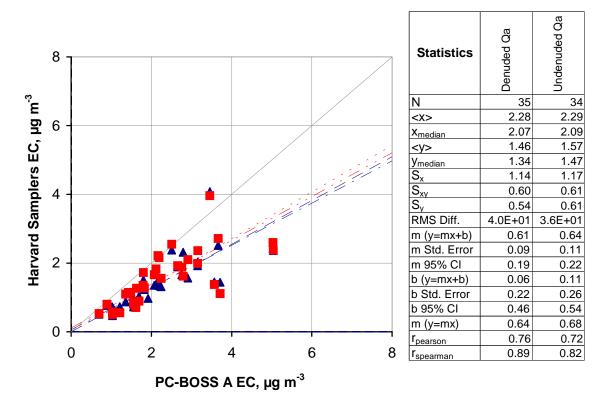


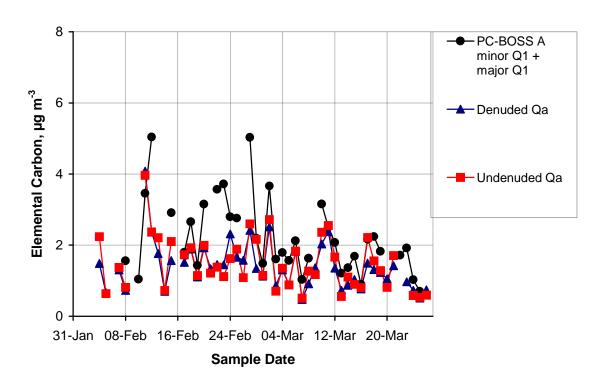
Figure 74A Elemental carbon: denuded (DEN) and undenuded (UND) Harvard Carbon Sampler front filters ( $Q_a$ ) vs. PC-BOSS minor flow quartz + major flow quartz filters at all sites.



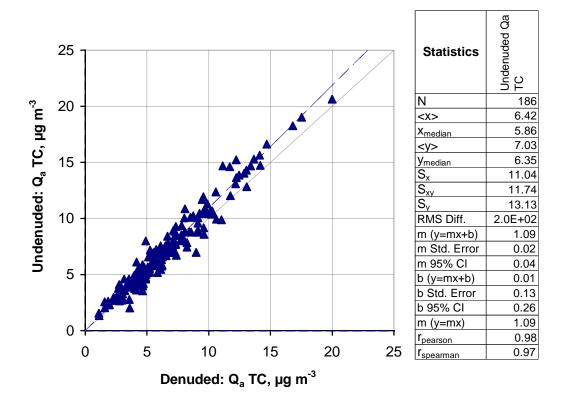


 $\label{eq:Figure 74R} Figure 74R \qquad \hbox{Elemental carbon: denuded (DEN) and undenuded (UND) Harvard} \\ \qquad \hbox{Carbon Sampler front filters } (Q_a) \ vs. \ PC-BOSS \ minor flow \ quartz + major \\ \qquad \hbox{flow quartz filters at Riverside.}$ 





 $\label{eq:Figure 74B} Figure 74B \qquad \hbox{Elemental carbon: denuded (DEN) and undenuded (UND) Harvard} \\ \qquad \hbox{Carbon Sampler front filters } (Q_a) \ vs. \ PC-BOSS \ minor flow \ quartz + major \\ \qquad \hbox{flow quartz filters at Bakersfield.}$ 



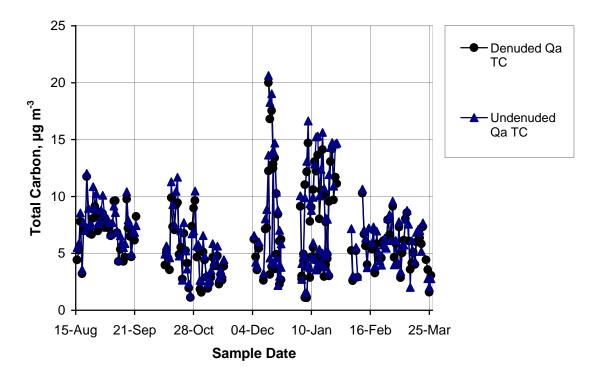
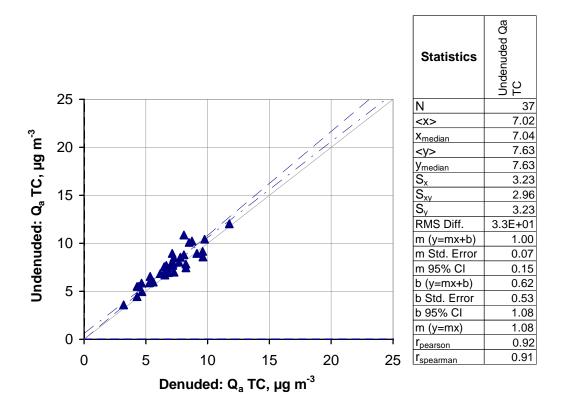


Figure 75A Total carbon: denuded (DEN) vs. undenuded (UND) Harvard Carbon Sampler front quartz filter  $(Q_a)$  at all sites.



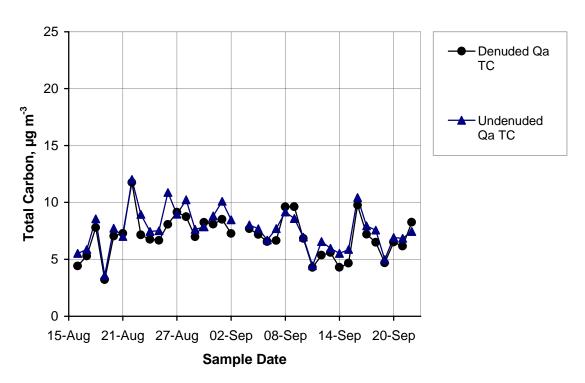
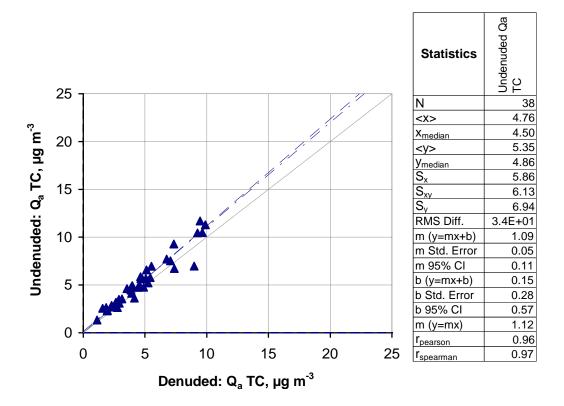


Figure 75R Total carbon: denuded (DEN) vs. undenuded (UND) Harvard Carbon Sampler front quartz filter  $(Q_a)$  at Riverside.



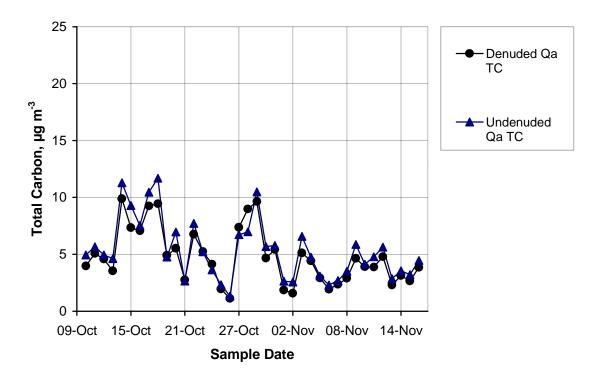
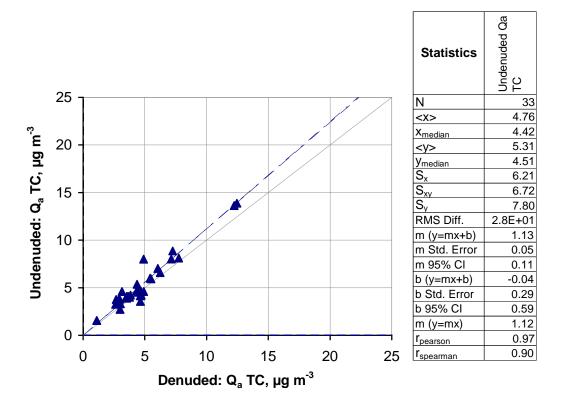


Figure 75C Total carbon: denuded (DEN) vs. undenuded (UND) Harvard Carbon Sampler front quartz filter  $(Q_a)$  at Chicago.



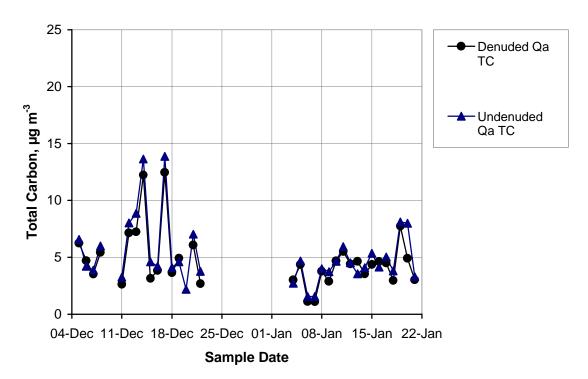
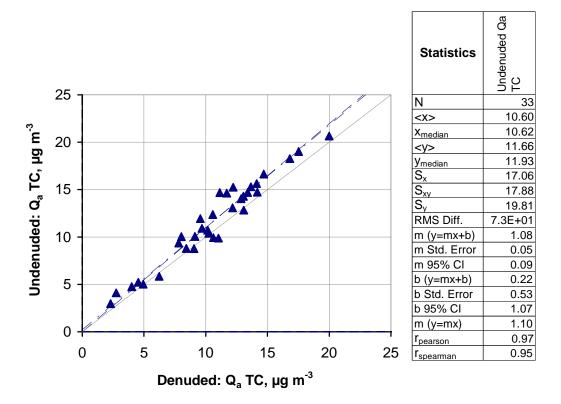


Figure 75D Total carbon: denuded (DEN) vs. undenuded (UND) Harvard Carbon Sampler front quartz filter  $(Q_a)$  at Dallas.



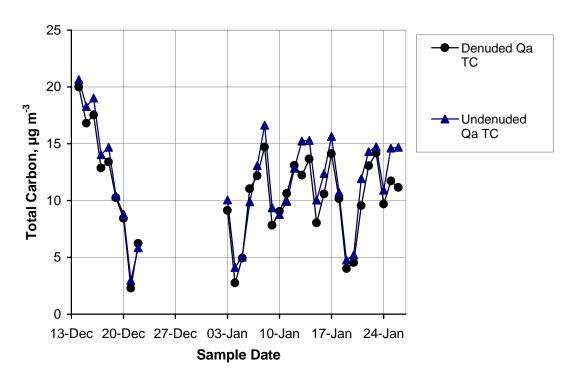
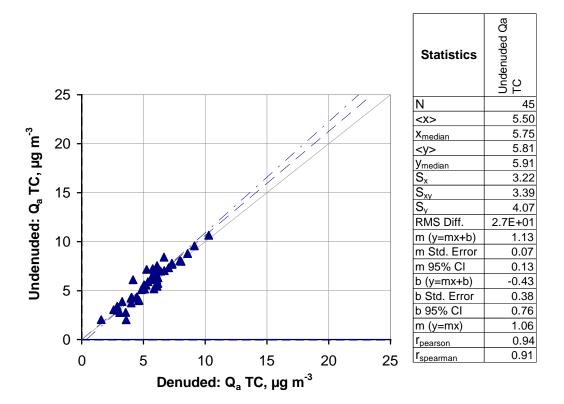


Figure 75P Total carbon: denuded (DEN) vs. undenuded (UND) Harvard Carbon Sampler front quartz filter  $(Q_a)$  at Phoenix.



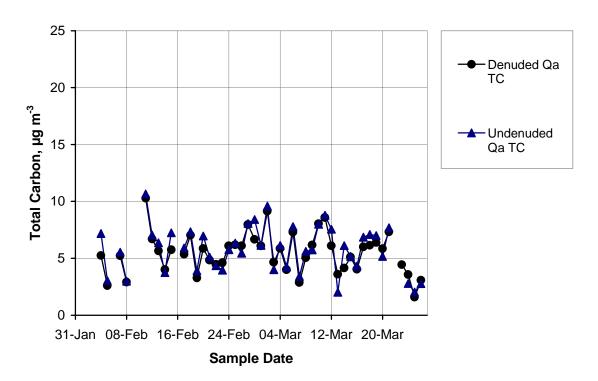
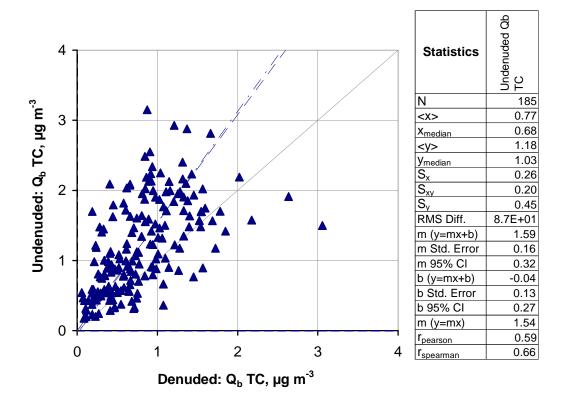


Figure 75B Total carbon: denuded (DEN) vs. undenuded (UND) Harvard Carbon Sampler front quartz filter  $(Q_a)$  at Bakersfield.



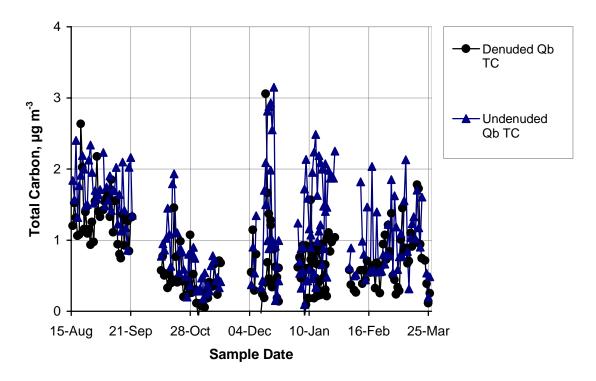
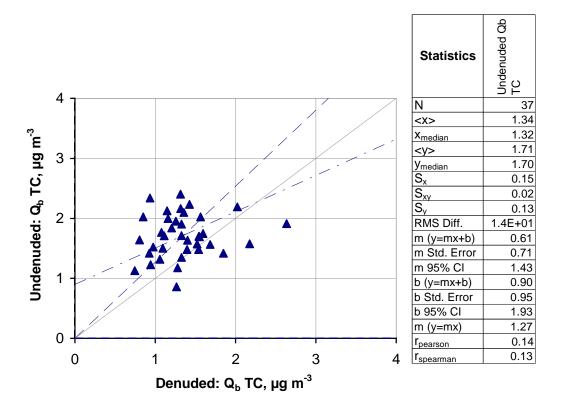
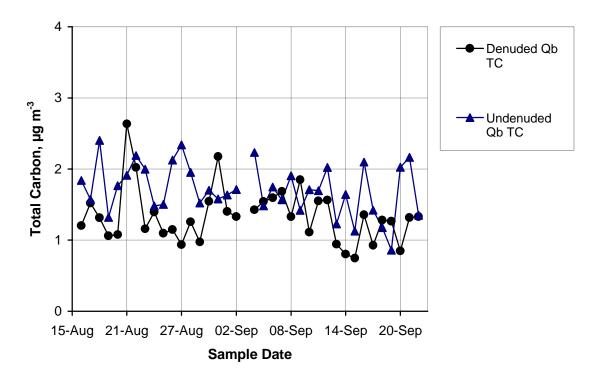
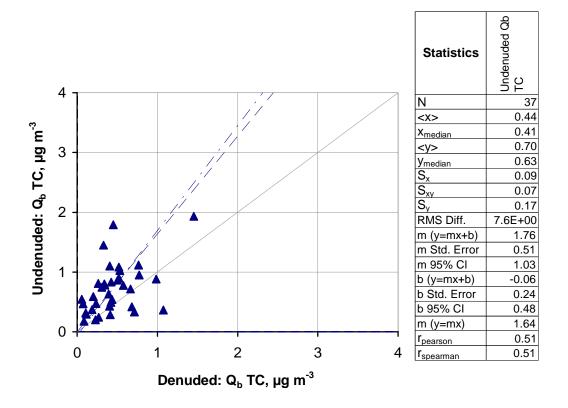


Figure 76A Total carbon: denuded (DEN) vs. undenuded (UND) Harvard Carbon Sampler back quartz filter  $(Q_b)$  at all sites.





**Figure 76R** Total carbon: denuded (DEN) vs. undenuded (UND) Harvard Carbon Sampler back quartz filter (Q<sub>b</sub>) at Riverside.



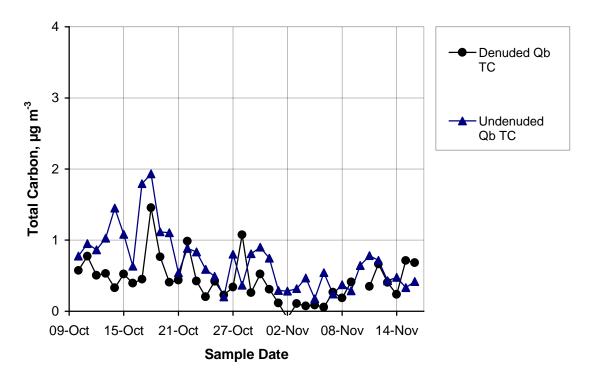
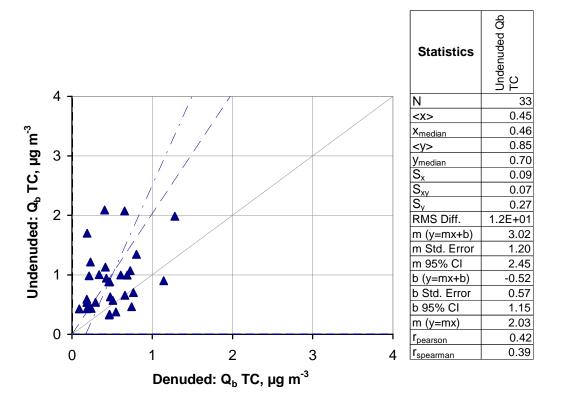
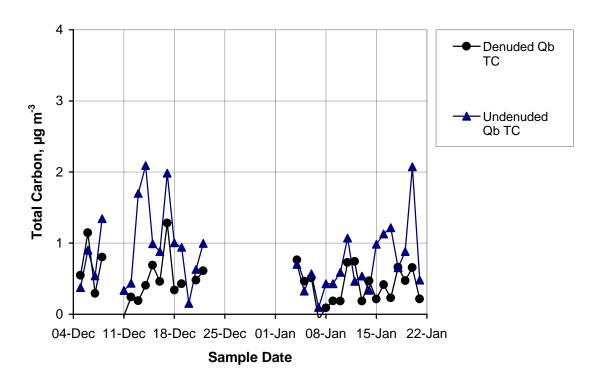
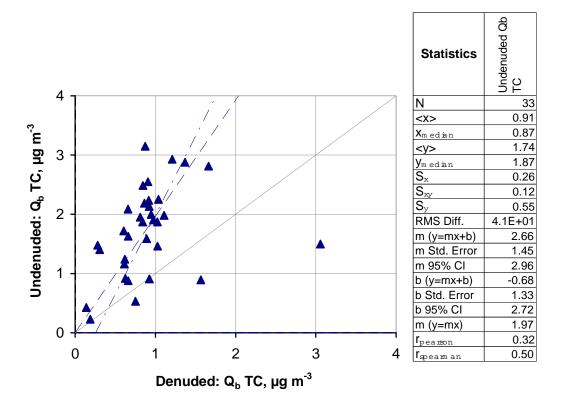


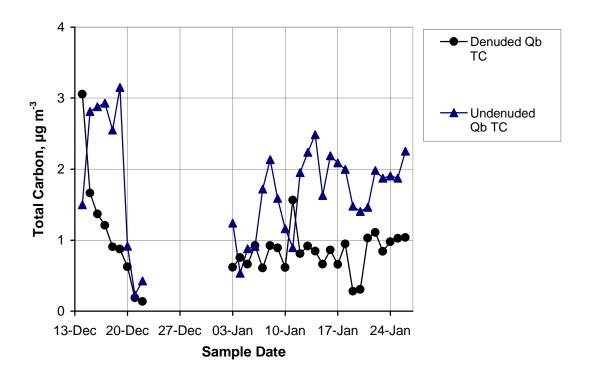
Figure 76C Total carbon: denuded (DEN) vs. undenuded (UND) Harvard Carbon Sampler back quartz filter  $(Q_b)$  at Chicago.



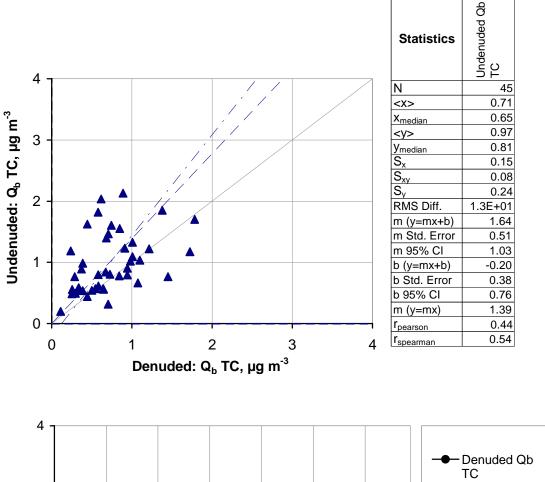


 $\begin{tabular}{ll} \textbf{Figure 76D} & Total \ carbon: denuded (DEN) \ vs. \ undenuded (UND) \ Harvard \ Carbon \\ & Sampler \ back \ quartz \ filter \ (Q_b) \ at \ Dallas. \end{tabular}$ 





 $\label{eq:Figure 76D} \begin{array}{ll} \textbf{Figure 76D} & \textbf{Total carbon: denuded (DEN) vs. undenuded (UND) Harvard Carbon} \\ & \textbf{Sampler back quartz filter } (Q_b) \text{ at Phoenix.} \end{array}$ 



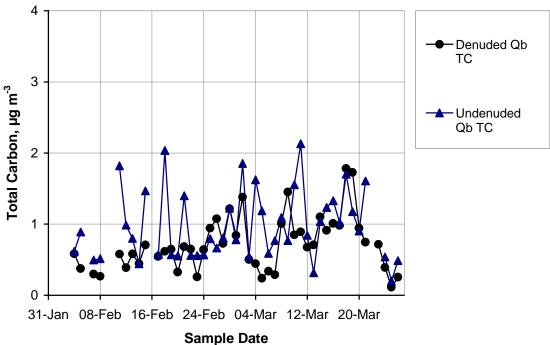
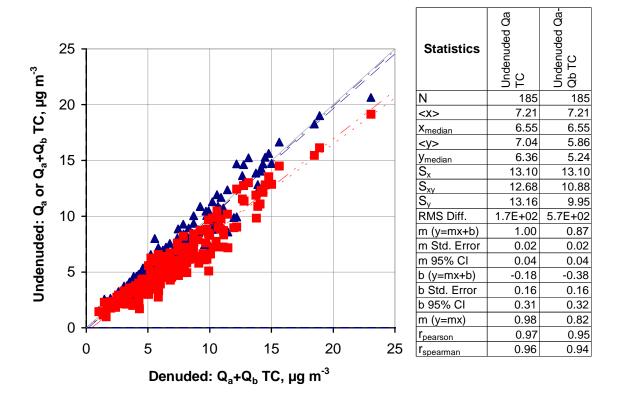
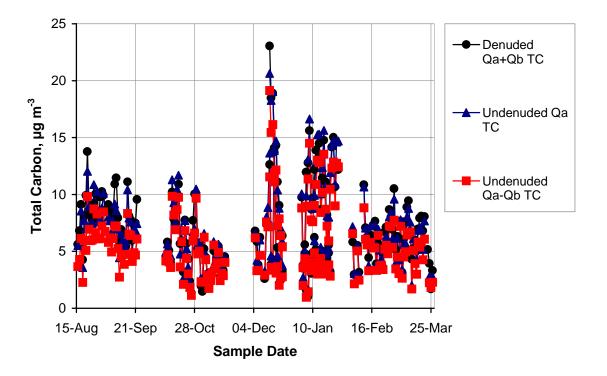
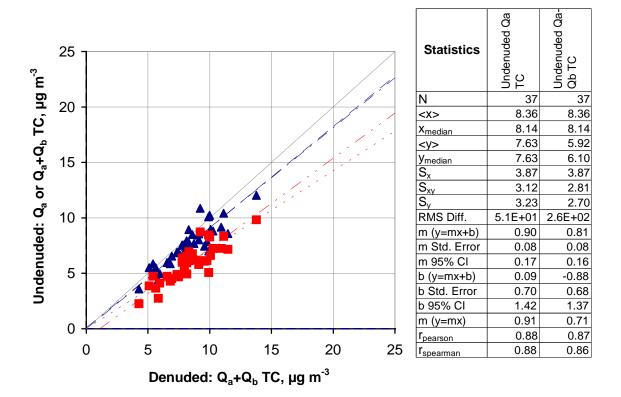


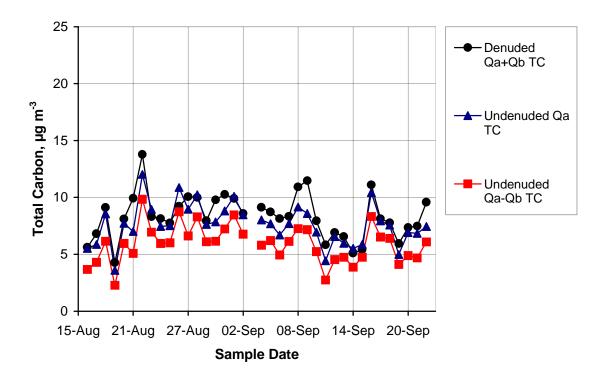
Figure 76B Total carbon: denuded (DEN) vs. undenuded (UND) Harvard Carbon Sampler back quartz filter  $(Q_b)$  at Bakersfield.



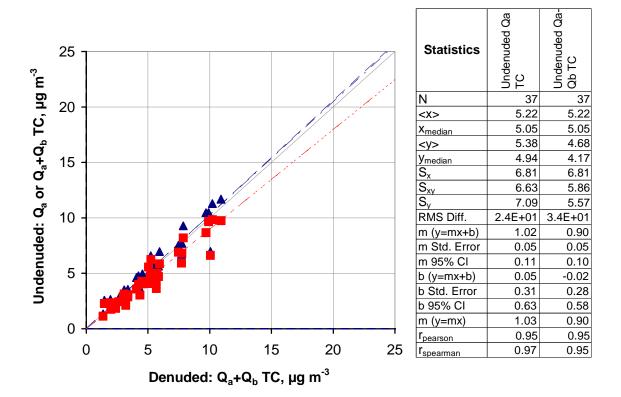


**Figure 77A** Total carbon: Harvard Carbon Sampler undenuded (UND) front filter  $(Q_a)$  and front – back filter  $(Q_a - Q_b)$  vs. denuded (DEN) front + back  $(Q_a + Q_b)$  at all sites.





**Figure 77R** Total carbon: Harvard Carbon Sampler undenuded (UND) front filter  $(Q_a)$  and front – back filter  $(Q_a - Q_b)$  vs. denuded (DEN) front + back  $(Q_a + Q_b)$  at Riverside.



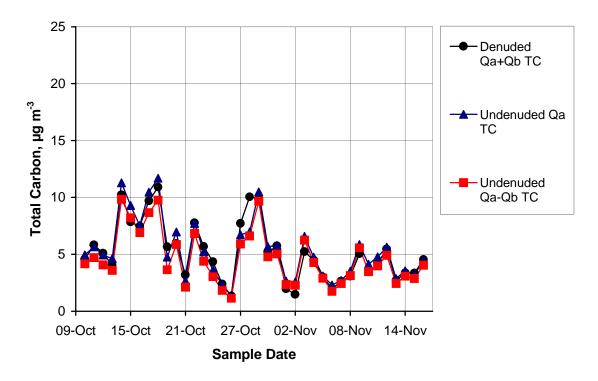
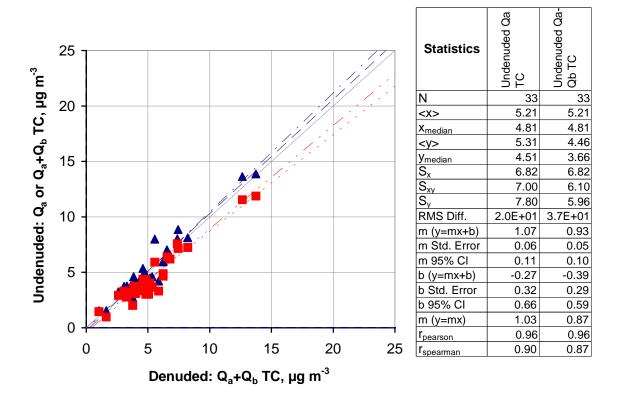
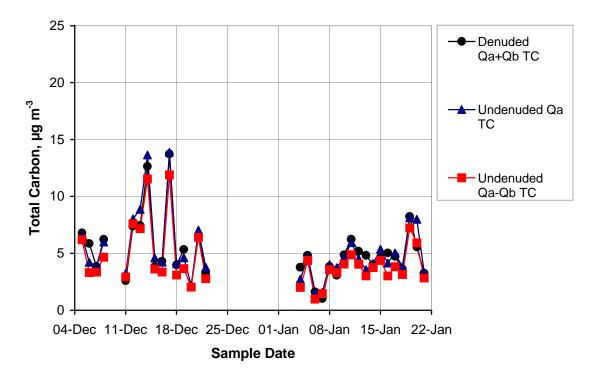
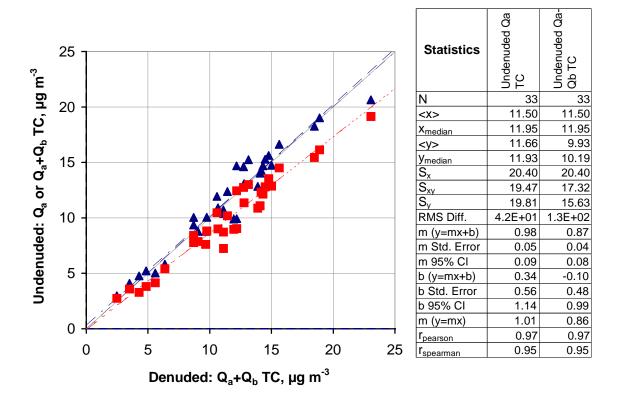


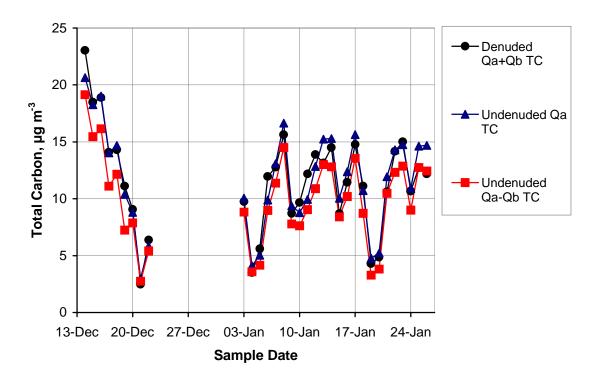
Figure 77C Total carbon: Harvard Carbon Sampler undenuded (UND) front filter  $(Q_a)$  and front – back filter  $(Q_a - Q_b)$  vs. denuded (DEN) front + back  $(Q_a + Q_b)$  at Chicago.



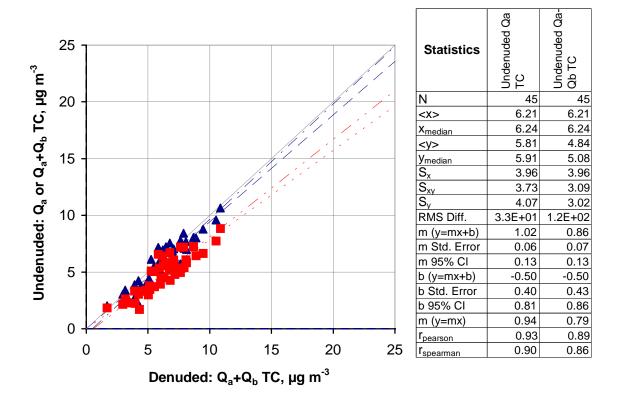


**Figure 77D** Total carbon: Harvard Carbon Sampler undenuded (UND) front filter  $(Q_a)$  and front – back filter  $(Q_a - Q_b)$  vs. denuded (DEN) front + back  $(Q_a + Q_b)$  at Dallas.





**Figure 77D** Total carbon: Harvard Carbon Sampler undenuded (UND) front filter  $(Q_a)$  and front – back filter  $(Q_a - Q_b)$  vs. denuded (DEN) front + back  $(Q_a + Q_b)$  at Phoenix.



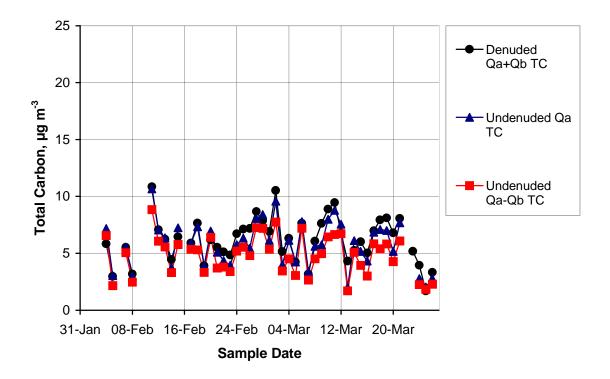
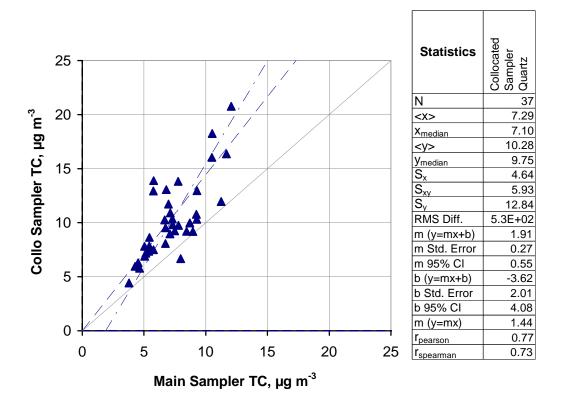


Figure 77B Total carbon: Harvard Carbon Sampler undenuded (UND) front filter  $(Q_a)$  and front – back filter  $(Q_a - Q_b)$  vs. denuded (DEN) front + back  $(Q_a + Q_b)$  at Bakersfield.



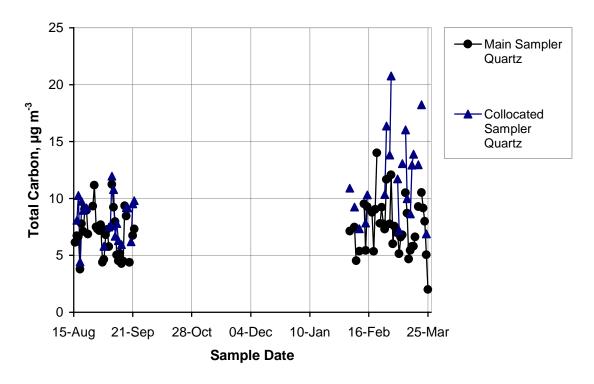
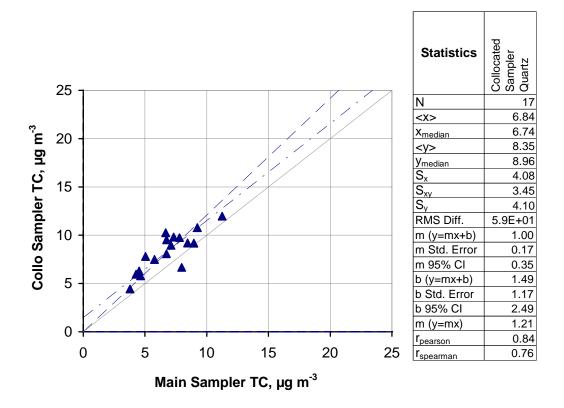


Figure 78A Total carbon: collocated Big BOSS quartz + Empore filters at all sites.



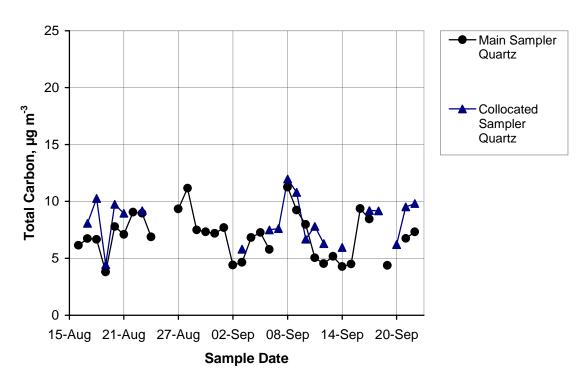
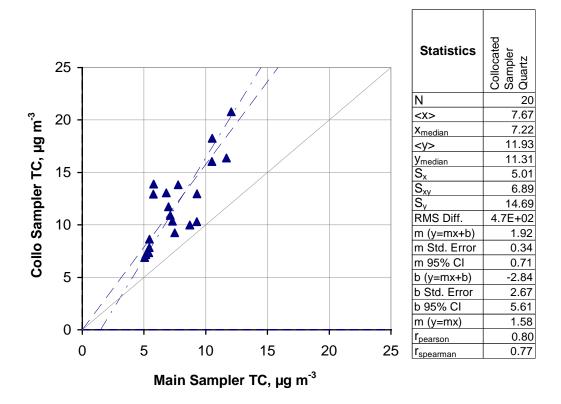


Figure 78R Total carbon: collocated Big BOSS quartz + Empore filters at Riverside.



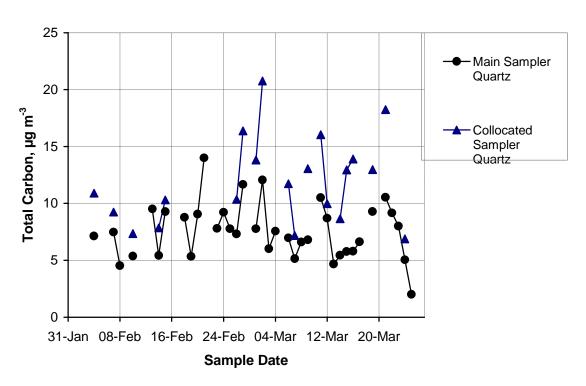
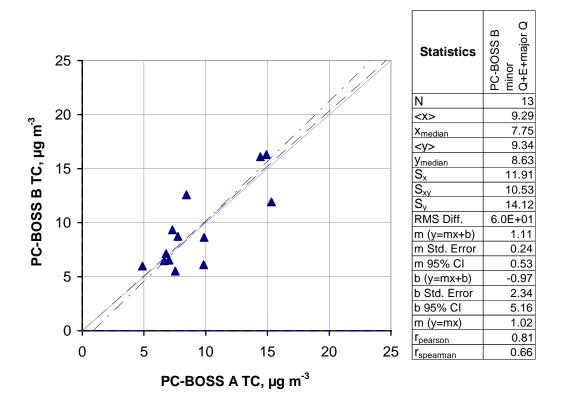
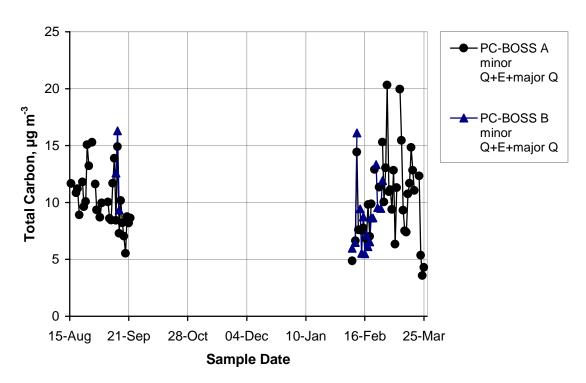
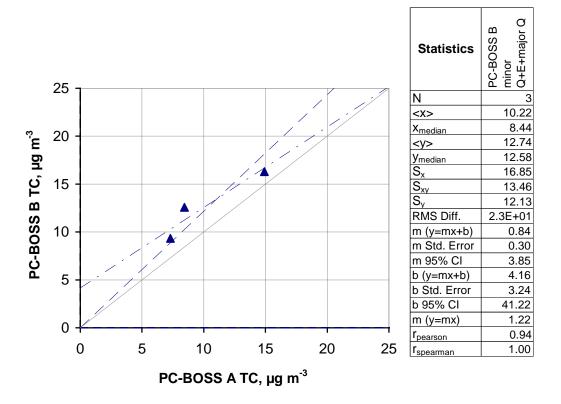


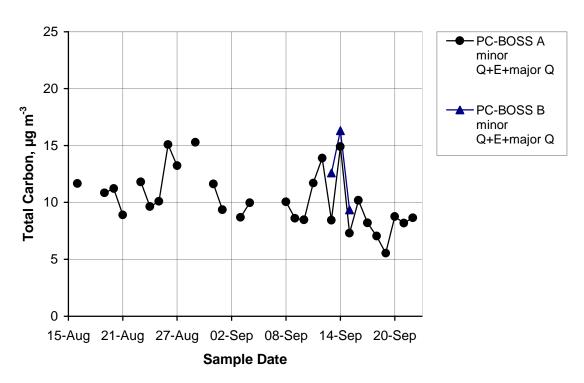
Figure 78B Total carbon: collocated Big BOSS quartz + Empore filters at Bakersfield.



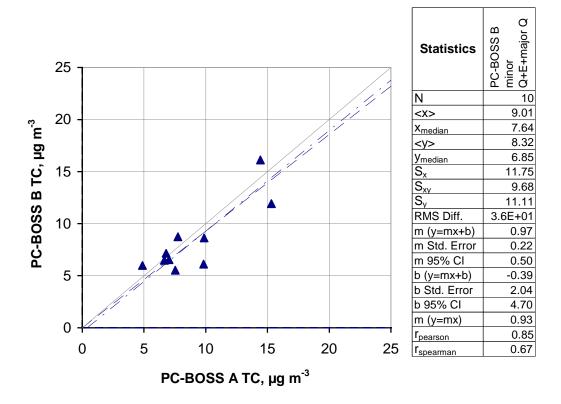


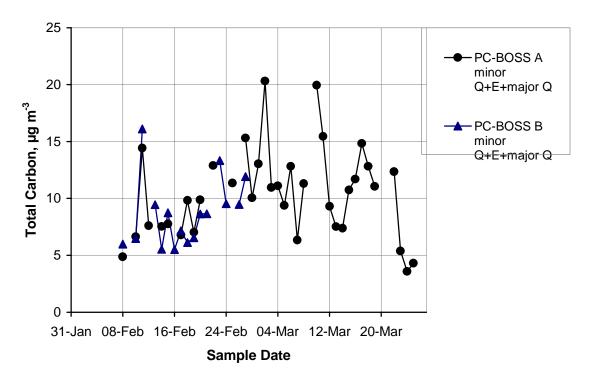
**Figure 79A** Total carbon: collocated PC-BOSS minor flow quartz + Empore + major flow quartz filters at all sites.



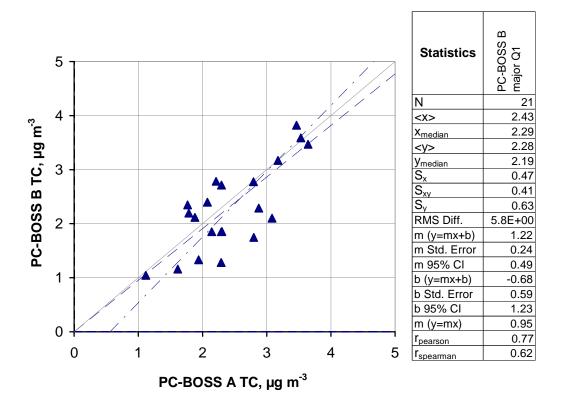


**Figure 79R** Total carbon: collocated PC-BOSS minor flow quartz + Empore + major flow quartz filters at Riverside.





**Figure 79B** Total carbon: collocated PC-BOSS minor flow quartz + Empore + major flow quartz filters at Bakersfield.



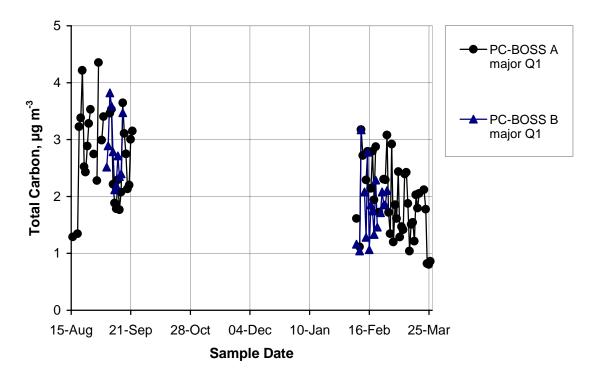
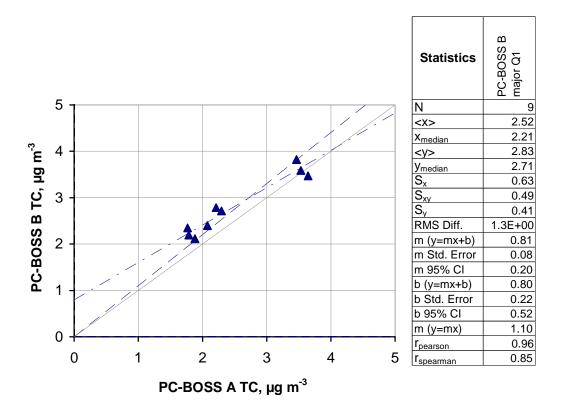


Figure 80A Total carbon: collocated PC-BOSS major flow quartz filters at all sites.



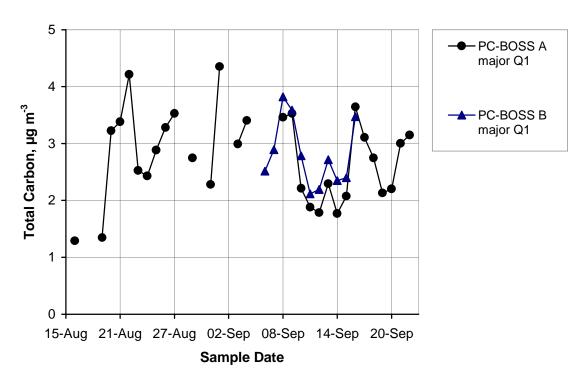
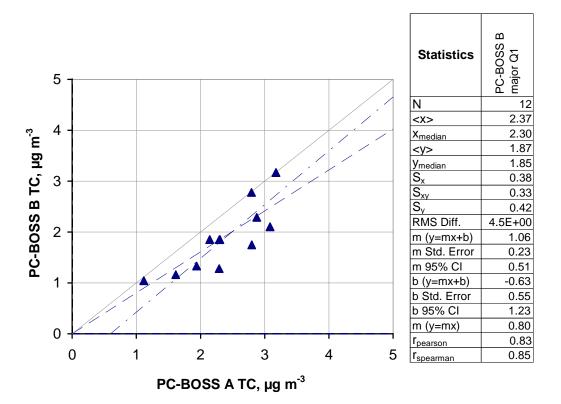
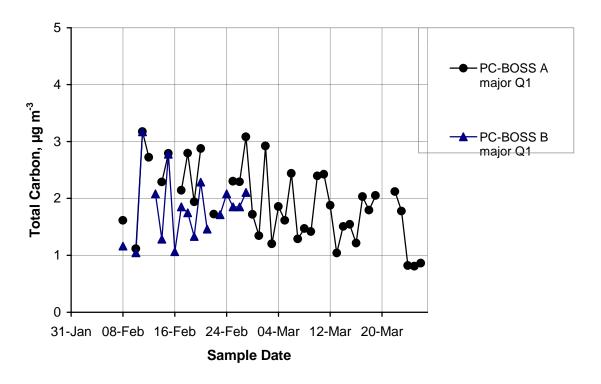
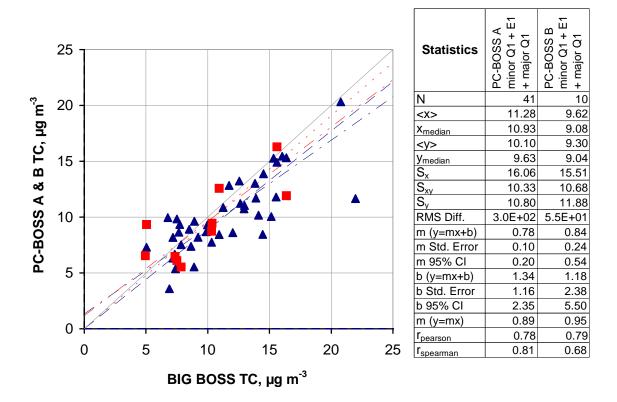


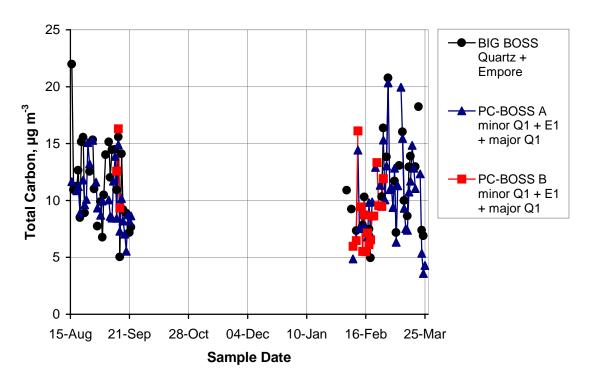
Figure 80R Total carbon: collocated PC-BOSS major flow quartz filters at Riverside.



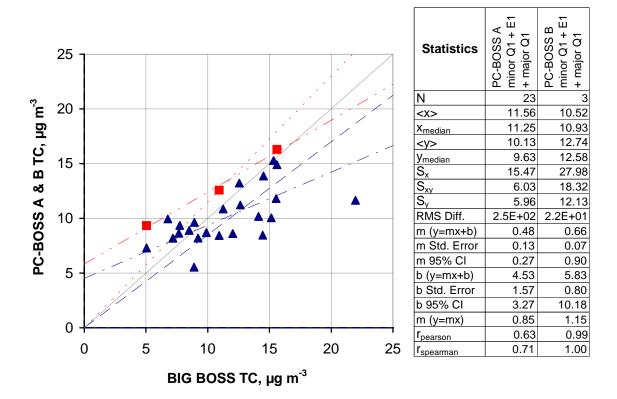


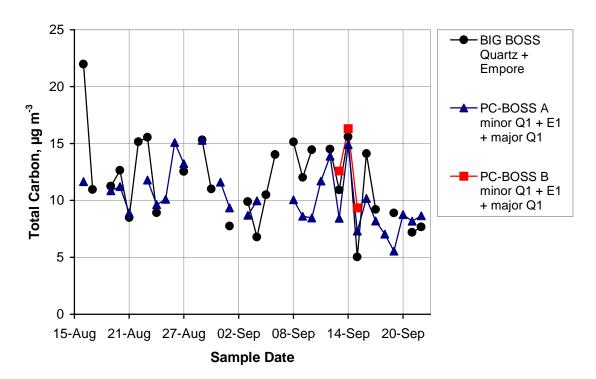
**Figure 80B** Total carbon: collocated PC-BOSS major flow quartz filters at Bakersfield.



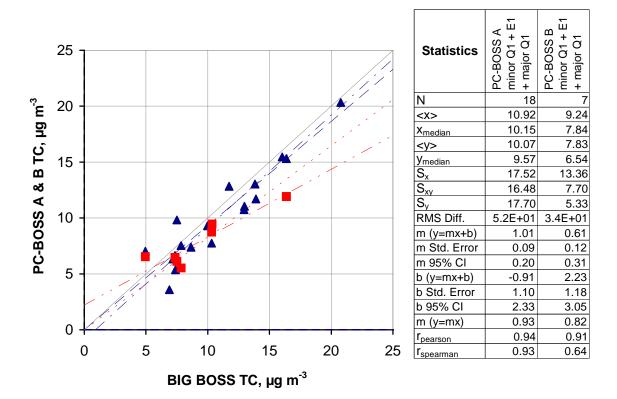


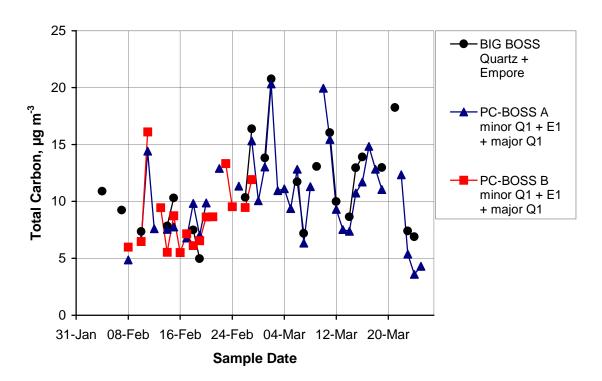
**Figure 81A** Total carbon: Big BOSS quartz + Empore filters vs. PC-BOSS A minor quartz + Empore + major flow quartz filters at all sites.



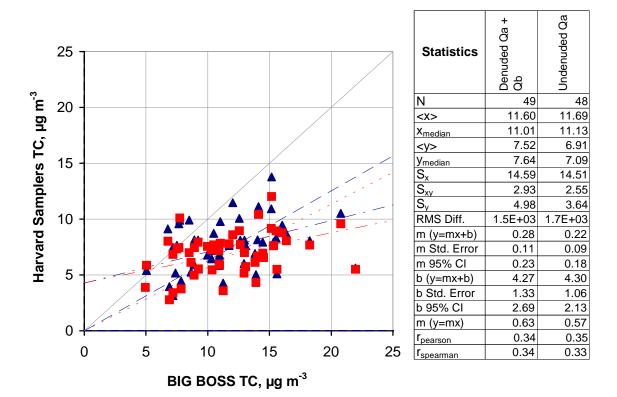


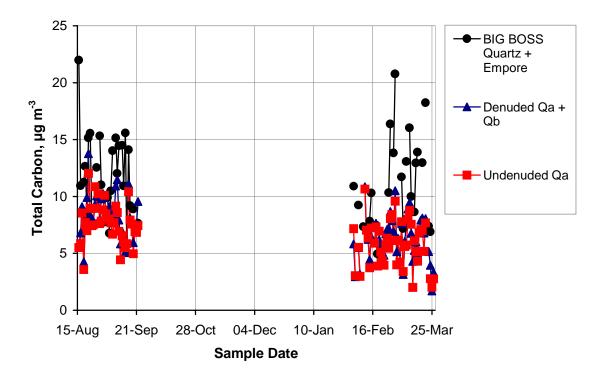
**Figure 81R** Total carbon: Big BOSS quartz + Empore filters vs. PC-BOSS A minor quartz + Empore + major flow quartz filters at Riverside.



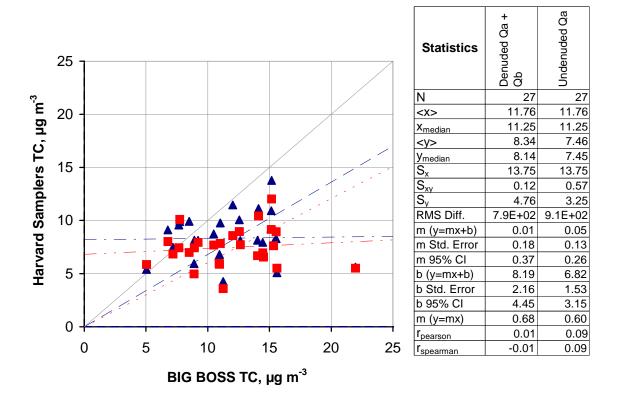


**Figure 81B** Total carbon: Big BOSS quartz + Empore filters vs. PC-BOSS A minor quartz + Empore + major flow quartz filters at Bakersfield.





 $\label{eq:Figure 82A} \begin{array}{ll} \textbf{Figure 82A} & \textbf{Total carbon: Harvard Carbon Sampler denuded (DEN) front + back} \\ & \textbf{quartz filters } (Q_a + Q_b) \ \text{and undenuded (UND) front filter } (Q_a) \ \text{vs. Big} \\ & \textbf{BOSS quartz} + \textbf{Empore filters at all sites.} \end{array}$ 



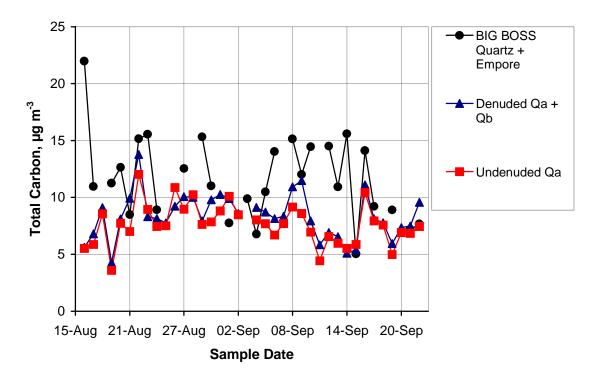
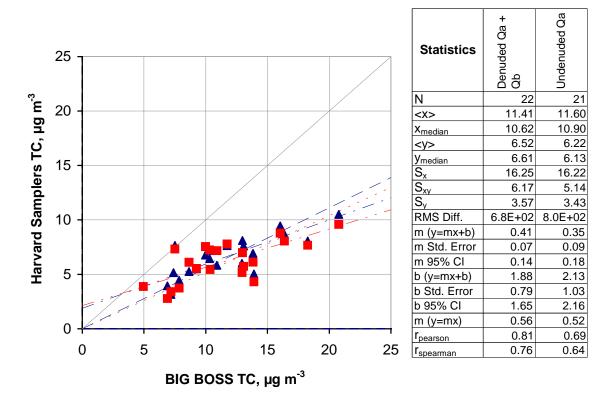
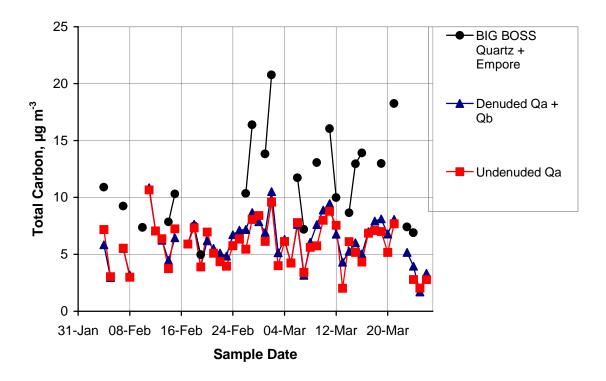
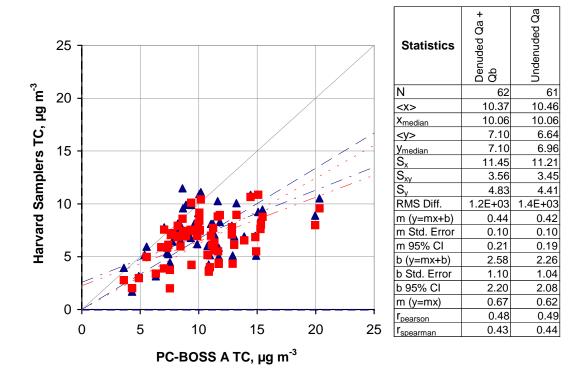


Figure 82R Total carbon: Harvard Carbon Sampler denuded (DEN) front + back quartz filters  $(Q_a + Q_b)$  and undenuded (UND) front filter  $(Q_a)$  vs. Big BOSS quartz + Empore filters at Riverside.





 $\label{eq:Figure 82B} \begin{array}{ll} \textbf{Figure 82B} & \textbf{Total carbon: Harvard Carbon Sampler denuded (DEN) front + back} \\ & \textbf{quartz filters } (Q_a + Q_b) \ \text{and undenuded (UND) front filter } (Q_a) \ \text{vs. Big} \\ & \textbf{BOSS quartz} + \textbf{Empore filters at Bakersfield.} \end{array}$ 



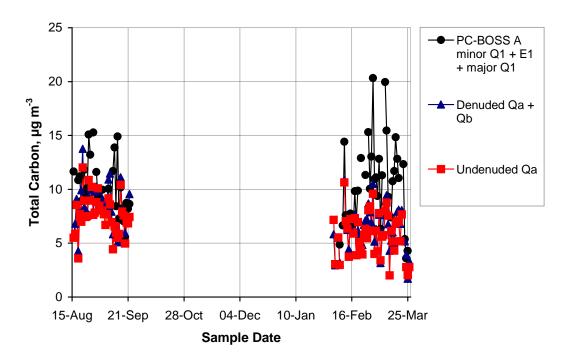
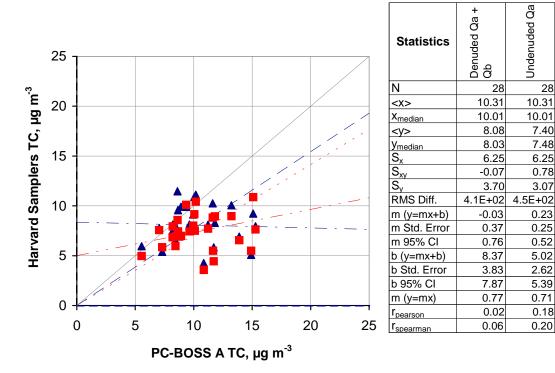


Figure 83A Total carbon: Harvard Carbon Sampler denuded (DEN) front + back quartz filters  $(Q_a + Q_b)$  and undenuded (UND) front filter  $(Q_a)$  vs. PC-BOSS A minor flow quartz + Empore + major flow quartz filters at all sites.



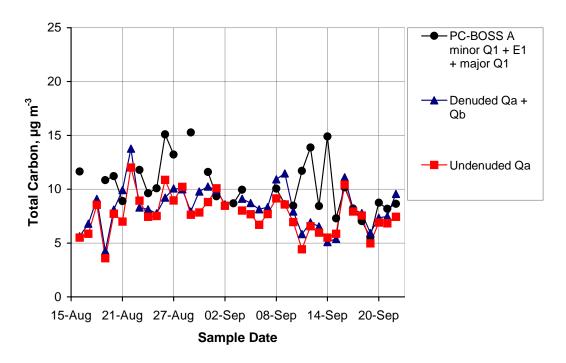
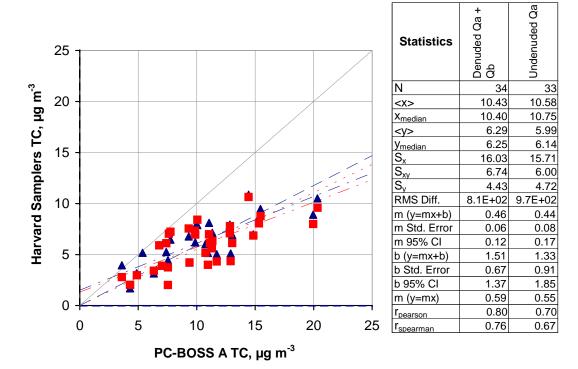
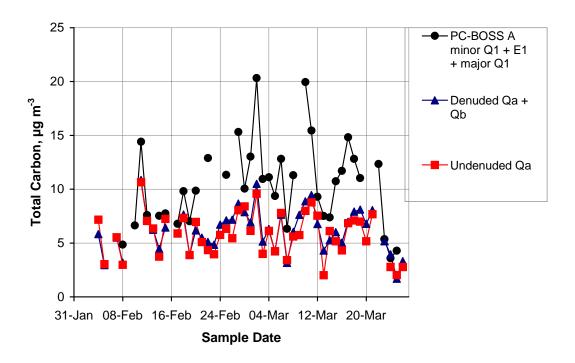
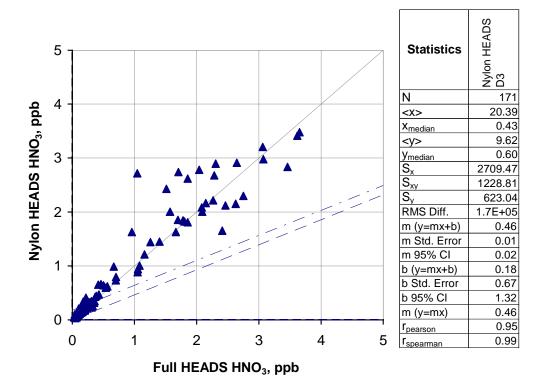


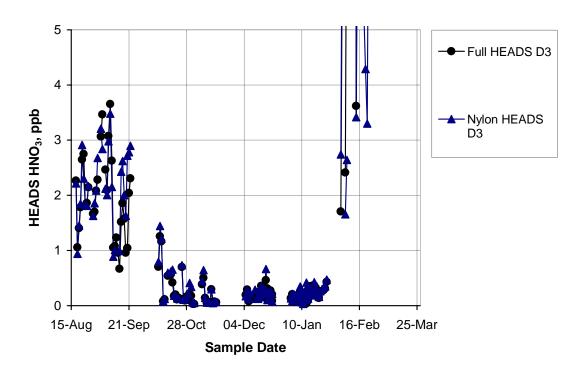
Figure 83R Total carbon: Harvard Carbon Sampler denuded (DEN) front + back quartz filters  $(Q_a + Q_b)$  and undenuded (UND) front filter  $(Q_a)$  vs. PC-BOSS A minor flow quartz + Empore + major flow quartz filters at Riverside.



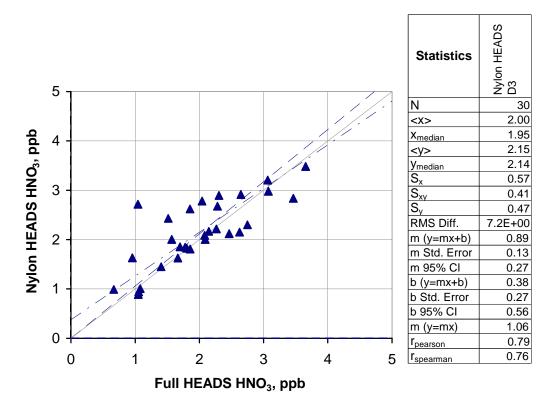


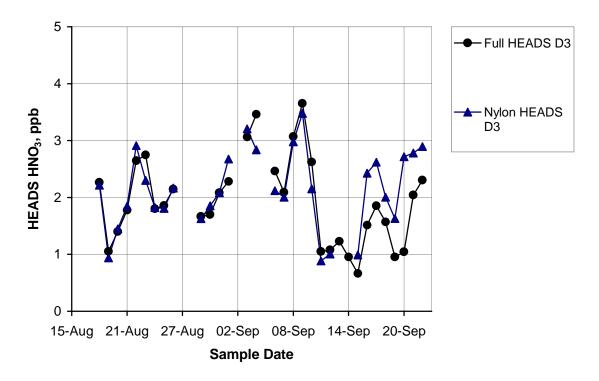
 $\label{eq:Figure 83B} \begin{array}{ll} \textbf{Total carbon: Harvard Carbon Sampler denuded (DEN) front + back} \\ \textbf{quartz filters } (Q_a + Q_b) \ and \ undenuded \ (UND) \ front \ filter \ (Q_a) \ vs. \ PC-BOSS \ A \ minor \ flow \ quartz + Empore + major \ flow \ quartz \ filters \ at \\ \textbf{Bakersfield.} \end{array}$ 



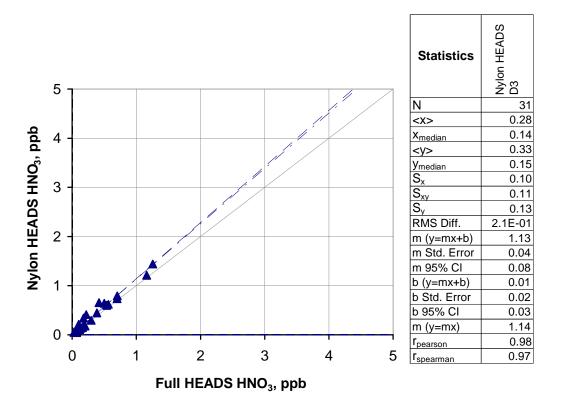


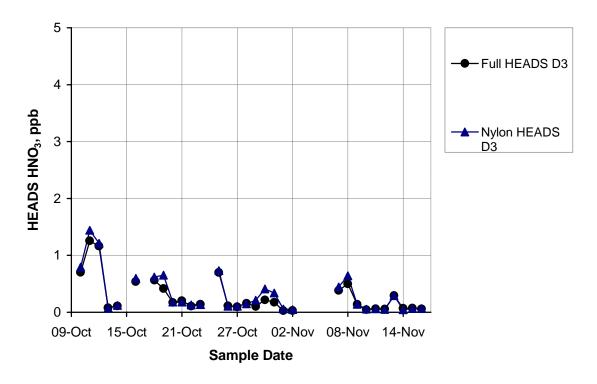
**Figure 84A** Gas-phase nitric acid: Full HEADS sodium carbonate denuder (D1) vs. Nylon HEADS D1 at all sites. For Bakersfield data (off scale here), see Figure 84B.



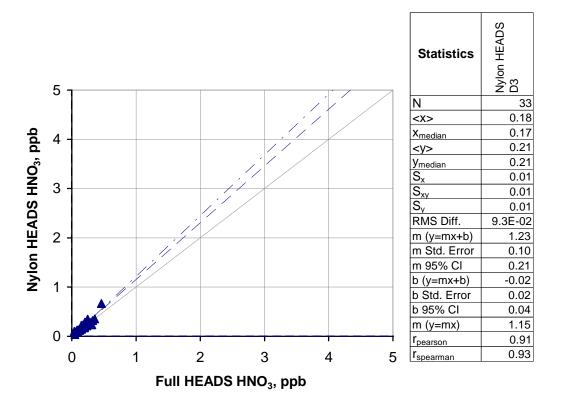


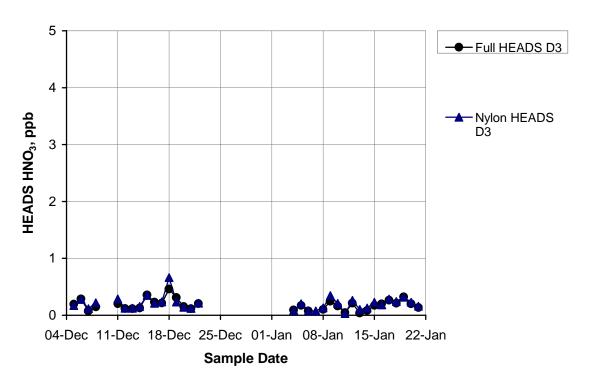
**Figure 84R** Gas-phase nitric acid: Full HEADS sodium carbonate denuder (D1) vs. Nylon HEADS D1 at Riverside.



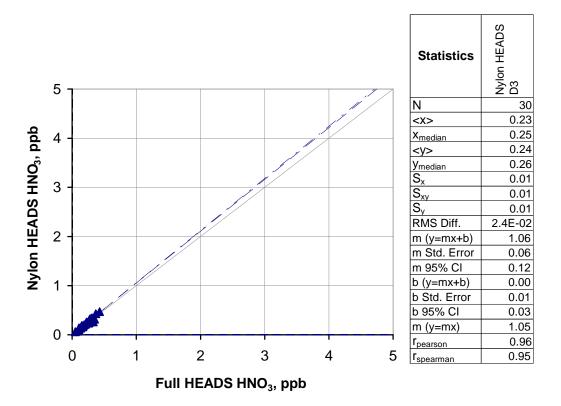


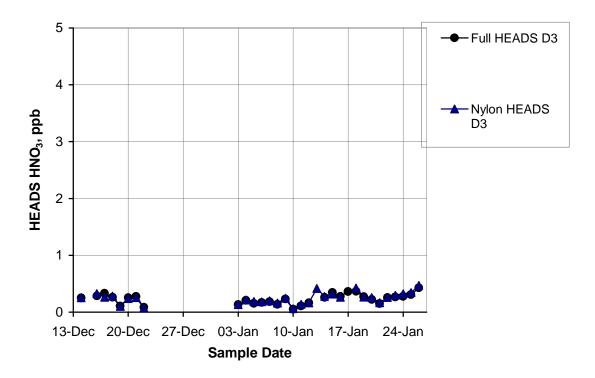
**Figure 84C** Gas-phase nitric acid: Full HEADS sodium carbonate denuder (D1) vs. Nylon HEADS D1 at Chicago.



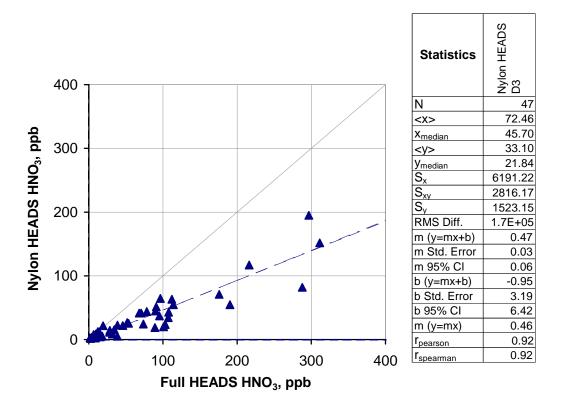


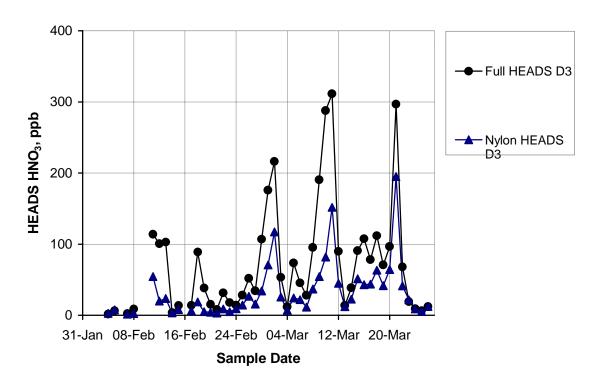
**Figure 84D** Gas-phase nitric acid: Full HEADS sodium carbonate denuder (D1) vs. Nylon HEADS D1 at Dallas.



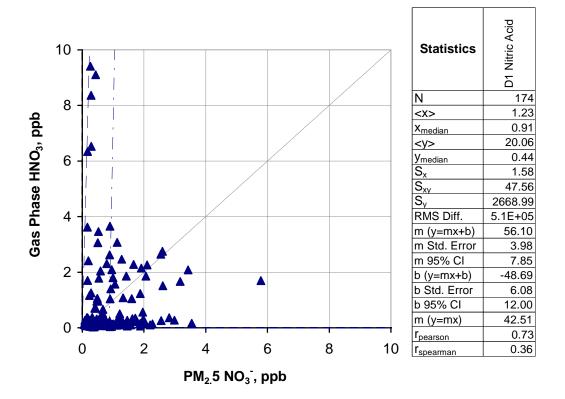


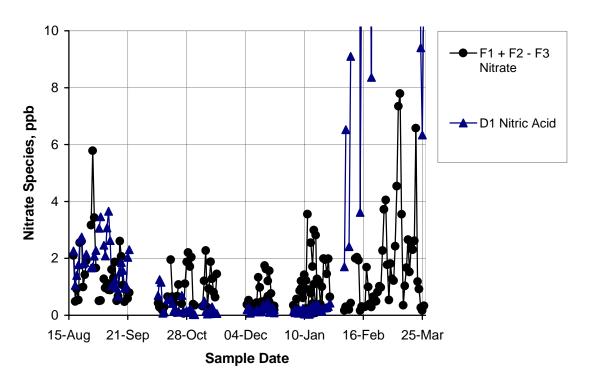
**Figure 84P** Gas-phase nitric acid: Full HEADS sodium carbonate denuder (D1) vs. Nylon HEADS D1 at Phoenix.



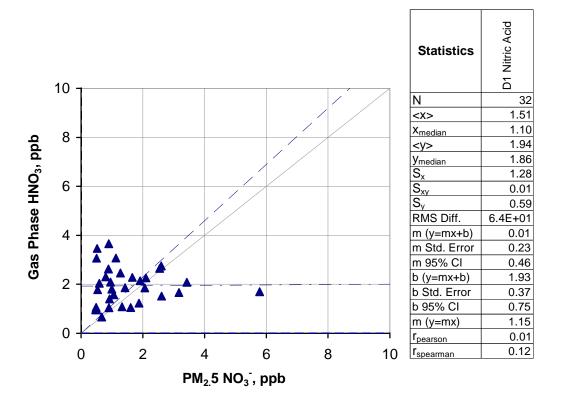


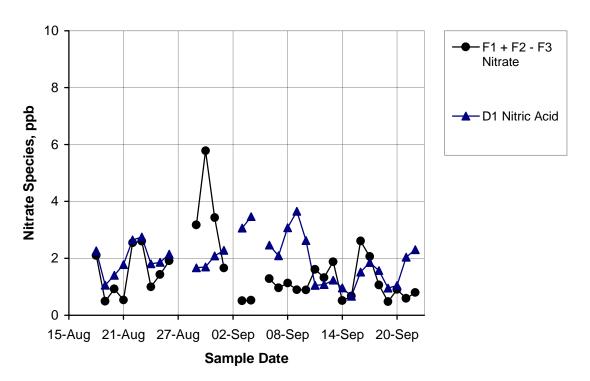
**Figure 84B** Gas-phase nitric acid: Full HEADS sodium carbonate denuder (D1) vs. Nylon HEADS D1 at Bakersfield.



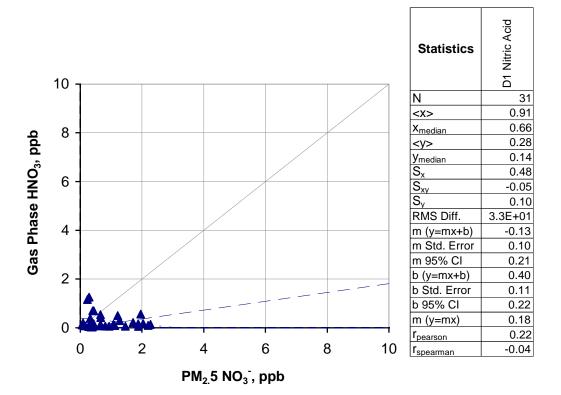


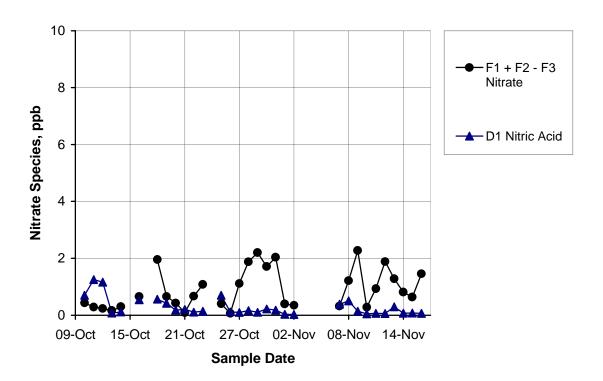
**Figure 85A** Nitrate gas-particle distribution: Full HEADS gas-phase nitric acid (D1) vs. filter nitrate (F1 + F2 - F3) at all sites.



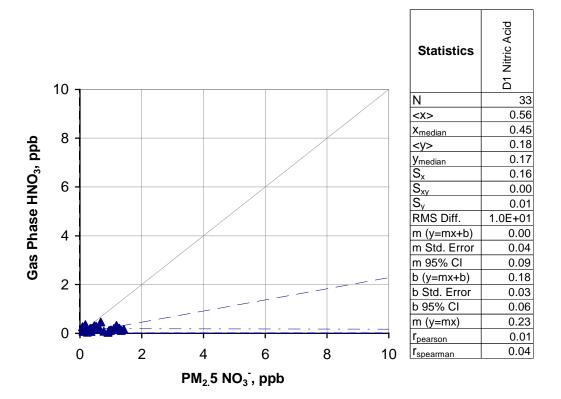


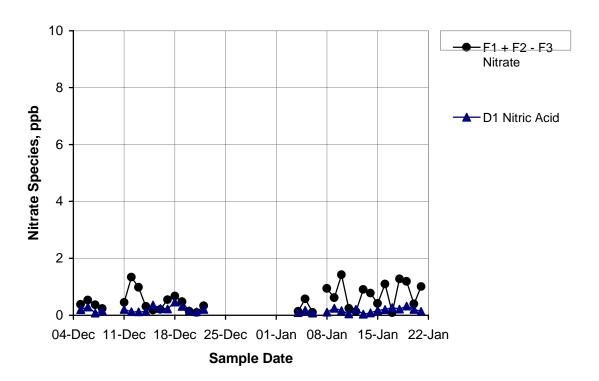
**Figure 85R** Nitrate gas-particle distribution: Full HEADS gas-phase nitric acid (D1) vs. filter nitrate (F1 + F2 - F3) at Riverside.



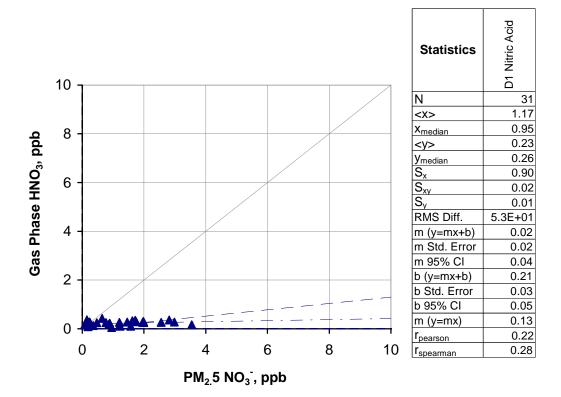


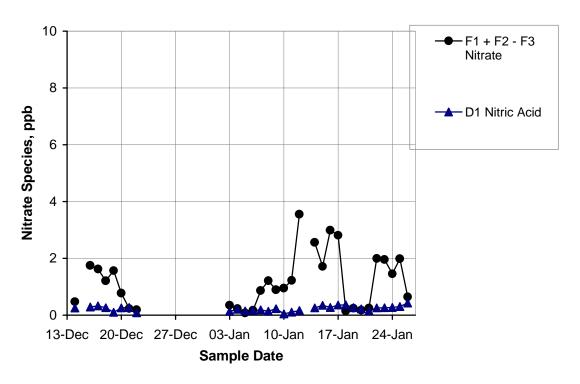
**Figure 85C** Nitrate gas-particle distribution: Full HEADS gas-phase nitric acid (D1) vs. filter nitrate (F1 + F2 - F3) at Chicago.



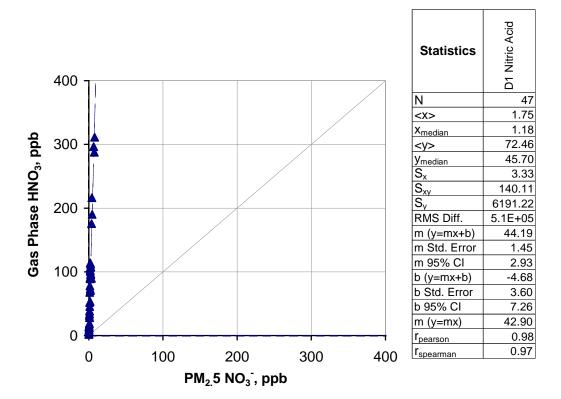


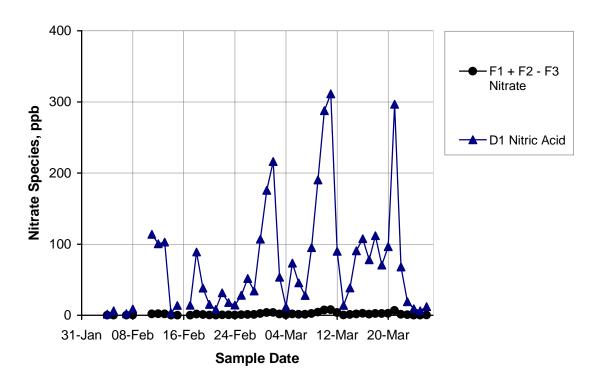
**Figure 85D** Nitrate gas-particle distribution: Full HEADS gas-phase nitric acid (D1) vs. filter nitrate (F1 + F2 - F3) at Dallas.



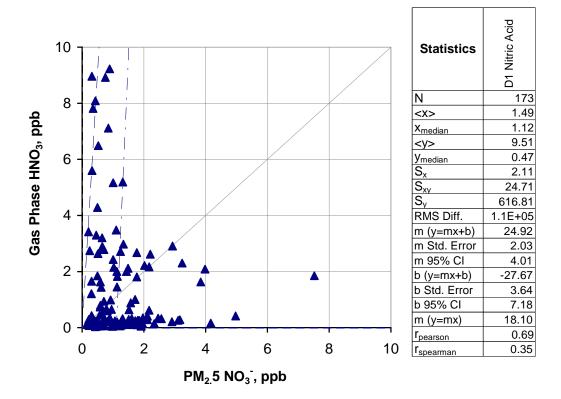


**Figure 85P** Nitrate gas-particle distribution: Full HEADS gas-phase nitric acid (D1) vs. filter nitrate (F1 + F2 - F3) at Phoenix.





**Figure 85B** Nitrate gas-particle distribution: Full HEADS gas-phase nitric acid (D1) vs. filter nitrate (F1 + F2 - F3) at Bakersfield.



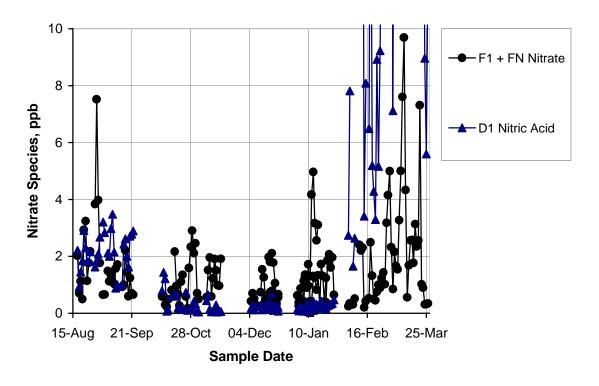
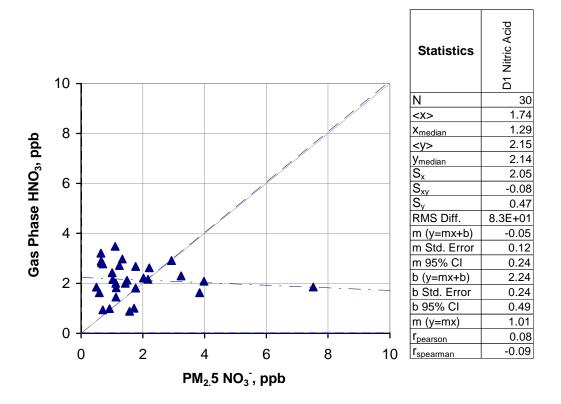
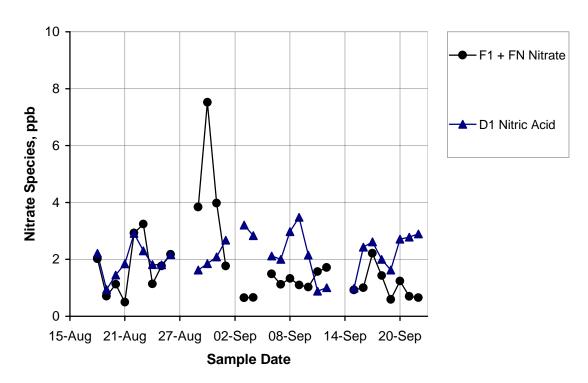
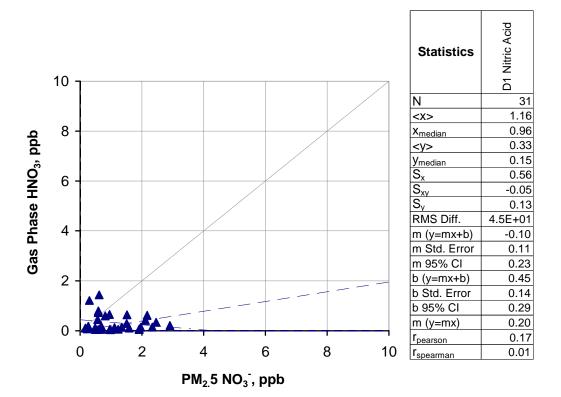


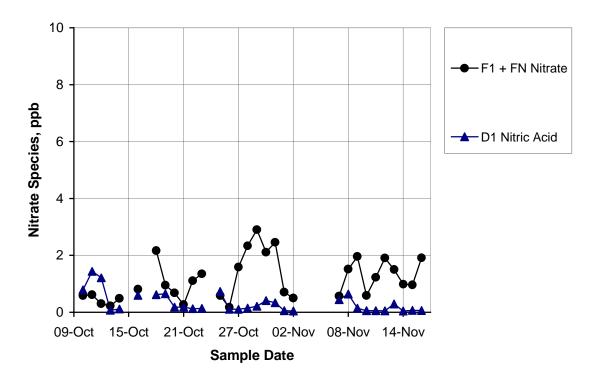
Figure 86A Nitrate gas-particle distribution: Nylon HEADS gas-phase nitric acid (D1) vs. filter nitrate (F1 + FN) at all sites.



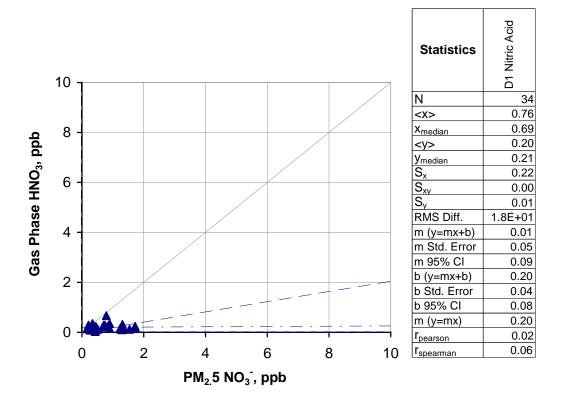


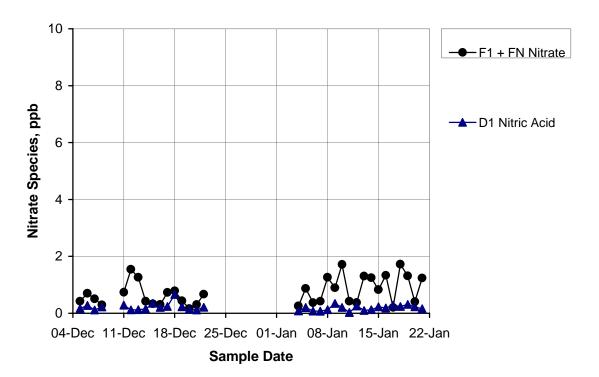
**Figure 86R** Nitrate gas-particle distribution: Nylon HEADS gas-phase nitric acid (D1) vs. filter nitrate (F1 + FN) at Riverside.



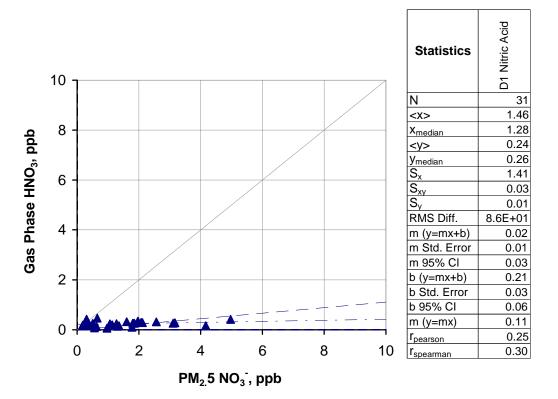


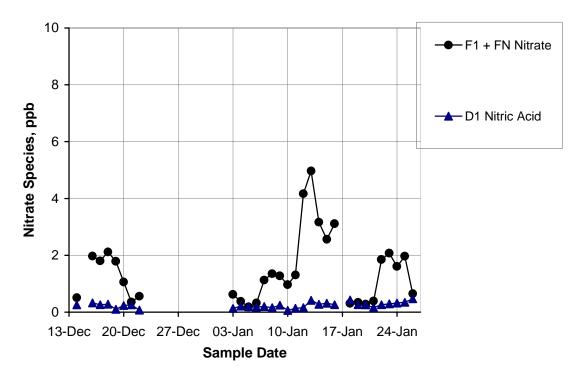
**Figure 86C** Nitrate gas-particle distribution: Nylon HEADS gas-phase nitric acid (D1) vs. filter nitrate (F1 + FN) at Chicago.



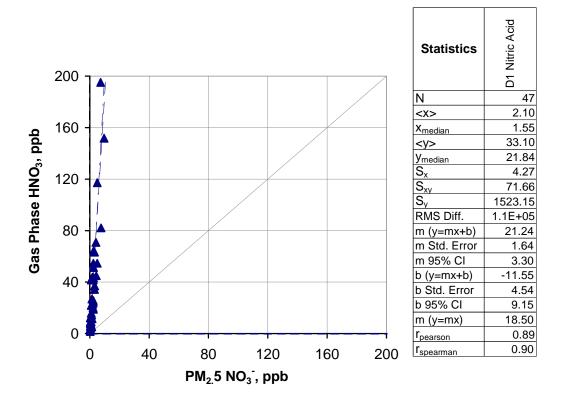


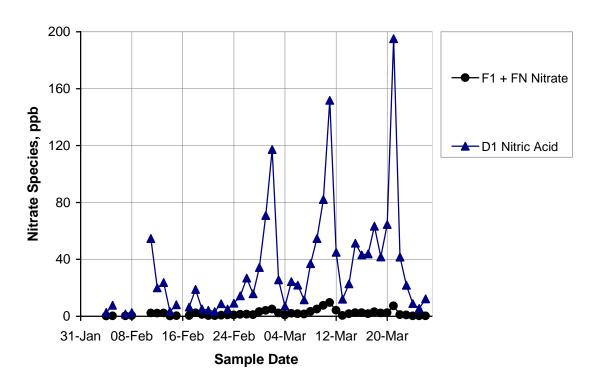
**Figure 86D** Nitrate gas-particle distribution: Nylon HEADS gas-phase nitric acid (D1) vs. filter nitrate (F1 + FN) at Dallas.



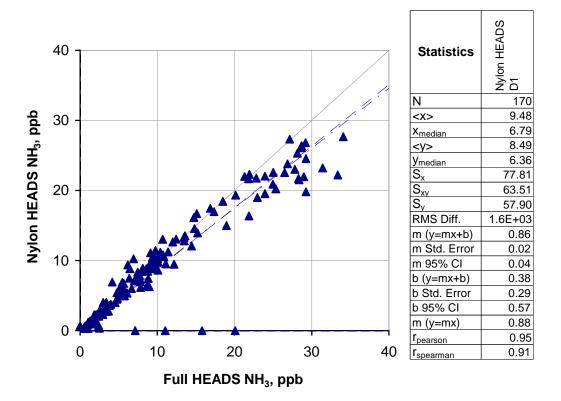


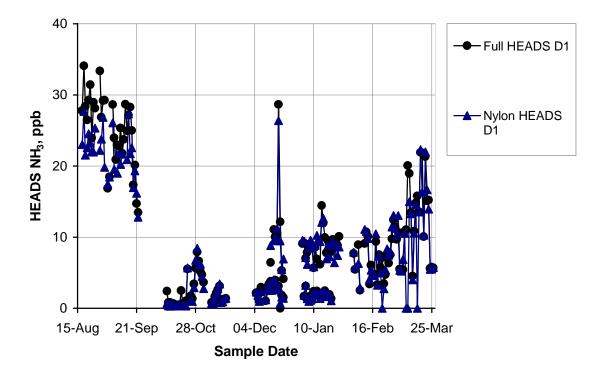
**Figure 86P** Nitrate gas-particle distribution: Nylon HEADS gas-phase nitric acid (D1) vs. filter nitrate (F1 + FN) at Phoenix.



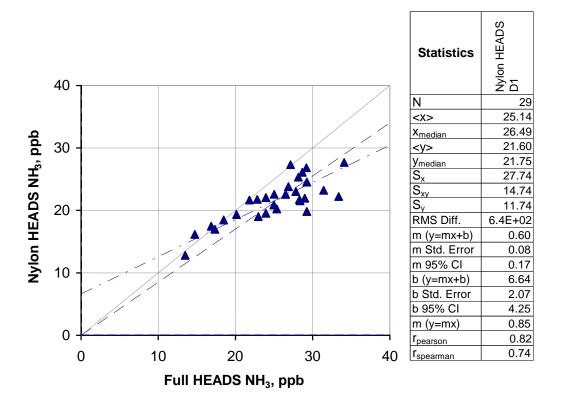


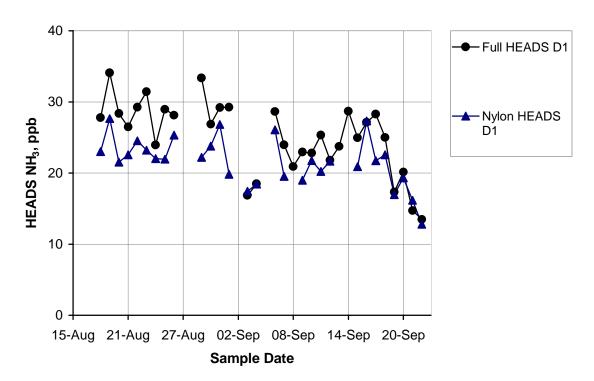
**Figure 86B** Nitrate gas-particle distribution: Nylon HEADS gas-phase nitric acid (D1) vs. filter nitrate (F1 + FN) at Bakersfield.



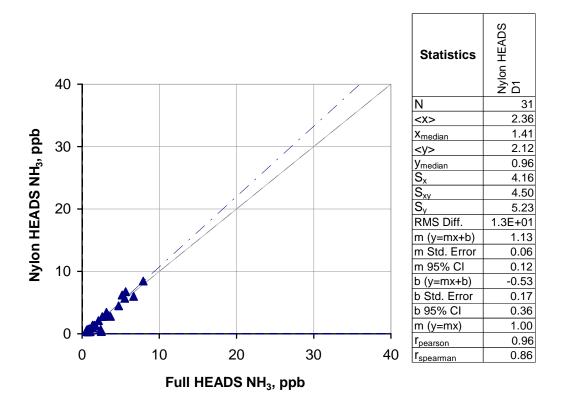


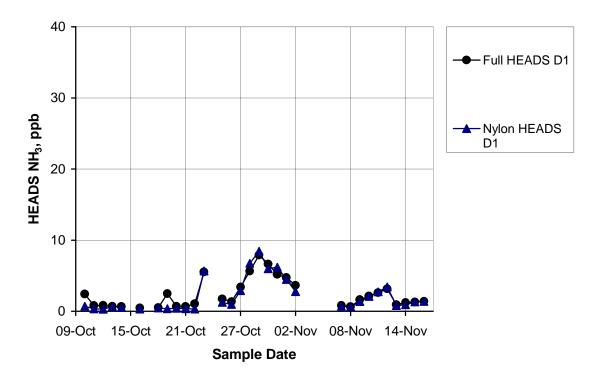
**Figure 87A** Gas-phase ammonia: Full HEADS citric acid denuder (D3) vs. Nylon HEADS D3 at all sites.



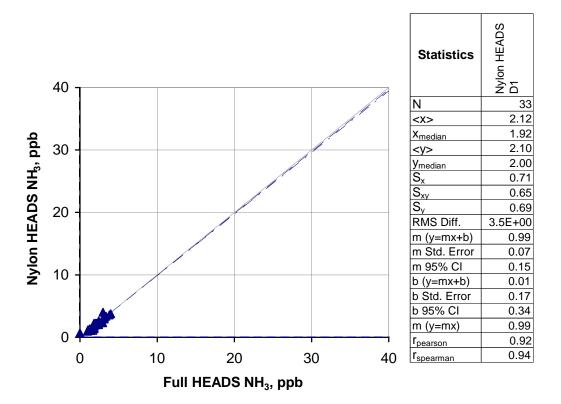


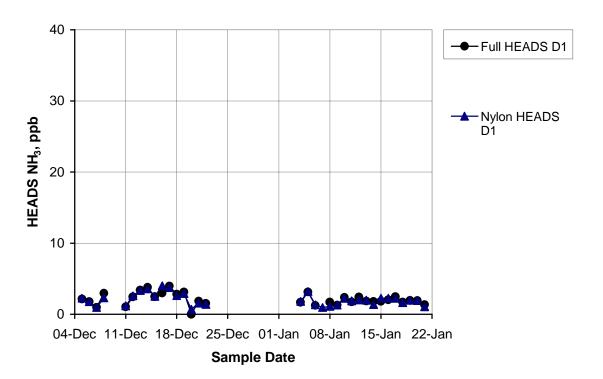
**Figure 87R** Gas-phase ammonia: Full HEADS citric acid denuder (D3) vs. Nylon HEADS D3 at Riverside.



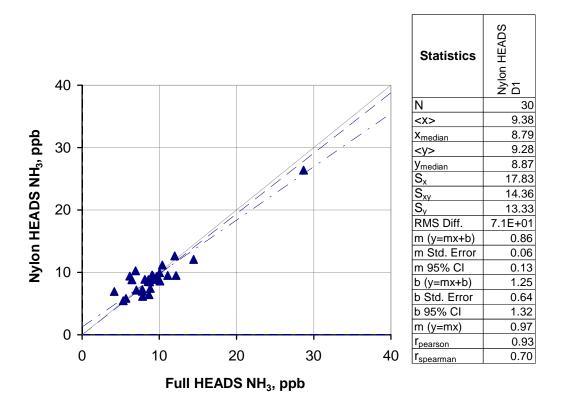


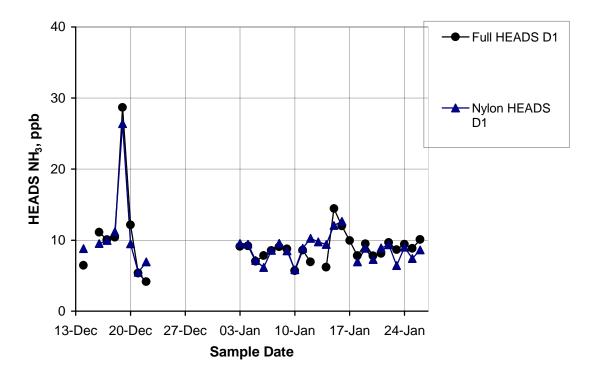
**Figure 87C** Gas-phase ammonia: Full HEADS citric acid denuder (D3) vs. Nylon HEADS D3 at Chicago.



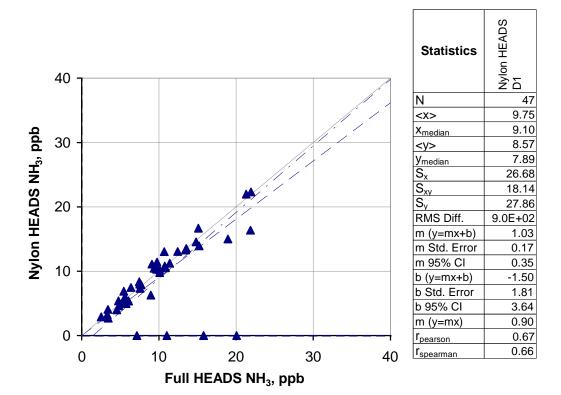


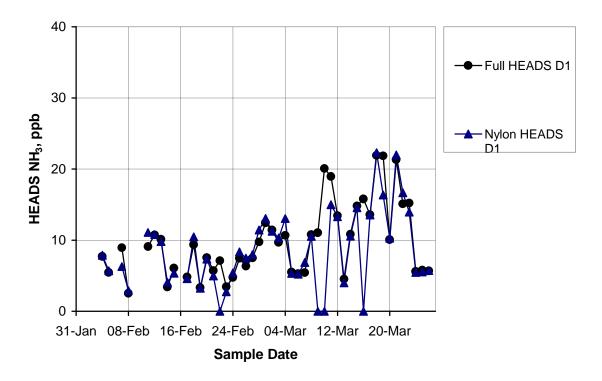
**Figure 87D** Gas-phase ammonia: Full HEADS citric acid denuder (D3) vs. Nylon HEADS D3 at Dallas.



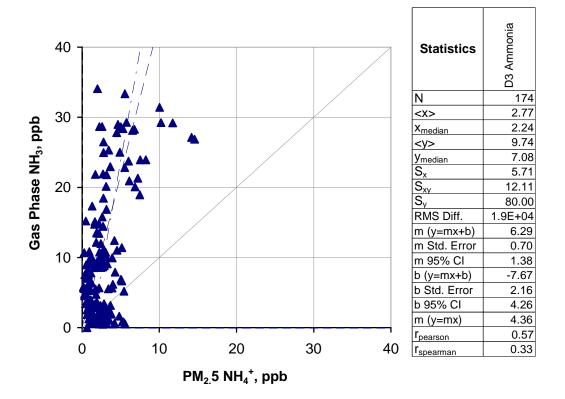


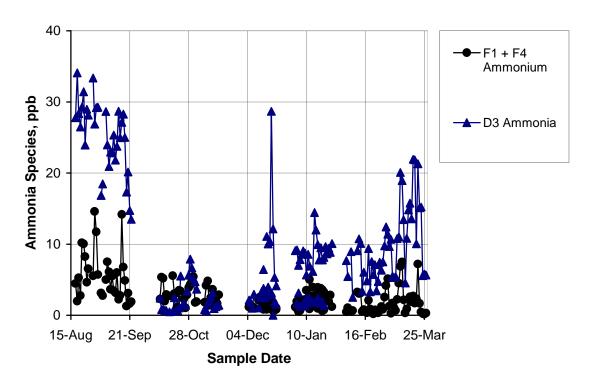
**Figure 87P** Gas-phase ammonia: Full HEADS citric acid denuder (D3) vs. Nylon HEADS D3 at Phoenix.



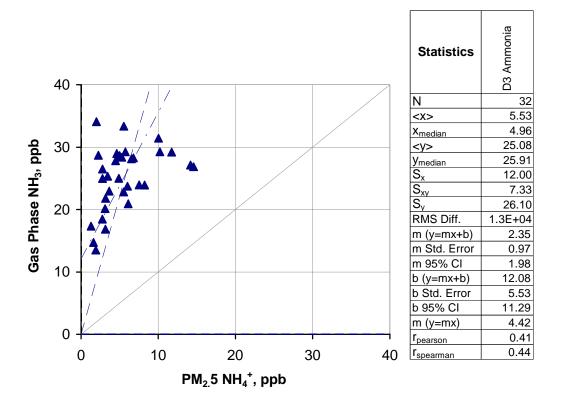


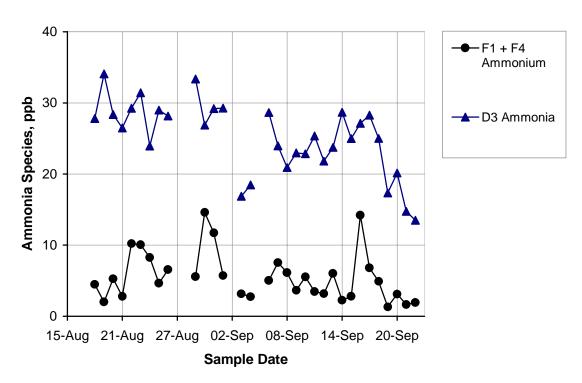
**Figure 87B** Gas-phase ammonia: Full HEADS citric acid denuder (D3) vs. Nylon HEADS D3 at Bakersfield.



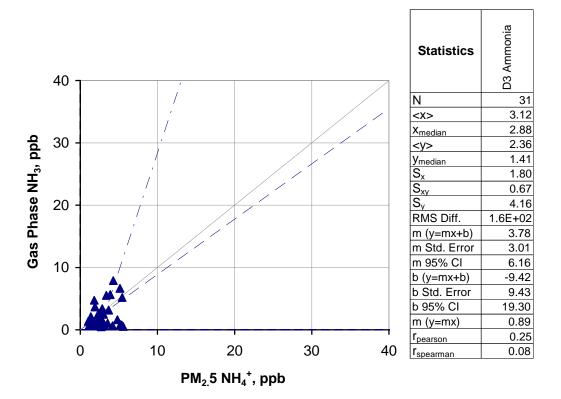


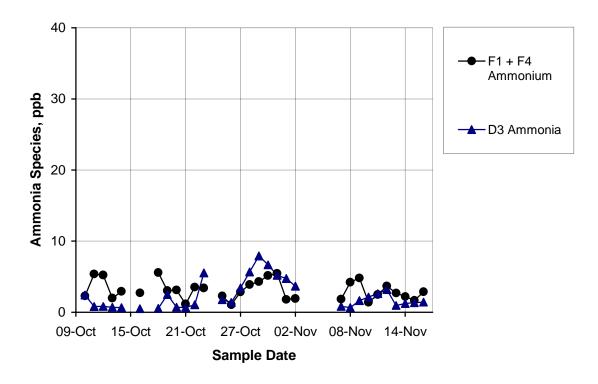
**Figure 88A** Ammonia gas-particle distribution: Full HEADS gas-phase ammonia (D3) vs. filter ammonium (F1 + F4) at all sites.



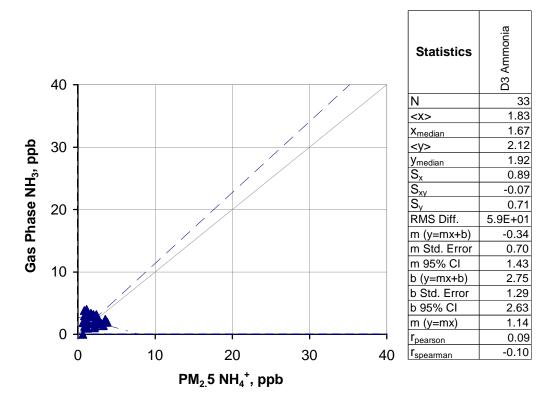


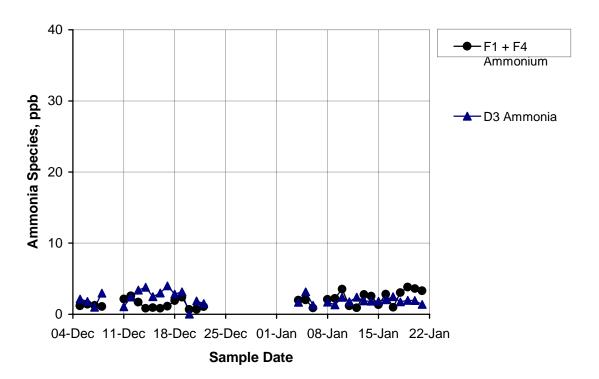
**Figure 88R** Ammonia gas-particle distribution: Full HEADS gas-phase ammonia (D3) vs. filter ammonium (F1 + F4) at Riverside.



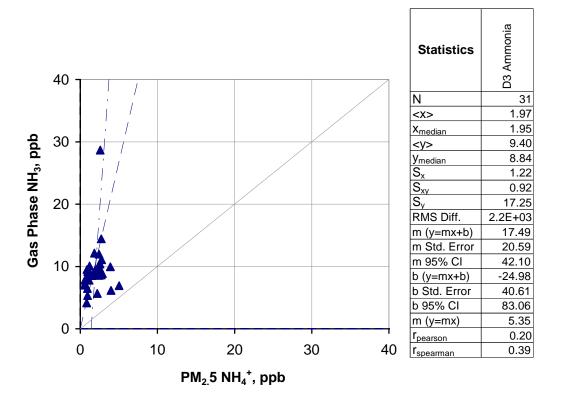


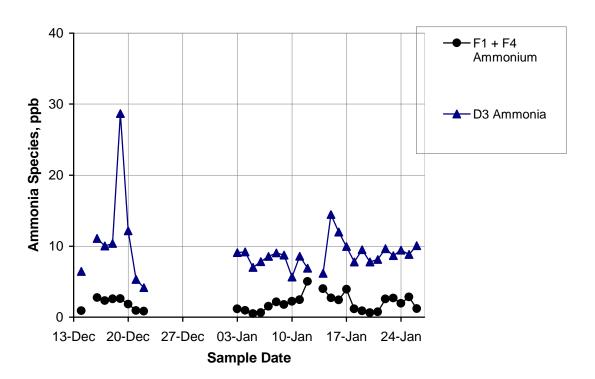
**Figure 88C** Ammonia gas-particle distribution: Full HEADS gas-phase ammonia (D3) vs. filter ammonium (F1 + F4) at Chicago.



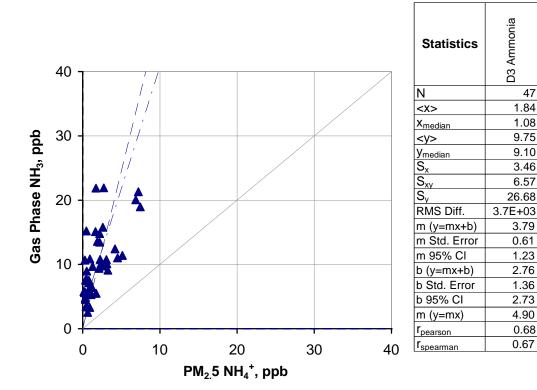


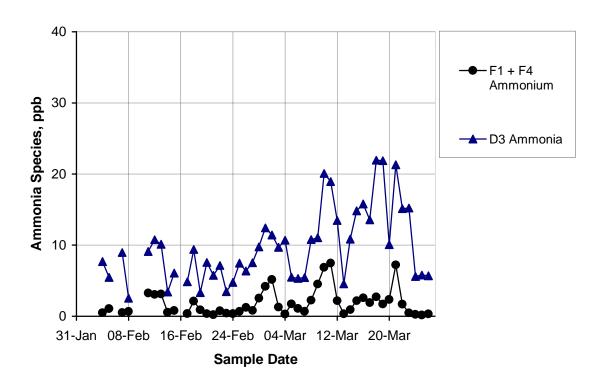
**Figure 88D** Ammonia gas-particle distribution: Full HEADS gas-phase ammonia (D3) vs. filter ammonium (F1 + F4) at Dallas.



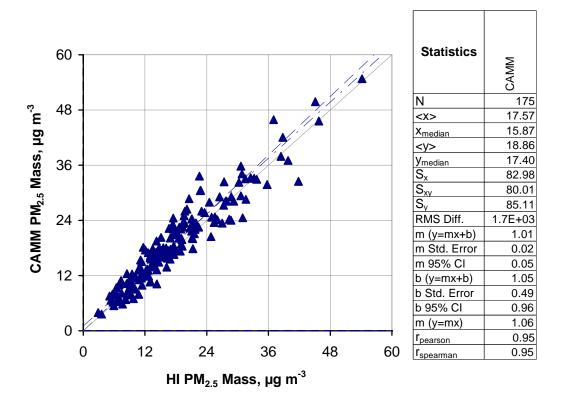


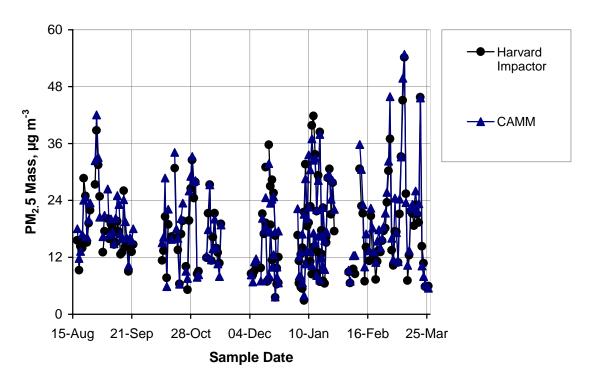
**Figure 88P** Ammonia gas-particle distribution: Full HEADS gas-phase ammonia (D3) vs. filter ammonium (F1 + F4) at Phoenix.



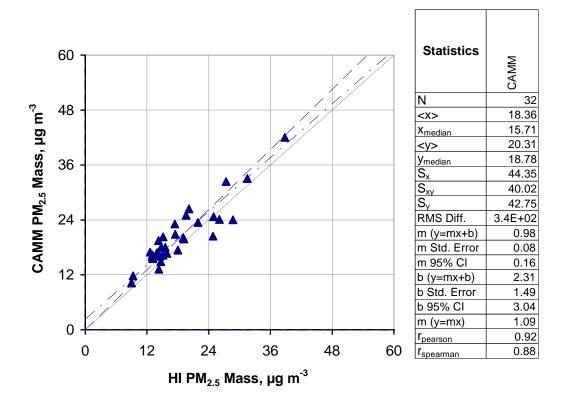


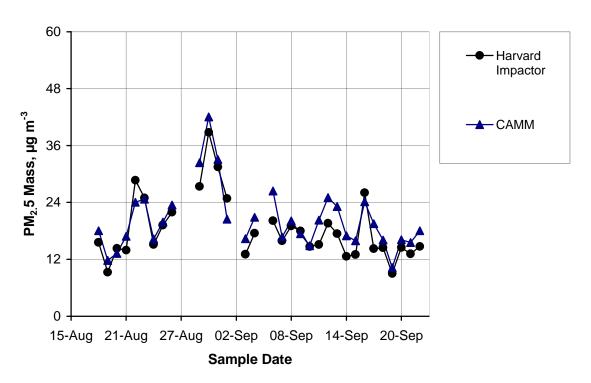
**Figure 88B** Ammonia gas-particle distribution: Full HEADS gas-phase ammonia (D3) vs. filter ammonium (F1 + F4) at Bakersfield.



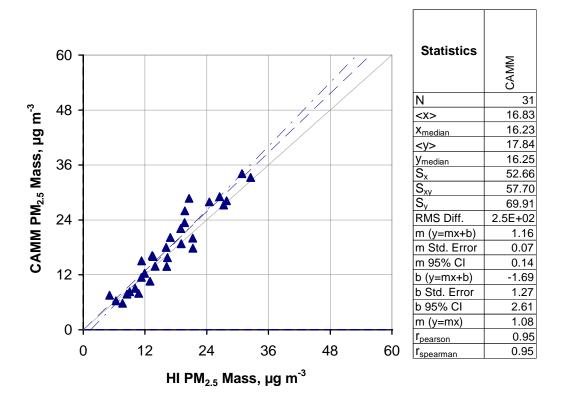


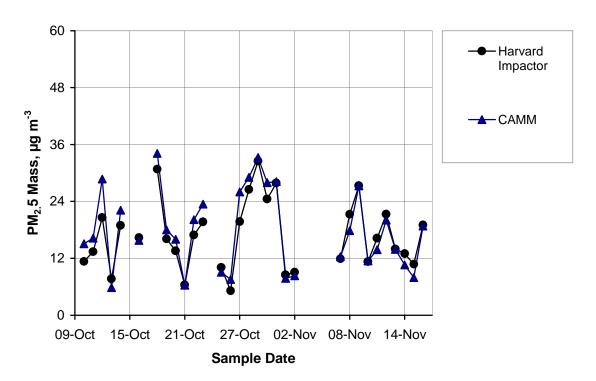
**Figure 89A** Continuous-discrete mass measurement comparison: 23-h averaged CAMM mass vs. Harvard Impactor at all sites.



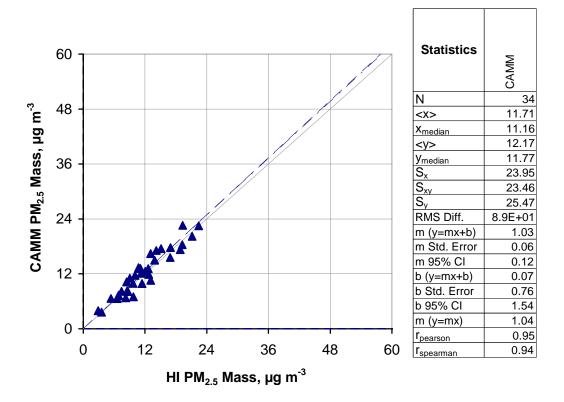


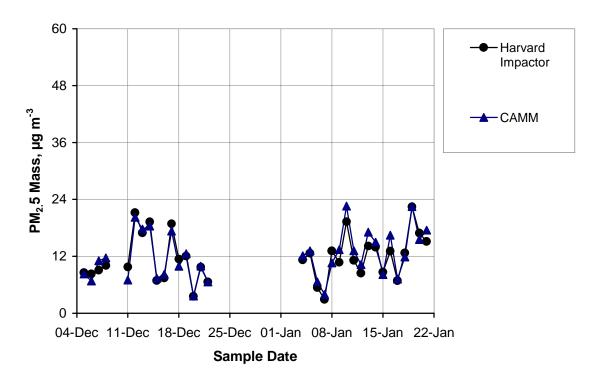
**Figure 89R** Continuous-discrete mass measurement comparison: 23-h averaged CAMM mass vs. Harvard Impactor at Riverside.



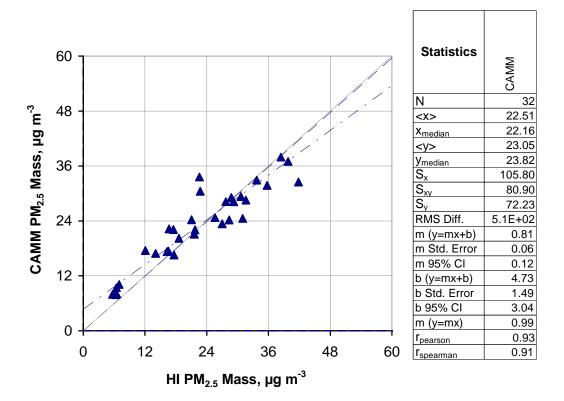


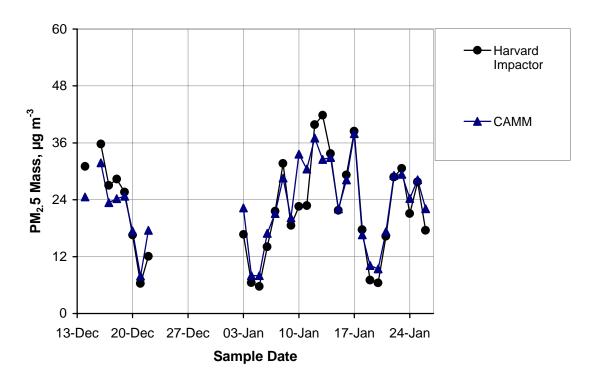
**Figure 89C** Continuous-discrete mass measurement comparison: 23-h averaged CAMM mass vs. Harvard Impactor at Chicago.



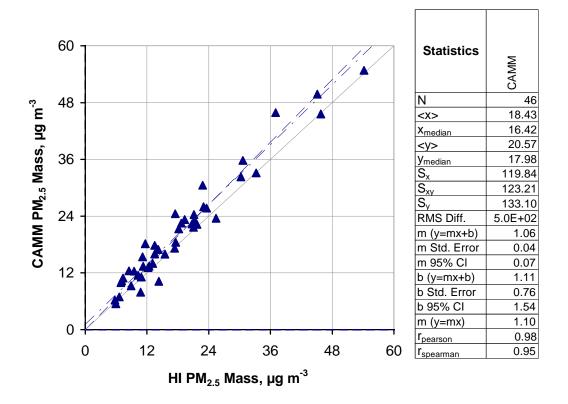


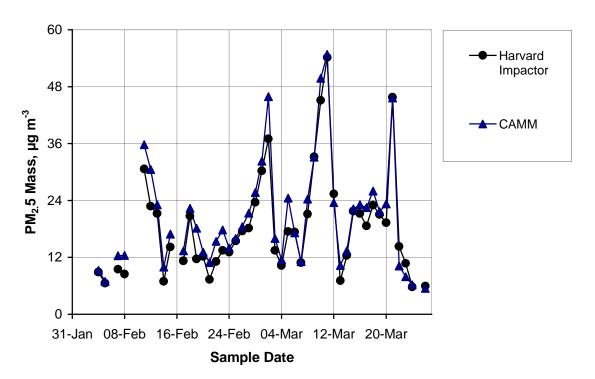
**Figure 89D** Continuous-discrete mass measurement comparison: 23-h averaged CAMM mass vs. Harvard Impactor at Dallas.



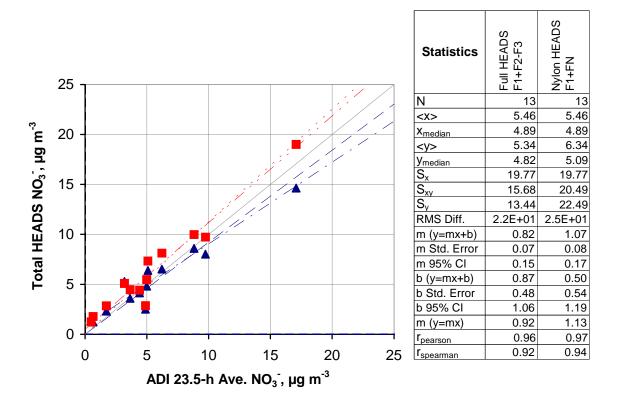


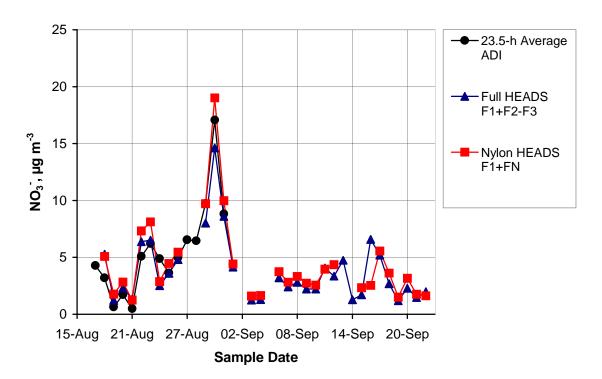
**Figure 89P** Continuous-discrete mass measurement comparison: 23-h averaged CAMM mass vs. Harvard Impactor at Phoenix.



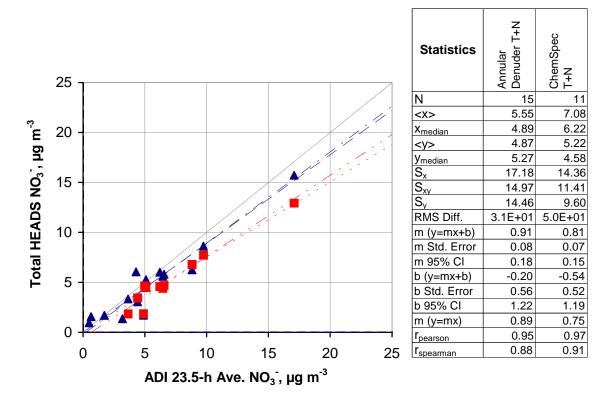


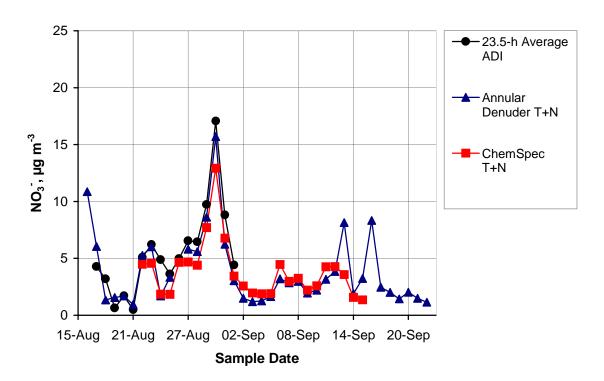
**Figure 89B** Continuous-discrete mass measurement comparison: 23-h averaged CAMM mass vs. Harvard Impactor at Bakersfield.



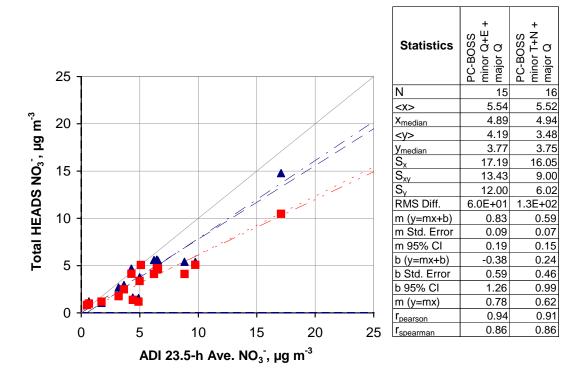


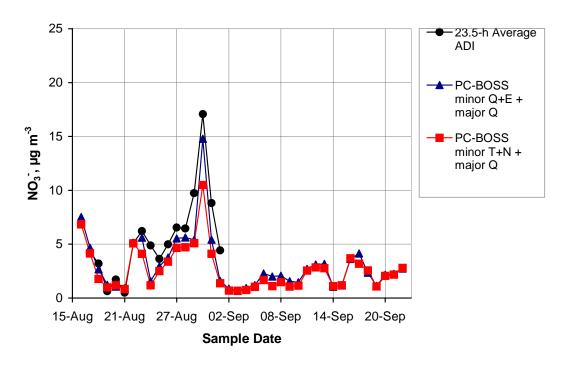
**Figure 90R** Continuous-discrete nitrate measurement comparison: 23-h averaged ADI nitrate monitor vs. Nylon HEADS F1 + FN and Full HEADS F1 + F2 – F3 at Riverside.



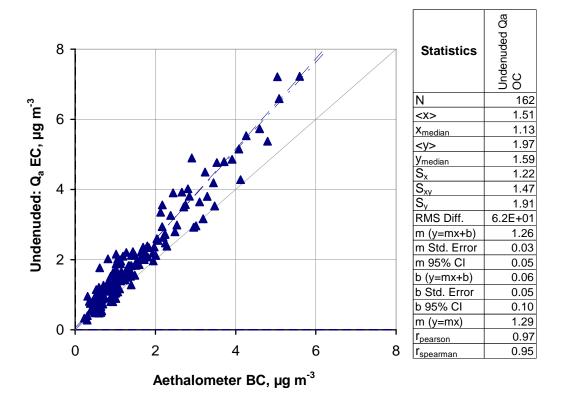


**Figure 91R** Continuous-discrete nitrate measurement comparison: 23-h averaged ADI nitrate monitor vs. ADS Teflon + nylon filters and CSS Teflon + nylon filters at Riverside.





**Figure 92R** Continuous-discrete nitrate measurement comparison: 23-h averaged ADI nitrate monitor vs. PC-BOSS minor flow quartz + Empore + major flow quartz filters and PC-BOSS minor flow Teflon + nylon + major flow quartz filters at Riverside.



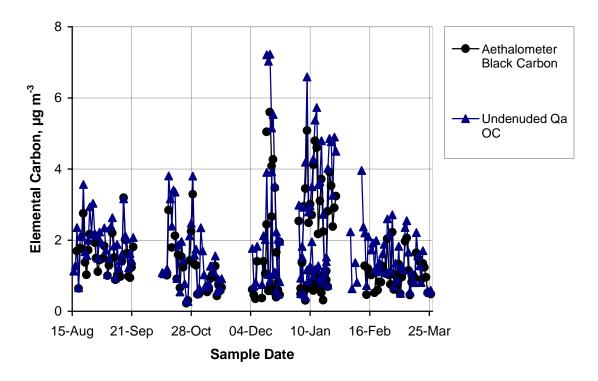
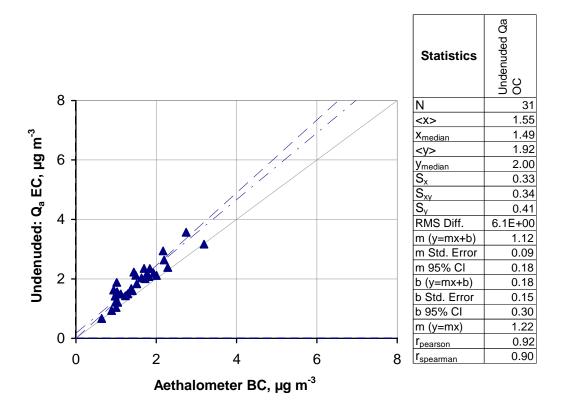


Figure 93A Continuous-discrete carbon measurement comparison: 23-h averaged aethalometer black carbon mass vs. undenuded Harvard Carbon Sampler (UND) front filter  $(Q_a)$  elemental carbon at all sites.



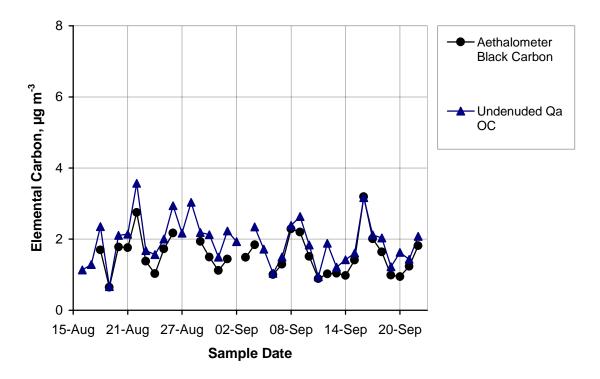
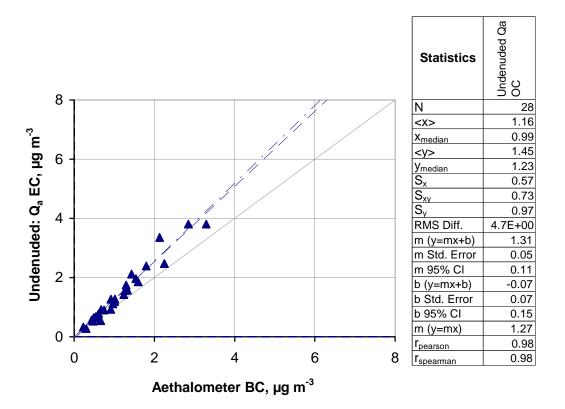


Figure 93R Continuous-discrete carbon measurement comparison: 23-h averaged aethalometer black carbon mass vs. undenuded Harvard Carbon Sampler (UND) front filter  $(Q_a)$  elemental carbon at Riverside.



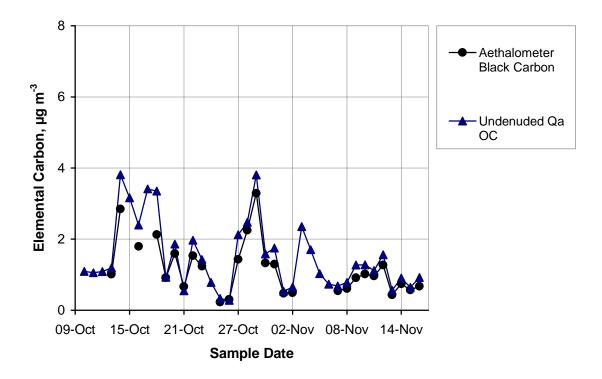
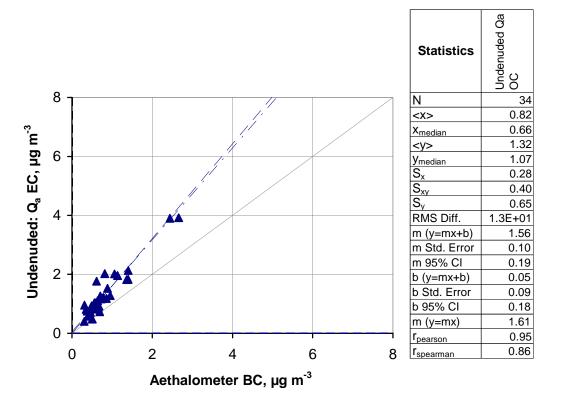


Figure 93C Continuous-discrete carbon measurement comparison: 23-h averaged aethalometer black carbon mass vs. undenuded Harvard Carbon Sampler (UND) front filter ( $Q_a$ ) elemental carbon at Chicago.



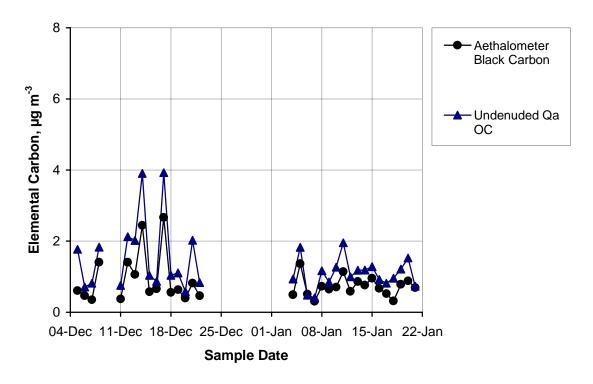
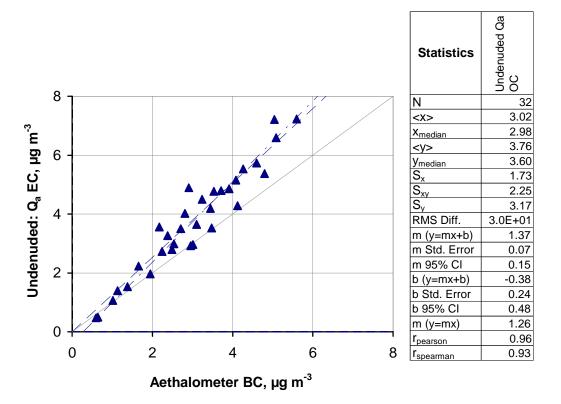


Figure 93D Continuous-discrete carbon measurement comparison: 23-h averaged aethalometer black carbon mass vs. undenuded Harvard Carbon Sampler (UND) front filter ( $Q_a$ ) elemental carbon at Dallas.



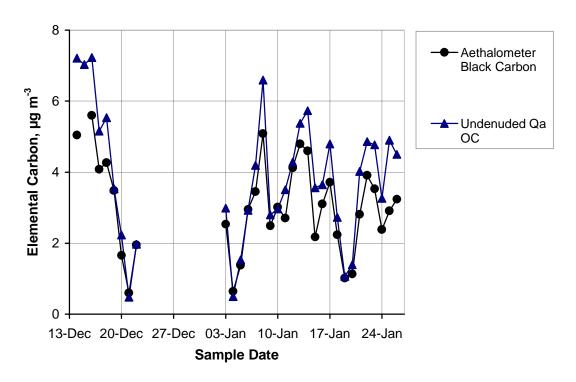


Figure 93P Continuous-discrete carbon measurement comparison: 23-h averaged aethalometer black carbon mass vs. undenuded Harvard Carbon Sampler (UND) front filter ( $Q_a$ ) elemental carbon at Phoenix.

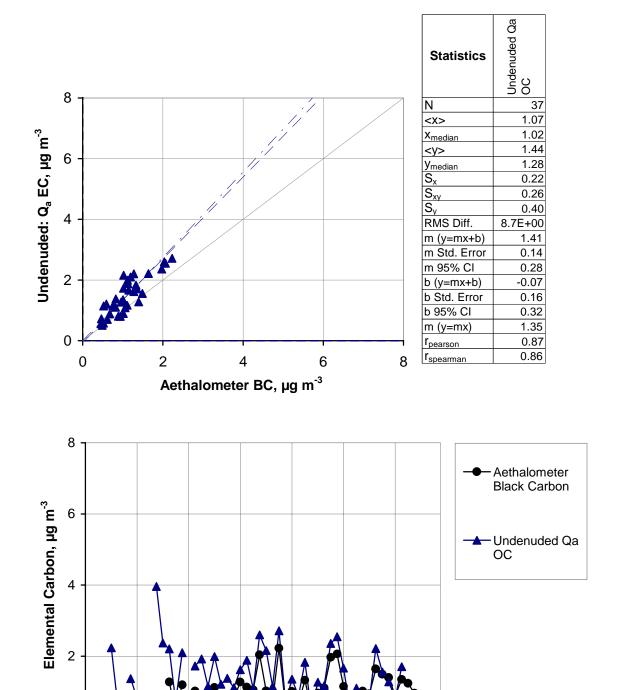
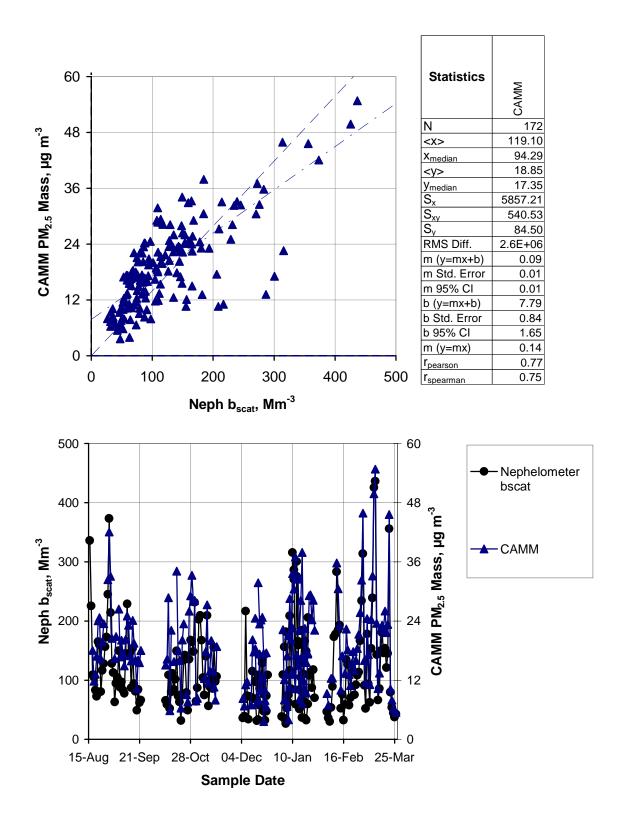


Figure 93B Continuous-discrete carbon measurement comparison: 23-h averaged aethalometer black carbon mass vs. undenuded Harvard Carbon Sampler (UND) front filter ( $Q_a$ ) elemental carbon at Bakersfield.

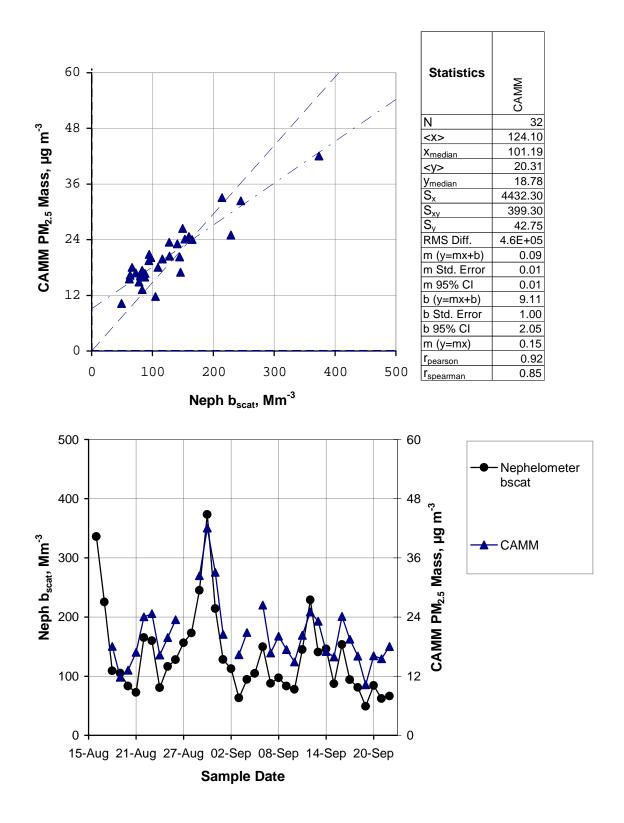
31-Jan 08-Feb 16-Feb 24-Feb 04-Mar 12-Mar 20-Mar

**Sample Date** 

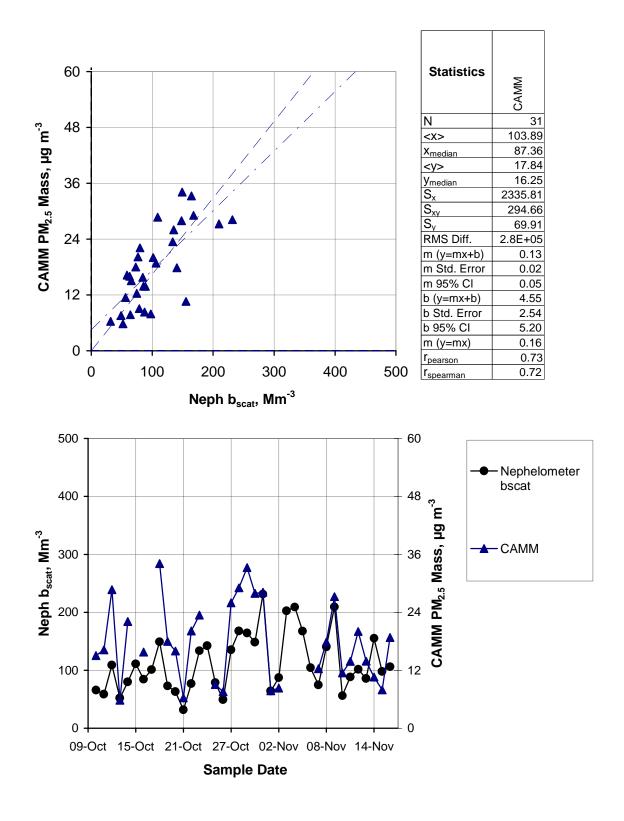
0



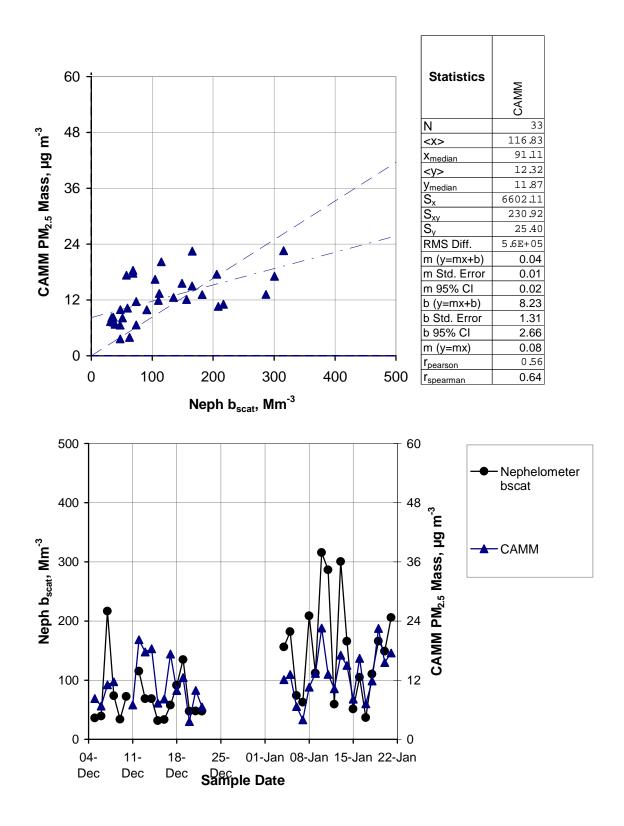
**Figure 94A** Comparison of 23-h averaged continuous-nephelometer scattering coefficient data with Harvard Impactor mass at all sites.



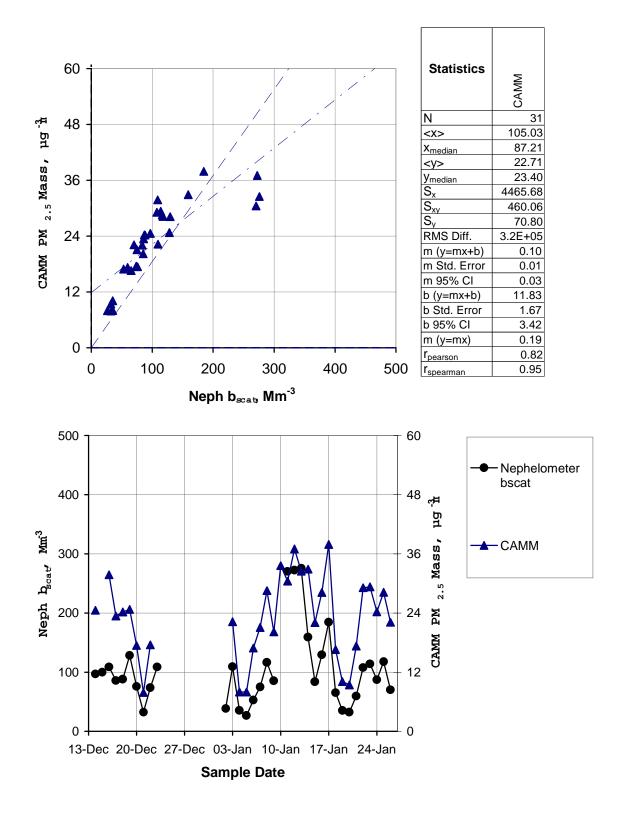
**Figure 94R** Comparison of 23-h averaged continuous-nephelometer scattering coefficient data with Harvard Impactor mass at Riverside.



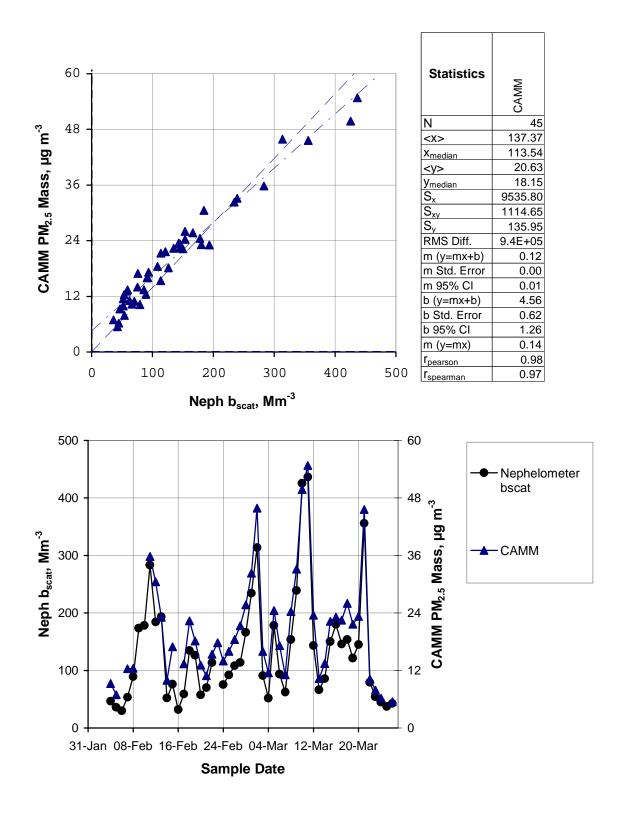
**Figure 94C** Comparison of 23-h averaged continuous-nephelometer scattering coefficient data with Harvard Impactor mass at Chicago.



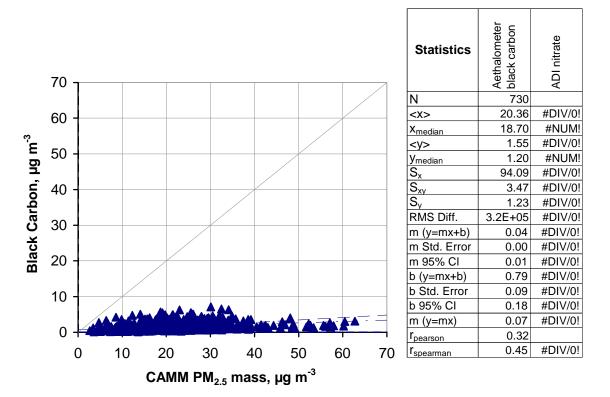
**Figure 94D** Comparison of 23-h averaged continuous-nephelometer scattering coefficient data with Harvard Impactor mass at Dallas.

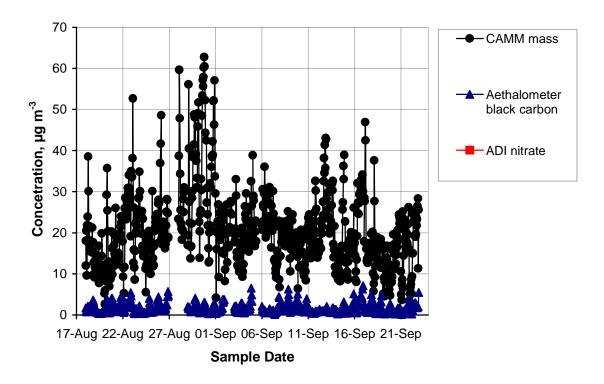


**Figure 94P** Comparison of 23-h averaged continuous-nephelometer scattering coefficient data with Harvard Impactor mass at Phoenix.

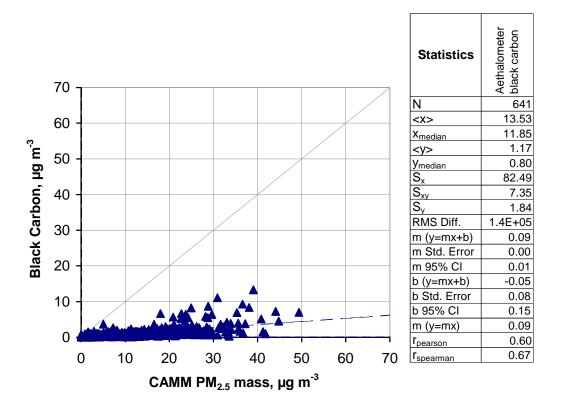


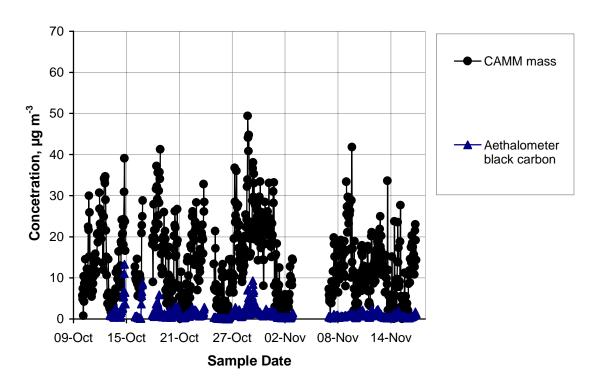
**Figure 94B** Comparison of 23-h averaged continuous-nephelometer scattering coefficient data with Harvard Impactor mass at Bakersfield.



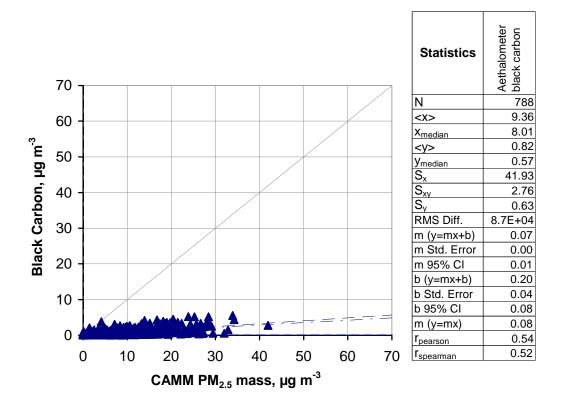


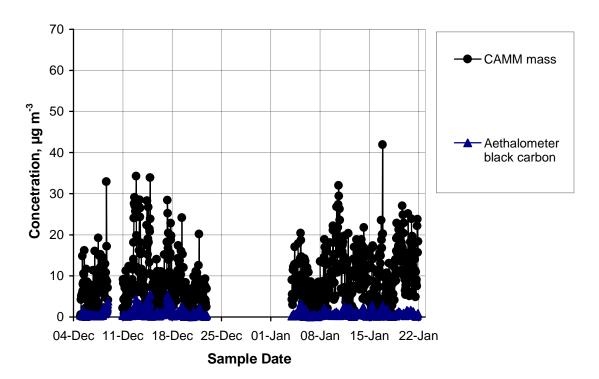
**Figure 95R** Correlations between 1-h average measurements collected by CAMM (mass), ADI sampler (nitrate), and aethalometer (black carbon) at Riverside.



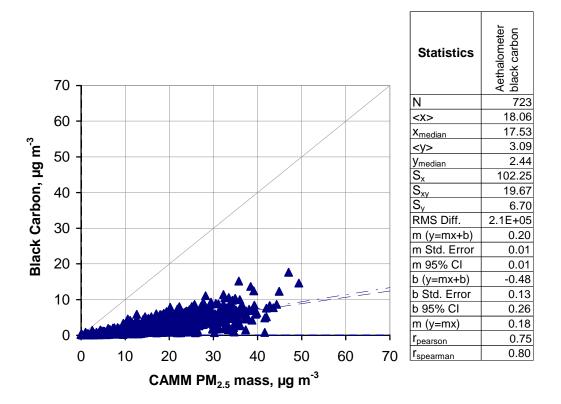


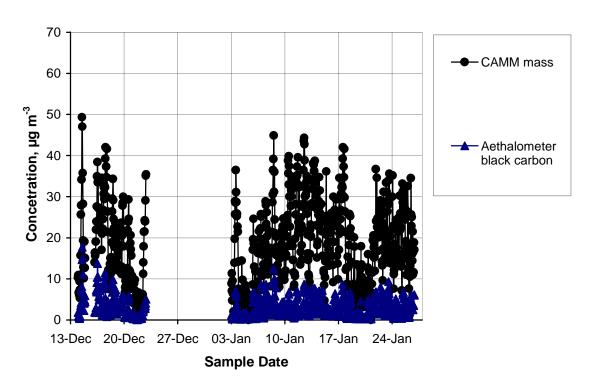
**Figure 95C** Correlations between 1-h average measurements collected by CAMM (mass) and aethalometer (black carbon) at Chicago.



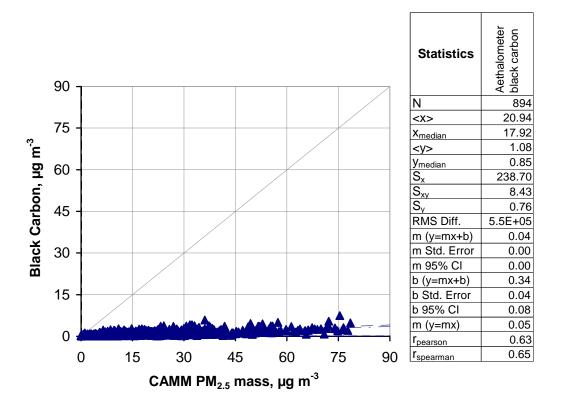


**Figure 95D** Correlations between 1-h average measurements collected by CAMM (mass) and aethalometer (black carbon) at Dallas.





**Figure 95P** Correlations between 1-h average measurements collected by CAMM (mass) and aethalometer (black carbon) at Phoenix.



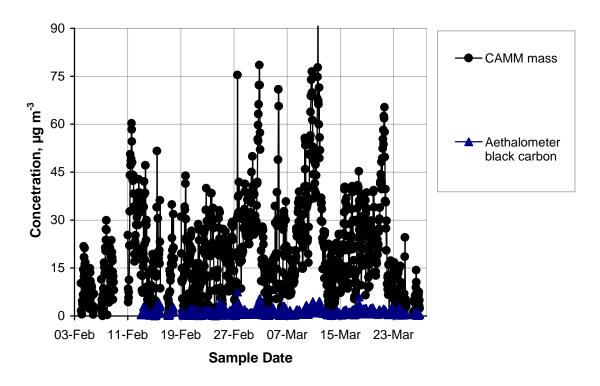


**Figure 95B** Correlations between 1-h average measurements collected by CAMM (mass) and aethalometer (black carbon) at Bakersfield.

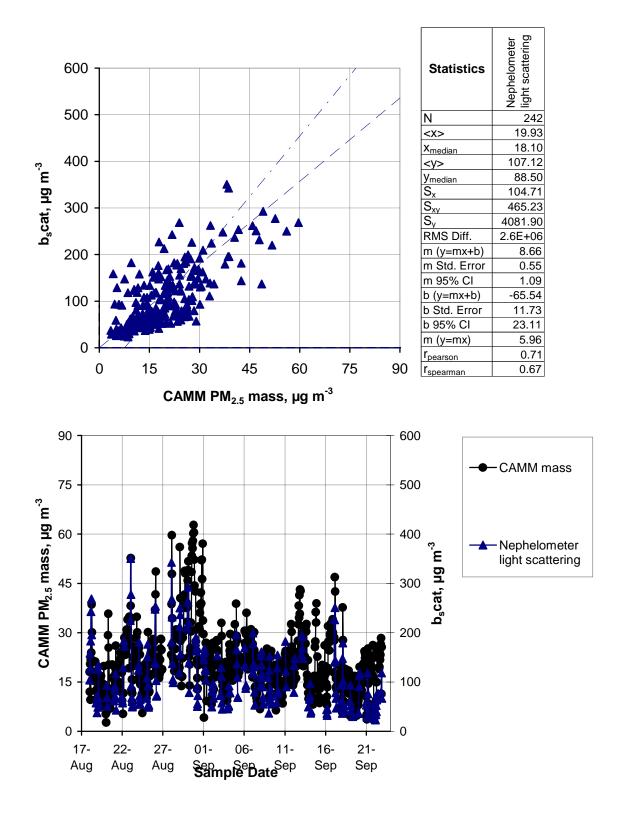


**Figure 96R** Correlations between 1-h average measurements collected by CAMM (mass) and nephelometer (light scattering)at Riverside.

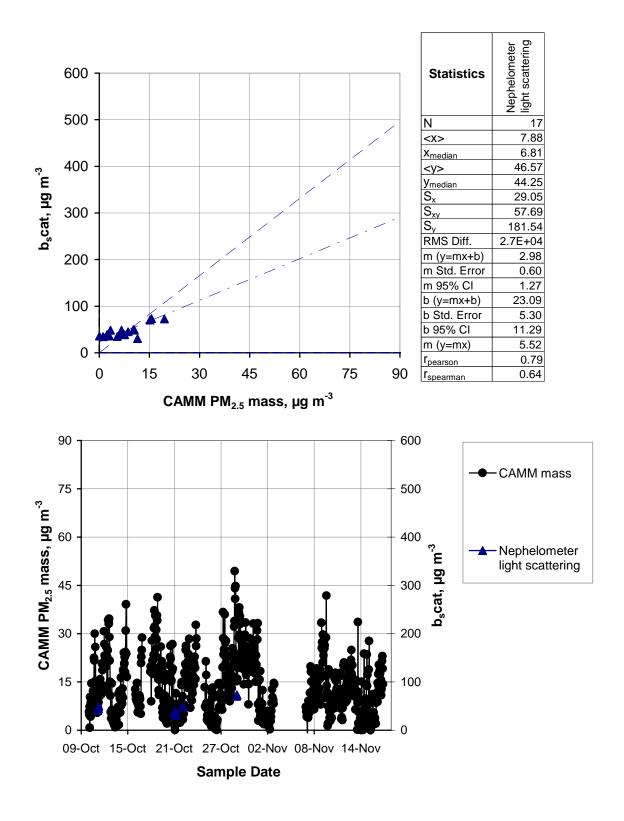


**Figure 96C** Correlations between 1-h average measurements collected by CAMM (mass) and nephelometer (light scattering)at Chicago.

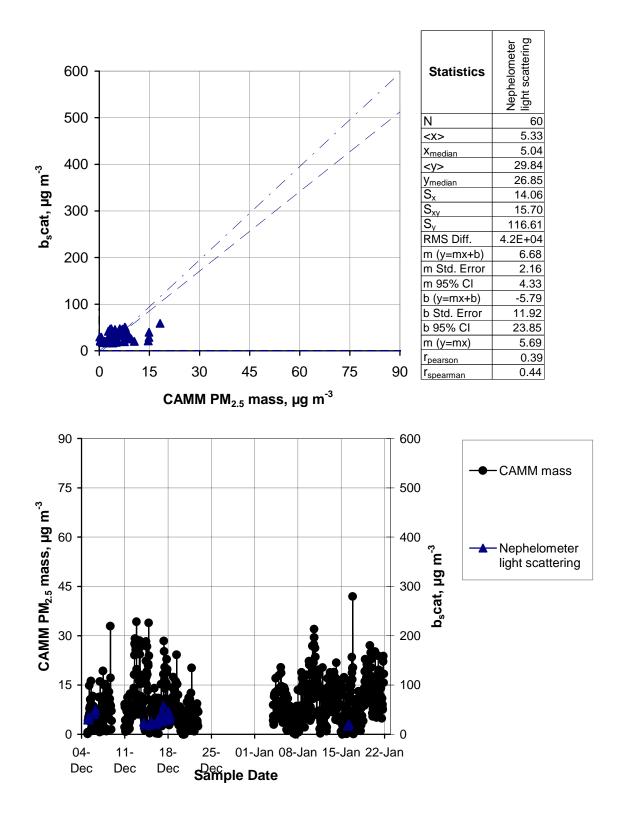


**Figure 96D** Correlations between 1-h average measurements collected by CAMM (mass) and nephelometer (light scattering)at Dallas.

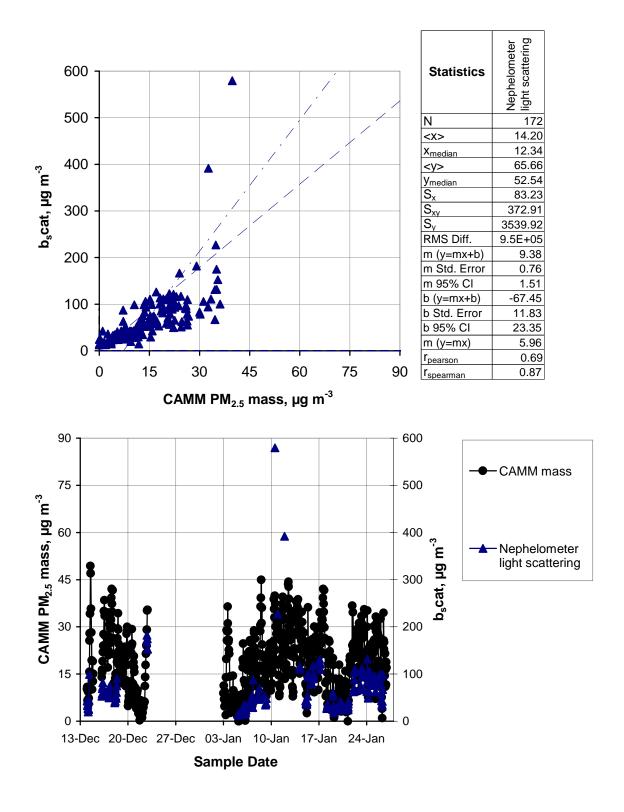


**Figure 96P** Correlations between 1-h average measurements collected by CAMM (mass) and nephelometer (light scattering)at Phoenix.

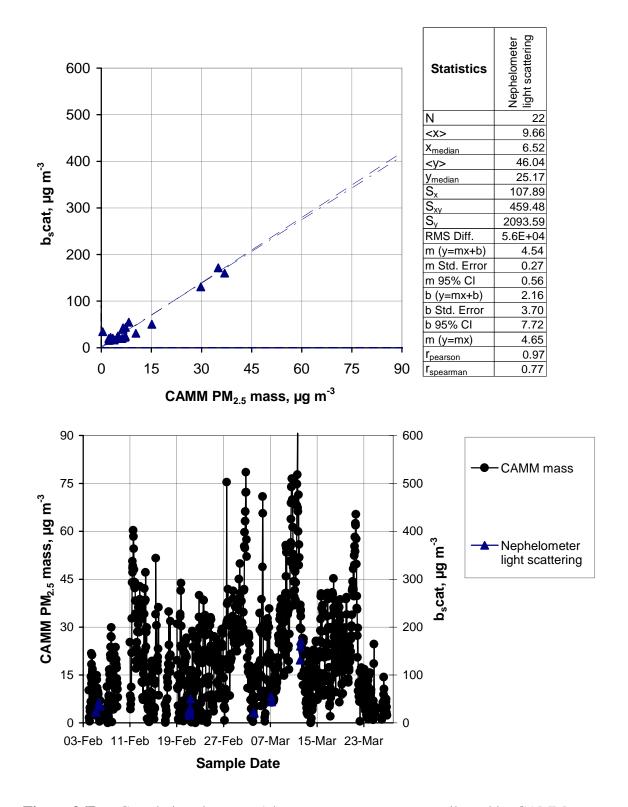


**Figure 96B** Correlations between 1-h average measurements collected by CAMM (mass) and nephelometer (light scattering)at Bakersfield.

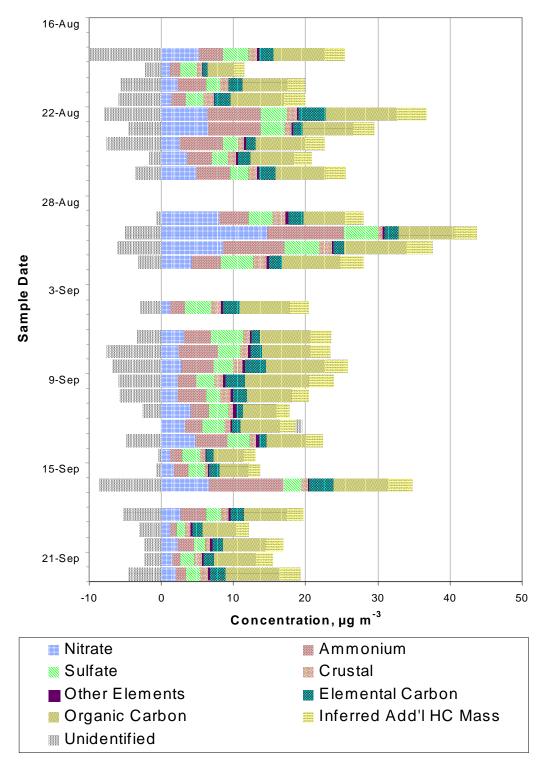


**Figure 97R** Daily average chemical composition estimates for PM<sub>2.5</sub> based on Full HEADS and DEN Harvard carbon sampler measurements at Riverside. A negative unidentified fraction indicates that the 24-h average reconstructed mass exceeded the HI mass.

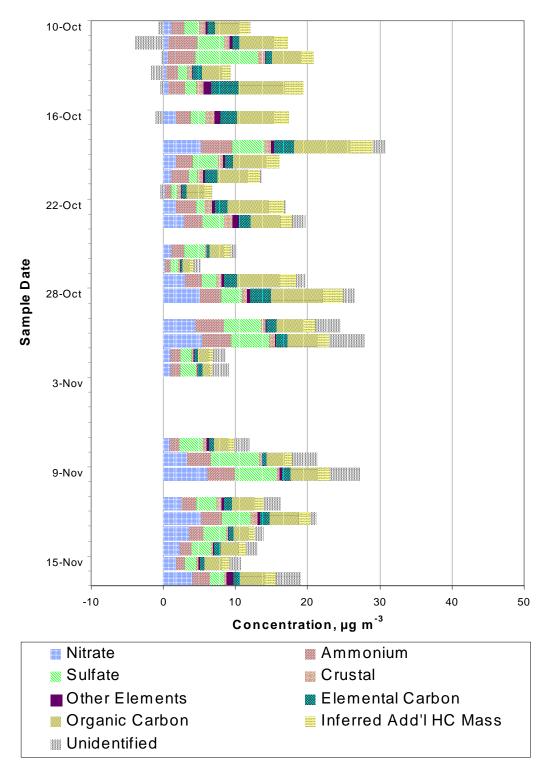


**Figure 97C** Daily average chemical composition estimates for PM<sub>2.5</sub> based on Full HEADS and DEN Harvard carbon sampler measurements at Chicago. A negative unidentified fraction indicates that the 24-h average reconstructed mass exceeded the HI mass.

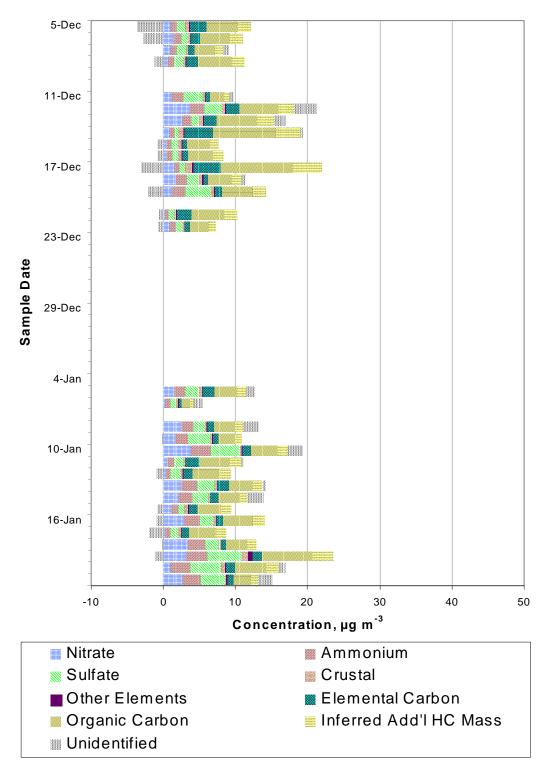


**Figure 97D** Daily average chemical composition estimates for PM<sub>2.5</sub> based on Full HEADS and DEN Harvard carbon sampler measurements at Dallas. A negative unidentified fraction indicates that the 24-h average reconstructed mass exceeded the HI mass.

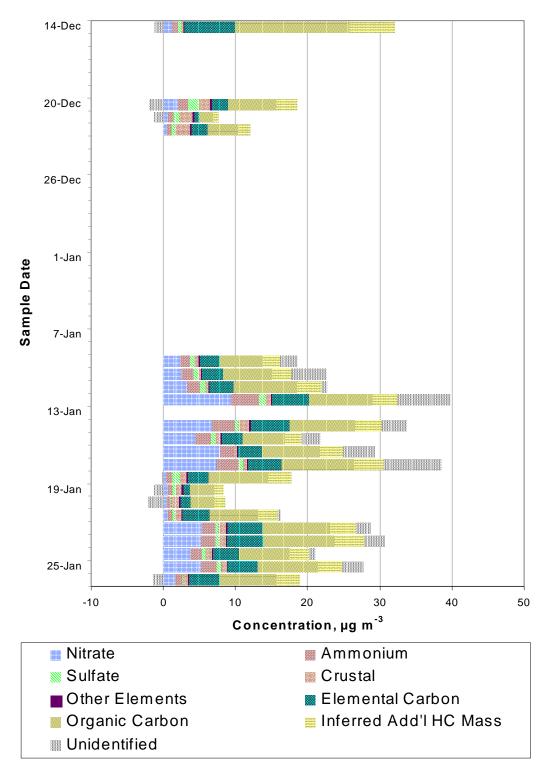


**Figure 97P** Daily average chemical composition estimates for PM<sub>2.5</sub> based on Full HEADS and DEN Harvard carbon sampler measurements at Phoenix. A negative unidentified fraction indicates that the 24-h average reconstructed mass exceeded the HI mass.

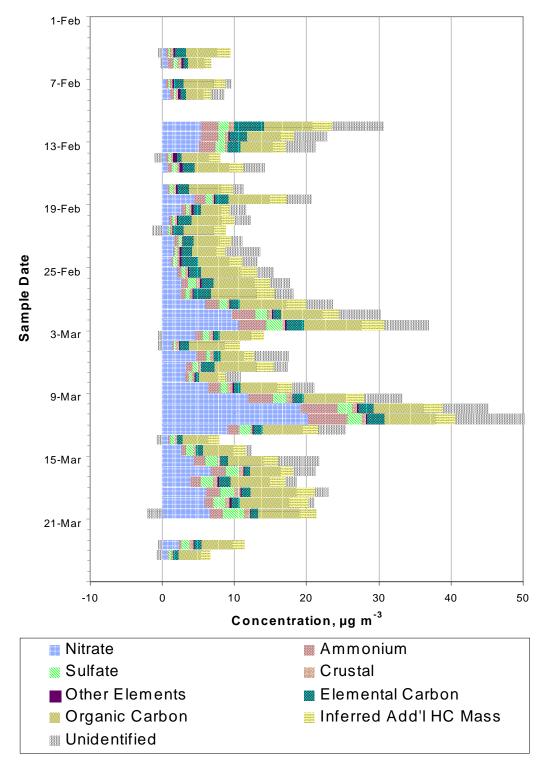
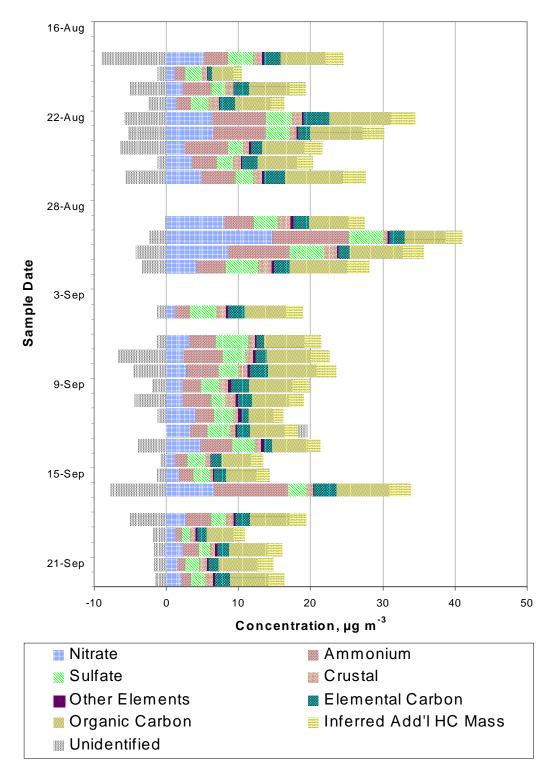
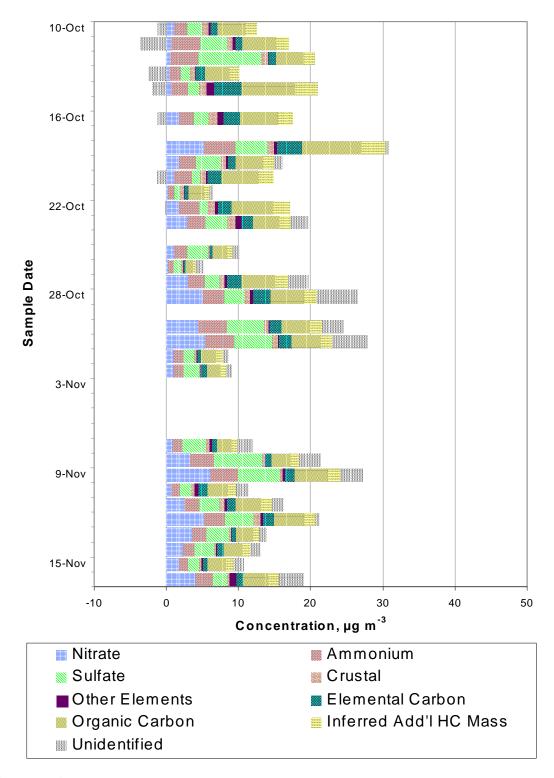


Figure 97B Daily average chemical composition estimates for PM<sub>2.5</sub> based on Full HEADS and DEN Harvard carbon sampler measurements at Bakersfield. A negative unidentified fraction indicates that the 24-h average reconstructed mass exceeded the HI mass.



**Figure 98R** Daily average chemical composition estimates for PM<sub>2.5</sub> based on Full HEADS and UND Harvard carbon sampler measurements at Riverside. A negative unidentified fraction indicates that the 24-h average reconstructed mass exceeded the HI mass.



**Figure 98C** Daily average chemical composition estimates for PM<sub>2.5</sub> based on Full HEADS and UND Harvard carbon sampler measurements at Chicago. A negative unidentified fraction indicates that the 24-h average reconstructed mass exceeded the HI mass.

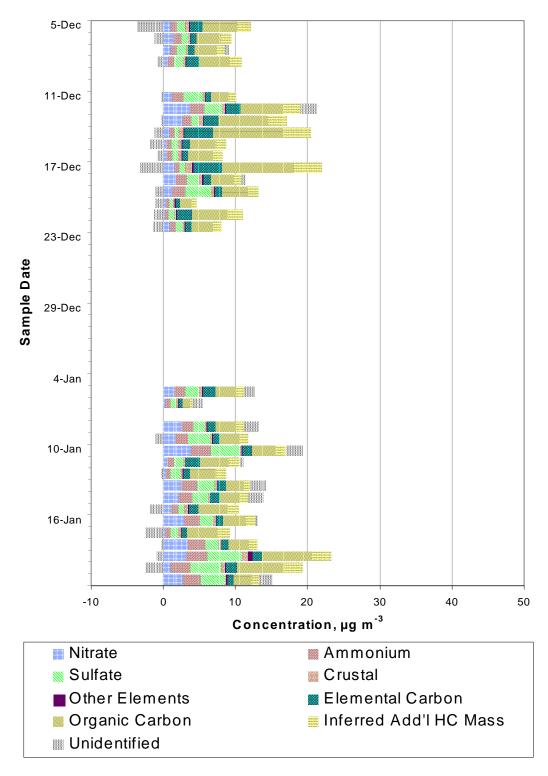


**Figure 98D** Daily average chemical composition estimates for PM<sub>2.5</sub> based on Full HEADS and UND Harvard carbon sampler measurements at Dallas. A negative unidentified fraction indicates that the 24-h average reconstructed mass exceeded the HI mass.

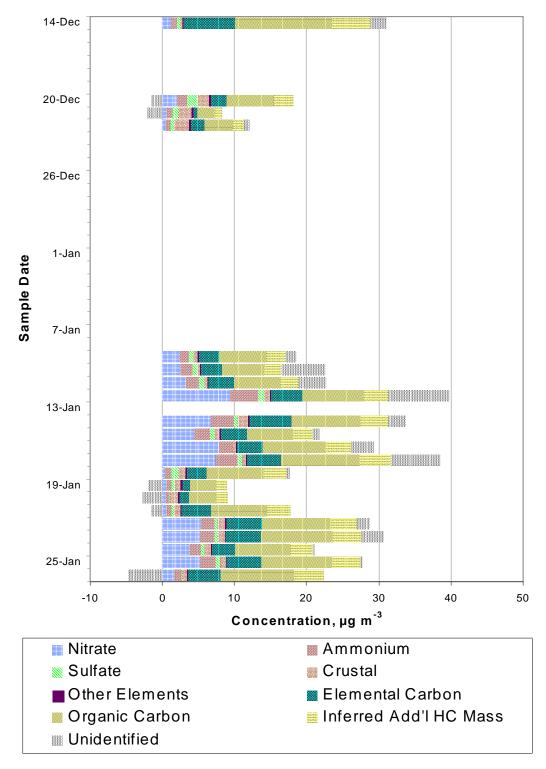


**Figure 98P** Daily average chemical composition estimates for PM<sub>2.5</sub> based on Full HEADS and UND Harvard carbon sampler measurements at Phoenix. A negative unidentified fraction indicates that the 24-h average reconstructed mass exceeded the HI mass.

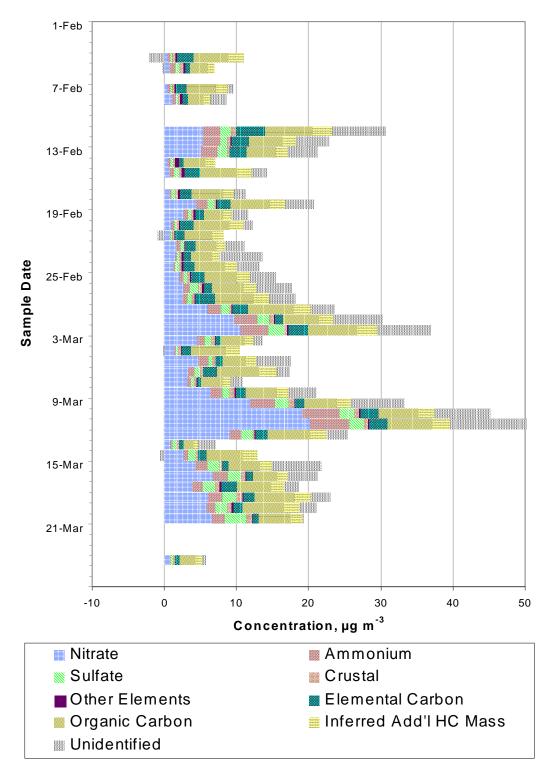
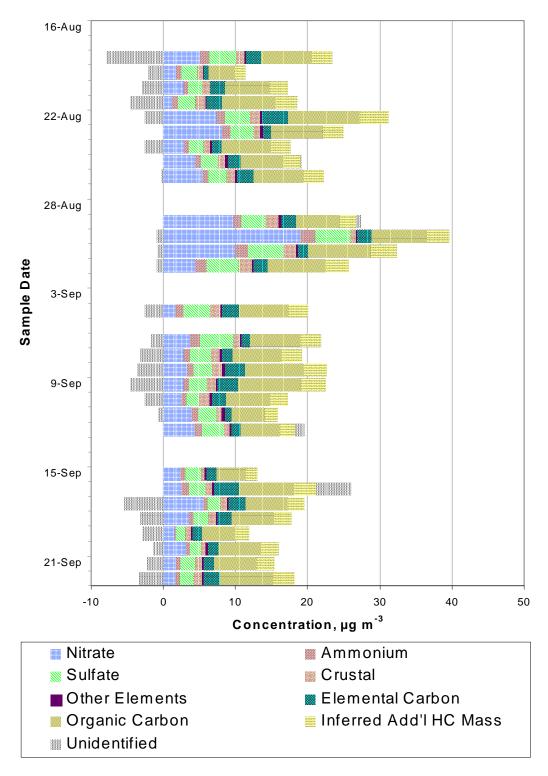
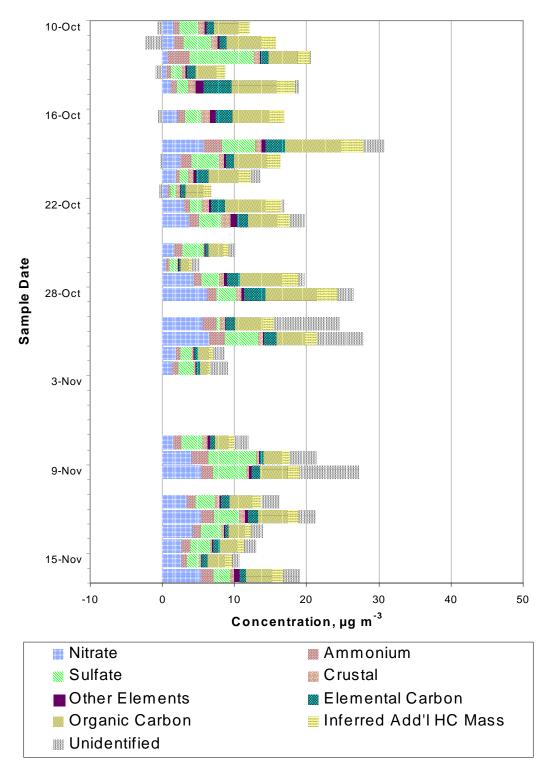


Figure 98B Daily average chemical composition estimates for PM<sub>2.5</sub> based on Full HEADS and UND Harvard carbon sampler measurements at Bakersfield. A negative unidentified fraction indicates that the 24-h average reconstructed mass exceeded the HI mass.



**Figure 99R** Daily average chemical composition estimates for PM<sub>2.5</sub> based on Nylon HEADS and DEN Harvard carbon sampler measurements at Riverside. A negative unidentified fraction indicates that the 24-h average reconstructed mass exceeded the HI mass.



**Figure 99C** Daily average chemical composition estimates for PM<sub>2.5</sub> based on Nylon HEADS and DEN Harvard carbon sampler measurements at Chicago. A negative unidentified fraction indicates that the 24-h average reconstructed mass exceeded the HI mass.

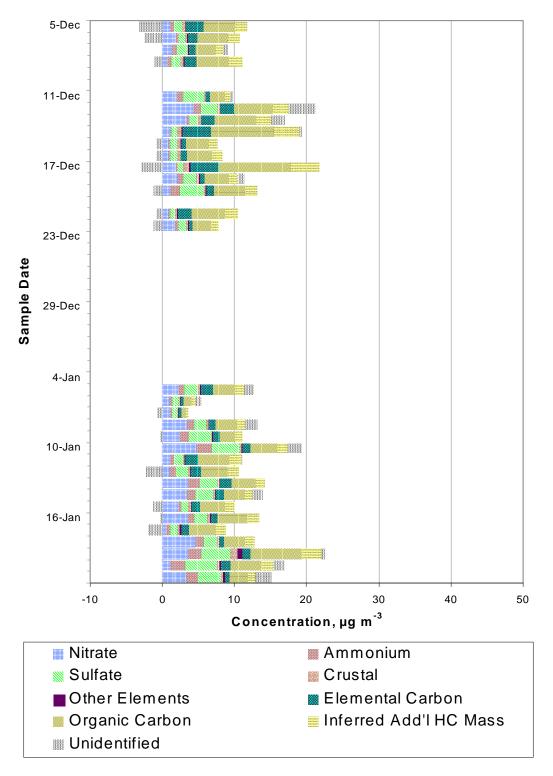


**Figure 99D** Daily average chemical composition estimates for PM<sub>2.5</sub> based on Nylon HEADS and DEN Harvard carbon sampler measurements at Dallas. A negative unidentified fraction indicates that the 24-h average reconstructed mass exceeded the HI mass.

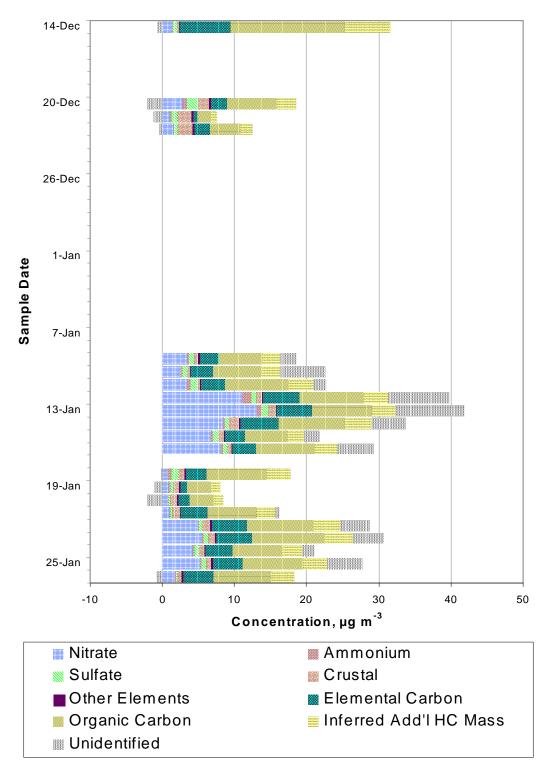


**Figure 99P** Daily average chemical composition estimates for PM<sub>2.5</sub> based on Nylon HEADS and DEN Harvard carbon sampler measurements at Phoenix. A negative unidentified fraction indicates that the 24-h average reconstructed mass exceeded the HI mass.

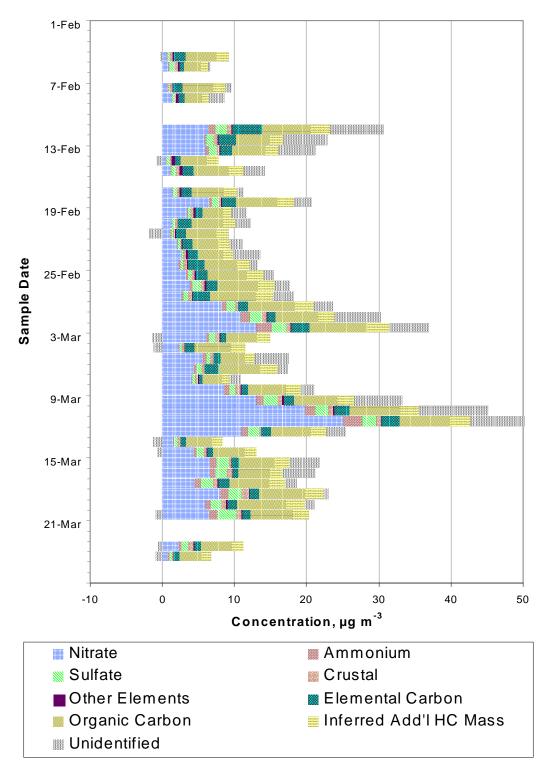


**Figure 99B** Daily average chemical composition estimates for PM<sub>2.5</sub> based on Nylon HEADS and DEN Harvard carbon sampler measurements at Bakersfield. A negative unidentified fraction indicates that the 24-h average reconstructed mass exceeded the HI mass.

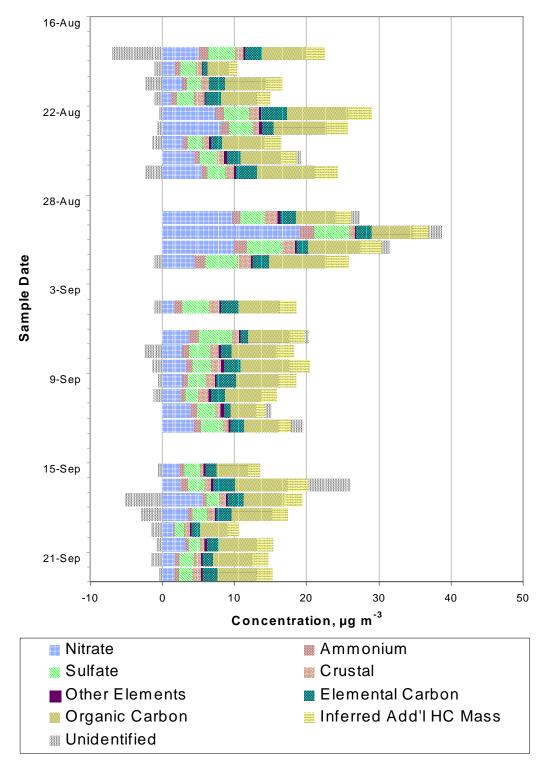


**Figure 100R** Daily average chemical composition estimates for PM<sub>2.5</sub> based on Nylon HEADS and UND Harvard carbon sampler measurements at Riverside. A negative unidentified fraction indicates that the 24-h average reconstructed mass exceeded the HI mass.

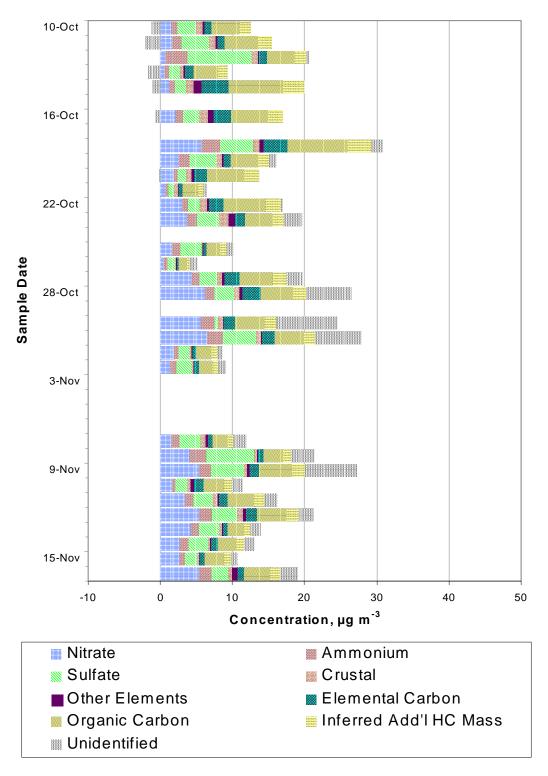
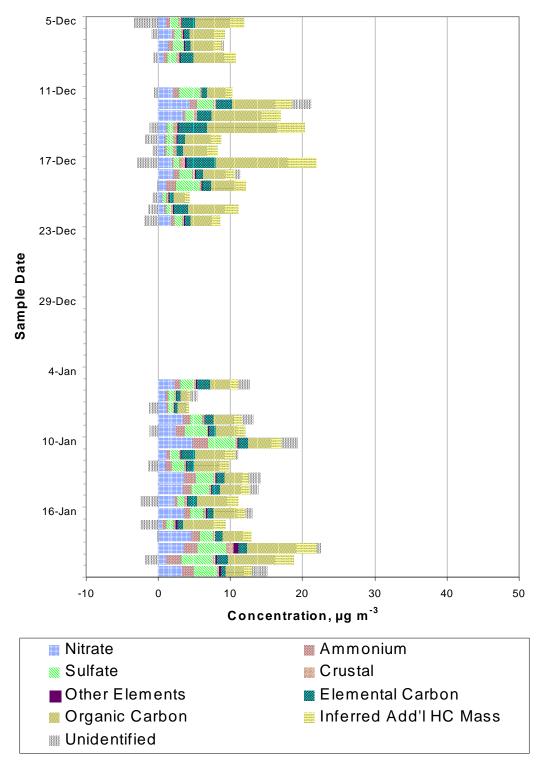
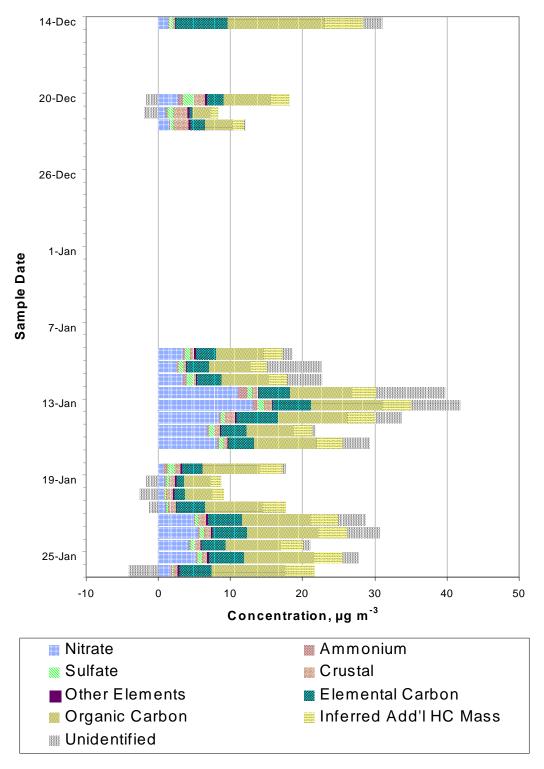


Figure 100C Daily average chemical composition estimates for  $PM_{2.5}$  based on Nylon HEADS and UND Harvard carbon sampler measurements at Chicago. A negative unidentified fraction indicates that the 24-h average reconstructed mass exceeded the HI mass.



**Figure 100D** Daily average chemical composition estimates for PM<sub>2.5</sub> based on Nylon HEADS and UND Harvard carbon sampler measurements at Dallas. A negative unidentified fraction indicates that the 24-h average reconstructed mass exceeded the HI mass.



**Figure 100P** Daily average chemical composition estimates for  $PM_{2.5}$  based on Nylon HEADS and UND Harvard carbon sampler measurements at Phoenix. A negative unidentified fraction indicates that the 24-h average reconstructed mass exceeded the HI mass.

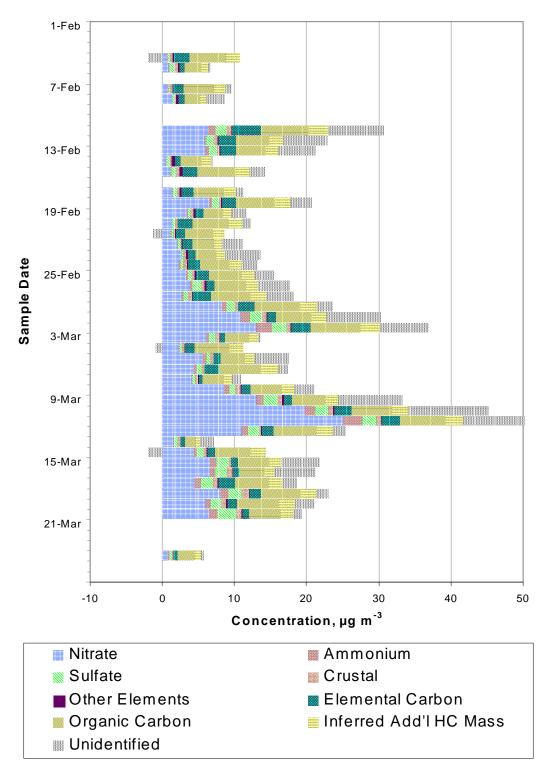


**Figure 100B** Daily average chemical composition estimates for PM<sub>2.5</sub> based on Nylon HEADS and UND Harvard carbon sampler measurements at Bakersfield. A negative unidentified fraction indicates that the 24-h average reconstructed mass exceeded the HI mass.

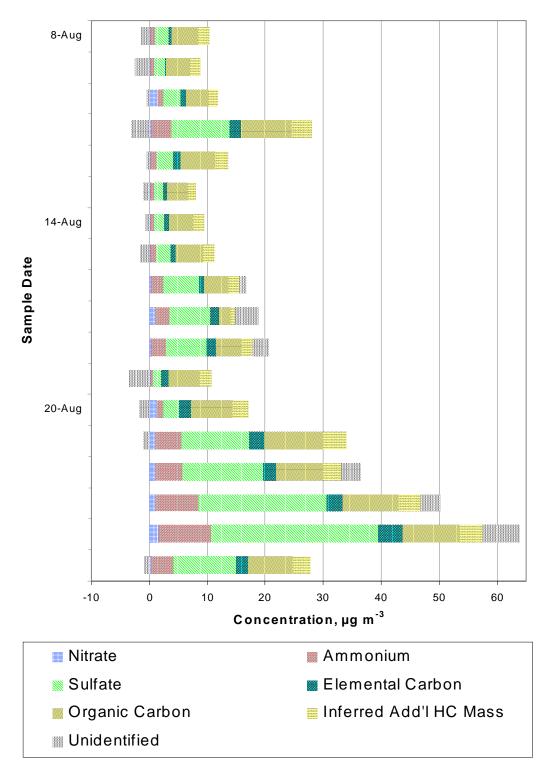


Figure 100F Daily average chemical composition estimates for PM<sub>2.5</sub> based on Nylon HEADS and UND Harvard carbon sampler measurements at Philadelphia. A negative unidentified fraction indicates that the 24-h average reconstructed mass exceeded the HI mass.

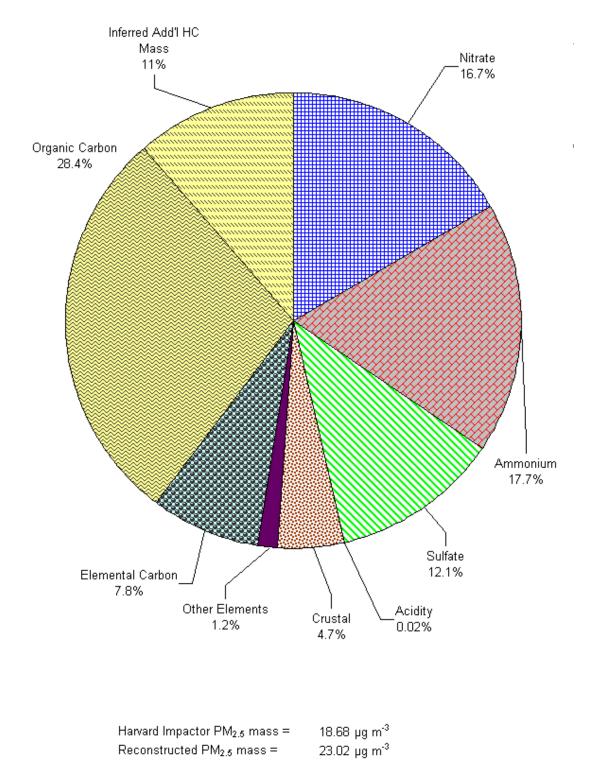
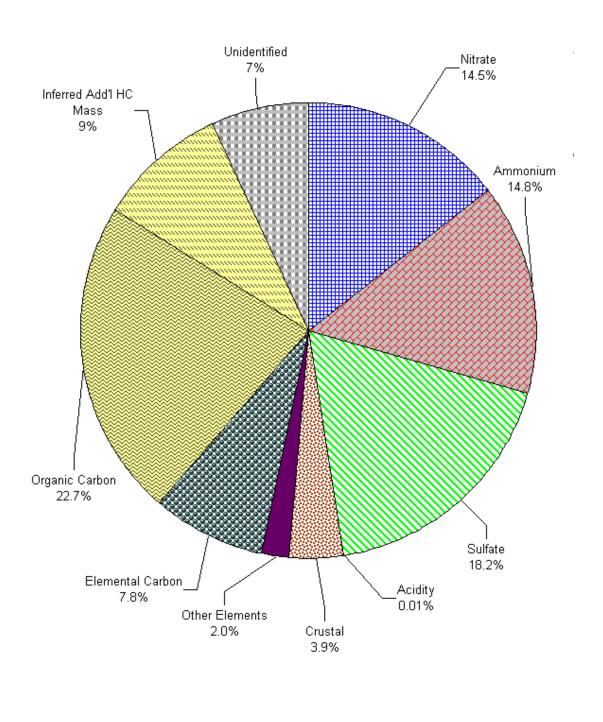
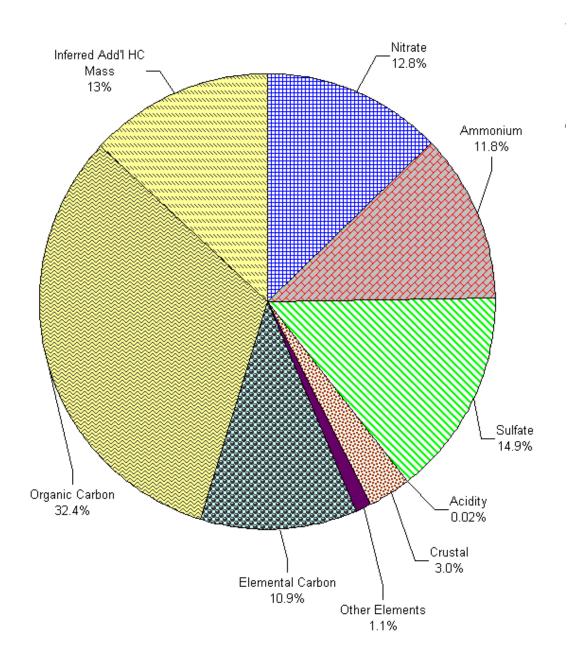


Figure 101R Study average chemical composition estimates for  $PM_{2.5}$  based on Full HEADS and DEN Harvard carbon sampler measurements at Riverside



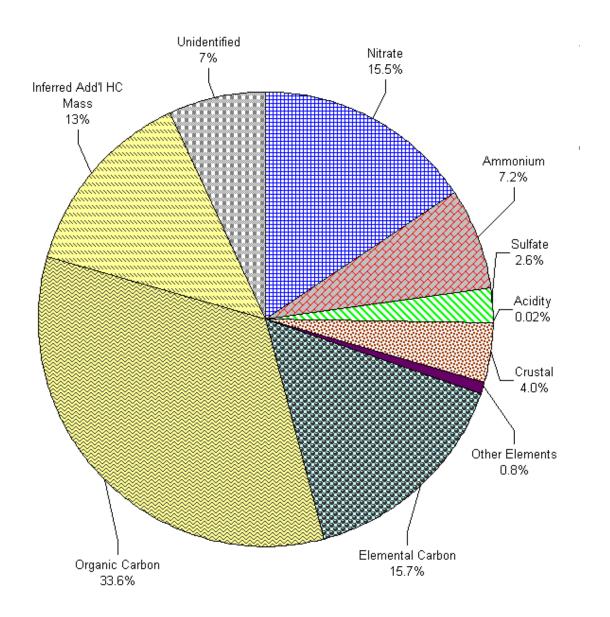
Harvard Impactor PM<sub>2.5</sub> mass =  $16.48 \ \mu g \ m^{-3}$ Reconstructed PM<sub>2.5</sub> mass =  $15.34 \ \mu g \ m^{-3}$ 

Figure 101C Study average chemical composition estimates for  $PM_{2.5}$  based on Full HEADS and DEN Harvard carbon sampler measurements at Chicago.



Harvard Impactor PM<sub>2.5</sub> mass =  $12.27 \ \mu g \ m^{-3}$ Reconstructed PM<sub>2.5</sub> mass =  $12.35 \ \mu g \ m^{-3}$ 

Figure 101D Study average chemical composition estimates for  $PM_{2.5}$  based on Full HEADS and DEN Harvard carbon sampler measurements at Dallas.



Harvard Impactor  $PM_{2.5}$  mass = 22.18  $\mu g m^{-3}$ Reconstructed  $PM_{2.5}$  mass = 20.61  $\mu g m^{-3}$ 

Figure 101P Study average chemical composition estimates for  $PM_{2.5}$  based on Full HEADS and DEN Harvard carbon sampler measurements at Phoenix.

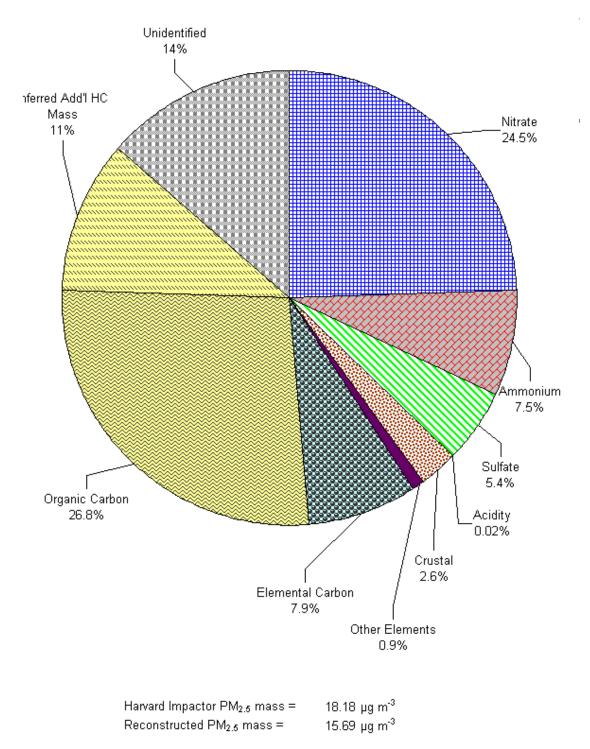
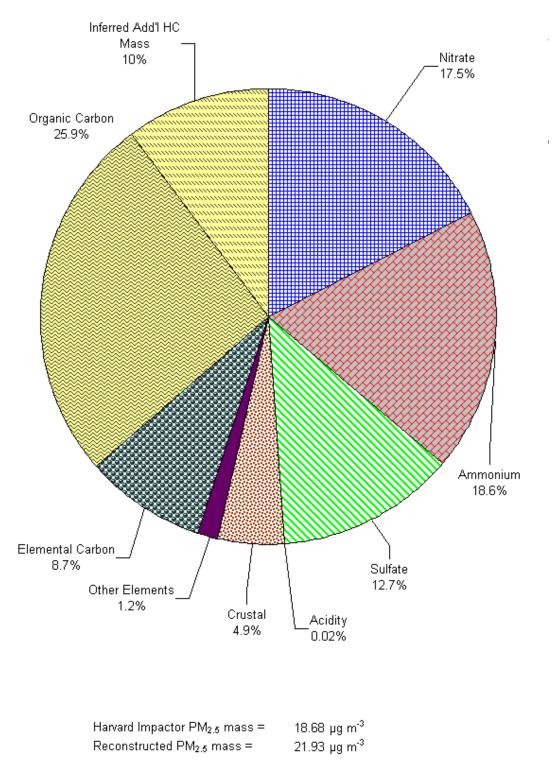
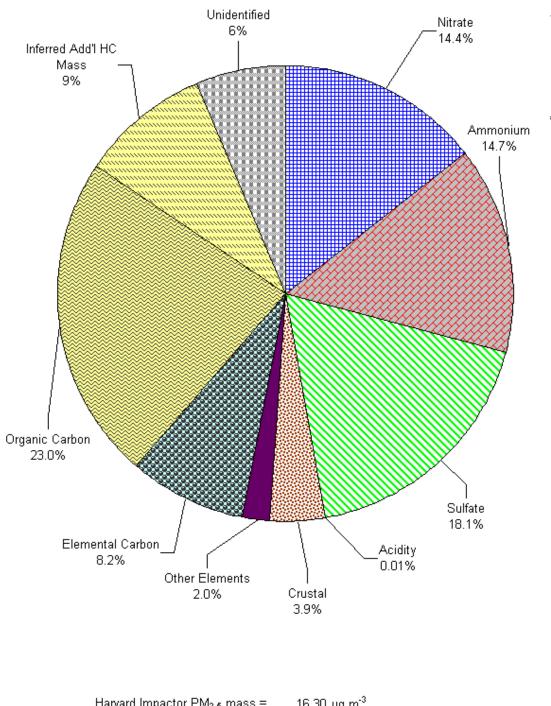


Figure 101B Study average chemical composition estimates for  $PM_{2.5}$  based on Full HEADS and DEN Harvard carbon sampler measurements at Bakersfield.



**Figure 102R** Study average chemical composition estimates for PM<sub>2.5</sub> based on Full HEADS and UND Harvard carbon sampler measurements at Riverside



Harvard Impactor PM<sub>2.5</sub> mass =  $16.30 \ \mu g \ m^{-3}$ Reconstructed PM<sub>2.5</sub> mass =  $15.25 \ \mu g \ m^{-3}$ 

Figure 102C Study average chemical composition estimates for  $PM_{2.5}$  based on Full HEADS and UND Harvard carbon sampler measurements at Chicago.

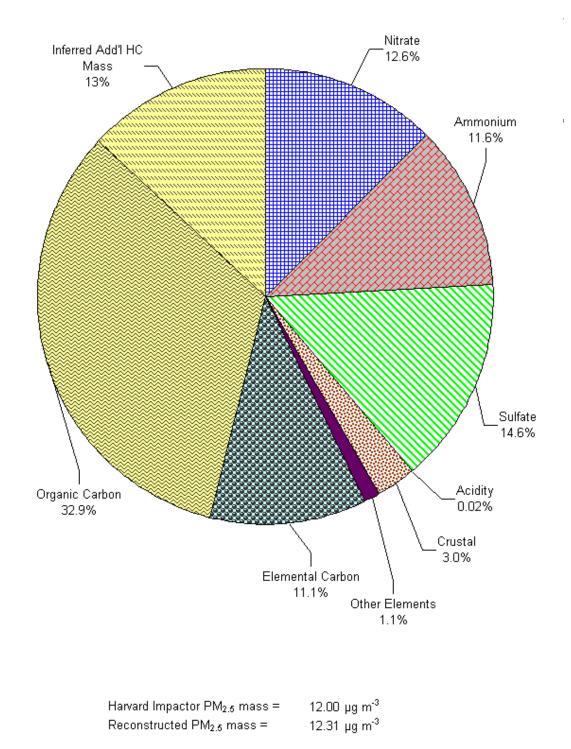
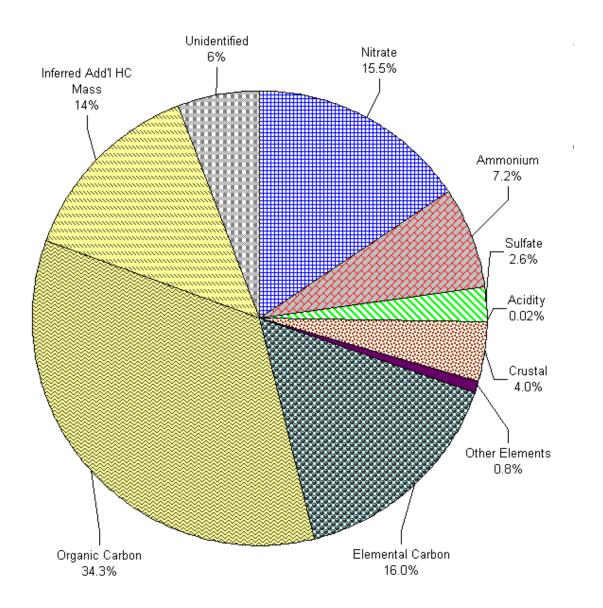
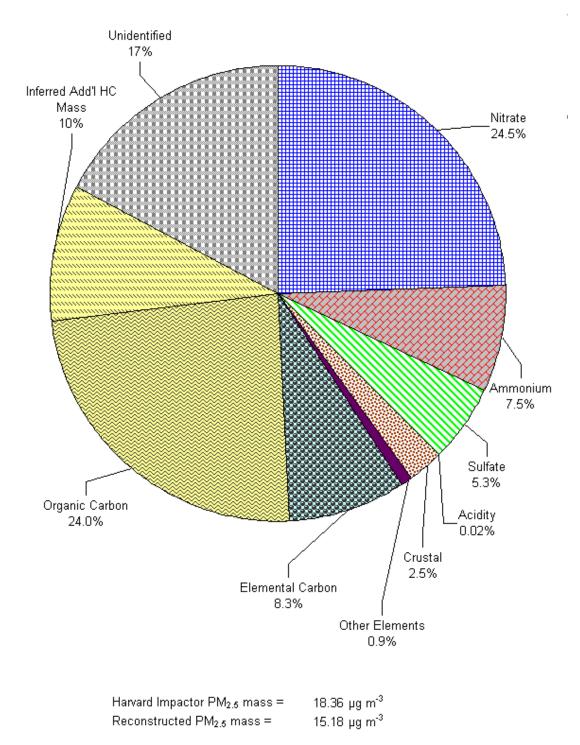


Figure 102D Study average chemical composition estimates for  $PM_{2.5}$  based on Full HEADS and UND Harvard carbon sampler measurements at Dallas.

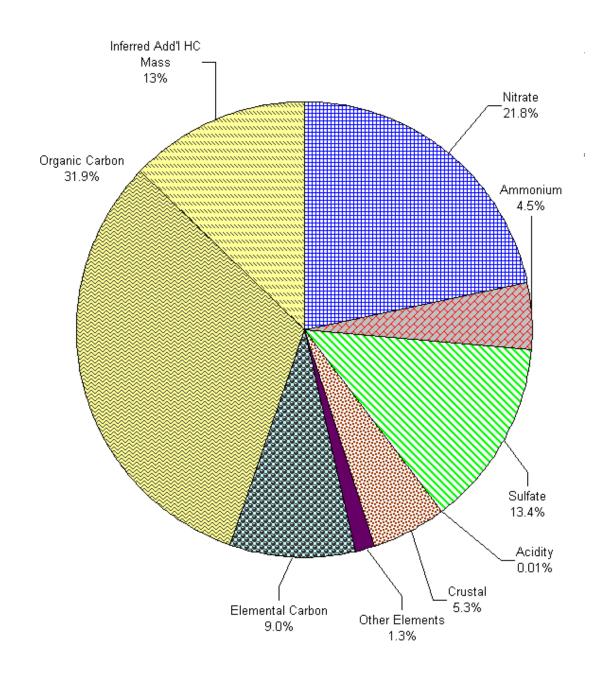


Harvard Impactor PM<sub>2.5</sub> mass =  $22.18 \mu g m^{-3}$ Reconstructed PM<sub>2.5</sub> mass =  $20.90 \mu g m^{-3}$ 

Figure 102P Study average chemical composition estimates for  $PM_{2.5}$  based on Full HEADS and UND Harvard carbon sampler measurements at Phoenix.

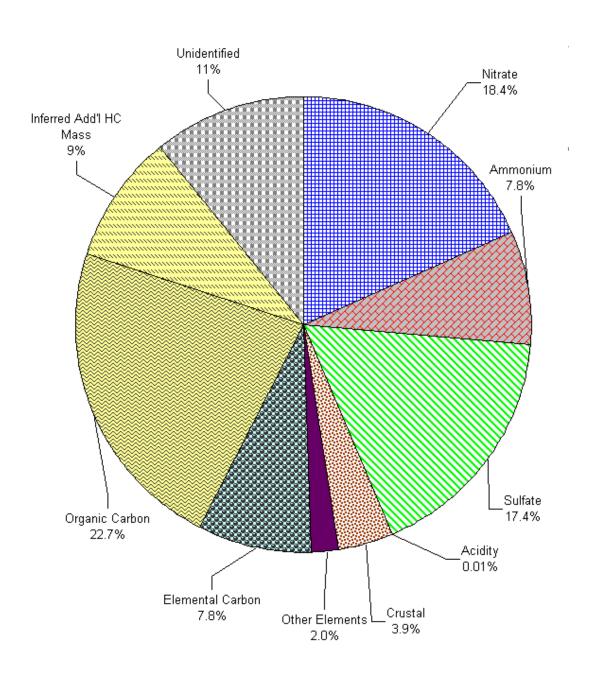


**Figure 102B** Study average chemical composition estimates for PM<sub>2.5</sub> based on Full HEADS and UND Harvard carbon sampler measurements at Bakersfield.



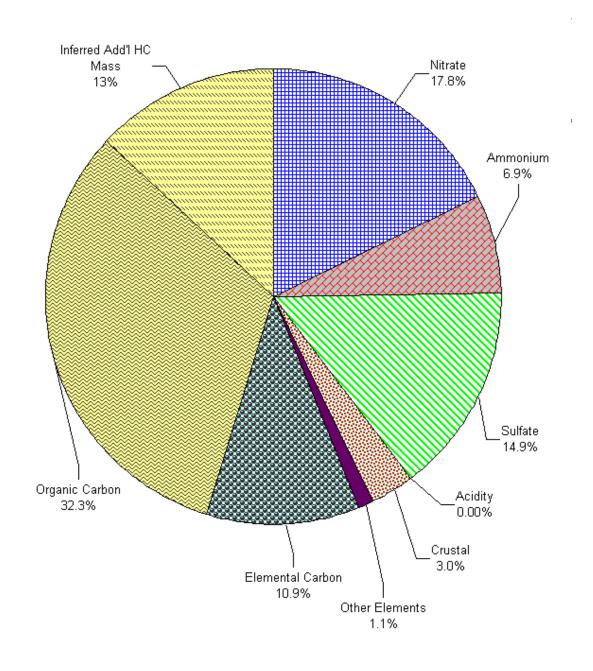
Harvard Impactor PM<sub>2.5</sub> mass =  $19.12 \ \mu g \ m^{-3}$ Reconstructed PM<sub>2.5</sub> mass =  $21.02 \ \mu g \ m^{-3}$ 

**Figure 103R** Study average chemical composition estimates for PM<sub>2.5</sub> based on Nylon HEADS and DEN Harvard carbon sampler measurements at Riverside



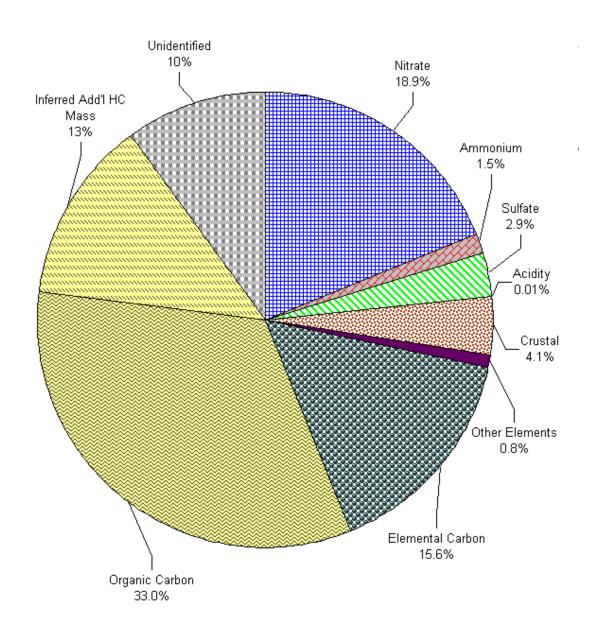
Harvard Impactor PM<sub>2.5</sub> mass =  $16.48 \mu g m^{-3}$ Reconstructed PM<sub>2.5</sub> mass =  $14.70 \mu g m^{-3}$ 

Figure 103C Study average chemical composition estimates for  $PM_{2.5}$  based on Nylon HEADS and DEN Harvard carbon sampler measurements at Chicago.



Harvard Impactor PM<sub>2.5</sub> mass =  $11.98 \ \mu g \ m^{-3}$ Reconstructed PM<sub>2.5</sub> mass =  $12.05 \ \mu g \ m^{-3}$ 

Figure 103D Study average chemical composition estimates for  $PM_{2.5}$  based on Nylon HEADS and DEN Harvard carbon sampler measurements at Dallas.



Harvard Impactor PM<sub>2.5</sub> mass =  $22.34 \ \mu g \ m^{-3}$ Reconstructed PM<sub>2.5</sub> mass =  $20.11 \ \mu g \ m^{-3}$ 

**Figure 103P** Study average chemical composition estimates for PM<sub>2.5</sub> based on Nylon HEADS and DEN Harvard carbon sampler measurements at Phoenix.

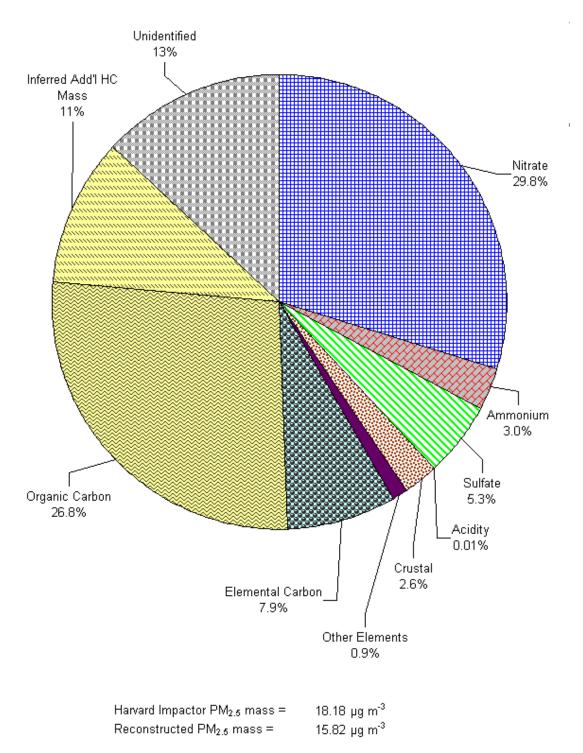
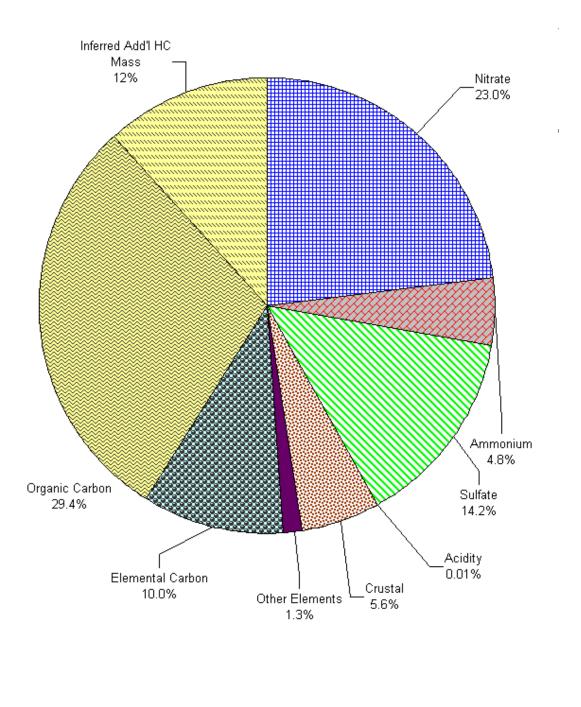
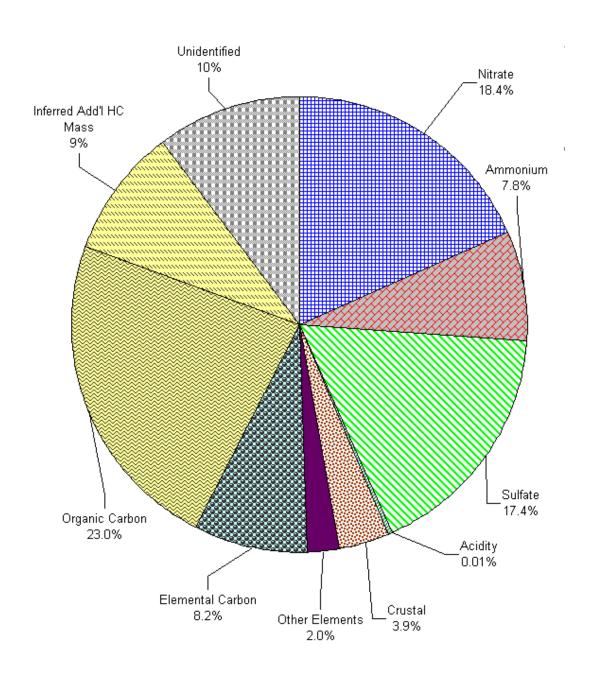


Figure 103B Study average chemical composition estimates for  $PM_{2.5}$  based on Nylon HEADS and DEN Harvard carbon sampler measurements at Bakersfield.



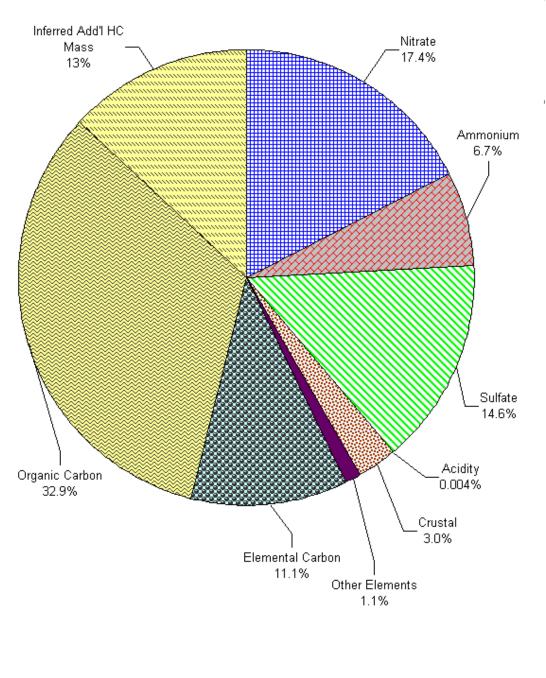
Harvard Impactor PM<sub>2.5</sub> mass =  $19.12 \ \mu g \ m^{-3}$ Reconstructed PM<sub>2.5</sub> mass =  $19.91 \ \mu g \ m^{-3}$ 

**Figure 102R** Study average chemical composition estimates for PM<sub>2.5</sub> based on Nylon HEADS and UND Harvard carbon sampler measurements at Riverside



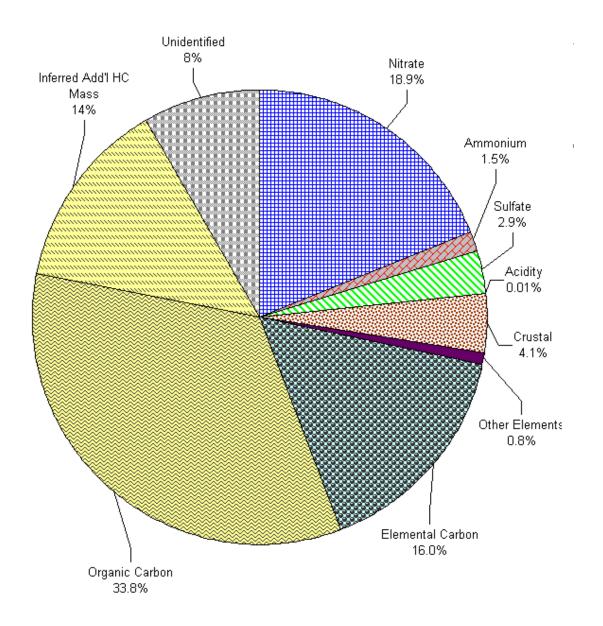
Harvard Impactor PM<sub>2.5</sub> mass =  $16.30 \ \mu g \ m^{-3}$ Reconstructed PM<sub>2.5</sub> mass =  $14.64 \ \mu g \ m^{-3}$ 

**Figure 102C** Study average chemical composition estimates for PM<sub>2.5</sub> based on Nylon HEADS and UND Harvard carbon sampler measurements at Chicago.



Harvard Impactor PM<sub>2.5</sub> mass =  $11.72 \ \mu g \ m^{-3}$ Reconstructed PM<sub>2.5</sub> mass =  $12.05 \ \mu g \ m^{-3}$ 

Figure 102D Study average chemical composition estimates for  $PM_{2.5}$  based on Nylon HEADS and UND Harvard carbon sampler measurements at Dallas.



Harvard Impactor PM<sub>2.5</sub> mass =  $22.34 \mu g m^{-3}$ Reconstructed PM<sub>2.5</sub> mass =  $20.47 \mu g m^{-3}$ 

**Figure 102P** Study average chemical composition estimates for PM<sub>2.5</sub> based on Nylon HEADS and UND Harvard carbon sampler measurements at Phoenix.

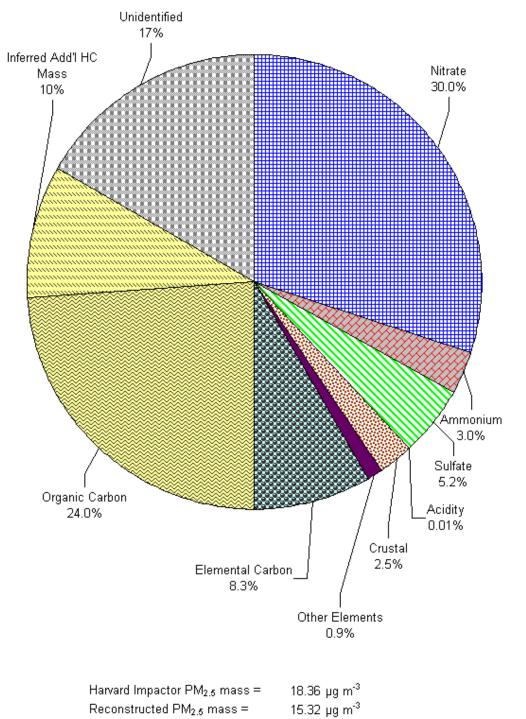
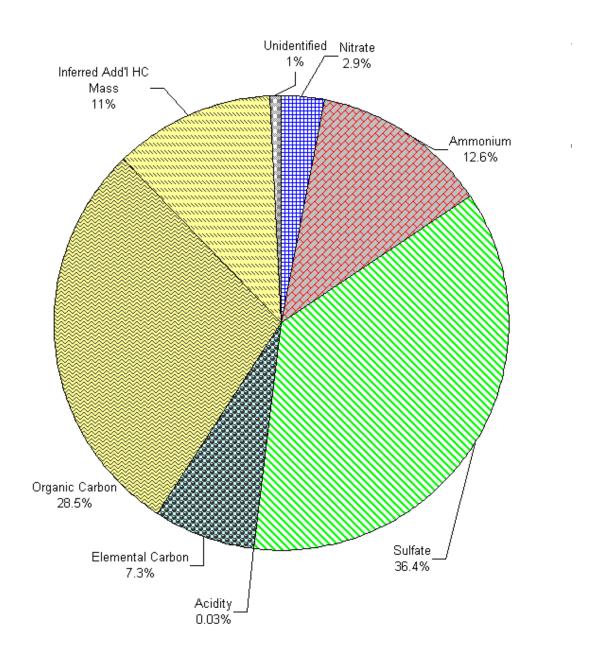
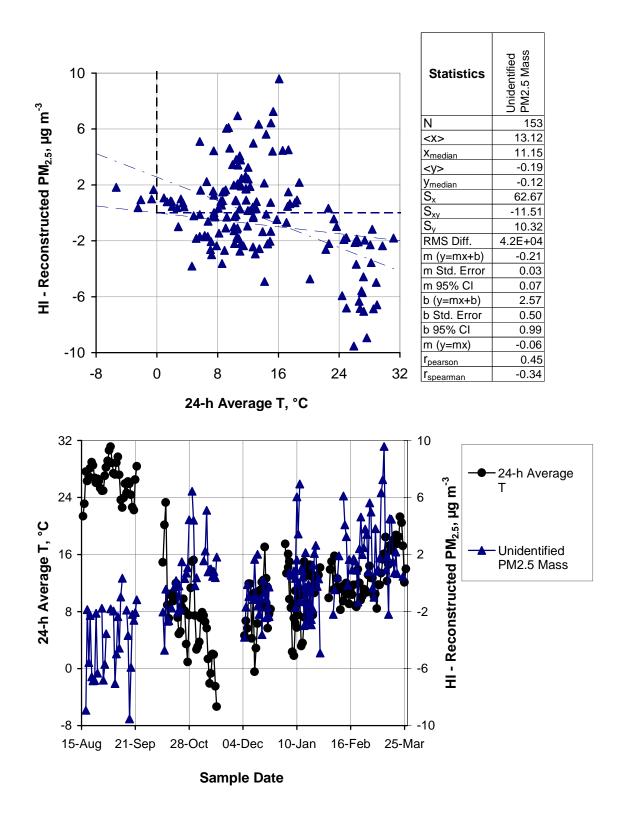


Figure 102B Study average chemical composition estimates for PM<sub>2.5</sub> based on Nylon HEADS and UND Harvard carbon sampler measurements at Bakersfield.



Harvard Impactor  $PM_{2.5}$  mass = 21.07  $\mu g m^{-3}$ Reconstructed  $PM_{2.5}$  mass = 20.90  $\mu g m^{-3}$ 

**Figure 102F** Study average chemical composition estimates for PM<sub>2.5</sub> based on Nylon HEADS and UND Harvard carbon sampler measurements at Philadelphia.



**Figure 105A** Exploration of observed disagreements between reconstructed and Harvard Impactor mass: HI mass – Reconstructed Mass 4 (see Table 16) vs. average daily temperature at all sites.

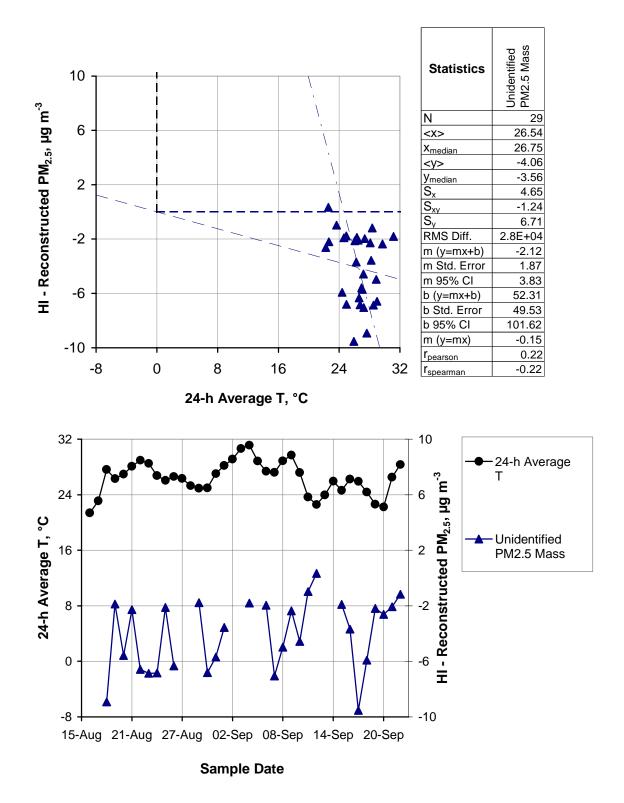


**Figure 105R** Exploration of observed disagreements between reconstructed and Harvard Impactor mass: HI mass – Reconstructed Mass 4 (see Table 16) vs. average daily temperature at Riverside.

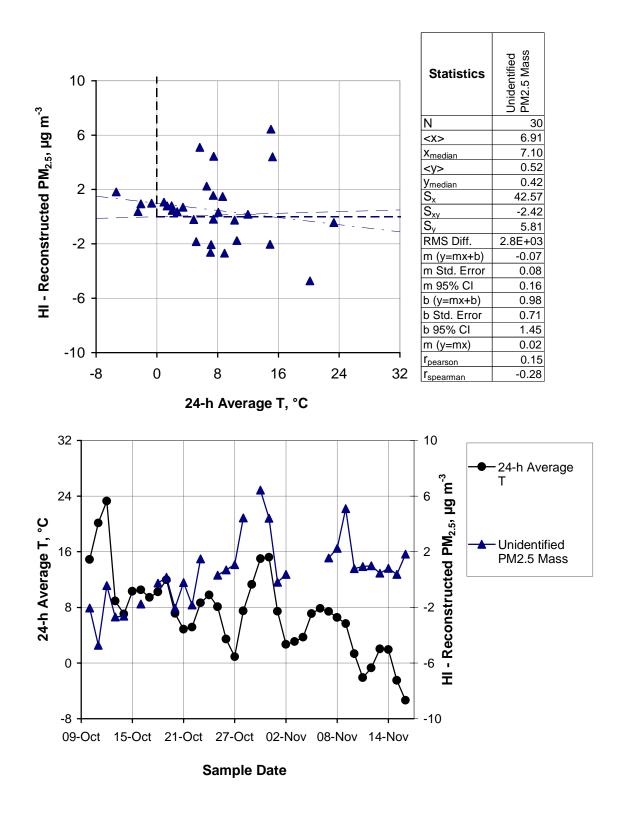


**Figure 105C** Exploration of observed disagreements between reconstructed and Harvard Impactor mass: HI mass – Reconstructed Mass 4 (see Table 16) vs. average daily temperature at Chicago.

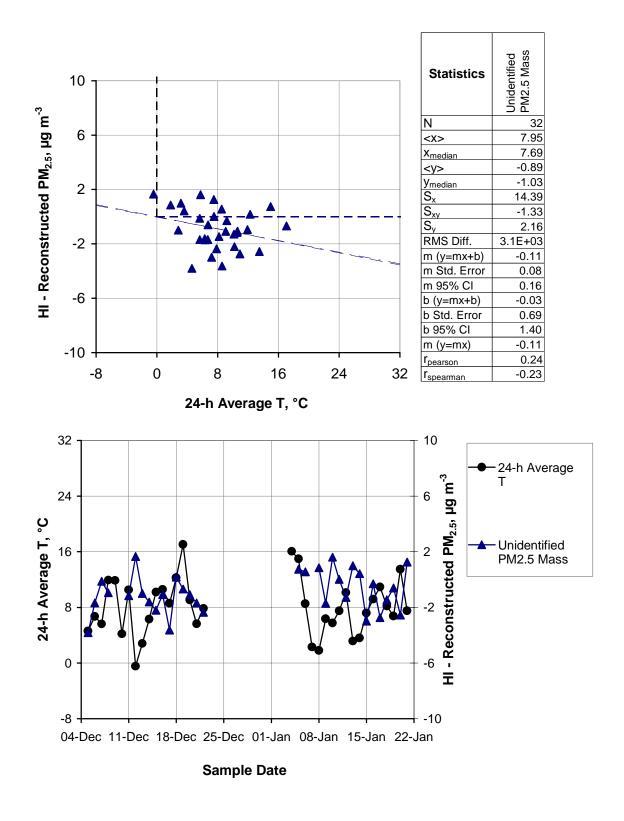


**Figure 105D** Exploration of observed disagreements between reconstructed and Harvard Impactor mass: HI mass – Reconstructed Mass 4 (see Table 16) vs. average daily temperature at Dallas.

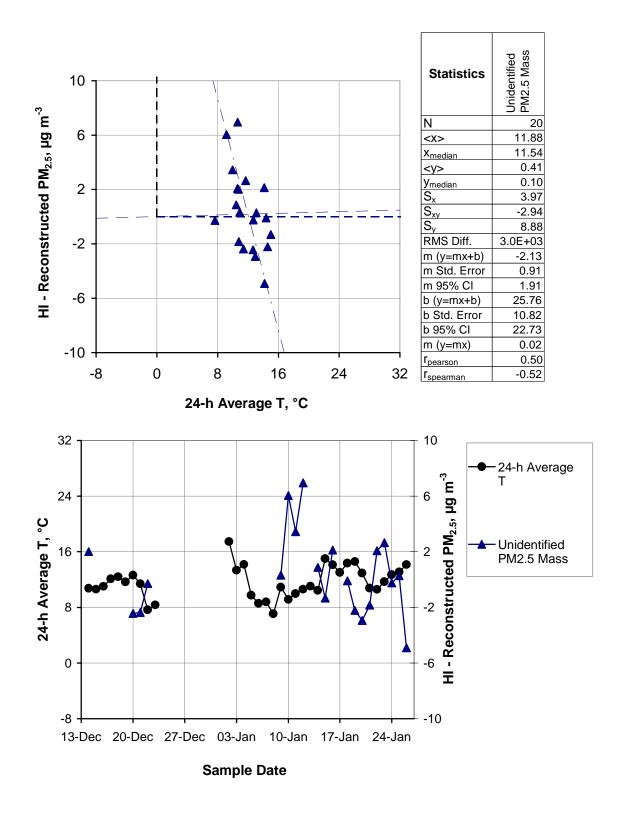


**Figure 105P** Exploration of observed disagreements between reconstructed and Harvard Impactor mass: HI mass – Reconstructed Mass 4 (see Table 16) vs. average daily temperature at Phoenix.

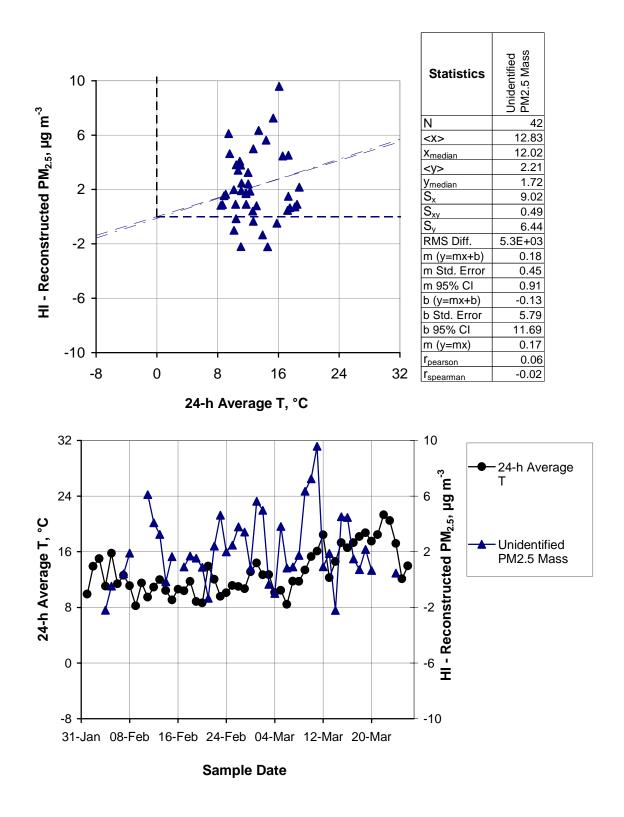


**Figure 105B** Exploration of observed disagreements between reconstructed and Harvard Impactor mass: HI mass – Reconstructed Mass 4 (see Table 16) vs. average daily temperature at Bakersfield.

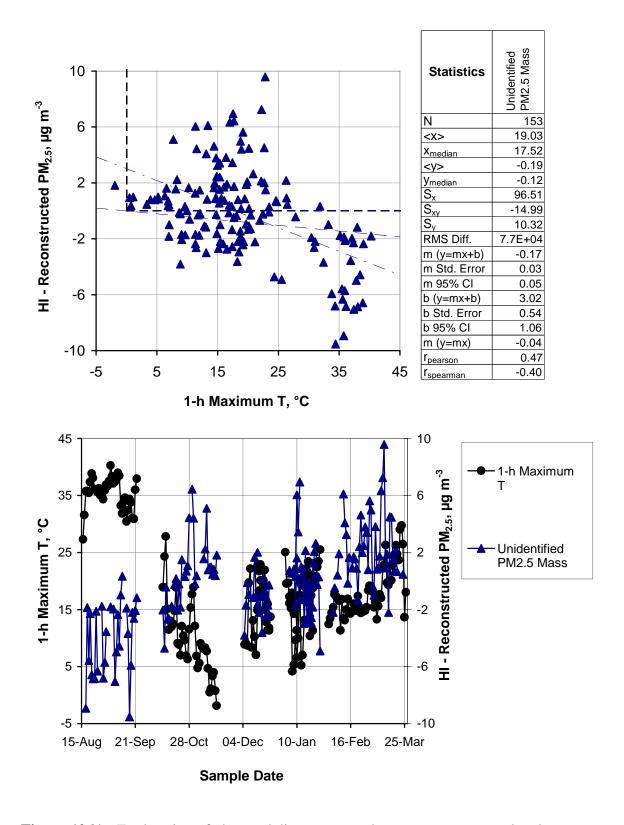


**Figure 106A** Exploration of observed disagreements between reconstructed and Harvard Impactor mass: HI mass – Reconstructed Mass 4 (see Table 16) vs. daily one hour maximum temperature at all sites.

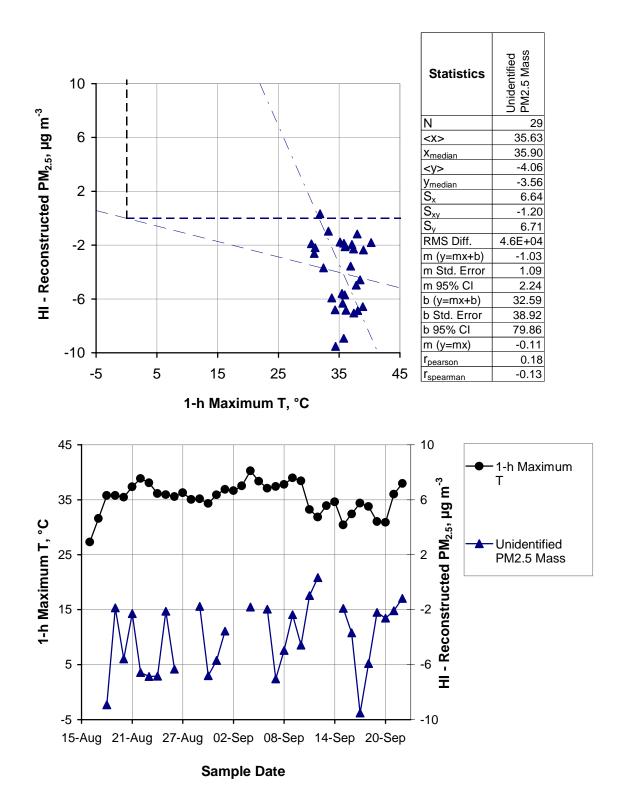


**Figure 106R** Exploration of observed disagreements between reconstructed and Harvard Impactor mass: HI mass – Reconstructed Mass 4 (see Table 16) vs. daily one hour maximum temperature at Riverside.

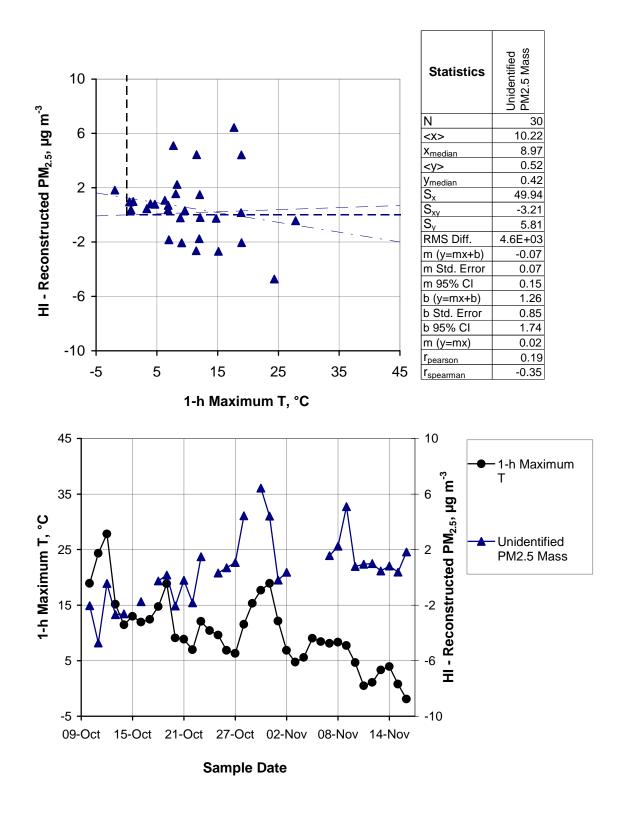


**Figure 106C** Exploration of observed disagreements between reconstructed and Harvard Impactor mass: HI mass – Reconstructed Mass 4 (see Table 16) vs. daily one hour maximum temperature at Chicago.

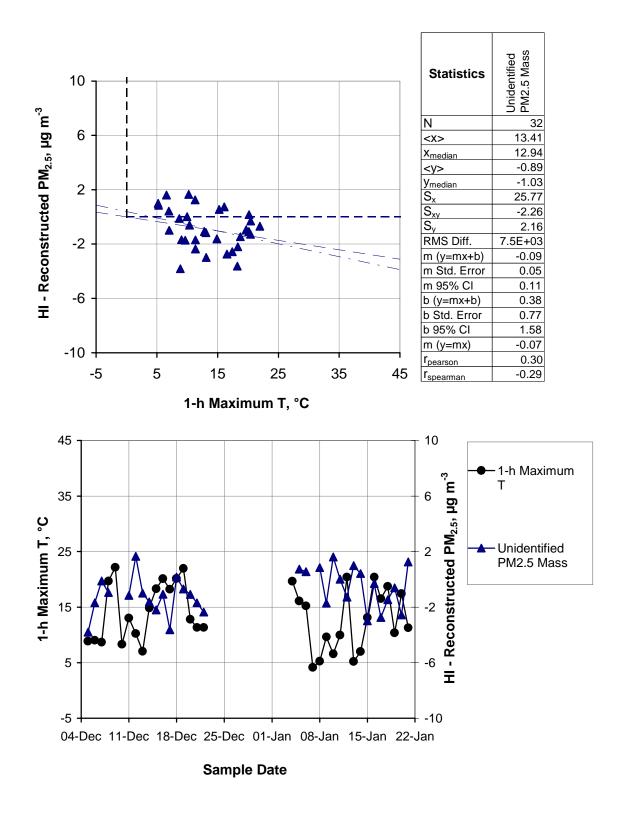


**Figure 106D** Exploration of observed disagreements between reconstructed and Harvard Impactor mass: HI mass – Reconstructed Mass 4 (see Table 16) vs. daily one hour maximum temperature at Dallas.

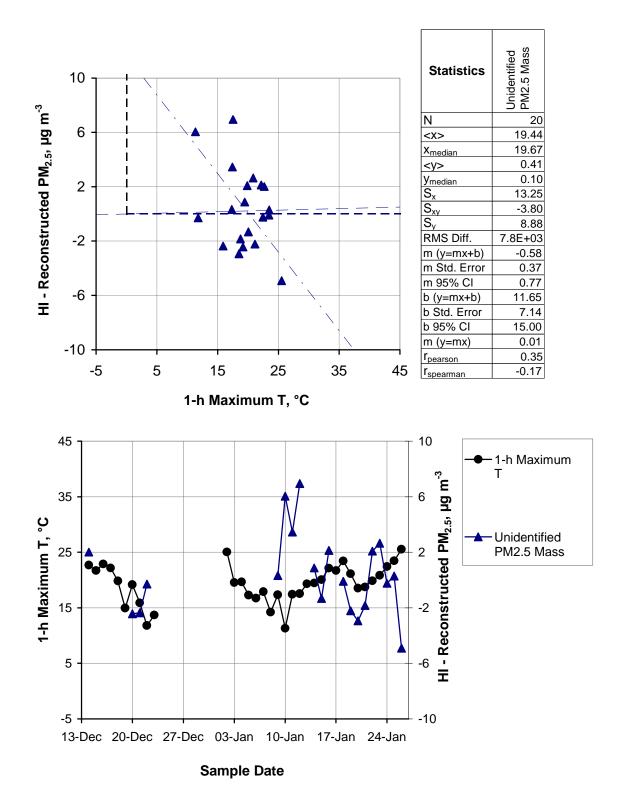


**Figure 106P** Exploration of observed disagreements between reconstructed and Harvard Impactor mass: HI mass – Reconstructed Mass 4 (see Table 16) vs. daily one hour maximum temperature at Phoenix.

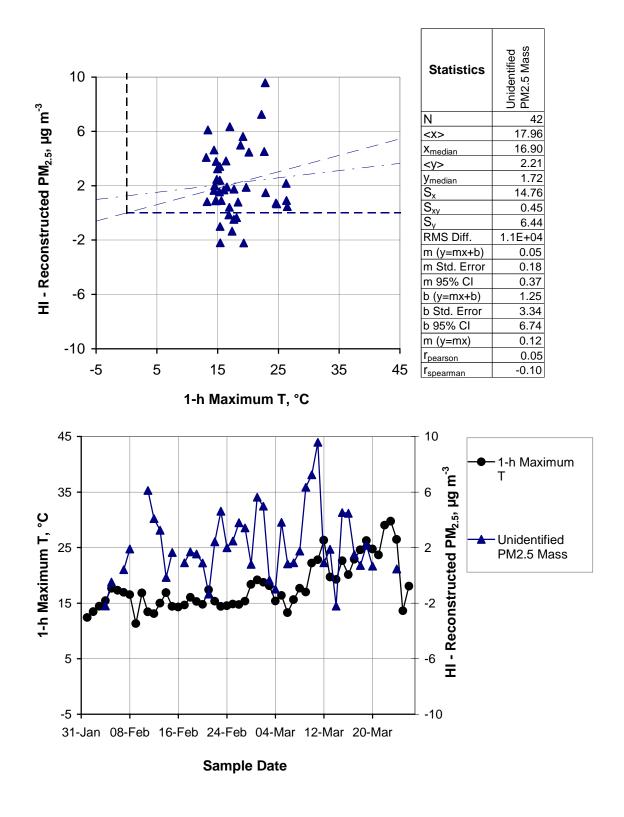


**Figure 106B** Exploration of observed disagreements between reconstructed and Harvard Impactor mass: HI mass – Reconstructed Mass 4 (see Table 16) vs. daily one hour maximum temperature at Bakersfield.

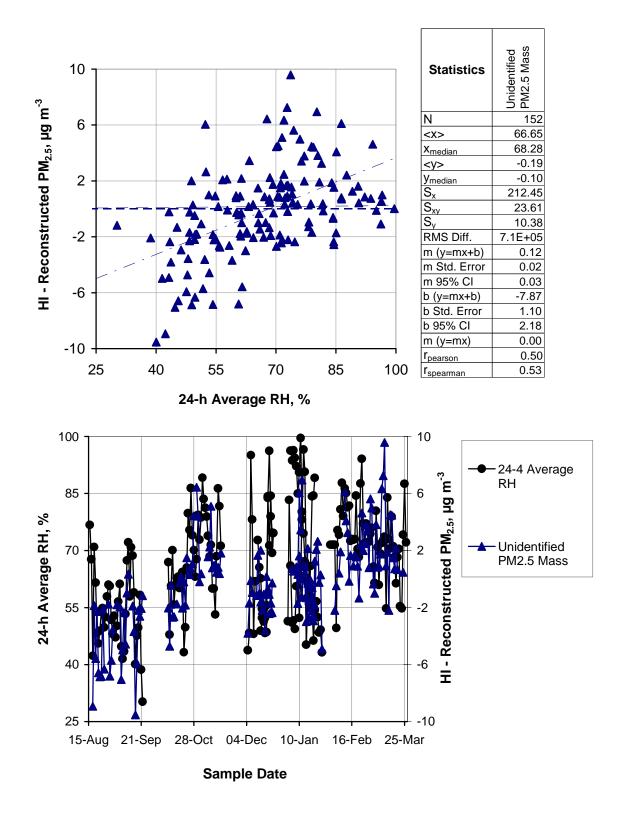


**Figure 107A** Exploration of observed disagreements between reconstructed and Harvard Impactor mass: HI mass – Reconstructed Mass 4 (see Table 16) vs. average daily relative humidity at all sites.

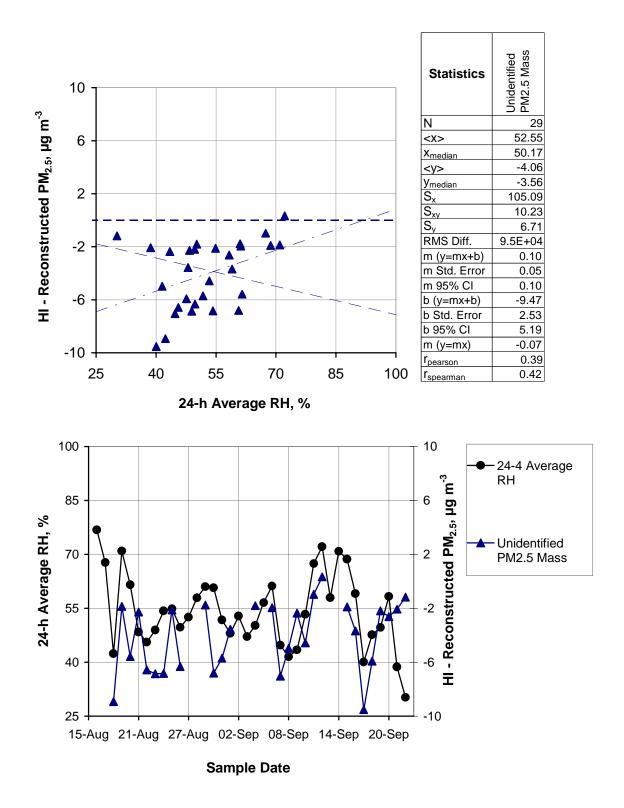


**Figure 107R** Exploration of observed disagreements between reconstructed and Harvard Impactor mass: HI mass – Reconstructed Mass 4 (see Table 16) vs. average daily relative humidity at Riverside.

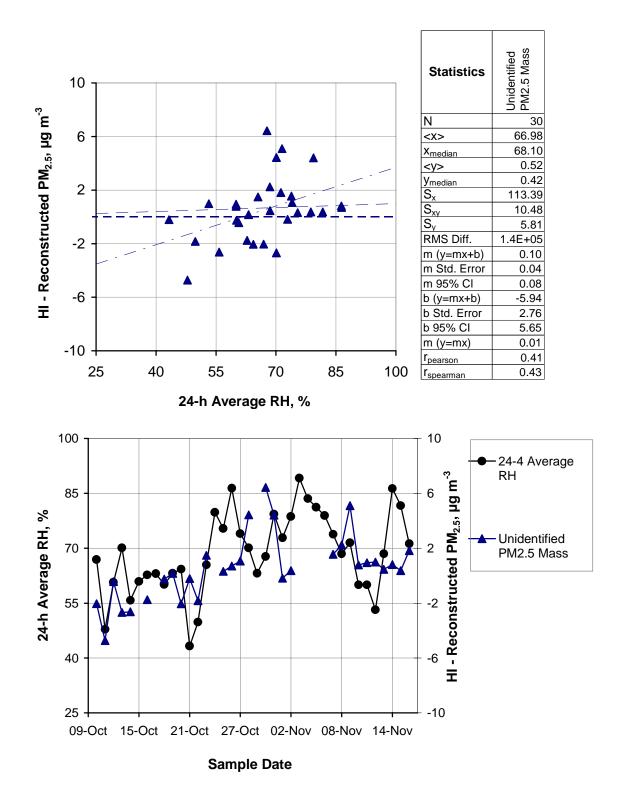


**Figure 107C** Exploration of observed disagreements between reconstructed and Harvard Impactor mass: HI mass – Reconstructed Mass 4 (see Table 16) vs. average daily relative humidity at Chicago.

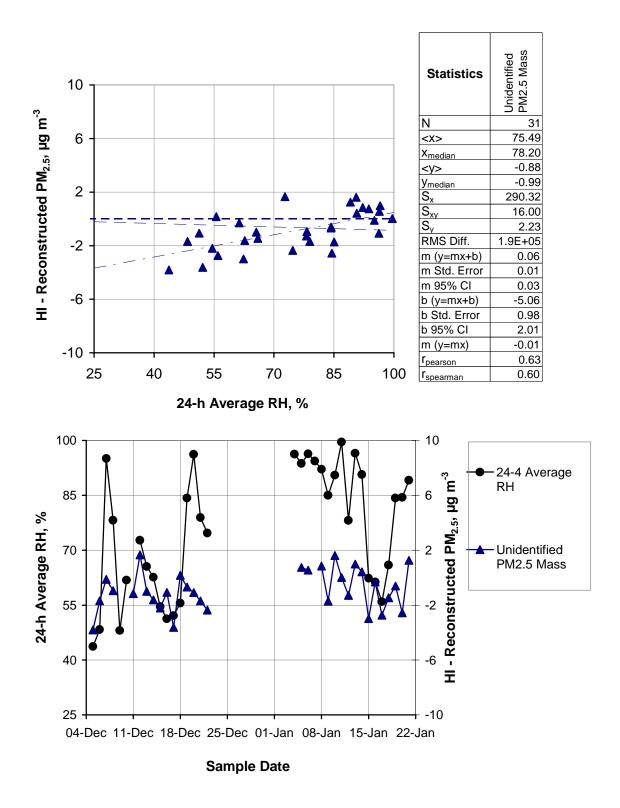


**Figure 107D** Exploration of observed disagreements between reconstructed and Harvard Impactor mass: HI mass – Reconstructed Mass 4 (see Table 16) vs. average daily relative humidity at Dallas.

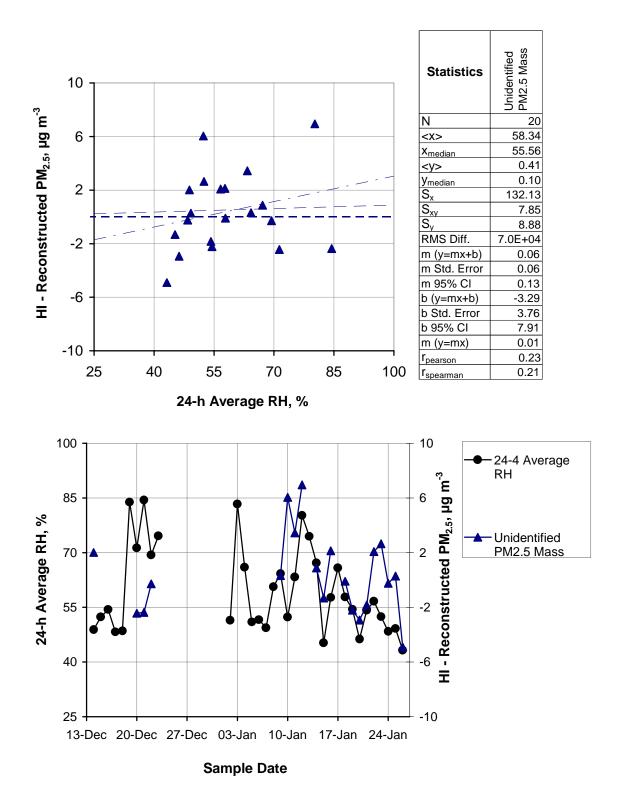


**Figure 107P** Exploration of observed disagreements between reconstructed and Harvard Impactor mass: HI mass – Reconstructed Mass 4 (see Table 16) vs. average daily relative humidity at Phoenix.

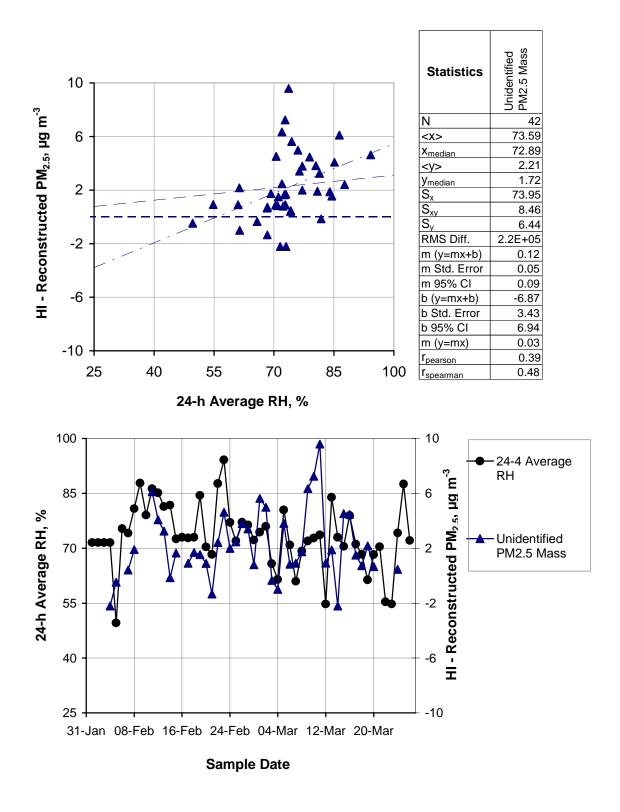


**Figure 107B** Exploration of observed disagreements between reconstructed and Harvard Impactor mass: HI mass – Reconstructed Mass 4 (see Table 16) vs. average daily relative humidity at Bakersfield.

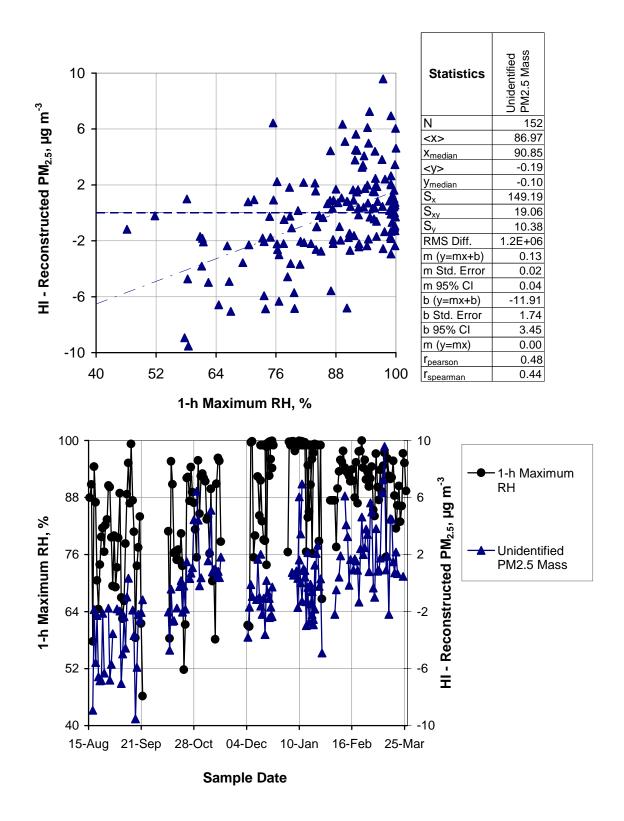


**Figure 108A** Exploration of observed disagreements between reconstructed and Harvard Impactor mass: HI mass – Reconstructed Mass 4 (see Table 16) vs. daily one hour maximum relative humidity at all sites.

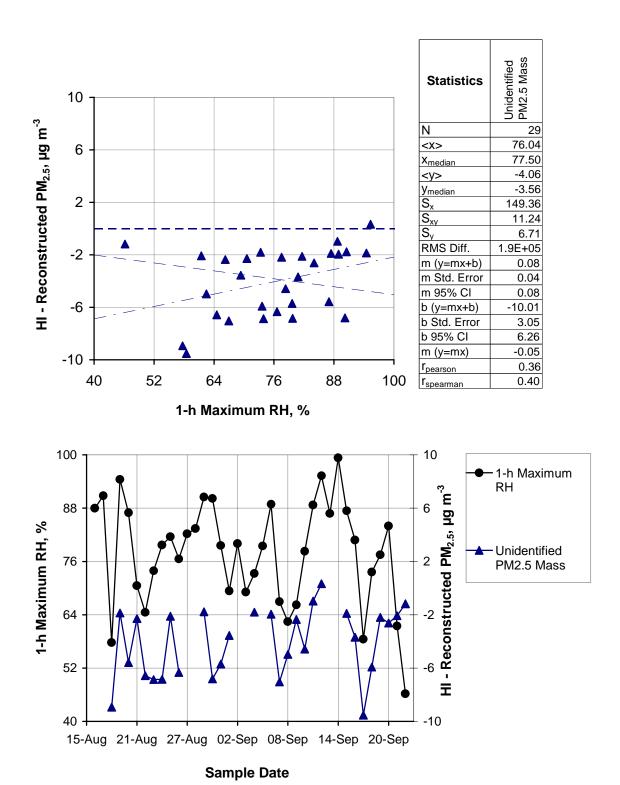


**Figure 108R** Exploration of observed disagreements between reconstructed and Harvard Impactor mass: HI mass – Reconstructed Mass 4 (see Table 16) vs. daily one hour maximum relative humidity at Riverside.

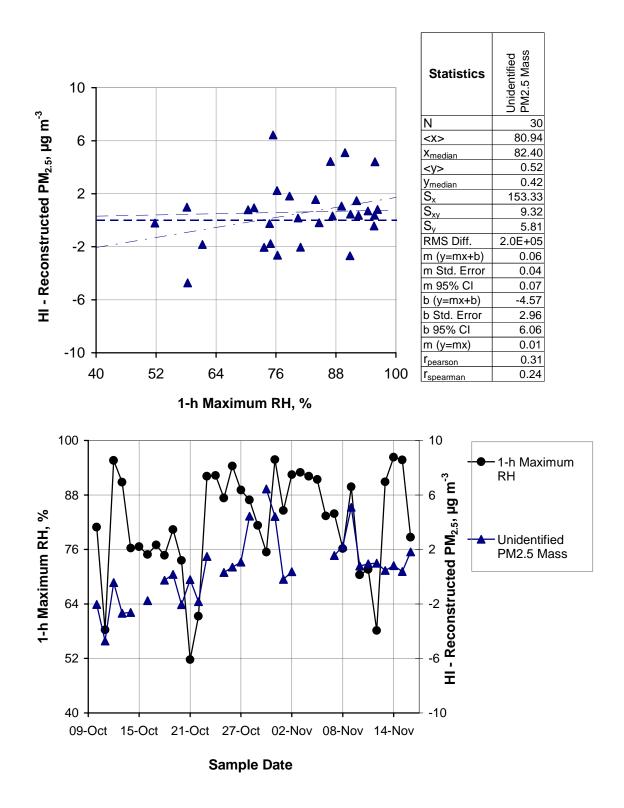


**Figure 108C** Exploration of observed disagreements between reconstructed and Harvard Impactor mass: HI mass – Reconstructed Mass 4 (see Table 16) vs. daily one hour maximum relative humidity at Chicago.

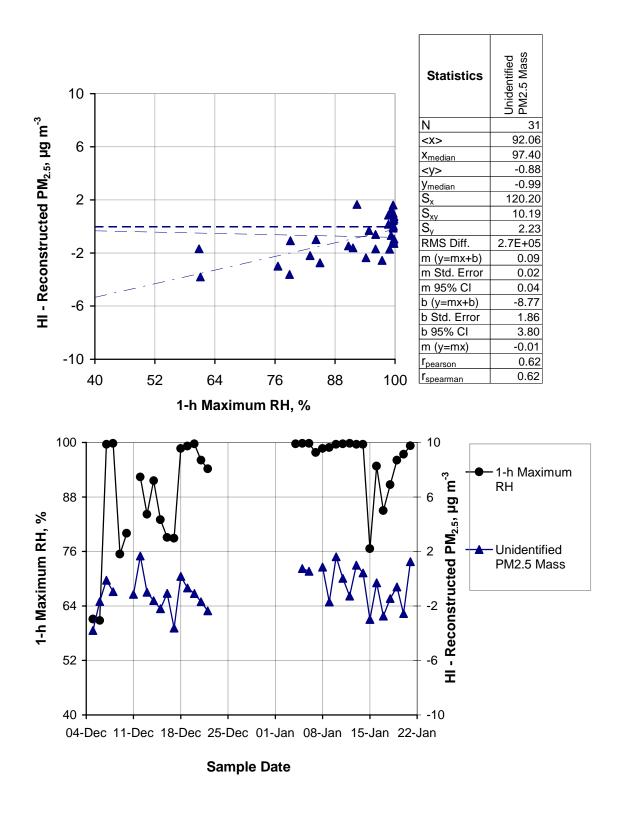


**Figure 108D** Exploration of observed disagreements between reconstructed and Harvard Impactor mass: HI mass – Reconstructed Mass 4 (see Table 16) vs. daily one hour maximum relative humidity at Dallas.

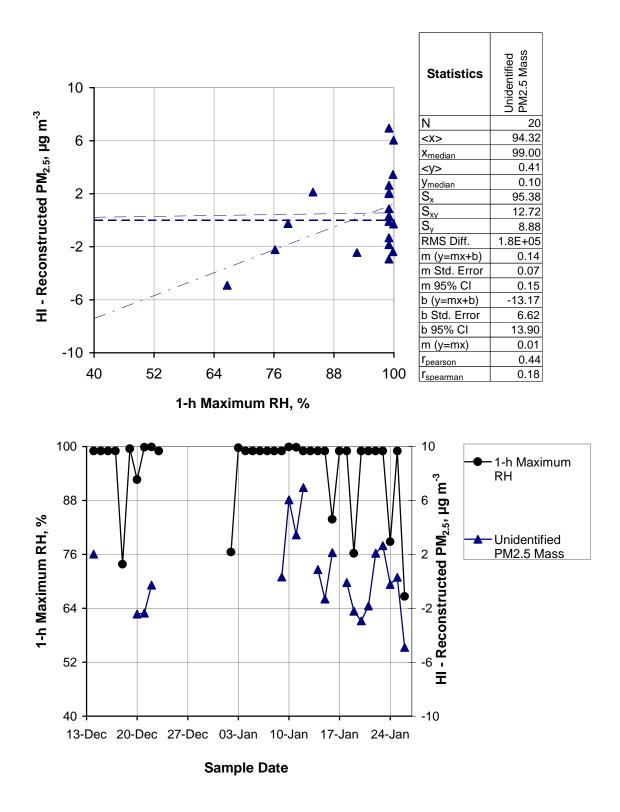


**Figure 106P** Exploration of observed disagreements between reconstructed and Harvard Impactor mass: HI mass – Reconstructed Mass 4 (see Table 16) vs. daily one hour maximum relative humidity at Phoenix.

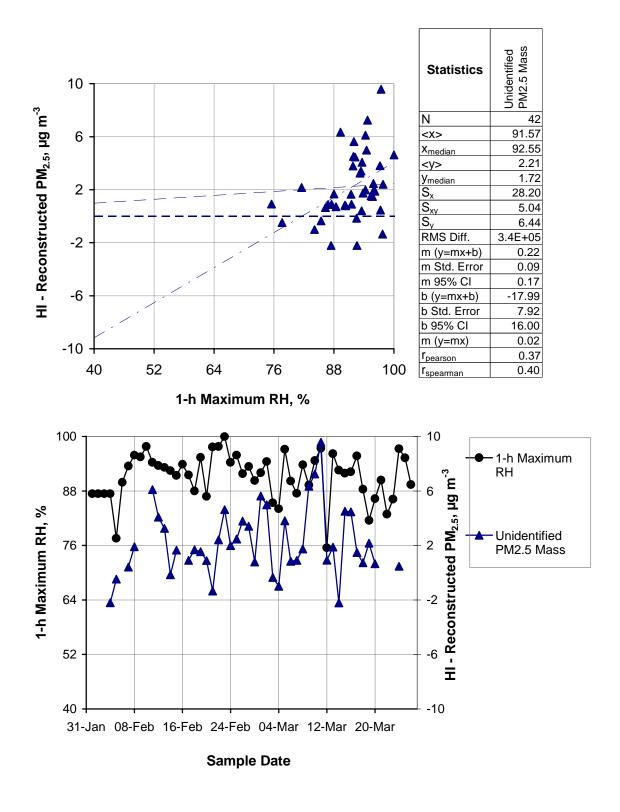


**Figure 106B** Exploration of observed disagreements between reconstructed and Harvard Impactor mass: HI mass – Reconstructed Mass 4 (see Table 16) vs. daily one hour maximum relative humidity at Bakersfield.